THE IMPACT OF ERAP1 FUNCTIONS ON INNATE AND ADAPTIVE IMMUNITY IN HUMAN DISEASE MODELS

By

Maja Kristin K Blake

A DISSERTATION

Submitted to
Michigan State University
in partial fulfillment of the requirements
for the degree of

Pharmacology and Toxicology– Doctor of Philosophy

2022

ABSTRACT

ERAP1 has long been appreciated for its role in antigen presentation during the adaptive immune response. It is a peptidase in the endoplasmic reticulum that trims peptide antigens prior to their loading onto awaiting MHC-1. However, ERAP1 has also been shown to play an important role in innate immune responses, although the mechanisms underlying these associations have been unclear. The ERAP1 gene has also been linked to a number of autoimmune diseases including, but not limited to Multiple Sclerosis, Ankylosing Spondylitis, and Ulcerative Colitis. In addition, it is known to be altered in various tumor types as a means of immune evasion, and inhibitors for ERAP1 have shown promising results against tumors *in vitro*. Therefore, ERAP1's significance in the susceptibility to diverse diseases is vast, and further study into how this protein participates in both innate and adaptive immune response mechanisms is justified. Our lab has previously published that immune cells and animals deficient in ERAP1 display proinflammatory phenotypes. In this dissertation, the mechanism as to how disruptions in normal ERAP1 function leads to proinflammatory phenotypes is studied. First, proinflammatory mechanisms within a critical innate immune cell, macrophages, are discerned using both *ex vivo* models and an *in vivo* inducible colitis mouse model. ERAP1 deficiency in the setting of a murine model of autoimmunity is also evaluated, revealing both disturbances in B cell development and function as dependent on normal ERAP1 activity, and that these disturbances can lead to exaggerated neuroinflammation in several murine models of MS. ERAP1 dependent proinflammatory mechanisms within B cells are further studied *ex vivo* using global RNA sequencing technology along with flow cytometry-based methods. Together, the results of these studies reveal that loss of ERAP1 function causes enhanced ER stress within the cell, leading to UPR activation, increased inflammasome activity, and evidence of increased

pyroptosis. Given the broad spectrum of ERAP1 functions on immune cell functions, we capitalized on these insights to determine how ERAP1 inhibition might impact diseases such as cancer. Specifically, our results confirmed that that ERAP1 inhibition promoted NK cell directed tumor killing, a modality that had never been attempted until now. In conclusion, this dissertation capitalizes upon insights gained from human genetic studies associating ERAP1 with a variety of human disease susceptibilities, identifying the molecular mechanisms underlying these associations, and also illuminates possible new therapies for human diseases derived from study of ERAP1.

This thesis is dedicated to my incredible husband and best friend Todd Blake. Thank you for always believing in me and selflessly supporting me throughout this journey.

ACKNOWLEDGMENTS

The work presented here would not have been possible without the hard work, expertise, and support of many individuals. First and foremost, I would like to thank my mentor Dr. Andrea Amalfitano. His expertise and intelligence are truly unparalleled. The first day I met Dr. Amalfitano he said, “Call me Andy”, and over the course of half a decade, he proved to be the most respectful, kind, and humble leader I’ve had the pleasure of working with. As busy as Andy became, he always made time for me and responded quickly to any poster or paper edits I needed, or any data questions I had. His input on experimental design and data analysis was always so critical for me moving projects forward. His unique perspective as a physician made him challenge me to think about how the work we were doing would impact humans, and ensure that the end goal was never lost. I hope I can one day not only be a caring and data-driven physician like he is, but also a genuine and humble co-worker and mentor. I cannot thank Andy enough for his support and encouragement during my graduate training at MSU. Thank you for allowing me to join your team and learn about immunology and genetics in such a translational manner. I am truly honored to have been able to contribute to your lab’s work.

Similarly, thank you to the entire Amalfitano lab, both past and present. In particular, thank you to Dr. Yasser Aldhamen for teaching me everything about various immune receptors and immunology as a whole, and teaching me how to think like a scientist. Thank you for continuously taking time out of your day to plan or analyze an experiment with me. I will always remember your white board drawings and our long discussion sessions. I appreciate your mentorship and support throughout this journey so much. Also, I would like to thank all of the other graduate students who helped train me and teach me. Specifically, I would like to thank Patrick O’Connell for involving me in many different projects of his, and working together with

me to complete our joint projects. I would also like to thank all of the undergrads who helped me with experiments and made the lab environment so much fun during my training. And finally, last but most definitely not least, thank you to Sarah Roosa. Thank you for ordering all of the reagents and helping me with many *in vivo* experiments. Thank you for always holding the lab and personnel to the highest standards, and for providing so many laughs and good times along the way.

Next, I would like to thank the DO-PhD program directors and staff. Thank you to Dr. Brian Schutte and Dr. John Goudreau for providing support for me financially throughout my training, and for always having the students' best interests in mind. I would never have been able to work towards my dream of becoming a physician scientist without the program's support. Thank you to Michele Volker for making sure my "i's were dotted and t's were crossed", and always being a trusting friendly face. Also, thank you to Dr. Justin McCormick for taking a chance on me when I applied to this program, and Bethany Heinlein for making sure I received a spot here. Without their believing in me, I would not be on my way to becoming a physician scientist, and for that I am eternally grateful.

I would like to sincerely thank my guidance committee: Dr. Anne Dorrance, Dr. Karen Liby, Dr. Cheryl Rockwell, and Dr. John Goudreau. I am so grateful for all your support and constructive criticism throughout this journey. Thank you for seeing the value of my medical training and for always encouraging me. Thank you for providing each of your unique perspectives to my project and training. I learned so much from each committee meeting, and learned to look at my data from a different perspective, which not only helped the project but also my own personal growth as a scientist.

Thank you to the Pharmacology and Toxicology department and it's amazing leadership: Dr. Anne Dorrance and Dr. Karen Liby. The environment of the department and its people are so kind, and I thank everyone for being so friendly to me from Day 1. The Pharm/Tox department is truly such a special place, and everyone in it made my time here so fun and I will remember everyone fondly. I would also like to thank Dr. Richard Neubig for letting me do a rotation in his laboratory when I started and for being a mentor ever since. Similarly, thank you to the IPSTP T32 training program through the Pharmacology and Toxicology department. The unique experience of working with other graduate students from different departments was truly invaluable and I learned so much through the training sessions. Thank you for supporting me financially throughout my final graduate school year, and for providing a strong sense of community.

I would also like to thank you to all of the core facilities at MSU, without which I would not have been able to do this work. Thank you to Dr. Louis King and Dr. Matt Bernard in the flow cytometry core. Your expertise in flow cytometry helped me not only complete this dissertation but also publish the manuscripts. Also, thank you to the animal facilities and CAR. Your oversight of our *in vivo* studies and close care of the animals made these studies possible.

And finally, thank you to my family and friends for all of your support. These past years have not been easy, and your unconditional love got me through the tough days. To all of the friends I made along this journey, I thank you for the encouragement and laughs. And to my family, thank you for always believing in me and thinking I could accomplish anything I put my mind to. I'm still amazed I made it to the other side, and I truly believe I could not have achieved this without your unwavering support.

TABLE OF CONTENTS

LIST OF ABBREVIATIONS

ERAP1	Endoplasmic Reticulum Aminopeptidase 1
SNP	Single Nucleotide Polymorphism
PRR	Pattern Recognition Receptor
PAMP	Pathogen Associated Molecular Patterns
TLR	Toll-Like Receptor
RLR	RIG-I-Like Receptors
NLR	NOD-Like Receptors
IFN	Interferon
TNF	Tumor Necrosis Factor
WT	Wild Type
KO	Knockout
DSS	Dextran Sodium Sulfate
NLRP1	NOD-, LRR- and Pyrin domain–containing 1
NLRP3	NOD-, LRR- and Pyrin domain–containing 3
NLRC4	NOD-, LRR- and Caspase recruitment domain–containing 4
AIM2	Absent In Melanoma 2
MHC	Major Histocompatibility Complex
HLA	Human Leukocyte Antigen
ASC	Apoptosis-Associated Speck-like
CNS	Central Nervous System
MTB	Mycobacterium Tuberculosis
EAE	Experimental Autoimmune Encephalomyelitis

UMAP	Uniform Manifold Approximation and Projection
FACS	Fluorescence-Assisted Cell Sorting
PMBCs	Peripheral Blood Mononuclear Cells
RNA-seq	RNA sequencing
Treg	Regulatory T cell
MS	Multiple Sclerosis
BAMs	Border-Associated Macrophages
MdCs	Myeloid-derived Cells
BCR	B Cell Receptor
TCR	T Cell Receptor
iEN	Immunological Elastic Net
I.T.	Intra-Tumoral
I.P.	Intra-Peritoneal
I.V.	Intra-Venous
tSNE	t-distributed Stochastic Neighbor Embedding
UMAP	Uniform Manifold Approximation and Projection
ADCC	Antibody-Dependent Cellular Cytotoxicity
MDS	Multidimensional Scaling
AS	Ankylosing Spondylitis
Breg	Regulatory B cell
FO	Follicular
MZ	Marginal Zone
APC	Antigen Presenting Cell

ER	Endoplasmic Reticulum
DEG	Differentially Expressed Gene
CFA	Complete Freund's Adjuvant
NK	Natural Killer
BMDM	Bone Marrow-Derived Macrophages
dsDNA	double stranded DNA
LPS	Lipopolysaccharide
FLICA	Fluorescent-Labeled Inhibitor of Caspases
NF-kb	Nuclear Factor kappa B
JNK	c-Jun N-terminal Kinase
TUDCA	Tauroursodeoxycholic acid
sXBP1	spliced X-Box Binding Protein 1
SEM	Standard Error of the Mean
MSU	Monosodium Urate
UPR	Unfolded Protein Response
GSDMD	Gasdermin D
CFSE	Carboxyfluorescein Succinimidyl Ester
CTV	CellTrace violet
PD-1	Programmed cell Death protein
ACK	Ammonium-Chloride-Potassium
UC	Ulcerative Colitis
GWAS	Genome Wide Associated Studies
HPV	Human Papillomavirus

SARS-Cov-2	Severe Acute Respiratory Syndrome Coronavirus 2
RAAS	*Renin* Angiotensin Aldosterone system
BD	Behçet's Disease
MOG	Myelin Oligodendrocyte Glycoprotein
SLAMF7	SLAM family member 7
TME	Tumor Microenvironment
CyTOF	Cytometry by Time Of Flight
Atg	Autophagy related gene
MDR	MitoTracker Deep Red
MG	MitoTracker Green
ERAD	Endoplasmic Reticulum-Associated Degradation
qRT-PCR	Real-Time Quantitative Reverse Transcription Polymerase Chain Reaction
CLL	Chronic Lymphocytic Leukemia
CATALYST	Cytometry dATa analysis Tools
SOMs	Self-Organizing Maps
UMIs	Unique Molecular Identifiers

LIST OF SYMBOLS

α	Alpha
β	Beta
γ	Gamma
κ	Kappa
μ	Mu

Chapter 1: Introduction

The role of the immune system is to rapidly and specifically identify foreign invasion of the host and respond accordingly. It is no wonder that the immune system has evolved to encompass a vast landscape of coordinated intracellular and extracellular signaling, fostering cell-cell interactions to eliminate infection and return the host to baseline as rapidly as possible. As a result, it can be predicted that even mild perturbations in normal immune system functions would have significant consequences, resulting in a myriad of diseases. Specifically, the balance between initiating pro-inflammatory and anti-inflammatory innate immune and adaptive immune responses is an intricate process, that requires a variety of molecular checks and balances to maintain homeostasis even in the face of overwhelming infection. However, when these immune regulatory responses go unchecked, are inherently unstable due to genetic predisposition, or are overwhelmed, problematic diseases can occur, including autoimmunity and cancer. In general, autoimmune diseases involve the hyper-activity of proinflammatory cells such as B and T lymphocytes (1). In relatively common autoimmune diseases such as the neurodegenerative and currently incurable neuroinflammatory disease Multiple Sclerosis (MS), it is primarily thought that autoreactive T and B cells can cause proinflammatory cytokine secretion, immune recruitment, and damage to surrounding neuronal tissue (1). In contrast, cancers many times downregulate the surveillance capacity of immune cells (i.e.: T lymphocytes and Natural Killer (NK) cells) to identify cancer cells as abnormal, promoting cancer cell survival and spread (2). Cancer cells can alter the immune microenvironment and cause reduced immune surveillance, such as upregulating exhaustion markers on T lymphocytes triggering early cell death, as a means of avoiding immune recognition and destruction of tumor cells (2). Therefore, autoimmune responses and cancer immunology reflect two extremes of a dysregulated immune system, i.e.: two sides of a double-edged sword. Many processes governing autoimmunity are

implicated in cancer immunology as well, and many molecules have been identified as contributing to both processes, most notably Endoplasmic Reticulum Aminopeptidase 1 (ERAP1).

Autoimmunity and genetic associations

The definition of autoimmune disease is the attack of healthy cells by an individual's own immune system (1). Autoimmune diseases affect 3-5% of the human population, with significant effects on human mortality and morbidity (1). Most, if not all autoimmune diseases often require lifelong treatment and cause significant costs on the healthcare system. Therefore, new, more sustainable treatments for autoimmune disease are of vital importance for study. The attack of autoimmunity on healthy tissues is diverse and therefore causes a wide variety of symptoms, from joint pain in rheumatoid arthritis to neurological deficits in multiple sclerosis.

To identify possible therapies and interventions to either minimize or fully prevent the tissue destruction caused by autoimmunity, it is essential to identify common factors found in individuals affected by such diseases. Known contributors to autoimmunity including sex, age, geographical location, and genetics to name a few (1). For example, multiple sclerosis is very rare in tropical climates, but more common in temperate climates (1, 3). MS affects women twice as much as men, whereas inflammatory bowel disease affects both men and women equally (1). These are just a few of the myriad associations identified in those affected by autoimmune diseases.

Various monozygotic twin studies and genome wide associated studies (GWAS) have revealed the correlation between genetics and autoimmunity. GWAS are a technique to identify markers in specific patient populations, identifying mutations associated with a specific disease in humans. There are two types of mutations: synonymous and nonsynonymous. Synonymous

mutations are evolutionarily neutral and do not change the amino acid sequence of a protein, where non-synonymous mutations do. Thus, most disease related variants associated with protein function are non-synonymous.

The most well documented genetic association with autoimmune disease is with the MHC-1 genes. Indeed, many studies have demonstrated specific MHC-1 polymorphisms being associated with increased susceptibility to specific autoimmune diseases (1, 3–5). The gene products of the MHC locus are the human leukocyte antigens (HLA) and the presence of specific HLA variants are recurrently altered in a multitude of autoimmune diseases. Specifically, HLA-II: DQ2 and DQ8, HLA-I: HLA-A and DQB1*0602 have been associated with type 1 diabetes and HLA-II: DR4; HLA-III: TNF have been associated with rheumatoid arthritis (1, 4), as some specific examples.

Although variants in the HLA genes are the most commonly associated gene associated with risk for autoimmune disease, a large number of other genes have been associated with susceptibility to autoimmune diseases as well. For example, variants of the cytokine genes IL-17 and IL-23 can be associated with spondylarthritis diseases (6, 7). In ankylosing spondylitis (AS), more than 10% of patients do not express the common HLA mutation HLA-B*27, although this marker is commonly used for diagnosis of the illness. In multiple sclerosis, over 100 genes have been associated with genetic MS risk (3, 8), and HLA mutations make up only a small percentage of these, supporting the notion that there is involvement of other genes beyond the HLA cluster in these same diseases. For example, the second most common gene mutation associated with risk for development of AS, and other autoimmune diseases, is in the Endoplasmic Reticulum Aminopeptidase 1 (ERAP1). ERAP1 has been linked to a wide range of autoimmune diseases and has been found in epistasis with HLA mutations as well, although the

reason as to why it does this is not fully understood. This dissertation will explore the impact of ERAP1 polymorphisms on human disease further.

ERAP1

The *ERAP1* gene is a highly polymorphic gene located on human chromosome 15 (9). It is composed of 47379 base pairs arranged in 20 exons, encoding a protein. ERAP1 is an aminopeptidase belonging to the M1 zinc metallopeptidase family, which is localized to the ER (38, 39). ERAP1 acts as a "molecular ruler" in the cell, processing antigenic peptides at their N-terminus prior to major histocompatibility complex 1, or MHC-1, loading and antigen presentation (38, 39). In review, during antigen processing for subsequent MHC I presentation, peptides are selected by transporter associated with antigen presentation 1 (TAP1) after proteasome processing and targeted to the endoplasmic reticulum (ER). TAP1 selects peptides which are 9-16 residues long specifically (10). ERAP1 then further modifies these peptides and trims them to 8-13 residues (11). These processed peptides can then bind to the peptide-binding domain on an HLA molecule and HLA associates with β2 microglobulin (β2m). This molecule is now called MHC-I, and ready to interact with CD8+ T-cells and NK cells at the cell surface. These pathways involving ERAP1 are represented in Figure 1.

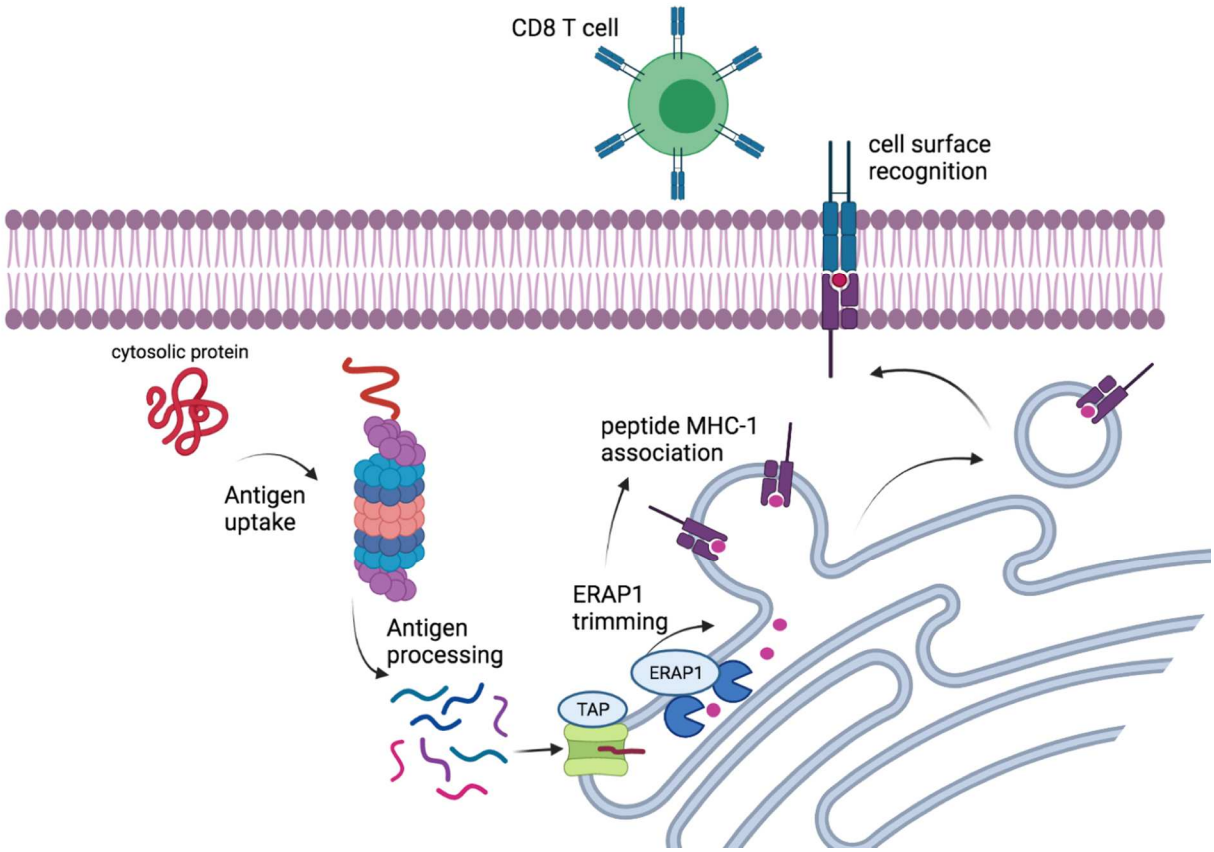

Figure 1: The mechanism of action of ERAP1 within antigen presenting cells.

As ERAP1 mediates antigenic peptide trimming, it regulates the immunopeptidome of a cell, thus driving the presentation of various peptides to the immune system which will ultimately determine immune response. Indeed, our group and others have shown that ERAP1 modulation alters the immunopeptide and T effector responses (12). In fact, a completely unique peptidome was present on the cell surface of ERAP1 modified splenocytes, which caused a shift in the peptide immunodominance and altered T cell memory responses (12). Furthermore, mice with ERAP1 variants developed unique T cell clones, due to this unique immunopeptidome, in response to vaccination (13). In mice with deficient ERAP1 or ERAP1 variants, MHC-1 surface expression was also reduced, due to inactive peptide trimming and therefore reduced loading (12,

13). This deficient ERAP1 activity led to cellular ER stress within immune cells and proinflammatory consequences (14).

ERAP1 deficient mice also have altered amounts of adaptive immune cell types. Notably, type 1 regulatory (Tr1) T cells were reduced in ERAP1$^{-/-}$ mice (15). Tr1s are a less well-studied cousin of the T regulatory (Treg) cell, carrying the same immunosuppressive function. Furthermore, we discovered that ERAP1$^{-/-}$ mice have altered B cell responses to recombinant MOG (1-125) during experimental autoimmune encephalitis (EAE) (16). This altered B cell response caused enhanced EAE phenotype in ERAP1-deficient mice. Tr1s and B cells have been implicated in a number of diseases, which have also been correlated with ERAP1 polymorphisms, supporting the translational power of our studies.

ERAP1 and innate immunity

In addition to ERAP1's role in antigen presentation, it is also a direct regulator of innate immune responses (17, 18). Our lab has extensively shown that ERAP1 modulation affects cytokine production in multiple cell types and animal disease models. Indeed, ERAP1 is a known cleavage enzyme for receptor shedding for various cytokines including TNF-R1 and IL-6, and is therefore a "receptor sheddase" (19). In addition to its role within the ER, ERAP1 can also be secreted. Goto *et al*. discovered that secreted ERAP1 causes the activation of macrophages, enhancing their phagocytic activity in response to lipopolysaccharide (LPS) and interferon (IFN)-y (20). This group further outlined TLR stimulation as causing ERAP1 secretion and thereby IFN-b and TNF-a induction, in a mechanism dependent on the calmodulin pathway (21).

Our lab used a unique ERAP1-deficient mouse model to explore the innate immune activity within these mice. We published that ERAP1$^{-/-}$ mice demonstrated enhanced innate immune activity, characterized by NK and NKT activation and proinflammatory cytokine

production such as IL-12 and MCP-1 (13). This increased IL-12 production correlated with more phagocytic activity of dendritic cells (DCs) and macrophages (17). Within human cells, ERAP1 variants can also cause innate immune activation. For example, our group demonstrated that human PBMCs treated with human ERAP1 variants had enhanced cytokine production and cell activation (18). Furthermore, PBMCs with ERAP1 overexpression show similar enhancement of innate immune responses, supporting the notion that ERAP1 modulation affects innate immunity.

Other than through cytokines, ERAP1 is also known to affect NK cells directly. For example, mice with deficient ERAP1 show increased amounts of terminally mature and licensed NK cells (13). Furthermore, stimulated splenocytes from ERAP1-deficient mice have enhanced NK cell activity, represented by elevated NK cell activation markers and proinflammatory cytokine secretion (13). Notably, IL-1β and IL-6 were both upregulated in ERAP1-/- splenocytes, supporting a proinflammatory phenotype. Furthermore, NK cells with either absent ERAP1 or an ERAP1 over-trimming variant, show enhanced activity and can even target and kill tumor cells significantly more than WT NK cells (13). This biology may in part be explained by ERAP1 controlling NK cell function, through perturbing the ability for cells to engage NK Inhibitory receptors (22).

We published that ERAP1-deficient bone marrow derived macrophages (BMDMs) were increasingly sensitive to inflammasome activation, and had increased secretion of IL-1β, IL-18, and other proinflammatory cytokine production in response to various inflammasome stimuli (14). This increased inflammasome activity was also seen *in vivo* in a mouse model of colitis (14). Altogether, this data proves that ERAP1 modulation is directly associated with innate

immune responses. The elevated innate immune activation we see may in part explain why ERAP1 variants are associated with so many immune-based diseases.

ERAP1 SNPs and associations with human diseases

More than a decade ago, genome wide associated studies (GWAS) revealed various polymorphisms within the *ERAP1* gene as being genetically linked with susceptibility to a multitude of diseases (23, 24). As previously mentioned, *ERAP1* is a highly polymorphic gene with common non-synonymous mutations. In humans, there is an *ERAP2* gene in addition to *ERAP1* (9), however, unlike *ERAP1*, *ERAP2* SNPs and their correlation to human disease is not a major topic of study. This is because although *ERAP2* is polymorphic as well, most mutations in *ERAP2* are synonymous, and therefore *ERAP2* SNPs have not been linked with many human diseases (9).

There are multiple published *ERAP1* SNPs associated with autoimmune disease, with the top most common being rs27044, rs17482078, rs10050860, rs30187, and rs2287987 (25–27). All of these variants within *ERAP1* exchange one amino acid for another in the coding region of the gene (27). ERAP1 activity can be both enhanced as well as reduced based on certain polymorphisms, resulting often in an "over-trimming" effect on peptides and therefore improper antigen presentation (28–30). This is in fact a common precursor to tumor immune evasion, a topic which will be discussed later in this dissertation. In general, the "over-trimming" of ERAP1 is more commonly associated with immune evasion by tumors while "loss-of-function" in ERAP1 enzymatic activity is associated more so with autoimmune disease development.

Many of these non-synonymous genetic polymorphisms in *ERAP1* are known to alter the aminopeptidase activity, and they are located at key enzymatic sites of the ERAP1 protein. Interestingly, all of the SNPs found in ERAP1 that are associated with certain diseases were

found at the interdomain junction or a peptide binding area of ERAP1, thereby all theoretically affecting the trimming ability of ERAP1. The location of these SNPs along within the ERAP1 protein can be appreciated in Figure 2. Although over 40,000 ERAP1 SNPs have been found, two (rs30187 and rs27044) are the most common in the human population (31). The SNP rs30187 involves the exchange of lysine for arginine at amino acid 528 (Table 1), and is the most common single variant in *ERAP1* that has been linked with multiple autoimmune diseases. In functional studies, this SNP was found to reduce the peptide trimming ability of ERAP1. The SNP rs27044 also showed altered peptide trimming specificity in functional studies. The combination of such SNPs is additive as well, where multiple SNPs in combination reduce ERAP1 trimming activity to a greater extent (23, 27, 32).

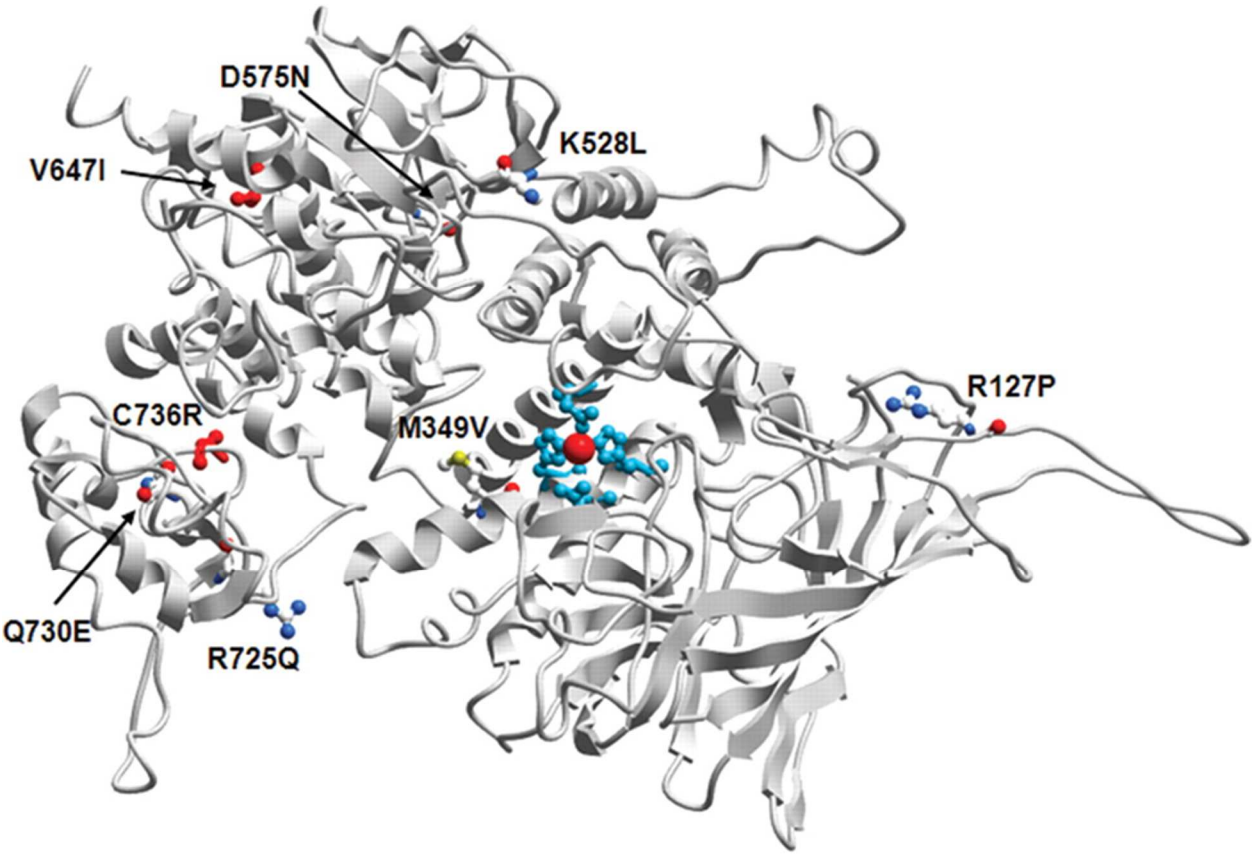

Figure 2: The ribbon protein structure of ERAP1 and location of SNPs. This figure represents a ribbon model of a proposed ERAP1 structure and the location of various non-synonymous SNPs. The red central atom represents the active site of the enzyme (33). This figure is from an Open access journal which allows for unrestricted non-commercial use, distribution, and reproduction in any medium. *Hum Mol Genet*, Volume 18, Issue 21, 1 November 2009, Pages 4204–4212, https://doi.org/10.1093/hmg/ddp371

ERAP1 SNPs are spread across the protein, and where they occur dictates downstream implications the SNP has on enzyme activity. For example, the rs2287987 variant causes a switch from methionine to valine at amino acid 349, which is located at the active site on ERAP1

and thus presumably affects direct enzyme activity (Table 1). Whereas ERAP1 SNPs rs27044 and rs17482078 are located at the internal surface of ERAP1, likely influencing substrate specificity. Furthermore, the SNPs rs30187, rs10050860, and rs26653 all occur at the junctional domain which can influence either enzyme activity or specificity. Table 1 illustrates the locations of these various ERAP1 SNPs, the diseases correlated with each specific polymorphism, and the variant's possible impact on enzyme activity.

SNP	**Amino acid change**	**Disease correlation**	**Enzyme location on ERAP1 and possible effect**
rs2287987 (34)	M349V	AS, Behçet's disease	Active site, influencing direct enzyme activity
rs27044 (35)	Q730E	AS, HPV-associated cervical carcinoma, Psoriasis	Internal Surface, influencing substrate specificity
rs17482078 (23)	R725Q	AS, Behçet's disease	Internal Surface, influencing substrate specificity
rs30187 (36)	K528R	AS, MS, Psoriasis, essential hypertension	Junction domain, influencing either enzyme activity or specificity
rs10050860 (37)	D575N	AS, Behçet's disease	Junction domain, influencing either enzyme activity or specificity
rs26653 (24)	R127P	AS, HPV-associated cervical carcinoma, psoriasis	Junction domain, influencing either enzyme activity or specificity

Table 1: Characteristics of ERAP1 SNPs. Adapted from Babaie et al. (31)

Our lab previously created and published a mouse model expressing the combination of 5 of these SNPs (rs27044, rs17482078, rs30187, rs10050860, rs2287987), which are the ones most altered in AS, a disease which will be discussed later in this introduction (13). We labeled this animal model "ERAP1 High", as the combination of these SNPs caused a high risk of AS development. Studies on these immune cells showed similarities between ERAP1 deficient cells, supporting that these variants are loss of function mutations in enzyme activity. Importantly, these ERAP1 deficient cells had loss of protein function and enzymatic activity, albeit a truncated ERAP1 protein was still present. These cells also showed significant alterations in innate immune activity as well as the immunopeptidome.

As one can appreciate, ERAP1 SNPs have been associated with a wide range of immune-based diseases. However, ERAP1 variants have also been genetically associated with other diseases as well, including hypertension and most recently, severe acute respiratory syndrome coronavirus 2 (SARS-CoV-2). Polymorphisms in ERAP1 were even discovered to be linked to more advanced SARS-CoV-2 infection, likely due to its regulatory role in the renin-angiotensin system (38). ERAP1 mediates the metabolism of angiotensin II, and loss of function variant in humans (rs30187) is associated with essential hypertension (39). This could in part explain worse SARS-CoV-2 outcomes, as the infectious disease also upregulates the renin-angiotensin-aldosterone system (RAAS) (40). Furthermore, there appears to be sex differences between biological male and biological female mice with ERAP1 deficiency in the way their RAAS responds to aldosterone (41). Similarly, ERAP1 may also play an important role is preeclampsia during pregnancy, as ERAP1 protein levels were increased on placental tissue in patients with preeclampsia, likely in part due to its role in angiotensin II metabolism (42, 43). Together, these associations implicate ERAP1 in having diverse roles in normal human physiology at a variety of

levels, and illustrate that ERAP1 has been linked to a wide variety of immune based human pathologies. This further highlights the central role ERAP1 plays in normal functions of the human immune system.

ERAP1-related autoimmune diseases

Ankylosing Spondylitis

Ankylosing Spondylitis (AS) is a debilitating spondylarthritis affecting mostly young adults (44). The disease is characterized by early onset inflammation at the sacroiliac joint, sacroiliitis, and can progress to bony fusions in the entirety of the spine, causing both lack of flexibility and pain. In addition to these symptoms, AS patients also have enhanced susceptibility to inflammation of the colon, or colitis (44). AS is therefore a multi-system inflammatory disorder. The disease is mainly treated first line with nonsteroidal anti-inflammatory medications (NSAIDs), followed by TNF-α inhibitors if needed. Other possible therapies include IL-17 inhibitors and disease modifying drugs such as methotrexate and sulfasalazine (45). Unfortunately, these treatments can help the symptoms of AS and pain, but there is no known cure for the disease.

The main genetic contributor to AS disease risk is presence of the HLA-B*27 variant, which is present in 88% of the AS patient population (7). Specifically, HLA-B*27 increases the risk of developing AS to 5-10% in individuals with the HLA-B*27 mutation (44). However, this mutation only accounts for about 20% of the heritability of AS, meaning that a small number of people carrying this HLA mutation will actually acquire AS. This suggests that other environmental or genetic components may be involved. The second strongest gene association to AS is ERAP1. ERAP1 mutation was linked with AS development in 2007, and to date 5 SNPs have been appreciated for their association (see Table 1), including rs30187. Indeed, ERAP1

mutation confers a 26% risk of developing AS, and in combination with HLA-B*27, the risk for AS developments increases even more as ERAP1 and HLA-I often have an epistatic relationship in this disease setting (46), whereby mutation in ERAP1 increases the likelihood of mutation in HLA-I. There are five associated ERAP1 SNPs with AS (rs27044, rs17482078, rs30187, rs10050860, rs2287987).

Our group published that ERAP1 deficient mice not only have exaggerated immune responses when vaccinated (18), but also show phenotypic signs very similar to patients with AS, including spontaneous onset of bony fusions and increased susceptibility to a dextran sodium sulfide (DSS) inducible colitis model (15). Both colons and sacroiliac joints were also found to have present inflammatory infiltrates in ERAP1 deficient mice (15). Interestingly, lower levels of Tr1 cells were also noted in ERAP1$^{-/-}$ mice, in comparison to WT mice (15). Another common symptom of AS patients is gut dysbiosis, and often patients with AS also have colitis. We discovered that mice with deficient ERAP1 also showed enhanced colitis scoring in comparison to WT mice (15). These mice also showed elevated immune infiltration in the colons, and elevated proinflammatory cytokine secretion (14, 15). Furthermore, humans with AS have enhanced ERAP1 methylation and reduced ERAP1 gene expression, further supporting ERAP1's role in AS pathophysiology and supporting the use of ERAP1$^{-/-}$ mice as a model for studying AS (47). Together, this data begins to identify the mechanisms that underlie the genetic association of ERAP1 with human AS.

Behçet's disease

Behçet's disease (BD) is a multi-system autoimmune disease characterized by recurrent genital and oral ulcers, uveitis, and other system involvement such as skeletal, cardiovascular, nervous and gastrointestinal systems (48, 49). Disease usually begins around the 3rd or 4th decade

of life, with sex and race playing an important role in disease prevalence (50). Patients with BD seem to have enhanced proinflammatory cytokine secretion, namely IL-17, IFN-g, and IL-23, and enhanced Th1 and Th17 responses, where affected organs have enhanced immune infiltration (48–50). Patients with Behçet's disease are treated primarily with corticosteroids, with colchicine as first line for mucocutaneous lesions (51). And, despite newer biologics options for the lesion treatment, the disease remains incurable (51).

Like other autoimmune diseases mentioned here, Behçet's disease also has a significant genetic component. The strongest genetic association contributing to BD is HLA-B*51, and is specific to non-Caucasian populations (25). However, the ERAP1 variant rs17482078 is also linked to BD, and is also known to be in epistasis with this HLA variant (52). Indeed, these two variants in conjunction altered the peptidome and reduced peptide binding affinity by HLA-B*27 in Behçet's disease models (52).

Multiple Sclerosis

Multiple Sclerosis (MS) is an autoimmune disease characterized by progressive CNS inflammation and deterioration of neurological functions, and is the most common neurological disease in young adults. More than 2.5 million people are living with MS worldwide today, and despite new therapies for MS, the disease remains incurable and severely debilitating for many people (5). The disease is highly heterogenous in its symptoms, course of disease, and prognosis. There are four main pathological features of MS: 1) inflammation leading to tissue damage; 2) demyelination; 3) axonal damage or loss; and 4) gliosis or the astrocyte reaction to CNS damage and scar formation (53).

The most common form of multiple sclerosis is relapsing-remitting MS (RRMS), which is characterized by periods of worsening neurological symptoms with periods of remission and

no apparent progression of disease (54). Primary progressive MS (PPMS), on the other hand, is consistent worsening of neurological symptoms and disease, without any periods of remissions or acute relapses. Secondary progressive MS (SPMS) begins as relapsing remitting, but then becomes steadily progressive like PPMS. The final form of MS is progressive relapsing MS (PRMS) which is steadily worsening disease and neurological function, with acute relapses as well.

Physicians diagnose and track disease severity with MRI, where white matter lesions are visualized. Active lesions or enhancing lesions are signs of disease and are a marker of activity. Various biomarkers can be used to assess for disease and subtype, although these are not commonly used in the clinic. The most common biomarker seen is IgM bands in the CSF, but other biomarkers include CSF C-X-C motif chemokine 13 (CXCL1), CSF chitinase-3-like protein 1(CHI3L1), and CSF neurofilament light chain (NfL) (54). Higher levels of IgM bands in the CSF were correlated with greater relapse rates and earlier progression to SPMS, and increased CHI3L1 levels in the CSF were correlated with more severe disability in RRMS patients (54). In addition, serum miR-223 and miR-15b can be used to distinguish PPMS from RRMS (54).

Risk factors known to increase susceptibility of developing MS include both non-genetic and genetic causes, with twin studies and GWAS showing 30% of patients to have a genetic cause (55). MS is a partially heritable disease, where the risk of disease development increases from 1:1000 to 1:4 in identical twins if one twin is affected (56). MS affects biological females more than biological males, and disease activity is significantly reduced during pregnancy, supporting the important role of male and female sex hormones in disease development (5). In addition to genetic susceptibilities, environmental factors also drive MS disease susceptibility.

Very recently, a group published a high impact article showing that Epstein Bar Virus (EBV), which has been theorized as implicated in MS pathogenesis, does indeed contribute to MS development (57). As compelling as this is, it still does not explain all cases of MS and arguably more important, does not explain why a majority of people who are infected with EBV do not go on to have MS.

Despite characterizing MS quite well and understanding risk factors, the disease remains incurable. Historically, patients were treated with systemic corticosteroids during acute relapses, however, the discovery of disease modifying therapies changed the landscape of MS treatment greatly in the early 1990's (58). The first disease modifying therapy to be approved was INF-β, which is still used successfully today in many patients. How and why IFN-β therapy exactly works is unknown, however it is presumed to reduce anti-inflammatory immune responses (58). Today, most patients with MS are treated with a form of immunomodulatory therapy. Given the great success of these therapies, the immune aspect to MS disease has been increasingly appreciated.

CD4+ Th cells are a well-studied immune subset which are known to drive MS (55). More specifically, Th1 and Th17 cells are found in white matter lesions in patients with MS, and are known to be required for EAE development (55). These cells are arguably very important in MS and EAE pathogenesis, however depletion of CD4+ specifically does not improve clinical MS disease (55). Also, CD8+ T cells are the dominant immune cell subset in MS lesions (55). This confusion has led to more study into the immunology of MS, and the role of innate immune system has been proven to be ever important (3, 5, 59). Interestingly, patients who were treated with anti-CD20 monoclonal antibodies showed reduced inflammatory active lesions and less relapses (60). This brought to light the obvious importance of B cells in MS (60). B cells remain

understudied in MS today, and they represent a possible immune cell population which could be manipulated to better MS therapy.

Genetics is known to play a strong role in MS onset, and although hundreds of genes have been linked to MS, the mechanisms driving them has not been fully studied. *ERAP1* is one of these associated genes (8, 26). The r30187 SNP in *ERAP1* has been linked as a pathologic driver in MS with an odds ratio of 1.26 (26). Mutations in HLA class II and HLA class I have also been implicated in MS disease, although some mutations are protective and some drive disease risk (55), leading to unclear conclusions. We showed that in a mouse model of MS, ERAP1-deficient mice have a much more severe EAE phenotype, as will be discussed in the following sections of this dissertation (16). We further linked this phenotype with B cells, showing that an adoptive transfer of ERAP1-deficient B cells specifically, greatly enhanced EAE (16). To note, it remains unclear how or if these variants contribute to biomarkers of the disease. Further research into how the *ERAP1* SNP impacts MS pathogenesis is therefore needed, and will hopefully improve outcomes for individuals living with MS.

Animal models of induced Autoimmunity

Throughout this dissertation, animal models are utilized to gain insights into the genetic basis of human autoimmune diseases, and support the translation of experimental results to human applications. Specific autoimmune diseases are either spontaneous, such as the onset of spinal fusions in ERAP1$^{-/-}$ mice, or induced, the latter using well established protocols. Here, several inducible models of autoimmunity and their applications are more closely examined and explained.

DSS

The DSS-induced colitis model is a mouse model commonly used to mimic human inflammatory bowel disease (IBD), a disease closely associated with other autoimmune diseases such as AS, as well as an individual disease pathology on its own. Dextran sulfate sodium, or DSS, is a water soluble drug with a molecular weight of 40-50kDa, and when dissolved in water and imbibed by mice, induces an inflammatory colitis (61). It is unknown exactly how DSS induces colitis, but it is thought to disrupt the epithelial lining of the large intestine, allowing for intestinal bacteria and other contents an entryway into the stroma of the intestinal tissue (61). DSS is particularly useful for studying the innate immune system's role in colitis, as DSS induced colitis itself can still occur even in the absence of B and T cells (61, 62).

Monitoring colitis after DSS administration in animals is based on the quantification of a variety of variables. Disease induction occurs within 3-7 days after DSS administration. Animals are visually inspected, and weighed daily, and their stool is examined for blood, and these factors influence the clinical score of the colitis. During DSS, mice experience significant weight loss, diarrhea and hematochezia, and need to be monitored very closely. Although other models exist for studying colitis in mice, DSS is the most widely used due to its ease, reproducibility, and reliability.

Given the association of IBD with AS, our group previously published that in the absence of normal ERAP1 functions , ERAP1$^{-/-}$ mice experienced a significantly worsened colitis subsequent to DSS treatment, (weight loss, diarrhea and hematochezia) relative to identical DSS treatments of WT mice (15). Upon histological examination, the colons of DSS treated ERAP1$^{-/-}$ mice had significantly more inflammatory infiltrates. Also, colon homogenates from ERAP1-

deficient mice were found to contain increased levels of several overall proinflammatory cytokines, including the inflammasome-derived cytokines IL-1β and IL18 (14).

EAE models of autoimmunity

There are two animal models most widely utilized to study MS pathogenesis, causation, and potentially treatment: the Theiler's Virus-Induced Demyelinating Disease (TMEV-IDD) model for MS, and the Experimental Autoimmune Encephalomyelitis (EAE) model for MS (63). TMEV-IDD is a useful model for studying viral etiologies that underlie induction of neuroinflammation, while the EAE model allows for intricate analysis of how innate and adaptive immune responses contribute to MS pathogenesis. EAE pathology itself is highly similar to CNS pathology in MS patients, because both show demyelinated lesions in white matter with immune infiltration. Also, IgG bands are found in the cerebral spinal fluid of both humans and mice.

Within EAE, there are several methods utilized to initiate EAE and neuroinflammation, but they all are initiated by the immunization of mice with a single antigen (myelin oligodendrocyte glycoprotein, or MOG) resembling the human myelin and thus initiate a disease in mice similar to EAE (63). Specifically, a protein or peptide for myelin is injected into the mouse, in addition to an immune adjuvant and pertussis toxin to make the blood brain barrier unstable (63). Although EAE can be stimulated with different types of protein and peptides, the MOG_{35-55} peptide and MOG_{1-125} protein will be focused on during this dissertation and are most commonly utilized in the field. The MOG_{1-125} is a full length MOG protein, while the MOG_{35-55} is the most immunogenic peptide within the full length protein. Most EAE research uses the peptide form of MOG, although the differences in their actions to induce EAE is important to highlight. Specifically, the MOG peptide initiates a CD4+ T cell dependent EAE model, while

the full length MOG protein is a B cell-dependent EAE model, likely due to the ability for B cells to be antigen presenting cells (64). Some studies have shown that other cell types, namely CD8+ T cells, also drive MOG peptide-based EAE, for example, after their adoptive transfer into naïve mice (64). However, EAE is generally accepted as a CD4+ T cell mediated neuroinflammatory disease of the CNS, in part due to the vast amount of research on MOG peptide (63). However, more recent studies have demonstrated that B cells can also drive induction of EAE as well (64) and have brought to light the important role for other immune cell subtypes in neuroinflammation. Outside of MOG, EAE can also be induced by adoptive transfer of encephalotiogenic MOG-specific T cells derived from MOG peptide immunized mice (63, 64).

Upon induction of EAE, mice are monitored closely and scored for disease development. A scale of 0-5 is assigned corresponding to disease severity, and are graded as follows. Grade 0 is healthy and no signs of paralysis or muscle weakness in mice. Grade 1 is tail weakness. Grade 2 is hind limb weakness. Grade 3 is hind limb paralysis, and Grade 4 is front limb paralysis. Grade 4 is a humane endpoint for all of our studies. Grade 5 is death by EAE. This grading scale comes with the possibility of bias, so it is of the upmost importance for studies to be blinded when assessing different genotypes or treatments. Also, the same individual should score the mice each day to ensure scoring is consistent and reproducible from day to day, and study to study. Upon scoring, less subjective methods for assessing the experiment include histopathology and flow cytometry, in addition to many others.

Despite its vast use in MS research, EAE does bring some challenges unique to the model. First, it represents a monophasic disease process without relapses and remissions, unlike the most common form of human MS (65). Also, the spinal cord is mainly affected in EAE,

whereas the brain is mainly affected in MS (53). EAE also is unable to study remyelination, an important parameter of human MS. In addition, EAE elicits a CD4+ T cell specific response, where most human MS lesions are dominated by CD8+ T cells (53). However, despite, these important distinctions, EAE has been invaluable for studying the incurable disease MS. This model has directly brought drugs to market for MS, such as glatiramer acetate, an immunomodulator who's exact mechanism remains understudied, although a very common clinical therapy for MS.

Mechanisms underlying Autoimmunity

Despite the many known risk factors for autoimmune disease, much research has focused on studying the cellular and molecular mechanism underlying the causation of autoimmunity. More specifically, what drives the immune response to recognize formerly "self" antigens as "foreign" and what mechanisms are causing a shift to the proinflammatory nature of autoimmunity. While there are many facets to autoimmunity, in this thesis we are focused upon those mechanisms linked to ERAP1 functions, including inflammasome activation, the unfolded protein response, and autophagy.

ER stress and the UPR

Within the ER, proteins are post-translationally processed and folded prior to their release to other organelles, and displayed on the cell's surface or secreted. However, in certain disease states such as cancers, infection, neurodegeneration and inflammation, the protein folding capacity of the ER can be either disturbed or overwhelmed, leading to an increase in unfolded proteins (66). This accumulation of unfolded proteins can then lead to ER stress (66). This stress stimulates an unfolded protein response (UPR), fundamental cellular stress response evolved to rapidly reduce unfolded protein levels in the cell, avoiding cell death and therefore returning the

cell back to homeostasis. The initiation of UPR responses can be induced via activation of at least three different signaling pathway initiated by the PERK, IRE1a, and ATF6 proteins (66).

At baseline cellular conditions, glucose regulated protein 78 (Grp78), a chemical chaperone which facilities protein folding, is bound to PERK, IRE1a and ATF6 (67). However, when abnormal, and/or large amounts of unfolded proteins are present, Grp78 binds to the unfolded proteins rather than the PERK, IRE1a and ATF6 proteins, allowing each to initiate their signaling cascades (67), which all result in UPR target gene translation. IRE1a activity processes XBP1 which upregulates UPR genes related to maintaining homeostasis such as ER-associated protein degradation (ERAD), protein folding, quality control, and organelle biogenesis (68). PERK signaling reduces protein synthesis by phosphorylating eukaryotic translation initiator factor 2a (eIF2a) (68). eIF2a also allows for ATF4 translation, which induces genes involved in antioxidant responses, autophagy, and apoptosis, as well as controlling GADD34 and CHOP (68). ATF6 is activated in cells undergoing ER stress and controls the induction of other UPR target genes, similar ones to sXBP1 and ATF4 (68).

In the setting of acute stress, either or all of these pathways trigger other cellular processes such as autophagy, lipid biogenesis, and degradation of the unfolded proteins through ERAD (66). However, in the setting of chronic stress, these pathways are often overwhelmed and the UPR begins to drive cell death instead of survival, activating the inflammatory cascade and proinflammatory cytokine release. Dysregulation of these pathways have been linked with multiple human diseases, including autoimmunity. For example, ER stress in beta cells was found to drive type 1 diabetes, likely due to it creating neo-antigens after abnormal folding and post translational modifications, activating autoreactive T cells (69). In addition, UPR signaling is known to induce a variety of proinflammatory cytokines including IL-1β, IL-6, IL-23 and

TNF-a (69). Induction of IRE-a can lead to an assortment of immune changes causing autoimmunity including: a decrease in MHC-1 antigen presentation, an increase in ERAD, neoantigen creation, and increased Th1 immune responses (66, 69). Interestingly, these occurrences are also found in the setting of ERAP1 inhibition. Similarly to ERAP1 polymorphisms, enhanced IRE1a signaling has been linked with multiple autoimmune diseases such as Type 1 Diabetes, rheumatoid arthritis, and inflammatory bowel disease (66).

The NLRP3 Inflammasome and pyroptosis

The inflammasome is an important innate immune regulator or immune responses to various triggers such as microbes, danger signals, etc. The inflammasome has sensors which are triggered in response to such signals. It is a complex composed of a sensor, an adaptor protein, and pro-caspase 1 (70). The recognition receptor is either of the nucleotide oligomerization domain (NOD)-like receptor (NLR) nucleotide-binding domain (NBD) and leucine-rich repeat (LRR)-containing family, or the absent in melanoma 2 (AIM2)-like receptor (ALR) family (70). The adaptor protein is the apoptosis-associated speck-like (ASC) protein with a caspase recruitment domain (70). Together these different sensors and ASC make up the diverse family of inflammasomes.

The best characterized inflammasomes include NOD-, LRR- and pyrin domain–containing 1 (NLRP1), NOD-, LRR- and pyrin domain–containing 1 (NLRP3), NOD-, LRR- and caspase recruitment domain–containing 4 (NLRC4), and AIM2 (70). AIM2 is a sensor of nucleic acids and is thus stimulated by pathogen double stranded DNA (70). NLRP1 and NLRC4 are stimulated by PAMPs (70). NLRP3 is unique because it is stimulated by a wide variety of signals including but not limited to reactive oxygen species, DAMPs monosodium urate crystals, nigericin and ATP (70).

Although there are multiple inflammasomes, much focus of the immunology field has been studying the NLRP3 inflammasome. Activation of the inflammasome, including NLRP3, involves two steps: priming and activation (71). Priming is done through low doses of TLR4 agonist LPS, and activation is done through small molecules specific for various inflammasomes, such as Nigericin for NLRP3. Upon activation, an ASC speck molecule is formed which triggers the release of caspase 1 from pro-caspase 1 (71). Once caspase 1 is released, it can cleave pro-IL-1β and pro-IL-18 to form IL-1β and IL-18, releasing these proinflammatory cytokines from the cell (71). It can also cleave gasdermin D (GSDMD) which then forms pores in the membrane, allowing proinflammatory cytokines to escape, and potassium ion efflux from the cell (71, 72). Indeed, potassium efflux from the cell is a necessary upstream event of NLRP3 activation as it allows for the maturation of IL-1β (73), although the mechanism by which this occurs is not fully understood. GSDMD pore formation leads to a specific form of cell death.

Pyroptosis is a form of inflammatory cell death, which is heavily linked with the NLRP3 inflammasome (72). Specifically, GSDMD is a critical mediator of pyroptosis, a mechanism that is also characterized by IL-1β and IL-18 release and downstream cell death (73). This mechanism is reliant on Caspase 1 for cleavage of GSDMD, similar to the NLRP3 inflammasome pathway. Distinct to GSDMD, caspase 8 can also induce the maturation and downstream release of IL-1β and IL-18 through a non-canonical NLRP3 pathway or completely independent of NLRP3 (74). The release of K^+ is downstream of the pyroptosis pathway as well, and a marker of cellular demise.

The UPR, inflammasome, and human disease

The inflammasome has been linked with many human diseases. Specifically, gain of function mutations in NLRP3 are known to cause cryopyrin-associated periodic syndrome

(CAPS), a disease characterized by autoimmunity (75). The NLRP3 inflammasome has been implicated in many other autoimmune diseases as well, although likely not in a causal manner. To this point, multiple NLRP3 inhibitors have been developed as autoimmune treatment. Some are monoclonal antibodies blocking IL-1β cytokines while others inhibit the inflammasome itself. MCC950 for example, is a specific NLRP3 inhibitor and is efficacious in treating multiple autoimmune diseases including CAPS, EAE, diabetes, and colitis (76, 77). This drug indeed was studied in Phase II clinical trials but due to toxicity, failed clinical study.

AS has also been linked with the inflammasome. Indeed, inflammasome activation was increased in both patients with AS and rodent models of AS with increased IL-1β cytokine secretion (78). This inflammasome activation was also linked with gut dysbiosis (76). The inflammasome was linked with other ERAP1 associated diseases as well. BD pathogenesis may be due to many immune changes such as Th1, Th17, or IL-10 dysregulation, but also, BD patients have variants of unknown significance in the inflammasome pathway, mainly in NOD2 and NLRP3 (79). BD-like diseases were also found to have activated inflammasomes by macrophages. Although it is unknown whether these variants directly contribute to the disease, it is intriguing that ERAP1 deficient macrophages have enhanced inflammasome, namely NLRP3, activation as well (14). In addition, macrophages from BD patients have also shown enhanced UPR activation (80). Perhaps this is why ERAP1 genetic variations are associated with Behçet's disease, through a mechanism dependent on the inflammasome.

MS has also been associated with the inflammasome, in addition to the UPR, signifying the close relationship between the UPR and the inflammasome. Studies have shown the UPR to be upregulated in both human MS and mouse EAE diseases models in various cell types (81). Specifically, UPR mediator ATF4 as well as ER stress genes BiP and CHOP are increased in MS

lesions in MS patients. Furthermore, these markers and others, such as the UPR regulator p-PERK, are upregulated in immune cells and neuronal cells during EAE. However, the impact of ER stress and UPR activation in B cells, specifically, has not been fully studied in the context of neuroinflammation.

Not only are UPR and ER stress upregulated in MS, but the inflammasome is as well. In the early 2000's, markers of inflammasome activation such as IL-1β and IL18 cytokine secretion and caspase 1 cleavage were identified in peripheral blood mononuclear cells (PBMCs) from patient samples with MS never treated with disease modifying drugs (82). Recently, NLRP3 activation was recognized as an important marker of primary progressive MS (83). Although the inflammasome has been in part addressed for inducing neuroinflammation, its role remains murky and its influence on specific cell types important for MS pathogenesis, such as B cells, as not been fully studied. Furthermore, specific gene involved in the inflammasome network and reactive oxygen species production from ER stress remain plausible options as stimuli, but more study into the exact mechanism remains to be explored.

Autophagy

Autophagy is a supporting mechanism for the cell to maintain homeostasis by processing unfolded proteins, defective organelles, or infectious agents. It is a mechanism both induced, as well as inhibited, by inflammatory cytokines and it is involved in both innate and adaptive immune responses (84). The process involves the formation of an autophagosome, which fuses with the lysosome. The contents within the autophagosome are then degraded by lysosomal enzymes. Essentially, this process involves cell contents and intracellular pathogens being recycled to make new proteins. SNPs within autophagy-related genes have been linked with multiple autoimmune diseases such as rheumatoid arthritis, IBD, and multiple sclerosis (84). In

MS specifically, autophagy related gene (Atg) 5 increases are linked with worsened EAE in mice (85), and autophagy gene knockout mouse models show much improved phenotypes.

Autophagy is closely linked with other cellular mechanisms discussed here. Indeed, it is a regulator of inflammasome complexes (70). Autophagy and the inflammasome are inversely related, whereby autophagic action reduces inflammasome components and cytokines. Likewise, the inflammasome can regulate autophagy. Specifically, Atg5 is lost during caspase 1 activation and IL-1β production in macrophages (70). Atg7 is also lost during caspase 1 activation and IL-1β production, but in response to different stimuli than Atg5 (70). Conversely, during starvation, IL-1β production and caspase 1 activation is reduced in various cell types. While multiple sources demonstrate that autophagy reduced IL-1β production (86), another source has actually found that autophagy induced IL-1β production (87). Therefore, autophagy clearly represents a multifaceted mechanism with multiple contributors and various outputs, with an obvious but muddy association with the inflammasome.

Studies have supported the link between autophagy and the UPR as well. Data shows that autophagy can alleviate the UPR, and that the UPR can trigger autophagy (67). Specifically, the IRE-1/XBP1 axis has been characterized as an inducer of autophagy (67). Upon activation of IRE-1 signaling and downstream activation of sXBP1, multiple UPR genes are induced. But, in addition to the UPR genes, autophagy is indirectly induced by sXBP1 upregulation of BCL-2 (88). sXBP1 can also induce expression of beclin-1, an important autophagy related gene (89). Thus, the impact of sXBP1signaling on autophagy mechanisms occurs in a pro-survival manner. On the other hand, other sources have found that sXBP1 deficiency in neurons, specifically, causes induction in autophagy (90). Furthermore, patients with ALS were found to have better neuronal survival when IRE1a/sXBP1 was deficient (90). This once again represents an unclear

association between autophagy and other cellular processes, whereby survival or cell death due to autophagy varies greatly.

Potential mechanisms underlying ERAP1 associations

Multiple theories exist as to why variants in the ERAP1 gene have been associated with susceptibility to human diseases. Namely, the influence of ERAP1 aminopeptidase function on the unfolded protein response has been a promising theory, and parallels prior theories similarly attempting to address the long-known association of HLA alleles with human diseases. Specifically, these theories suggest that upon improper folding of HLA alleles such as HLA-B*27 due to mutation, misfolded HLA molecules can aggregate in the cell, leading to ER stress and UPR responses (68, 81, 91). Likewise, improper action of ERAP1 could cause reduced MHC-1 molecule generation in the ER, leading to the same unfolded protein responses. As has been discussed earlier, ERAP1 and HLA can potentially epistatically interact to hypothetically exacerbate these effects.

Indeed, the UPR is found to be activated in human macrophages with AS (92). Also, ER stress and IL-23 production was upregulated in human M1 macrophages from AS patients (93). Although not from AS patients directly, we discovered that ERAP1-deficient macrophages also had enhanced ER stress and IRE1a phosphorylation. Together, this supports that HLA processing is an important player in AS pathophysiology, and may be through UPR pathway dysregulation by ER stress. However, how all of this translates into the triggering of an overall proinflammatory state in an individual inheriting high risk ERAP1 variants remains unknown.

A double-edged sword to autoimmunity: tumor immunology

In contrast to my previous discussions regarding heightened immunity leading to pro-inflammatory states and autoimmunity, the inability of the immune system to recognize and/or

respond to the presence of damaged or abnormal cells can also lead to human diseases, in particular, cancer. The cancer cell/tumor microenvironment (TME) is a complex and diverse landscape into which a host's immune cells migrate to, and if they can enter, interact with tumorigenic cells to hopefully promote tumor cell clearance and return to homeostasis. These interactions can either be direct or indirect and involve many different non-cancer cell types including T cells, natural killer cells, macrophages, neutrophils, B cells, and fibroblasts, to name a few. The impact of immune cell dysregulation in the tumor microenvironment has been ever more appreciated in the past decade, in part due to the success of immune checkpoint inhibitors for cancer treatment.

Checkpoint inhibitors harness the T cell exhaustion mechanism. Specifically, in settings of chronic inflammation or cancer, T cells can become terminally exhausted and upregulate inhibitory receptors which reduce their efficacy, as a means of reducing inflammation (94). Such inhibitory receptors and exhaustion markers include T-lymphocyte-associated protein 4 (CTLA4), Programmed cell death protein 1 (PD-1), T-cell immunoglobulin and mucin-domain containing-3 (TIM-3), and lymphocyte-activation protein 3 (LAG-3) (94). The first checkpoint inhibitor utilized in oncology was an anti-CTLA4 therapy. CTLA4 is a protein with inhibits T cell functions, and thus by inhibiting this protein's signaling, early cell death and immune suppression could be overcome. More recently, other checkpoint inhibitors have been developed, namely anti-PD1 therapy. PD-1 is involved in inhibitory immune signaling and is upregulated in chronic inflammatory states, and like CTLA4, is upregulated on T cells in tumor microenvironments as means of cancer immune evasion (94). Both CTLA-4 and PD-1 checkpoint inhibitors have proven efficacious in multiple cancer types clinically, including advanced stage melanoma and relapsed/refractory Hodgkin's lymphoma (94). These therapies

proved that tumor control, and disease eradication in some cases, can be achieved by targeting the immune system, and not the tumor directly (95). Although an incredible success for the cancer field, many patients still fail to respond or develop resistance to these immune checkpoint inhibitors. Therefore, the need for understanding the immunological and genetic changes in responder patients, as well as developing new immunotherapies with different immune targets, are still greatly needed.

Cancer and ERAP1

As ERAP1 seems to play important roles in in susceptibility to autoimmunity, it also would make sense that ERAP1 also play a role in the immune system's ability to mitigate tumor progression in some cancers. ERAP1 functioning has been implicated in multiple cancers, and specific SNPs have even been linked with HPV driven cancers, mainly cervical carcinoma (32). Indeed, it has been discovered that human cancer cells have altered ERAP1 and MHC-1 expression, thereby altering the immunopeptidome on tumor cells and promoting immune evasion (96). In cervical carcinoma, ERAP1 polymorphism can increase risk of tumor development and metastasis, especially when other genetic SNPs in *TAP2* and *LMP7 are* present. These proteins are also active in the peptide processing and antigen presentation pathways (32).

How can loss of normal ERAP1 functions in one instance cause a pro-inflammatory state, but then in another be associated with cancer cell evasion of the immune system? One possible mechanism may be that when variant of ERAP1 over-trims peptides prior to presentation on MHC-1, incorrect antigens are presented and therefore neoantigens, the antigens specific for tumors, are ineffectively displayed to the immune system. Thus, T cells do not recognize tumor specific antigens because they are not present, and MHC-1 surface molecules are downregulated

as well. Cifaldi *et al*. determined that when ERAP1 was silenced in tumor cells, the tumors were subsequently rejected by NK cells (97). This is likely because when MHC-1 downregulation occurs on cancer cells as means of immune evasion, NK cells sense this downregulation and kill cancer cells on the spot. Overexpression of ERAP1 causes enhanced ERAP1 trimming activity, and this has been linked with cancers from HPV infection (98). Furthermore, reducing this ERAP1 expression to normal levels led to better tumor killing. ERAP1 function has also been correlated with tumor infiltrating lymphocyte (TIL) CD8+ numbers as its role in peptide presentation affects CD8+ infiltration at tumor sites (99). This affects prognosis of HPV driven cancer, by an anti-HPV T-cell response.

Therefore, efforts have been made to block this ERAP1 over-trimming activity as a means of cancer therapy. By inhibiting the over-trimming capability of ERAP1, more neoantigens are able to be presented to T cells for tumor destruction. Studies have shown that ERAP1 inhibitors alter the immunopeptide of cancer cells, inducing a greater T cell response towards such cancer cell (100). Furthermore, the combination of an ERAP1 inhibitor with a T cell checkpoint inhibitor, anti-PD1, resulted in dramatically less tumor growth in a xenograft melanoma mouse model (101). Other groups have identified ERAP1 inhibitors through large drug screens and optimized molecules for better safety and efficacy. DG013A, for example, has been used by various groups including ours, and has shown efficacy in reducing ERAP1-driven proinflammatory signals. Thimerosal was even discovered as a potent ERAP1 inhibitor. Although these drugs have not transitioned into clinical practice, they present a promising avenue for both autoimmune disease and cancer therapy.

Conclusion

With this background, the mechanisms underlying why variants that cause loss of normal ERAP1 functions may lead to human disease will be explored. In Chapter 2, we investigate innate immune modulation in ERAP1 deficient BMDMs, and will unveil a possible cause of enhanced innate immune activation: ER stress and inflammasome activity. Then in Chapter 3, we will examine the role of ERAP1 in a specific autoimmune disease using the murine model of MS, EAE. We will show that B cells, specifically, are responsible for driving elevated EAE disease in ERAP1 deficient animals. In Chapter 4, we will explore the mechanisms at play in these B cells, and again find elevated ER stress and inflammasome activation, by utilizing genomic based profiling techniques. Chapter 5 we will expand upon these findings, and demonstrate that use of an ERAP1 inhibitor may be capitalized upon as a possible new cancer immunotherapy, in that ERAP1 modulation in NK cells can lead to enhanced tumor cell targeting and death. Chapter 6 will review the unique methods developed for collection of the data presented in Chapter 2-5, and Chapter 7 will summarize the overall findings as well consider next steps of investigation and application. Together, this work contributes to the published understanding on the role of ERAP1 modulation in innate and adaptive immunity, and the mechanisms as to why ERAP1 polymorphisms have been repeatedly associated with risk for human disease.

Throughout this dissertation, we address the problem of how ERAP1 dysfunction impacts immune responses and causes autoimmune phenotypes in human disease models. We hypothesize that ERAP1 dysfunction impacts important intracellular mechanisms which drive proinflammatory responses including the inflammasome and UPR. Our aims are to first, study why ERAP1 dysfunction causes proinflammatory responses. Next, examine whether or not we

see similar immune dysregulation by ERAP1 modification in neuroinflammation. Then, we will try to identify molecular mechanisms driving the immune dysregulation during neuroinflammation. Finally, we will study apply this knowledge towards cancer where ERAP1 dysfunction promotes more immune surveillance towards tumor cells.

Chapter 2: ERAP1 is a critical regulator of inflammasome-mediated proinflammatory and ER stress responses

Authors: Maja K. Blake, Patrick O'Connell, Yuliya Pepelyayeva, Sarah Godbehere, Yasser A. Aldhamen, Andrea Amalfitano

This chapter is an adapted version of a manuscript published in BMC Immunology 2022, 23, 9.

Introduction

Polymorphisms in endoplasmic reticulum aminopeptidase 1 (ERAP1) have been linked to several important autoimmune diseases such as Ankylosing Spondylitis (AS), Type I diabetes, Multiple Sclerosis, and Behçet's disease, suggesting that causation of these conditions may share a common mechanism due to dysfunctions in ERAP1 (102). ERAP1 not only plays a canonical role in the adaptive immune system via its role in the ER as an aminopeptidase processing peptides destined for MHC I presentation to $CD8^+$ T cells (29, 103, 104), but ERAP1 functions are also required to suppress a number of proinflammatory, innate immune responses (13, 15, 17, 18).

We previously demonstrated an important regulatory role for ERAP1 in innate immunity by showing that $ERAP1^{-/-}$ mice elicit exaggerated innate immune responses following exposure to several pathogen-derived components (17, 18). TLR-stimulated $ERAP1^{-/-}$ mice produced significantly higher levels of multiple Th-1 skewing proinflammatory cytokines and chemokines such as MCP-1, RANTES, IL-12p40, and IL-12p70, as compared to WT mice (17). These exaggerated innate immune responses positively correlated with enhanced activation of innate (natural killer (NK) cells and dendritic cells (DCs)) as well adaptive immune cells in $ERAP1^{-/-}$ mice (13, 17). Several other independent studies have also indicated a critical role for ERAP1 in innate immune cell regulation (97, 105, 106). We have also demonstrated that human ERAP1 variants caused enhanced IL-1β production from human immune cells (18) in a mechanism that involves K+ influx (107), which is a well-known signal of NLRP3 inflammasome activation. However, the underlying mechanisms responsible for these ERAP1-dependent immune responses remain unknown.

Synthesis of inflammatory cytokines and chemokines by the innate immune system is primarily initiated by activation of various germline-encoded pattern-recognition receptors (PRRs), such as Toll-like receptors (TLRs), RIG-I-like receptors (RLR), and NOD-like receptors (NLRs) (108). Activation of these PRRs drive the coordinated activation of intracellular signaling pathways that regulate the transcription of inflammatory cytokine and chemokine genes, as well as other innate immune defense responses (108). For example, activation of caspase-1 by NLRP3, and other caspase-1-activating inflammasomes, results in the processing and release of the proinflammatory cytokines IL-1β and IL-18 (109, 110). Upon binding to their receptors and following recruitment of the MYD88 adaptor, IL-1β and IL-18 induce the expression and production of several proinflammatory cytokines and chemokines (109, 110). Interestingly, AS patients are known to have increased proinflammatory cytokine levels, including IL-1β (111).

Notably, inflammatory bowel disease has also been directly and indirectly associated with ERAP1 linked diseases, for example gut inflammation was found in 25%- 49% of AS patients (111). We previously demonstrated that ERAP1$^{-/-}$ mice not only have exaggerated innate and adaptive immune responses to various stimuli, but also demonstrate severe intestinal inflammation upon DSS treatment, with a phenotype paralleling patients with AS (15); however, the mechanisms underlying responsible for ERAP1's role in modulating these inflammatory responses have also not been identified.

Here, we hypothesized that ERAP1 may have an intrinsic immune regulatory function in innate immune cells in addition to its normal role in antigen trimming in the ER. We investigated the impact that ERAP1 functions have on inflammasome and TLR receptor regulation *ex vivo* using a BMDM-based model for analyzing inflammasome and ER stress responses, and *in vivo*

by utilizing the DSS-induced intestinal inflammation model. Our results suggest that deletion of ERAP1 aminopeptidase activity not only impacts cellular display of MHC-I peptides, but is correlated with the activation of multiple innate immune pathways and predisposes cells to increased ER stress, all phenomenon that are also present in several ERAP1-linked autoimmune diseases (68, 112, 113).

Results

ERAP1 dysfunction enhances NLR-dependent inflammasome responses in macrophages

We wished to determine the mechanism linking ERAP1 to regulation of inflammasome pathways; including IL-1β processing and release, using a BMDM-based model. We previously demonstrated that ERAP1 is involved in caspase-1-dependent IL-1β production from human immune cells (18), however the molecular mechanism(s) and the signaling pathway(s) underlying these ERAP1-dependent responses are not understood. To examine if ERAP1 is involved in regulating inflammasome responses, BMDMs derived from WT and ERAP1$^{-/-}$ mice were LPS-primed and stimulated with multiple inflammasome agonists, and subsequent production of IL-1β, IL-18, and caspase-1 activation was evaluated. Consistent with previous reports (114), stimulating WT mice-derived BMDMs with AIM-2 inflammasome agonists (double stranded DNA (dsDNA) and poly(dA:dT)), significantly enhanced IL-1β production (Fig. 3A). Interestingly, we found that stimulation of AIM2 in ERAP1$^{-/-}$ BMDMs produced significantly ($p<0.001$) higher levels of IL-1β, as compared to WT BMDMs (Fig. 3A). To determine if ERAP1 regulates immune responses derived from activation of other inflammasomes, LPS-primed WT and ERAP1$^{-/-}$ BMDMs were stimulated with NLRP3 (nigericin and alum), NLRP1 (MDP), and NLRC4 (flagellin) agonists. We again detected significantly ($p<0.001$) higher levels of IL-1β production from ERAP1$^{-/-}$ derived macrophages following nigericin, MPD, flagellin, and alum stimulation, as compared to WT-derived macrophages that were similarly treated (Fig. 3B-C). These results suggest that loss of ERAP1 functions results in exaggerated AIM2, NLRP1, NLRP3, and NLRC4 inflammasome responses. Similar to the IL-1β results, ERAP1$^{-/-}$ macrophages produced higher levels of IL-18 following poly(dA:dT), nigericin, and alum stimulation (Fig. 3D-F). We then investigated if loss of ERAP1 also results in increased caspase-1 activation. Indeed, ERAP1$^{-/-}$ macrophages possessed

significantly increased levels of caspase-1 activation after MDP, flagellin and alum stimulations, as compared to identically treated WT macrophages (Fig. 3G). To verify whether increased inflammasome activation was due to mature IL-1β production and not general elevation of baseline pro-IL-1β in ERAP1$^{-/-}$, we evaluated basal levels of pro-IL-1β using flow cytometry. We determined that basal levels were not significantly different between WT and ERAP1$^{-/-}$ cells, supporting the notion that ERAP1$^{-/-}$ BMDMs have increased inflammasome activation responses to agonists and therefore greater cleavage of pro-IL-1β into its active, secreted form (Fig. 3H). Although not significant, pro-IL-1β was reduced to a greater extent in ERAP1$^{-/-}$ cells, further supporting our data of increased IL-1β processing and release in ERAP1-deficient macrophages (Fig. 3I). Together with enhanced inflammasome responses, ERAP1$^{-/-}$ BMDMs also had increased surface expression of macrophage activation markers CD80 and CD86 following various exposures to inflammasome agonists (Fig. S1).

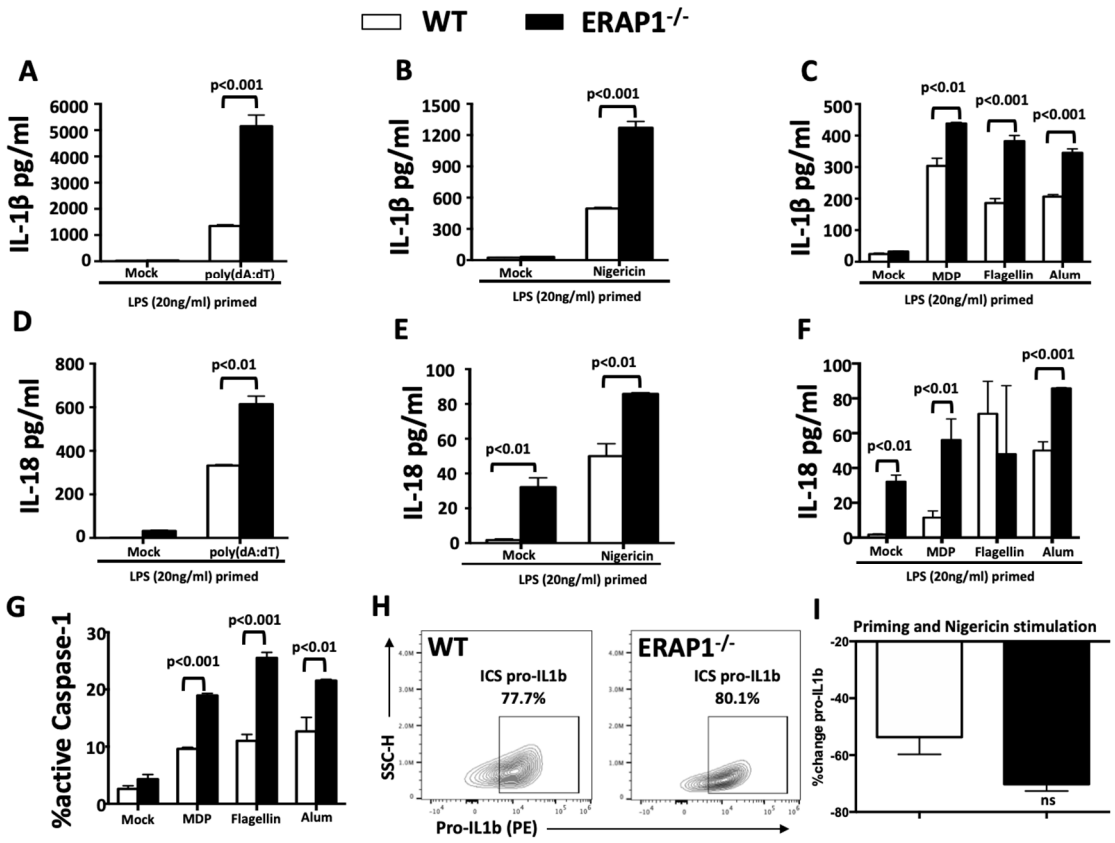

Figure 3: ERAP1 deficient macrophages have increased IL-1β, IL-18, and capsase-1 activation upon inflammasomes activation. Bone marrow-derived macrophages (5×10^5 cells) were plated into 24-well plates. Cells were primed with LPS (20ng/ml) for 16 hours, and then stimulated for another 24 hours with alum (1mg/ ml), nigericin (10ug/ml), MDP (10ug/ml), flagellin (250ng/ml), and poly(dA:dT) (8μM). Production of IL-1β (A-C) and IL-18 (D-F) in cell supernatant was performed. Caspase-1 activity (G) was evaluated using FLICA flow-based assay. Intracellular pro-IL1β was detected by flow cytometry using Cytek Aurora with various conditions. Baseline mock levels (H) as well as percent reduction of pro-IL-1β with priming and nigericin stimulation was compared in WT and ERAP1$^{-/-}$ (I). Cells were plated in quadruplicate. Data are expressed as means ± SEM. These figures are representative of four independent experiments.

Exaggerated cytokine and chemokine responses occur following inflammasome stimulation of ERAP1$^{-/-}$ macrophages

We next determined the impact that ERAP1 deficiency has on inflammasome-regulated cytokine and chemokine responses. Cytokines present in supernatants derived from inflammasome-activated WT and ERAP1$^{-/-}$ BMDM cultures were quantified using a 23-plex multiplex assay, as previously described (18). We observed significant increases in the production of IL-1α (Fig. 4A), G-CSF (Fig. 4B), IL-6 (Fig. 4C), MCP-1 (Fig. 4D), and TNFα (Fig. 4E) from ERAP1$^{-/-}$ macrophages, as compared to WT macrophages identically treated with MDP, flagellin, nigericin, alum, and poly(dA:dT). IL-10 levels were also significantly increased in MDP and flagellin (but not nigericin, alum, and poly(dA:dT)) stimulated ERAP1$^{-/-}$ BMDMs, as compared to WT BMDMs (Fig. 4F). It is important to note that ERAP1$^{-/-}$ macrophages were also more sensitive to LPS-priming as compared to WT macrophages, suggesting an inherently increased sensitivity of ERAP1$^{-/-}$ BMDMs to TLR4 stimulation (Fig 4A-3F). Following nigericin stimulation, a potent inducer of the NLRP3 inflammasome, multiplexed assays confirmed increased production of several cytokines including IL-1α, MCP-1, TNFα, MIP-1, IL-2, IL-13, and IL-9 from ERAP1$^{-/-}$ derived macrophages, as compared to WT-derived macrophages (Fig. S2). Together these data suggest that ERAP1 deficient macrophages are inherently more susceptible to innate immune stimulation and have exaggerated proinflammatory cytokine responses after exposure to inflammasome agonists.

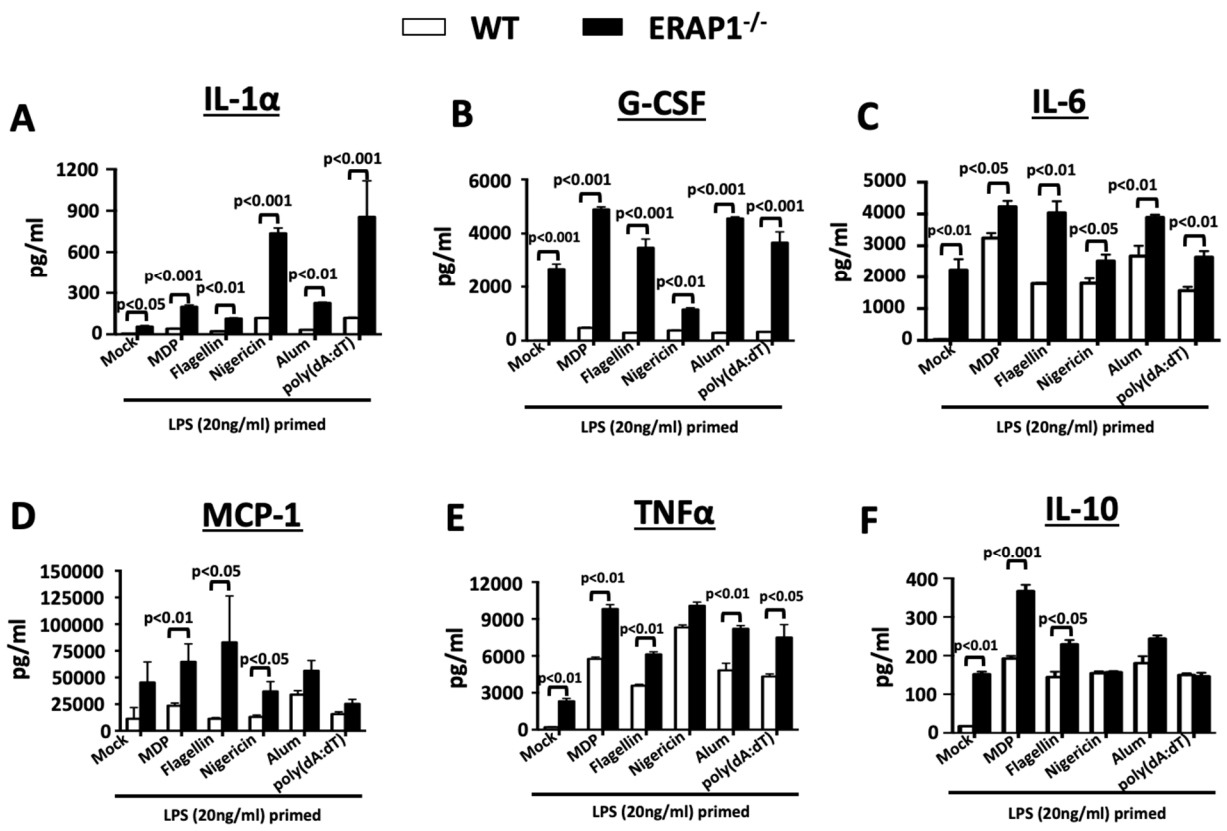

Figure 4: ERAP1 deficiency enhances cytokine and chemokine responses in macrophages following inflammasome stimulation. Bone marrow-derived macrophages (5×10^5 cells) were plated into 24-well plates. Cells were primed with LPS (20ng/ml) for 16 hours, and then stimulated for another 24 hours with various NLR inflammasome agonists, as indicated. Cell supernatants were collected, and a 23-plex multiplex assay was performed. Production of IL-1α, G-CSF, IL-6, MCP-1, TNFα, and IL-10 following NLRs stimulation is shown. Cells were plated in quadruplicate. Data are expressed as means ± SEM. These figures are representative of four independent experiments.

The effect of ERAP1 deficiency on TLR signaling pathways

As ERAP1 deficient cells are highly sensitive to LPS stimulation alone, we tested whether ERAP1$^{-/-}$ deficiency modulates TLR signaling, specifically via the NF-κb pathway (115). NF-κB is a known activator of proinflammatory cytokines such as IL-2, IL-6, IL-12, and TNFα and enhanced NF-κB activity could explain the increased proinflammatory cytokine secretion, albeit non-specifically. (116). To assess whether ERAP1$^{-/-}$ BMDMs have enhanced NF-κB activation, we evaluated p65 phosphorylation, the active subunit of NF-κB, by a phospho-flow-based assay (117). To our surprise, we found that LPS treated ERAP1$^{-/-}$ BMDMs had less phosphorylated p65 than identically treated WT BMDMs (Fig. 5A, Fig. 5B) at various timepoints. This data suggests that ERAP1 may be regulating proinflammatory responses through an NF-κB independent mechanism.

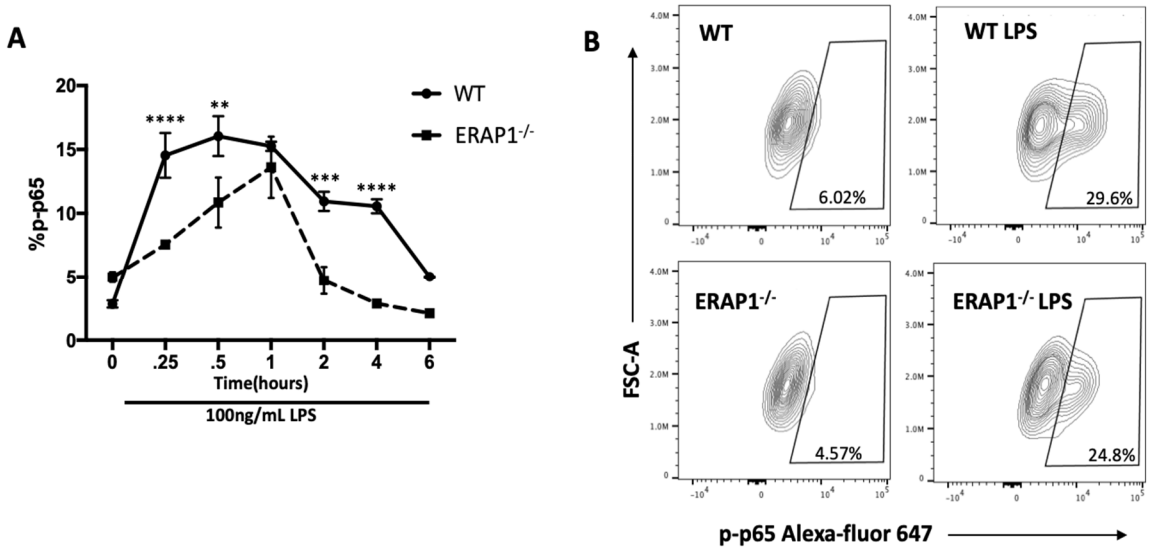

Figure 5: ERAP1 deficiency causes enhanced inflammatory responses through an NF-κB independent mechanism. Bone marrow derived macrophages (5 x 10^5 cells) were plated into 24 well plates, and activated with 100ng/mL LPS for various timepoints (15 minutes, 30 minutes, 1 hour, 2 hours, 4 hours, 6 hours). Cells were immediately fixed, permeabilized and stained for p-p65 using BD Phosphoflow Perm Buffer per manufacturer's guidelines. p-P65 activation was assessed with Cytek Aurora followed by analysis in FlowJo (A). Representative images of flow cytometry for mock and 1 hour LPS stimulation (B) Data are representatives of two independent experiments. Data are expressed as means ± SEM.

MHC-I dysregulation in ERAP1 deficient immune cells

Lack of ERAP1 functions can lead to deficient peptide loading onto awaiting MHC-I molecules, resulting in unfolded protein responses that may lead to ER stress (68, 91, 113, 118, 119). Prior studies utilizing ERAP1$^{-/-}$ mice transgenically expressing human ERAP1 variants, as

well as other studies, have supported that alterations in the enzymatic activity of ERAP1 diminishes the production of appropriately sized peptides for MHC-I loading, potentially resulting in the ER accumulation of empty MHC-I heavy chains (17, 18). Furthermore, HLA-B27 (the HLA allele most associated with AS, and found to be in epistasis in AS patients) misfolding has been linked to activation of the unfolded protein response (UPR) and production of proinflammatory cytokines via NF-κB, JNK1/2, p38 and/or Erk1/2 activation (68, 91). This may be due to multiple reasons such as lack of appropriate ERAP1 aminopeptidase activity reducing the pool of appropriately sized peptides available for MHC-I loading, leading to aggregation of incorrectly folded MHC-I molecules within the cell and reduced MHC-I expression on the cell surface(13, 30). Indeed, we show here that MHC-I surface expression was reduced on various ERAP1$^{-/-}$ immune cells, as compared to similarly assessed WT cells (Fig. 6). However, this reduction could be corrected with the provision of supranormal amounts of ovalbumin (ova) derived SINFEKL peptide, a procedure that bypasses the need for ERAP1 dependent processing, and thereby restores surface levels of MHC-I in ERAP1 deficient cells (119, 120).

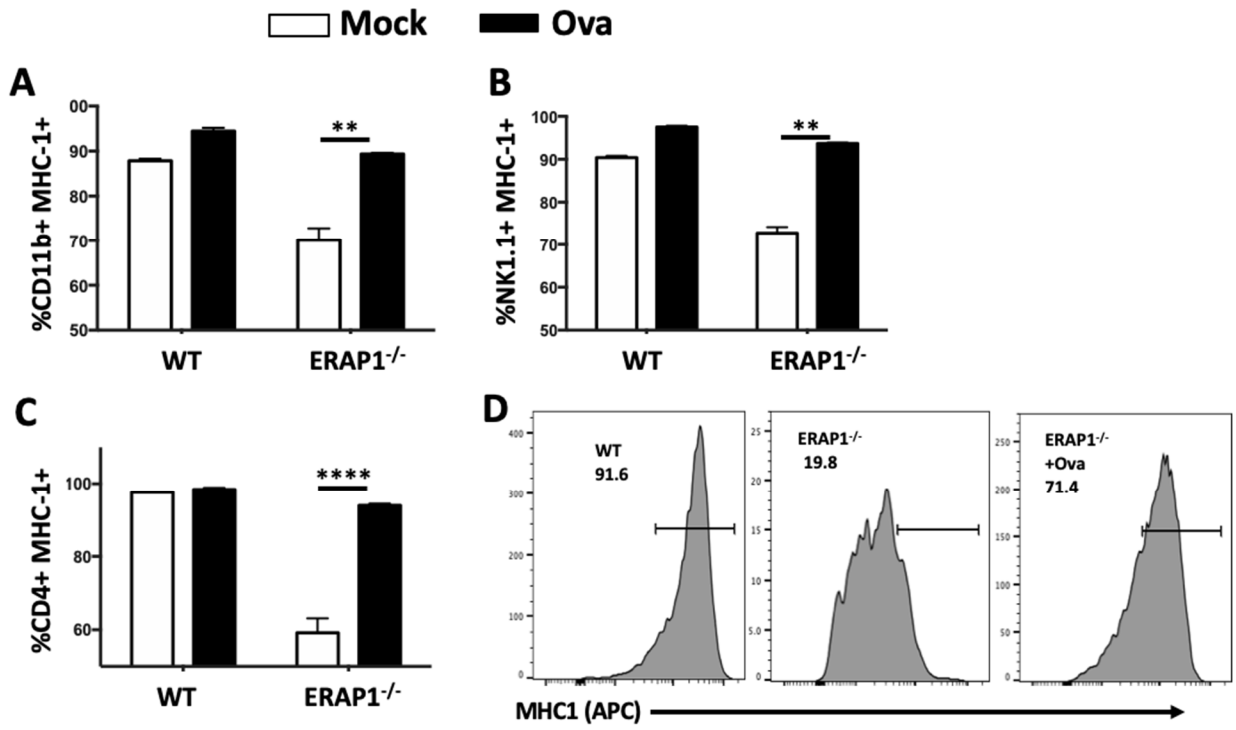

Figure 6: MHC-I surface expression is reduced on ERAP1$^{-/-}$ BMDMs. Total splenocytes were isolated from WT and ERAP1$^{-/-}$ and incubated with or without 25ug Synficol (Ova). Cells were incubated for 18 hours. Cell surface MHC-I (APC) expression was analyzed in CD4+, NK1.1+, and CD11b+ cells by flow cytometry (A-C). BMDMs were also cultured in the same manner and MHC-I surface expression was assessed (D). This figure is a representative of 3 independent experiment. Data are expressed as means ± SEM. * $p<0.05$, ** $p<0.01$, **** $p<0.00001$ significantly different from mock.

Increased expression of ER stress genes in ERAP1 deficient macrophages

It is also well known that a possible downstream effect of protein accumulation in the ER is ER stress-dependent NLRP3 inflammasome activation, as the NLRP3 inflammasome is indeed a sensor of ER stress (68, 112, 118). Given this, together with decreased surface MHC-I

expression in ERAP$^{-/-}$ cells, we hypothesized that increased innate signaling in ERAP deficient cells may be due to the presence of ER stress. More specifically, that the increased sensitivity of ERAP1$^{-/-}$ macrophages to inflammasome agonists might be associated with the presence of increased ER stress precipitated by lack of ERAP1-dependent peptide trimming functions. Using LPS-primed WT and ERAP1$^{-/-}$ BMDMs in the presence or absence of the ER stress inhibitor tauroursodeoxycholic acid (TUDCA), we quantified ER stress-associated gene expression by qRT-PCR. Interestingly, ERAP1$^{-/-}$ BMDMs had significant increases (30-fold) in ER stress chaperone BiP mRNA levels, as compared to BiP levels in WT BMDMs cultured under these same conditions (Fig. 7A). Also, we detected increased expression of the spliced variant of the X-box-binding protein 1(sXBP1) in ERAP1$^{-/-}$ BMDMs, as compared to WT BMDMs (Fig. 7A). Importantly, TUDCA significantly decreased these responses (Fig. 7A).

We further studied associations between ERAP1-dependent inflammatory responses and ER stress in additional immune cell types, particularly in subsets found to be altered in ERAP1$^{-/-}$ mice such as CD4^{+} T cells (15). We confirmed that significantly elevated levels of both BiP and sXBP1 were present in LPS-stimulated ERAP1$^{-/-}$ CD4^{+} T cells in comparison to similarly treated WT CD4^{+} T cells (Fig. 7B).

We next wished to study whether this induction in ER stress genes was linked with inflammasome activity. When ER stress was inhibited with TUDCA, this also reverted the enhanced IL-1β and IL-1α cytokine production in ERAP1$^{-/-}$ cells to WT levels (Fig. 7C), further supporting the importance of ER stress in ERAP1-modulated proinflammatory responses. These data suggest that ERAP1's role in inflammasome regulation is associated with increased ER stress.

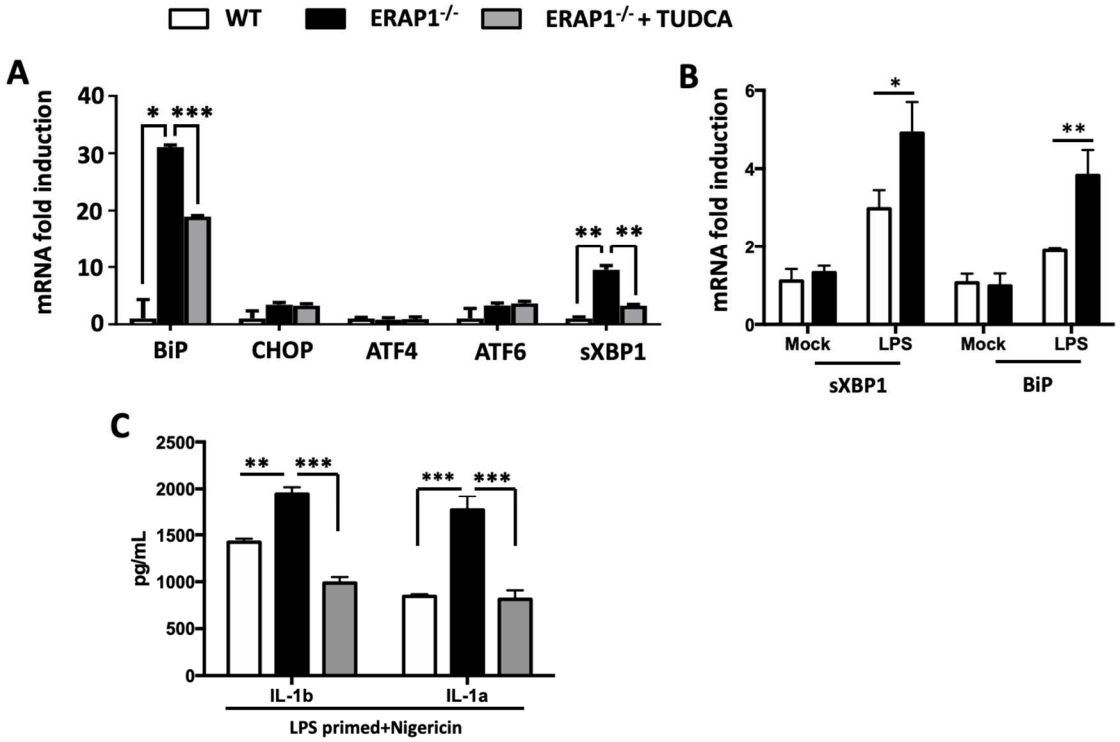

Figure 7: ERAP1 is a regulator of ER stress. Bone marrow-derived macrophages (2×10^6 cells) were plated into 6-well plates. Cells were either untreated or pretreated with 500ug/mL of TUDCA for 48 hours and were then stimulated with LPS (25ng/ml) for 18 hours. Cells were harvested for RNA isolation. mRNA levels of ATF6, ATF4, BiP, CHOP, sXBP1 and GAPDH were evaluated (A). $CD4^+$ T cells were isolated from total splenocytes, pooled, and plated at 3×10^6 cells per well into 6-well plates. Cells were stimulated with LPS (20ng/ml) for approximately 12 hours. Cells were harvested for RNA isolation. Cells were collected from 5 WT and 4 $ERAP1^{-/-}$ cells and kept separate during the experiment. mRNA levels of ER stress genes BiP and sXBP1 was assessed (B). BMDMs were primed with LPS overnight, incubated with TUDCA the next day, and then stimulated with nigericin for an additional 16 hrs. Supernatant was collected and 23-bead Bioplex was run for cytokine examination of IL-1β and IL-1α (C). Data are expressed as means ± SEM. These figures are representative of four independent experiments.

Increased proinflammatory cytokine and chemokine responses in colon tissues of ERAP1 deficient mice following DSS administration

Previously, we demonstrated that ERAP1$^{-/-}$ mice have enhanced susceptibility to DSS-induced colitis (15). DSS is not only a well-studied induction model for colitis, but DSS can also induce caspase-1 cleavage via activation of the NLRP3 inflammasome (62). As expected, colon homogenates from DSS-treated ERAP1$^{-/-}$ mice contain significantly higher levels of several proinflammatory cytokines and chemokines, as compared to identically treated WT mice (Fig. 8). Specifically, we observed dramatic increases in the production levels of several CC chemokines (MCP-1 ($p<0.001$), MIP-1α ($p<0.01$), RANTES ($p<0.001$), and MIP-1β) (Fig. 8A-D), Th-17- (IL-17α ($p<0.001$)) (Fig. 8E), Th-1- (IL-12p40 ($p<0.001$), IL-1β, and G-CSF) (Fig. 8F-H), and Th-2-skewing cytokines (IL-10 ($p<0.001$) and IL-6) (Fig. 8I-J) in colon homogenates of DSS treated ERAP1$^{-/-}$ mice, as compared to WT controls. We also noted increased trends towards increased production of other proinflammatory cytokines including IL-1α, IL-2, GM-CSF, and EOTAXIN in colon homogenates of DSS-treated ERAP1$^{-/-}$ mice as compared to DSS-treated WT controls; however, these trends did not reach statistical significance (data not shown). Together, these results suggest that ERAP1 deficiency also results in exaggerated colonic cytokine and chemokine responses during inflammasome (DSS)-induced intestinal inflammation.

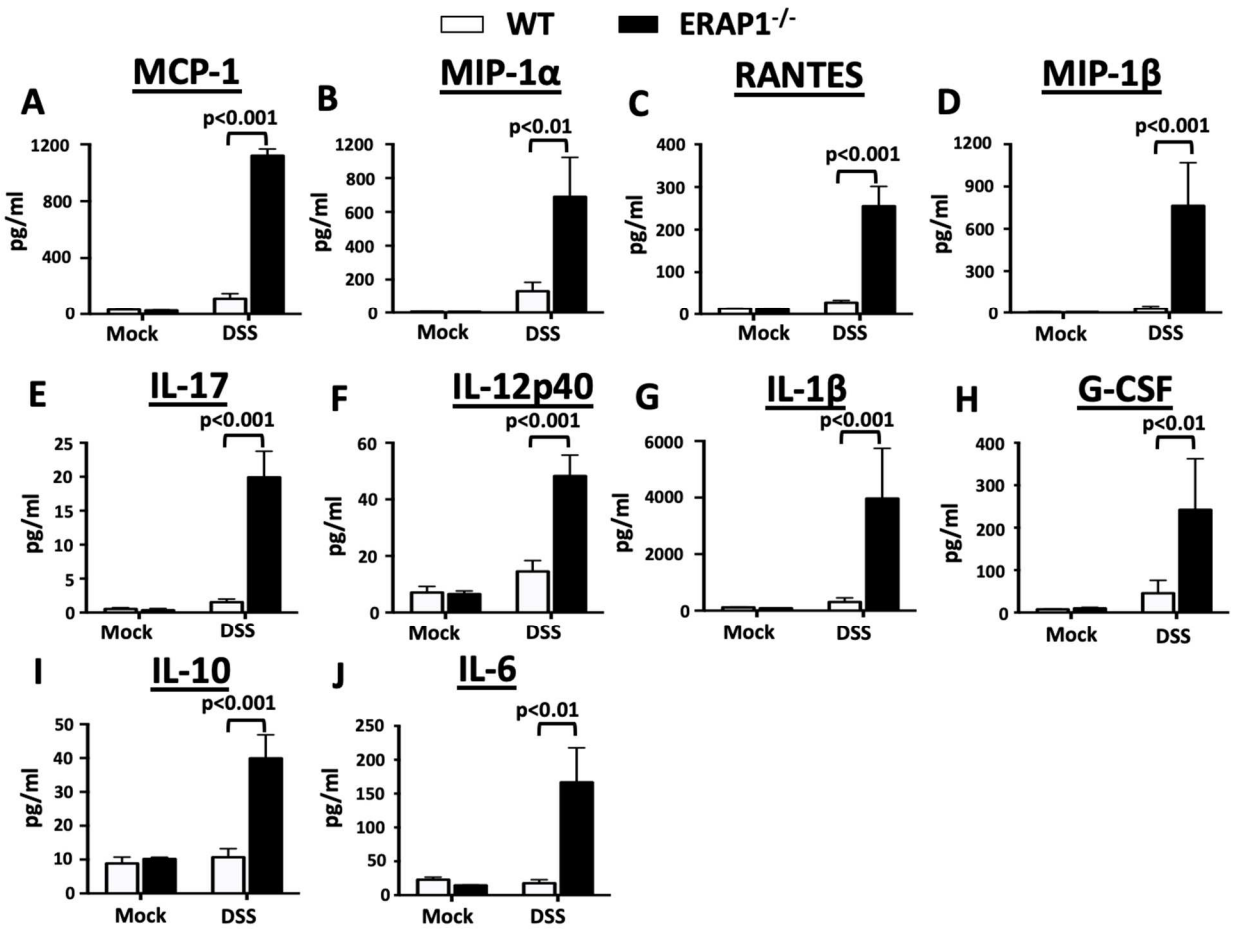

Figure 8: ERAP1 modulates colonic inflammatory cytokines and chemokines during DSS-induced colitis. Male WT and ERAP1$^{-/-}$ mice (n=7) were treated with a 3% DSS solution in drinking water for 7 days. Colon tissues were collected at day 7 following DSS treatment. Colon homogenates were prepared as described in Material and Methods. (A-J) A 23-plex multiplex analysis on colon lysate supernatants was used to evaluate the concentration of the indicated cytokines and chemokines. Data are expressed as means ± SEM.

Enhanced pro-inflammatory cytokines with Monosodium Urate Crystal

As ERAP1 polymorphisms have been linked with inflammatory arthritic disease

ankylosing spondylitis (48, 102, 121), we wished to study the role of ERAP1 in relation to the NLRP3 inflammasome specifically in arthritis-linked disorders. Monosodium urate (MSU) crystals are both potent NLRP3 inflammasome inducers as well as mediators of other inflammatory diseases such as gout (122). In addition to gout, MSU crystal deposits were discovered in the spines of patients with ankylosing spondylitis without gout, and these MSU crystals were correlated with more severe sacroiliac joint disease (123). Given that we previously published ERAP1 deficient mice have enhanced bony fusions in a phenotype similar to ankylosing spondylitis, and our results demonstrating that ERAP1-deficint BMDMs have elevated IL-1β production, we wished to study the impact of MSU crystals on ERAP$^{-/-}$ cells. We determined that ERAP1$^{-/-}$ BMDMs not only had increased production of IL-1β (Fig. 9A), but also increased IL-1α and IL-12 secretion (Fig. 9B, 9C), and conversely less IL-10 production (Fig. 9D) after exposure to MSU crystals. This data further supports ERAP1's important role in the inflammasome and innate immune regulation.

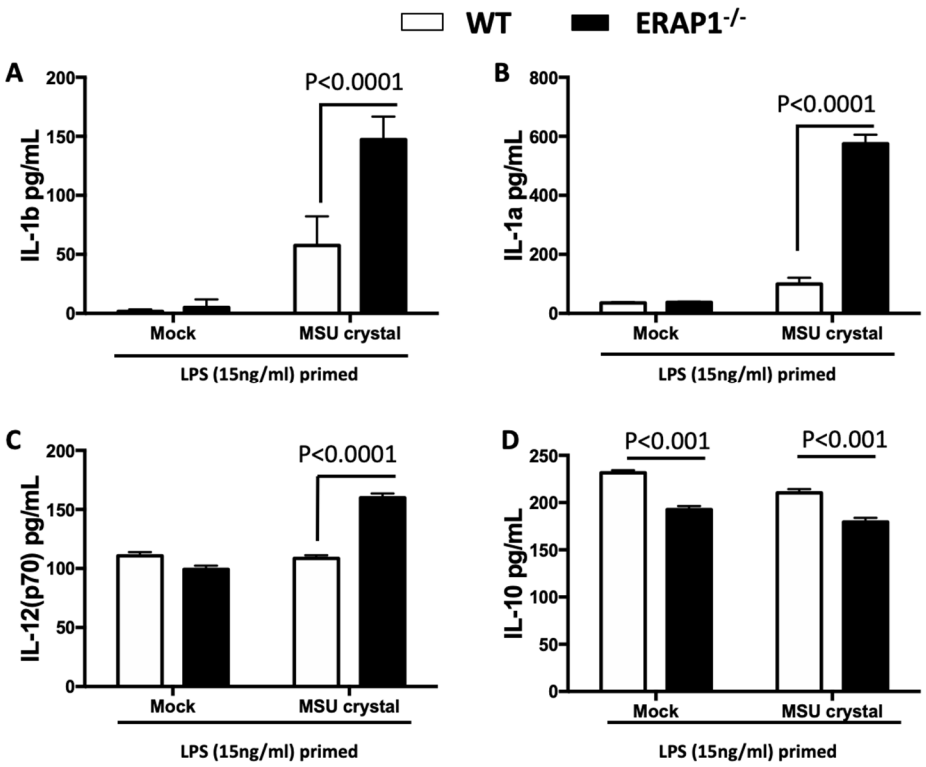

Figure 9: ERAP1 deficient macrophages are sensitive to NLRP3 activation by MSU crystals. Bone marrow-derived macrophages (2×10^6 cells) were plated into 6-well plates. Cells were primed overnight with 15ng/mL LPS, and then stimulated with or without 100ug/mL MSU crystals for approximately 18 hours. Cell supernatant was collected, and cytokine quantification was done by 23-plex Bioplex assay. Data is representative of two independent experiments and data are expressed as means ± SEM.

Discussion

Innate immune activation is a common denominator in the pathophysiology of autoimmune diseases, and is many times characterized by increases in immune mediators, such as cytokines like TNFα and IL6, and exaggerated inflammasome activity (17, 18, 102, 111). ERAP1 gene polymorphisms causing improper ERAP1 functions have been linked to several autoimmune diseases (102, 124–126); however, the exact molecular mechanisms underlying these associations are yet to be defined. Our previous studies illustrated that ERAP1 polymorphisms in human cells enhance innate signaling, and recognize this as a possible cause for enhanced susceptibility to ERAP1 linked autoimmune diseases (18). By utilizing *in vitro* and *in vivo* murine models, we can further study the role of ERAP1 in autoimmune diseases. Our results here confirm that loss of ERAP1 functions resulted in increased sensitivity to inflammasome stimulation, a phenomenon that results in exaggerated caspase-1 activation and production of proinflammatory cytokines and chemokines following AIM-2, NLRP1, NLRP3, and NLRC4 inflammasome activation.

The NF-κB pathway is one of the most well studied signaling pathways in immunology and is an important driver of innate immune responses. Activation of NF-κB can induce multiple cytokines, chemokines, and genes all involved in a proinflammatory response (87, 127). TLR4 activation by LPS can induce NF-κB activity through the adaptor molecule MYD88 (128, 129), and since we found enhanced cytokine production in ERAP1-deficient BMDMs with LPS priming alone, NF-κB activity was important for us to assess. In our studies we determined that NF-κB activation was actually statistically significantly reduced in ERAP1$^{-/-}$ BMDMs as compared to WT. This data suggests that although ERAP1$^{-/-}$ cells have enhanced proinflammatory cytokine and chemokine secretion, this may be occurring through an NF-κB

independent mechanism. As heightened induction of NF-κB in ERAP1$^{-/-}$ cells does not seem to be occurring, the potential importance of the inflammasome in these cells became paramount to determine.

One possibility as to why ERAP1 functions may be necessary to modulate the multiprotein inflammasome complexes may be that ERAP1 regulates inflammasome responses by directly interacting with the inflammasome complex in the ER, or other compartment of the cell. Intriguingly, resting NLRs, such as NLRP3, are also known to localize to ER structures, providing a direct mechanism as to how these pathways are modulated by lack of appropriate ER peptidase functions caused by mutations in ER proteins such as ERAP1 (130).

ER stress responses activate proinflammatory pathways (130–132) and previous studies have linked ER stress as a cause for DSS-induced colitis *in vivo specifically,* and in the pathophysiology of IBD in general (131, 132), both of which also share a strong correlation with NLRP3 inflammasome activation (62). Our current results confirm that ERAP1 is important for maintaining proper homeostasis of the ER, as evidenced by the increased expression levels of important ER stress-associated genes in the absence of a functional ERAP1 protein. Not only were ER stress genes elevated in ERAP1$^{-/-}$ BMDMs, but also in ERAP1$^{-/-}$ CD4^{+} T cells as compared to WT cells. Interestingly, prevention of ER stress prevented exaggerated inflammasome activation in stimulated ERAP1$^{-/-}$ cells, linking loss of ERAP1 to both ER stress induction and activation of the NLRP3 inflammasome.

Together, our results suggest that ERAP1$^{-/-}$ BMDMs may be inherently predisposed to exaggerated inflammasome responses upon encounter with typical inflammasome agonists as a result of increased ER stress being constitutively present in these cells. As one reason amongst several, this may be due to lack of efficient processing of MHC-I destined peptides and

translocation, as evidenced by loss of surface MHC-I on ERAP1 deficient cells (13, 17, 29). Here we show that MHC-I surface expression is indeed reduced on multiple immune ERAP1$^{-/-}$ cell types, and that this reduction can be overcome when incubated with an ovalbumin derived peptide, which is not reliant on ERAP1 processing for loading onto MHC-I. These data suggest that enhanced ER stress may be present in multiple cell types when ERAP1 functions in the ER are inadequate.

Patients with autoimmune disease such as AS have a high likelihood to also suffer from inflammatory bowel diseases (IBD) such as UC. We demonstrated here that loss of ERAP1 also results in excessive proinflammatory cytokine and chemokine responses during DSS-induced colitis. For example, the NLR inflammasome-mediated production of IL-1β and IL-18 is known to increase in the inflamed mucosa of UC patients (133), and our data suggest that loss of ERAP1 results in excessive production of IL-1β and IL-18 from activated inflammasomes ex vivo. This was independent of baseline pro-IL-1β levels. Importantly, NLRP3 polymorphisms that impact IL-1β and IL-18 production have also been previously associated with an increased susceptibility to UC in humans (134). In addition, increased caspase-1 activation and IL-1β production by the constitutively active autoimmune disease-associated variants of NLRP3 were also linked to autoimmune diseases (135), indicating a crucial need for appropriate NLRP3 activation and IL-1β production. Together, our current data reveal that the presence of ERAP1 is important for maintaining balanced IL-1β levels during episodes of intestinal inflammation.

There is clear overlap between ERAP1-regulated cytokine and chemokine responses and the cytokine and chemokine profile that is commonly present in UC patients. For example, an increased production of IL-6 and its soluble receptor (sIL-6R) is commonly observed in UC patients with active inflammation (136). Notably, in our studies we found that ERAP1 plays an

important role in regulating IL-6 in the colons of DSS-treated ERAP1$^{-/-}$ mice. ERAP1 is also known to cause shedding of IL-6 (137), further linking ERAP1 and regulation of IL-6 in colitis. Importantly, this data overall shows ERAP1's critical role in innate immune signaling. Although IL-1β is increased in ERAP1$^{-/-}$ colons, we found an overwhelming proinflammatory cytokine profile, indicating that ERAP1 may regulate global inflammatory responses not solely specific to the inflammasome.

In the past few years, studies have found that patients with AS also have MSU crystal deposition in their sacroiliac joints(123). As MSU crystals are a known inducer of the NLRP3 inflammasome, we wished to further study their role in relation to ERAP1 *ex vivo*. As expected, ERAP1-deficient macrophages showed enhanced inflammasome activity in response to NLRP3 activation by MSU crystals. Other pro-inflammatory cytokines were elevated with the stimuli in ERAP1$^{-/-}$ BMDMs including IL-12, but also the anti-inflammatory cytokine IL-10 was reduced, further supporting a pro-inflammatory signature in ERAP1$^{-/-}$ BMDMs. Together with the DSS studies shown here, this data further underpins the importance of ERAP1 in inflammatory diseases and begins to investigate how enhanced inflammation in ERAP1-deficient animals may be occurring through exaggerated activation of the inflammasome.

In summary, we demonstrated that ERAP1 is a regulator of innate inflammatory cytokines and the inflammasome. We discovered here that the presence of increased ER stress responses in ERAP1 deficient cells may explain why lack of ERAP1 function results in excessive activation of several caspase-1-activating inflammasomes and exaggerated production of cytokines following innate immune system activation. Our data suggest that the strong genetic associations between ERAP1 polymorphisms and various autoimmune diseases may be linked to ERAP1's role in innate immune regulation, including regulating proinflammatory cytokine and

chemokine responses during inflammasome activation. Here we also suggest the important connection between ERAP1 and ER stress, uncovering new potential targets for the treatment, and/or prevention of ERAP1 linked autoimmune diseases. Future studies into the definitive mechanism for which signaling molecules or chaperones are triggering inflammasome activation in ERAP1$^{-/-}$ cells should be explored.

Chapter 3: Absence of ERAP1 in B cells increases susceptibility to CNS autoimmunity, alters B cell biology, and mechanistically explains genetic associations between ERAP1 and Multiple Sclerosis

Authors: Patrick O'Connell*, Maja K. Blake*, Sarah Godbehere, Yasser A. Aldhamen, Andrea Amalfitano

*Both authors contributed equally to this work

This work is published in Journal of Immunology, 2021, 207 (12) 2952-2965 and is being used here with permission.

Author contributions: P.O. conceived the project. P.O., M.K.B., A.A., and Y.A.A., designed experiments. P.O. and M.K.B. performed all experiments. S.G. managed all mouse work. P.O. and M.K.B. analyzed data. P.O. carried out human scRNA-seq dataset integration and analyses. P.O. and M.K.B. wrote the manuscript, with input and revisions from all authors. Y.A.A. and A.A. supervised the study.

Introduction

Nearly 2.5 million people are living with Multiple Sclerosis (MS) worldwide, and despite new therapeutic strategies, this chronic neuroinflammatory disease remains incurable and severely debilitating for many (5, 138). Known risk factors for MS include both genetic and non-genetic components, with the role of innate inflammation becoming ever more important (3, 5, 59). Various immune cells contribute to disease pathogenesis, with characteristic brain lesions containing: monocytes, $CD4^+$ T cells, $CD8^+$ T cells, and B cells, amongst others (139, 140). Therapies targeting the immune response in MS patients have been developed to modulate inflammatory immune responses and include interferon-beta (58) and specific immune cell targeting monoclonal antibodies (141). More recently, B cells have been targeted for depletion, revealing them as a critical driver of MS (60). Despite great clinical benefit, these therapies are not effective for disease prevention or reducing lesions, especially in more severe MS subtypes, as well can result in significant immune-suppressive side-effects, limitations that together highlight the need to better understand mechanisms underlying MS pathogenesis.

Early studies of monozygotic twins revealed that approximately 30% of all MS risk can be attributed to genetic susceptibility (142), with subsequent genome-wide association studies identifying over 500 genetic regions highly linked to MS (143, 144). For example, one specific single nucleotide polymorphism (SNP) located within an important immune regulatory gene, *ERAP1,* has been linked with MS (26, 143). Endoplasmic reticulum aminopeptidase 1 (ERAP1) is a ubiquitously expressed protein located in the ER which trims peptides prior to loading onto MHC-I molecules, which are then presented on the cell surface for antigen identification (145). Given these roles, it is not surprising that ERAP1 plays an important role in adaptive immunity; however, it is also a well-known mediator of the innate immune responses (17, 18). ERAP1 also

plays a pivotal role in TLR regulation, and may be involved with the NLRP3 inflammasome as well (14). Critically, it has been shown that mice lacking ERAP1 spontaneously develop an autoimmune disease phenotype similar to that of Ankylosing Spondylitis, an autoimmune disease in which ERAP1 has also been genetically linked (15).

In this study, we investigated the mechanistic underpinnings of the genetic association of ERAP1 with MS using the well-studied experimental autoimmune encephalomyelitis (EAE) mouse model of antigen induced CNS autoimmunity (53). Utilizing a variety of EAE models, we confirmed that ERAP1$^{-/-}$ mice had exaggerated EAE severity and that this was B cell-dependent using a variety of animal models. We subsequently found that B cells lacking ERAP1 exhibit impaired proliferation during EAE in vivo, express higher levels of multiple activation markers, and have a specific deficit in the B1 cell compartment across the CNS and spleen. Correlating with these findings, integrated analysis of human B cells from multiple scRNA-seq datasets revealed that B cells containing the MS-linked K528R ERAP1 SNP exhibit dysregulation of several pathways, including over-activation of eIF2 signaling. Finally, we also present the first single-cell protein-level reference map of the murine CNS resident IL-10^{+} immune compartment in the presence and absence of EAE, and uncover ERAP1-specific impacts on this arm of the CNS immune response. Together, our results link the genetic association between ERAP1 and MS to an intrinsic effect on B cells, uncovering a novel immuno-modulatory role for ERAP1 which may suggest why ERAP1 has also been linked to a number of other autoimmune diseases beyond MS.

Results

ERAP1$^{-/-}$ mice have a worsened phenotype and CNS immune landscape following EAE induction as compared to WT mice.

Although polymorphisms in the ERAP1 gene in humans have been linked to MS, no studies have been performed to date examining if mice lacking ERAP1 are differentially susceptible to MOG-induced EAE (a well-established model for inducing CNS autoimmunity in mice) (53). When WT and ERAP1$^{-/-}$ mice had EAE induced with mouse-derived rmMOG$_{1-125}$, we found that ERAP1$^{-/-}$ mice had significantly increased EAE mean clinical scores (Fig. 10A). We next profiled of the CNS immune compartment in these mice via high dimensional spectral cytometry, utilizing a panel capable of identifying all CNS immune cell subsets (Fig. 10B). We found our panel capable of identifying all known CNS resident immune cell subsets, comparable to a previously published reference map (146), with the CNS being dominated by microglia, and significant lymphoid and myeloid cell infiltrates, indicative of active neuroinflammation (Fig. 10B). Comparison of immune cell subset frequencies between WT and ERAP1$^{-/-}$ mice during EAE revealed decreased border-associated macrophages (BAMs), increased NK cells, and increased myeloid-derived cells (MdCs) in the ERAP1$^{-/-}$ CNS (Fig. 10C). We also found that ERAP1$^{-/-}$ mice had increased total numbers of: B cells, BAMs, CD4^{+} T cells, Ly6C^{+} monocytes, NK cells, NKT cells, and MdCs (Fig. 10D); positively correlating with exaggerated EAE clinical symptoms in ERAP1$^{-/-}$ mice. Interestingly, we observed strong increases in the expression of Tim3 on multiple CNS myeloid cell types, suggesting that ERAP1 may be able to module this emerging myeloid cell modulatory receptor (147–149). Together these results imply the association of ERAP1 with MS is conserved in mice, since mice lacking ERAP1 exhibit enhanced neuroinflammation after induction of EAE.

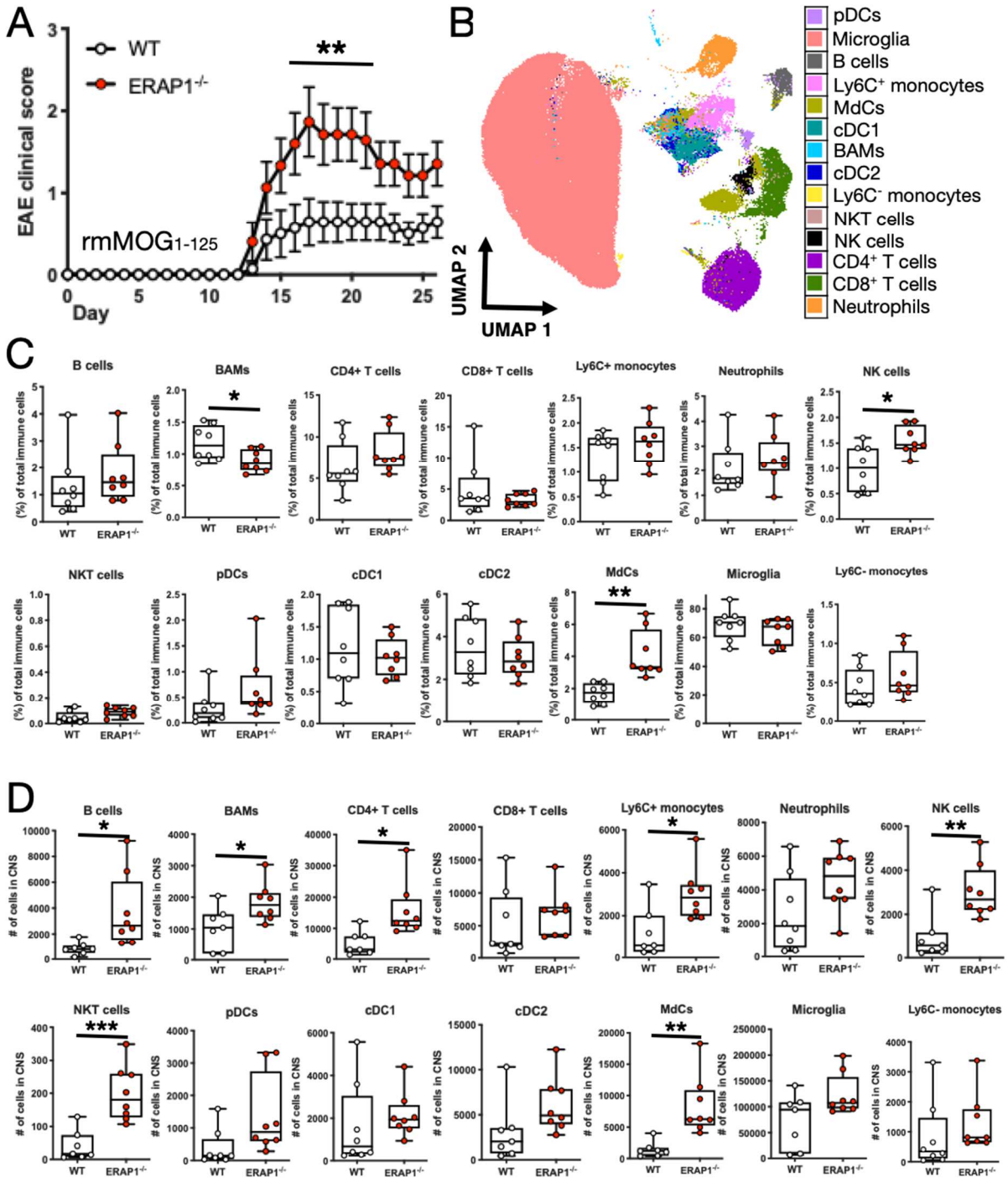

Figure 10: ERAP1$^{-/-}$ mice experience increased EAE mean clinical scores and exhibit alterations in the CNS immune landscape. (A) Clinical scores of WT and ERAP1$^{-/-}$ mice subjected to EAE induced with rmMOG$_{1\text{-}125}$. (B) UMAP projection of the entire CNS immune

Figure 10 (cont'd)

landscape in WT and ERAP1$^{-/-}$ mice subjected to EAE. The complete CNS immune landscape was assessed via high dimensional single-cell spectral cytometry. (C) Frequency of all CNS immune cell subsets from (B) between WT and ERAP1$^{-/-}$ mice. (D) Total number of various immune cell subsets in the CNS of WT and ERAP1$^{-/-}$ mice subjected to EAE. Groups in (A) compared with a two-way ANOVA with Tukey's multiple comparison test, displayed with mean ± SEM, and representative of two independent experiments showing similar results. Groups in (B, C) compared with unpaired two-way t-test and representative of two independent experiments showing similar results. *$p<0.05$, **$p<0.01$, ***$p<0.001$.

Exhaustive profiling of the resident CNS IL-10 immune compartment.

We previously published that mice lacking ERAP1 have decreased numbers of an important regulatory immune cell type (Tr1 cells), known to modulate immunity via production of IL-10 (15, 150, 151). Since IL-10 is also known to play an important role in MS/EAE pathogenesis (152–155), we examined IL-10 expressing cells in our EAE model. First, however, we combined our high dimensional single-cell spectral cytometry approach with IL-10^{GFP} mice , to generate a reference map of the CNS IL-10 immune compartment at steady state and during EAE. In addition to accurate detection of IL-10^{+} cells using GFP reporter mice, we also employed in vivo cell labeling to discriminate bona fide CNS resident from circulating immune cells (Fig. 11A, B). We first generated a reference map of all CNS immune cell subsets at steady state and during EAE, where cells are colored by FlowSOM-defined clusters (Fig. 11C). These cell subsets express markers as typically expected (Fig. 11D). The importance of IV labeling to discriminate CNS resident from circulating cells can be appreciated when examining the fraction

of each cell cluster staining IV^+ at steady state (Fig. 11E) and during EAE (Fig. 11F); non-resident cells were removed from downstream analysis. We found very few cells making IL-10 at steady state (Fig. 11G), but during active EAE one can appreciate a considerable portion of CD4+ T cells now making IL-10 (Fig. 11H). By restricting our analysis to just IL-10^+ cells, we find that at steady state in WT mice, microglia are the primary cell type responsible for IL-10 production (Fig. 11I). In contrast, during EAE, $CD4^+$ T cells dominate the CNS IL-10^+ compartment (Fig. 11J, K).

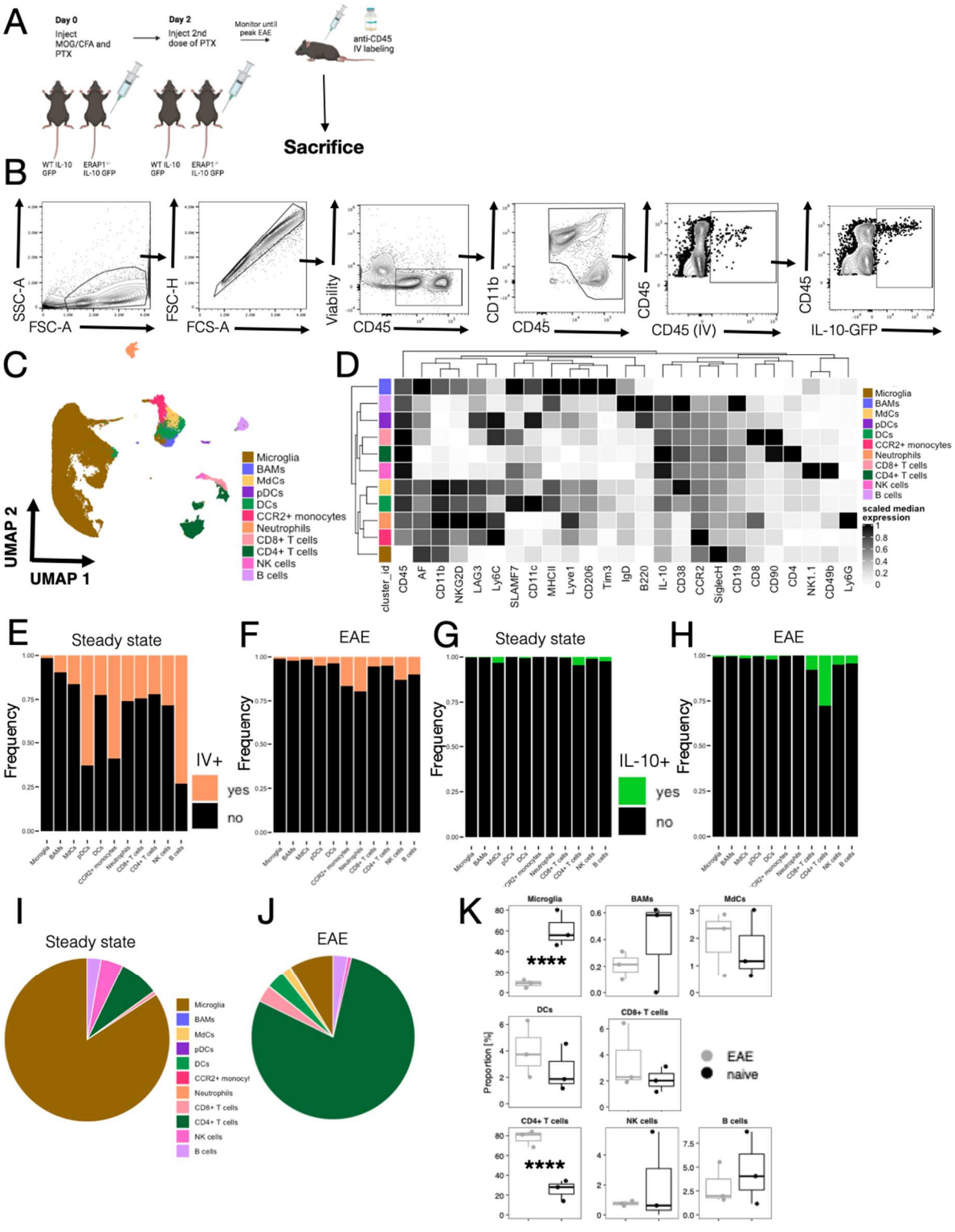

Figure 11: Single-cell profiling of the CNS resident IL-10^{+} immune compartment. (A) Graphical overview of experimental design. (B) CNS immune cell gating scheme. All

Figure 11 (cont'd)

combinations of IV^+/IV^- and $IL\text{-}10^+/IL\text{-}10^-$ were boolean gated and exported for high dimensional analysis. (C) UMAP projection of the entire CNS immune cell landscape from WT mice at steady state and with EAE, where cells are colored according to FlowSOM-defined clusters. (D) Heatmap of marker expression from all clusters in (C). (E, F) Frequency of non-resident (IV^+) immune cells across various subsets in WT mice at steady state (E) and during EAE (F). (G, H) Frequency of $IL\text{-}10^+$ cells across various immune subsets in WT mice at steady state (G) and during EAE (H). (I, J) Contributions of various $IL\text{-}10^+$ immune cells subsets to the entire CNS resident $IL\text{-}10^+$ immune compartment for WT mice at steady state (I) and during EAE (J). (K) Changes in contributions to the CNS resident $IL\text{-}10^+$ compartment between steady state and EAE in WT mice. Groups in (K) compared with a GLMM. Results in (B-K) representative of a single experiment. ****$p<0.0001$. AF: autofluorescence.

Comparison of CNS immune cell states and IL-10 production between WT and $ERAP1^{-/-}$ mice.

We next compared the CNS immune landscape of $WT/IL\text{-}10^{GFP}$ and $ERAP1^{-/-}/IL\text{-}10^{GFP}$ mice at steady state and during MOG-induced EAE. Global dimension reduction with MDS reveals samples clustering by disease status across the first MDS dimension and by genotype across the second MDS dimension (Fig. 12A). Comparing the composition of the CNS resident compartment at steady state, we find that while microglia make up about 80% of $IL\text{-}10^+$ cells in WT mice, in $ERAP1^{-/-}$ mice there are significantly less $IL\text{-}10^+$ microglia and more $CD4^+$ T cells (Fig. 12B). We also find there are significantly less total $IL\text{-}10^+$ cells in the $ERAP1^{-/-}$ CNS at steady state (Fig. 12C). Interestingly, during EAE, the CNS resident IL-10 compartment of WT

and ERAP1$^{-/-}$ mice is equivalent (Fig. 12D), as are total numbers of CNS IL-10^{+} cells (Fig. 12E). These findings may point to the potential for ERAP1 to be important in early processes controlling the development of CNS autoimmunity, and not during later stages when active resolution via IL-10-mediated immune suppression may be primarily occurring. We next compared all significantly differentially expressed markers across all CNS immune subsets between WT and ERAP1$^{-/-}$ mice at steady state (Fig. 12F) and during EAE (Fig. 12G). We found decreased expression of CD90 of multiple lymphoid cell types in ERAP1$^{-/-}$ mice at steady state (Fig. 12F) and decreased CD90 on multiple myeloid subsets in ERAP1$^{-/-}$ mice during EAE (Fig. 12G). Increases in Tim3 across myeloid cell subsets in ERAP1$^{-/-}$ mice are again observed, both at steady state (Fig. 12F) and during EAE (Fig. 12G). We also observe alterations in CD8^{+} T cell phenotypes, with ERAP1$^{-/-}$ CD8^{+} T cells expressing more SLAMF7, more CD38, more CD11c, and more IL-10 (Fig. 12F, G).

Due to the important role of various T cell subsets in MOG-induced EAE, we further narrowed our analysis to T cells and performed sub-clustering to investigate these cells on a more granular level. We identified nine T cell subsets (Fig. 12H) including two IL-10^{+} CD4^{+} T cell subsets (Fig. 12H, I). While none of these IL-10^{+} CD4^{+} T cell subsets displayed characteristic Tr1 cell markers (data not shown) (151), they were generally separable by their expression of CD90 (Fig. 12I). We found that during EAE, ERAP1$^{-/-}$ mice lack the CD90^{+}IL-10^{+}CD4^{+} T cell subset compared to WT mice and show significant changes in other T cell subsets (Fig. 12J). Altogether, these results identify important differences in the CNS immune compartment in mice lacking ERAP1, but do not reveal a defect in Tr1 cells per se. This implies that mechanisms underpinning the increased EAE mean clinical scores in ERAP1$^{-/-}$ mice, as well as AS, may not be primarily due to intrinsic defects in Tr1 cells.

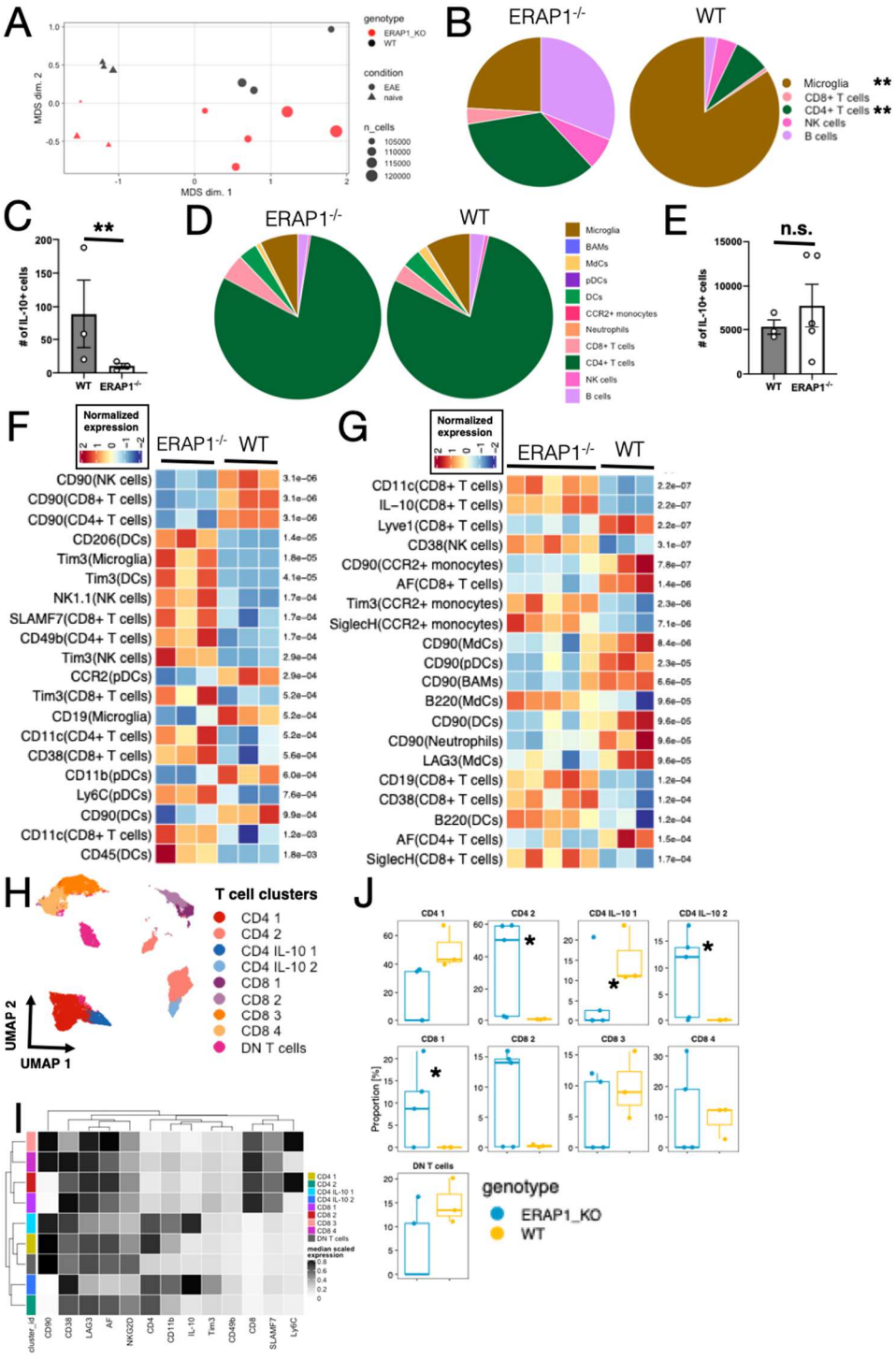

Figure 12: In depth comparison of resident CNS immune cell states and IL-10 production between WT and ERAP1$^{-/-}$ mice. (A) MDS plot of CNS immune cells from WT and ERAP1$^{-/-}$ mice at steady state and during EAE. (B) Comparison of the CNS resident IL-10^{+} immune cell

Figure 12 (cont'd)

compartment between WT and ERAP1$^{-/-}$ mice at steady state. (C) Number of total IL-10^{+} immune cells in the CNS of WT and ERAP1$^{-/-}$ mice at steady state. (D) Comparison of the CNS resident IL-10^{+} immune cell compartment between WT and ERAP1$^{-/-}$ mice during EAE. (E) Number of total IL-10^{+} immune cells in the CNS of WT and ERAP1$^{-/-}$ mice during EAE. (F, G) Heatmap of all statistically significant (FDR<0.05) differentially expressed markers between WT and ERAP1$^{-/-}$ mice at steady state (F) and during EAE (G). Adjusted p-values are listed next to each row. (H) UMAP of resident CNS T cell subsets colored by FlowSOM-defined clusters. (I) Marker expression on clusters from (H). (J) T cell subset frequency differences between WT and ERAP1$^{-/-}$ mice during EAE. Groups in (B, D, J) compared with a GLMM. Groups in (C, E) compared with an unpaired two-way t-test. Differentially expressed markers shown in (F, G) determined via a GLMM. Results in (A-K) representative of a single experiment. *p<0.05, **p<0.01, n.s. not significant.

ERAP1$^{-/-}$ susceptibility to EAE is B cell-dependent.

In an effort to better identify the specific, non-Tr1 cells that may be mediating EAE susceptibility in ERAP1$^{-/-}$ mice, we also induced EAE in WT and ERAP1$^{-/-}$ mice using the rhMOG$_{35-55}$ peptide, known to induce a primarily CD4^{+} T cell-dependent form of EAE (53, 156). Surprisingly, we observed identical EAE mean clinical scores between WT and ERAP1$^{-/-}$ mice using this antigen (Fig. 13A). This result, combined with prior studies demonstrating that EAE induced with rhMOG$_{1-125}$ protein (has 92% conserved identity to rmMOG$_{1-125}$) is known to be B cell-dependent (64, 156–158), and coupled with studies demonstrating that use of rmMOG$_{1-125}$ in B cell deficient mice can cause increased EAE symptoms relative to the identical treatment of

WT mice (159), led us to hypothesize that an intrinsic defect in ERAP1$^{-/-}$ B cells may be responsible for increased EAE mean clinical scores in ERAP1$^{-/-}$ mice. To confirm this, we adoptively transferred WT or ERAP1$^{-/-}$ B cells into mice genetically deficient in B cells (μMT mice) (160), confirmed equivalent transfer of cells, and then induced EAE with rmMOG$_{1-125}$. Indeed, μMT mice receiving ERAP1$^{-/-}$ B cells had higher EAE mean clinical scores compared to μMT mice receiving WT B cells, confirming this phenotype is at least partly due to an intrinsic defect in ERAP1$^{-/-}$ B cells (Fig. 13B).

During the late phase of EAE in these mice (day 38 post-EAE induction) we profiled the inguinal lymph nodes, spleen, and blood to assess B cell reconstitution and T cell phenotypes. Interestingly, we found that while WT B cells reconstituted the spleen and lymph nodes effectively (and to a lesser extent the peripheral blood), ERAP1$^{-/-}$ B cells were absent from all three locations (Fig. 13C-E). The observed decreases in B cells were likely not due to NK cell-mediated killing.

Assessing T cell phenotypes in the peripheral blood, mice reconstituted with ERAP1$^{-/-}$ B cells showed a skewing of CD4^{+} T cells away from GATA3^{+} Th2 cells towards Tbet^{+} proinflammatory Th1 cells (Fig. 13F, G), consistent with their more severe EAE phenotype (161, 162). Looking to other CD4^{+} T cell subsets important in EAE/MS pathogenesis (Th17 and Treg) we did not find any significant changes. Together, these findings not only point to an ERAP1-mediated dysfunction in B cells as responsible for the exaggerated EAE phenotype we originally observed in MOG protein treated ERAP1$^{-/-}$ mice, but identify a further defect in the ability of ERAP1$^{-/-}$ B cells to reconstitute secondary lymphoid organs, deficiencies that may bias immune responses during EAE and cause altered CD4^{+} T cell polarization.

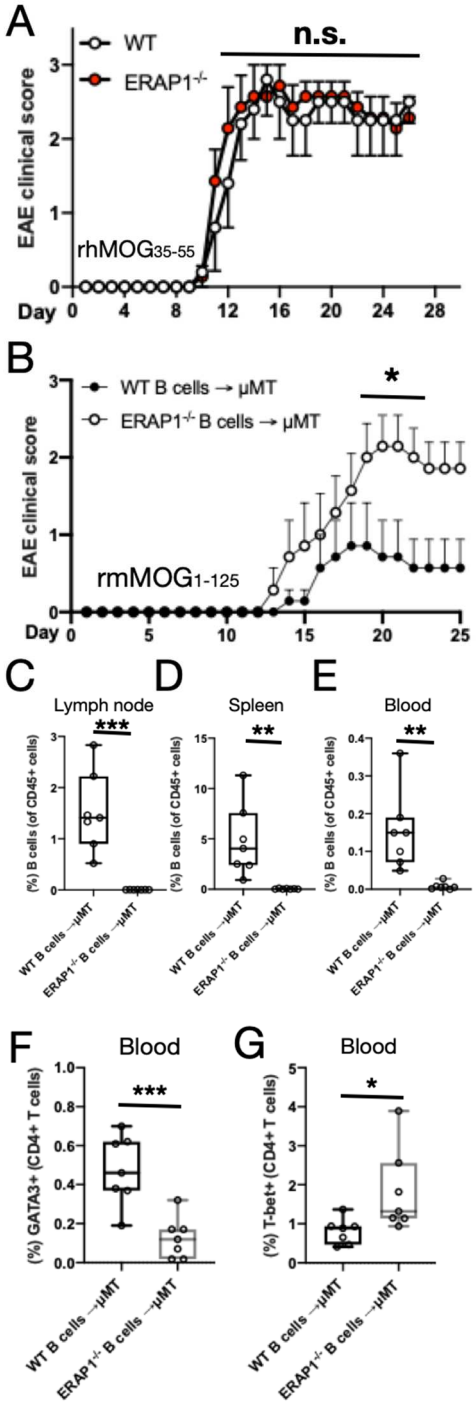

Figure 13: Loss of ERAP1 in B cells renders mice more susceptible to EAE. (A) Clinical scores of WT and ERAP1$^{-/-}$ mice subjected to EAE induced with rhMOG$_{35-55}$. (B) Clinical scores of µMT mice reconstituted with 1x10^{10} of WT or ERAP1$^{-/-}$ B cells five days before EAE induction with rmMOG$_{1-125}$. (C-E) Percent adoptively transferred B cells of total CD45^{+} cells

Figure 13 (cont'd)

from mice in (B) in the inguinal lymph nodes (C), spleen (D), and blood (E). (F) Percent $GATA3^+$ $CD4^+$ T cells (Th2 cells) in the blood of mice from (B). (G) Percent $Tbet^+$ $CD4^+$ T cells (Th1 cells) in the blood of mice from (B). Groups in (A, B) compared with a two-way ANOVA with Tukey's multiple comparison test, displayed with mean $\pm$ SEM, and representative of two independent experiments showing similar results. Groups in (C-G) compared with an unpaired two-way t-test and are representative of two independent experiments showing similar results. *$p<0.05$, **$p<0.01$, ***$p<0.001$, n.s. not significant.

Deep phenotyping of B cells during EAE reveal increased activation and specific decreases in B1 B cells in ERAP1$^{-/-}$ mice.

To better understand how ERAP1 modulates B cells, we designed an exhaustive B cell phenotyping panel to allow us to comprehensively profile all B cell subsets across the spleen and CNS. In the spleens of WT and ERAP1$^{-/-}$ mice at peak EAE, we identified 12 different B and plasma cell subsets via unbiased FlowSOM clustering (Fig. 14A), all expressing expected markers (Fig. 14B). Notably, using mice on an IL-10^{GFP} background allowed measurement of IL-10 across all B cell subsets, however, a distinct regulatory B cell (Breg) subset ($CD1d^+CD5^+$) we identified was clustered independently of IL-10 expression (Fig. 14A, B). We also used the same panel to profile the CNS B cell compartment of the same mice, revealing many of the same B cell subsets, except for the absence of follicular B cells, and the discovery of an undetermined subset (Fig. 14C, D). Comparison of the frequency of B cell subsets across the spleen and CNS in WT mice revealed compartment-specific differences in follicular, undetermined, B1b, and marginal zone subsets (Fig. 14E). Comparing the frequency of splenic B cell subsets between

WT and ERAP1$^{-/-}$ mice during peak EAE, we found significant decreases in both B1 cell subsets, and a minor decrease in plasma cells (Fig. 14F). Similarly, in the CNS during peak EAE we also found decreases in both B1 cell subsets in ERAP1$^{-/-}$ mice (Fig. 14G). Comparison of differentially expressed markers across all B cell subsets in the spleen uncovered higher expression of activation markers such as CD80, CD40, and GL7 on numerous ERAP1$^{-/-}$ B cell subsets (Fig. 14). This was also observed in the CNS, but to a lesser extent (Fig. 14I). Together, this demonstrates that a lack of ERAP1 expression in B cells results in excessive B cell activation and a specific decrease in the innate-like B1 cell subsets during peak EAE.

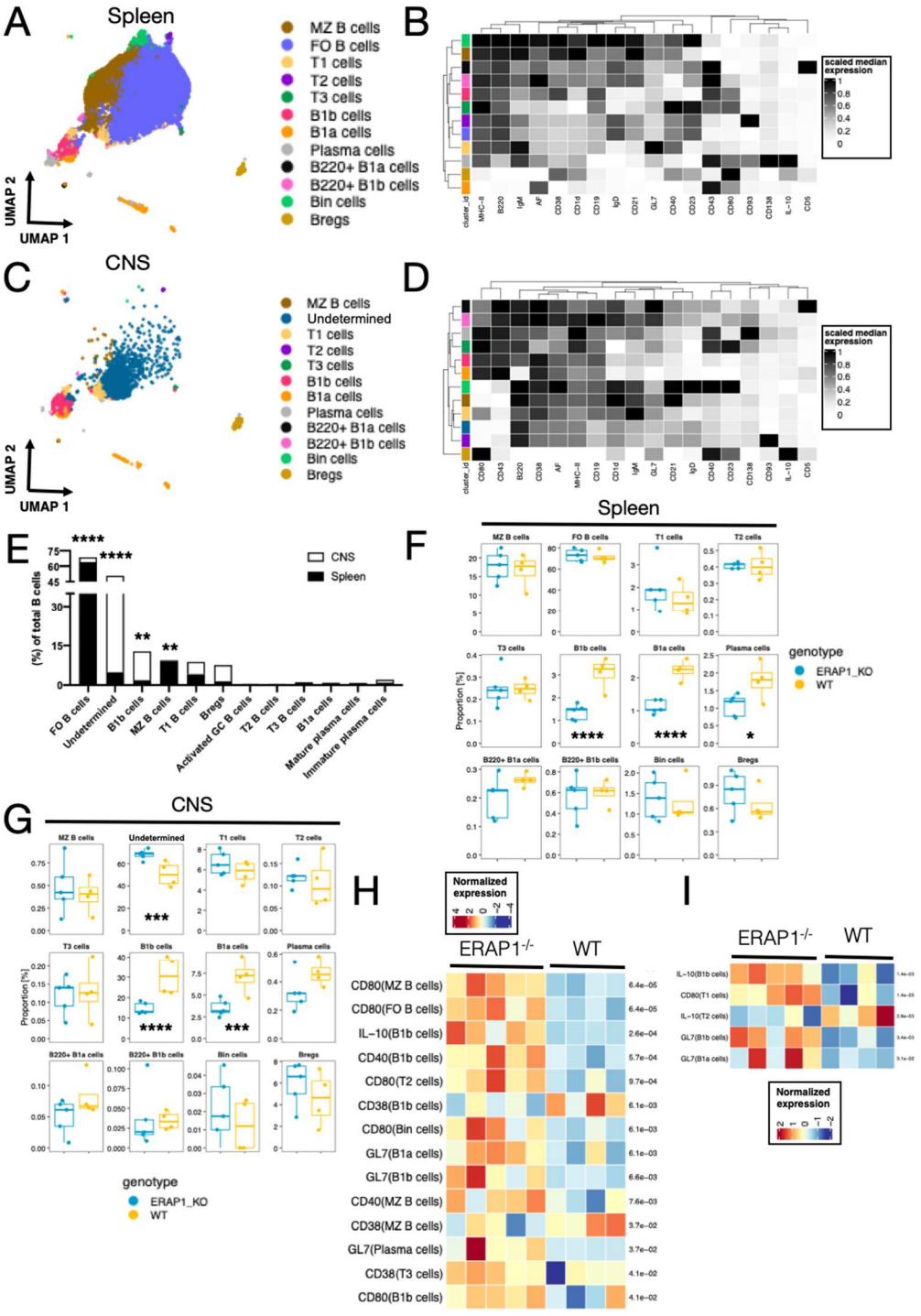

Figure 14: Reconstruction of the splenic and CNS B cell compartments during EAE reveal specific decreases in B1 cells and increased activation of ERAP1$^{-/-}$ B cells. (A) UMAP

Figure 14 (cont'd)

projection of all splenic B cells from WT mice during EAE with cells colored by FlowSOM-defined clusters. (B) B cell subset marker expression in cells from (A). (C) UMAP projection of all CNS B cells from WT mice during EAE with cells colored by FlowSOM-defined clusters. (D) B cell subset marker expression in cells from (C). (E) Comparison of B cell subset frequency across the spleen and CNS during EAE in WT mice. (F) Frequency of all immune cell subsets in the spleen of WT and ERAP1$^{-/-}$ mice during EAE. (G) Frequency of all immune cell subsets in the CNS of WT and ERAP1$^{-/-}$ mice during EAE. (H) Heatmap of all statistically significant (FDR<0.05) differentially expressed markers on splenic B cells during EAE between WT and ERAP1$^{-/-}$ mice. (I) Heatmap of all statistically significant (FDR<0.05) differentially expressed markers on CNS B cells during EAE between WT and ERAP1$^{-/-}$ mice. Groups in (E) compared with a two-way ANOVA with Sidak's multiple comparison test and representative of a single experiment. Groups in (F-G) compared with a GLMM and are representative of a single experiment. Differentially expressed markers shown in (H, I) determined via a GLMM. *p<0.05, ***p<0.001, ****p<0.0001, n.s. not significant. FO: follicular, MZ: marginal zone, Bin: B cells in inflamed nodes, Bregs: regulatory B cells.

Lack of ERAP1 in B cells leads to reduced proliferation *in vivo* and lack of B cell engraftment during EAE.

B cells are known to have different roles in the modulation of EAE during different stages of the disease (163, 164). Therefore, to help explain why μMT mice receiving ERAP1$^{-/-}$ B cells showed increased susceptibility to EAE, and to help identify why ERAP1$^{-/-}$ B cells could not be detected in these animals during the chronic phase of EAE, we developed a unique in vivo

assay (Fig. 14A). Here, we differentially labeled WT and ERAP1$^{-/-}$ B cells with CFSE and CellTrace Violet, mixed them in a 1:1 ratio, adoptively transferred them into μMT mice, induced EAE with rmMOG$_{1-125}$, and monitored B cell survival and proliferation at various timepoints during the EAE disease course (Fig. 15A). We found minor increases in the ratio of WT:ERAP1$^{-/-}$ B cells at day 2, with larger, more significant increases on day 5, 10, and especially day 20, reflecting a higher survival rate for WT B cells relative to ERAP1$^{-/-}$ B cells in mice experiencing EAE (Fig. 15B). By day 20, a consistent two-fold increase in the ratio of WT:ERAP1$^{-/-}$ B cells was evident across multiple environments, with very few ERAP1$^{-/-}$ B cells present overall (Fig. 15B). We found that the decreases in the numbers of ERAP1$^{-/-}$ B cells only occurred in mice with EAE, and did not occur when ERAP1$^{-/-}$ B cells were transferred into μMT mice that did not have EAE. Finally, since we labeled our cells with commonly used proliferation dyes, we were able to assess B cell proliferation in vivo. We found equivalent levels of WT and ERAP1$^{-/-}$ B cell proliferation across all locations up until day 10. By day 20, ERAP1$^{-/-}$ B cells exhibited a significant reduction in the ability to proliferate compared to WT B cells across all locations (Fig. 15C-E). These findings suggest that B cells lacking ERAP1 are not able to cope well in settings of prolonged immune activation, and that they may reach a threshold at which point they can no longer proliferate and survive.

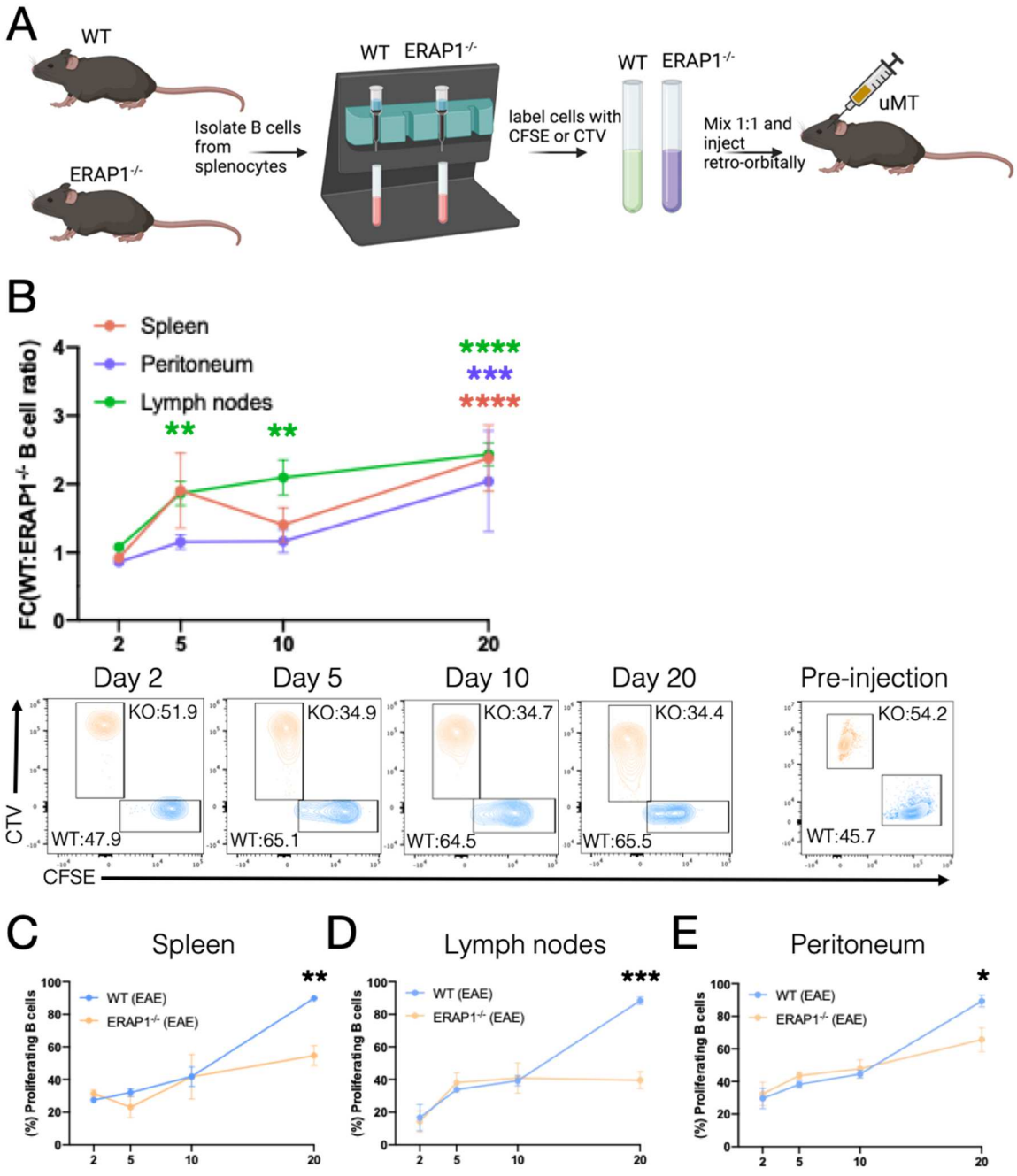

Figure 15: ERAP1$^{-/-}$ B cells display impaired proliferation in vivo during EAE. (A) Graphical overview of experimental design. (B) Top, Fold change in the ratio of WT to ERAP1$^{-/-}$ B cells transferred into the same μMT mouse and assessed across various lymphoid organs at multiple timepoints following induction of EAE with rmMOG$_{1-125}$. Bottom, representative FACS plots of differentially labeled WT and ERAP1$^{-/-}$ B cells at various timepoints during EAE. (C-E)

Figure 15 (cont'd)

Frequency of adoptively transferred B cells actively proliferating from the previous timepoint in mice subjected to EAE. Data in (B-E) representative of a single experiment with three mice analyzed per timepoint. Groups in (B, C) compared with a two-way ANOVA with Sidak's multiple comparison test. Comparisons in (B) were performed by comparing the fold change from baseline between WT and ERAP1$^{-/-}$ B cells. Groups in (D, E) compared with a mixed-effects analysis. *p<0.05, **p<0.01, ***p<0.001, ****p<0.0001. FC: fold change.

Human B cell subset dysregulation in individuals carrying the ERAP1 K528R SNP.

Murine B cells completely lacking the *ERAP1* gene show considerable differences from their WT counterparts, especially during induction of inflammation (17). In humans, the presence of specific SNPs in *ERAP1* results in dysfunction of the protein's ability to trim peptides for MHC-I, and these SNPs are also linked to multiple autoimmune diseases (26, 28). The most pathogenic of these, the K528R SNP, is genetically associated with MS (26, 143), and shows the strongest associations with other autoimmune diseases (165, 166). We have previously shown that the presence of this SNP induces the strongest changes in immune cell function (including dysregulation of the NLRP3 inflammasome) as compared to other ERAP1 variants (18). Therefore, we wanted to determine if human B cells carrying this pathogenic SNP exhibit dysregulated phenotypes. We accomplished this by sourcing data from multiple published scRNA-seq datasets containing data from PBMCs of 36 healthy individuals, across six studies, encompassing a total of 24,795 B cells (see Chapter 6) (Fig. 16A). Critically, using the raw sequencing data, we were able to determine which individuals carry the *ERAP1* K528R SNP, identifying seven out of the 36 individuals as having at least one copy of this SNP.

Unbiased clustering (See Chapter 6) identified five distinct B and plasma cell subsets (Fig. 16A) expressing numerous subset-defining genes (Fig. 16B). Each of the six studies contributed evenly to these subsets with the exception of the ”Exhausted B cell” subset which was almost entirely from Kang, H.M., et al. (167). We found that B cells expressing high levels of ERAP1 were evenly distributed across all subsets (Fig. 16C) and that the proportion of each subset per individual did not differ based on the presence of the K528R SNP (Fig. 16D). However, individuals carrying K528R had decreased expression of ERAP1 in their naive B cells, class-switched memory B cells, and plasma cells/blasts (Fig. 16E). For each B cell subset we also identified differentially expressed genes (DEGs) and pathways between cells with the K528R SNP and those without. We observed consistent findings across all cell subsets noting decreased expression of: *PTPRCAP*, *EEF1G*, *MT-ATP8*, and *MT-ND4L* (Fig. 16F, H, J, L), and increased expression of numerous ribosomal protein genes, *ATP5E*, and *TIPIN* (Fig. 16F, H, J, L) in K528R containing B cells. Most interesting were the conserved pathways enriched in B cell subsets carrying the K528R SNP, most notably upregulation of eIF2 signaling and oxidative phosphorylation (Fig. 16G, I, K, M). These results suggest that the presence of the K528R *ERAP1* SNP in human B cells correlates with an up-regulation of ribosomal translation machinery and altered metabolism; both of which are known to also affect immune cell functions (168–170).

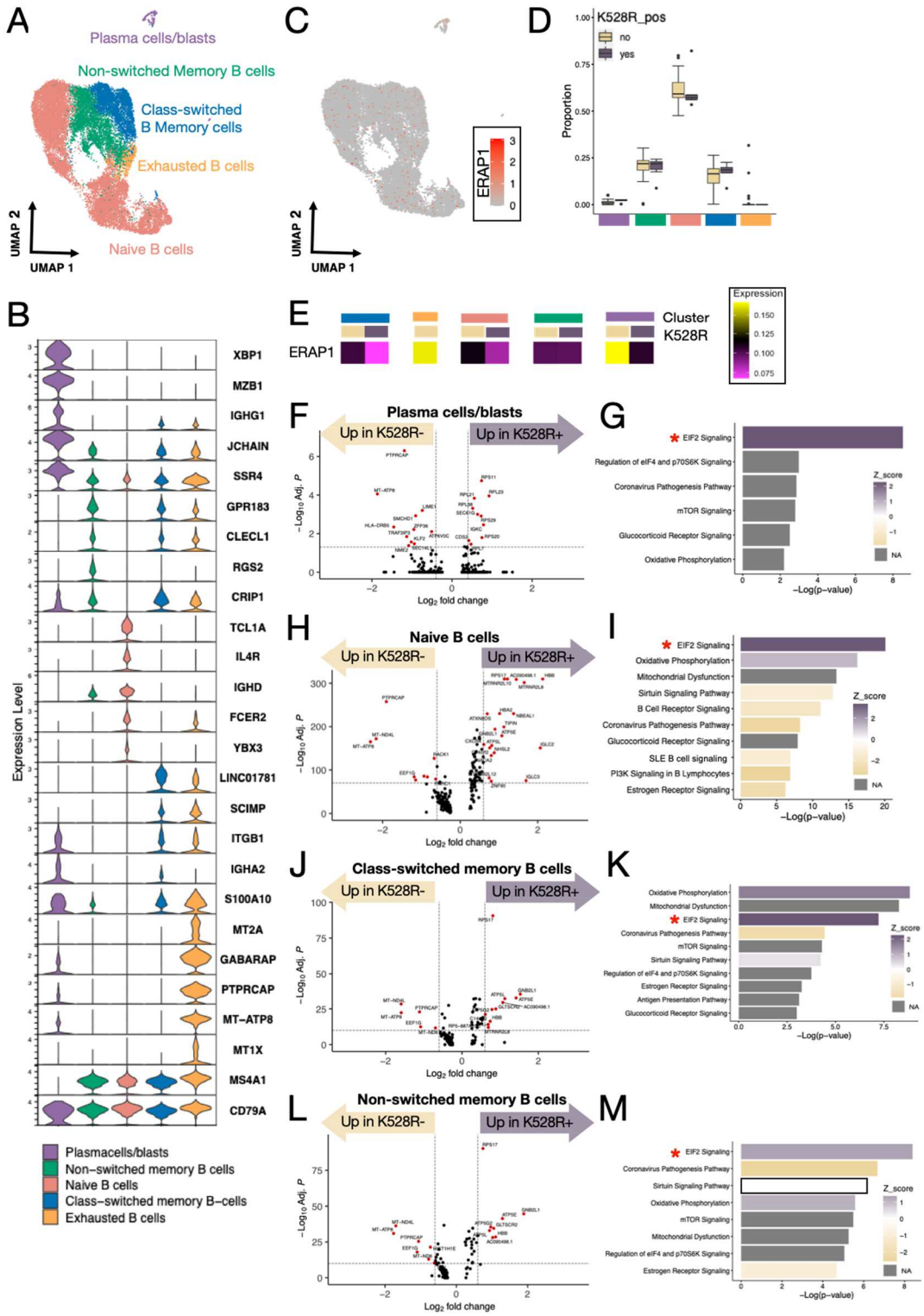

Figure 16: Integrated scRNA-seq analysis of human B cells reveal subset-conserved dysregulation in B cells carrying the K528R ERAP1 SNP. (A) UMAP of plasma cells/blasts

Figure 16 (cont'd)

and B cell subsets from an integrated analysis of six healthy human scRNA-seq datasets incorporating 36 individual samples and 24,795 cells. Cells are colored based on cluster-level annotations obtained using SingleR. (B) Stacked violin plots of expression of cluster-defining markers. (C) UMAP of the expression of ERAP1 on B cell subsets revealing equal distribution across clusters. (D) Proportion of various B cell subsets in individuals based on the presence or absence of the K528R SNP. (E) Heatmap of ERAP1 expression on B cell subsets split by cells containing the K528R SNP or not. The exhausted B cell subset contains only cells without the K528R SNP. (F) Volcano plot of differentially expressed genes (DEGs) in plasma cells/blasts based on the presence of the K528R ERAP1 SNP. (G) IPA canonical pathway analysis using DEGs from (F) with bars colored based on whether the pathway is up- or down-regulated in cells with the K528R SNP. Gray bars indicate no pathway directionality data is available. (H, I) Same as (F, G), but for Naive B cells. (J, K) Same as (F, G), but for Class-switched memory B cells. Same as (F, G), but for non-switched memory B cells. Differential expression in (B, F, H, J, and L) performed with MAST.

Discussion

Hundreds of genes have been linked to MS (143), yet we still understand little of the mechanisms underlying each of these associations. Identification of these mechanisms, may reveal conserved master pathogenesis archetypes responsible for MS, that can then be therapeutically targeted in patients. To this end, we sought to understand the mechanism(s) linking SNPs in the ERAP1 gene to MS. Identifying mechanisms underlying ERAP1's link to MS is significant as ERAP1 is linked to many other autoimmune diseases (28, 165). An understanding of the mechanisms underlying the genetic association of ERAP1 with MS susceptibility may also identify mechanisms across multiple other autoimmune diseases linked to ERAP1 including: AS, Psoriatic Arthritis, and Behçet's disease.

Our finding that mice lacking ERAP1 experience increased EAE mean clinical scores in a rodent form of autoimmune neuroinflammation that mirrors MS supports GWAS studies linking human ERAP1 SNPs with susceptibility to MS. Our finding that ERAP1$^{-/-}$ mice exhibit exaggerated EAE due to an intrinsic B cell defect narrows the possible immune mechanisms responsible for ERAP1's association with MS, and potentially other autoimmune diseases also linked to ERAP1.

The localization of ERAP1's contribution to CNS autoimmunity via B cells aligns well with current theories regarding MS pathogenesis since B cell depleting monoclonal antibodies are now a mainstay of MS treatment (141). Why depleting B cells leads to robust clinical responses in some MS patients is currently a heavily investigated topic, with a number of potential mechanisms postulated, including: B cell antigen presentation (171), B cell cytokine production (172), B cell-mediated T cell co-stimulation (171), Epstein-Barr virus infection of B cells (173), and contributions from Bregs (171). Importantly, B cell depletion therapies are far

from a cure, and show limited efficacy in MS patients with more severe forms of MS such as primary progressive MS (174). Accordingly, groups have been vigorously researching how B cells contribute to MS (171, 172), as well as if more precise B cell targeting can achieve superior responses. Our results show that B cells lacking ERAP1 have both exaggerated expression of T cell co-stimulatory/activation markers and fail to proliferate in vivo. Both of these may explain why mice lacking ERAP1 experience higher EAE mean clinical scores since increased B cell activation during the initiation phase of EAE and impaired B cell regulatory responses during the chronic phase of EAE are linked to more severe pathology. Such findings tie in with the currently appreciated divergent roles for B cells during the pathogenesis of CNS autoimmunity, where B cells are capable of harboring both disease-inducing roles early on and protective roles later during the resolution phase (163, 164). Regarding the undetermined CNS B cell subset we identified, since these cells are $IgD^{+}B220^{+}CD21^{-}CD23^{-}$, make up the majority of B cells in the CNS, and since it has been shown previously that most human CNS B cells are class-switched memory B cells (175), this unknown population may represent these cells.

Shedding light on this mechanism, we identified that mice lacking ERAP1 also have drastically reduced numbers of the innate-like B1 cell subsets during peak EAE. This effect is likely due to an intrinsic defect, but we cannot fully rule out an extrinsic one, such as NK cell-mediated depletion, however, our ex vivo studies and in vivo studies of B cell survival in mice not subjected to EAE argue against such a possibility. While B1 cells are understudied, they are known to be able to secrete auto-antibodies, function as APCs, secrete cytokines, and respond to pathogen infection in an innate manner (176). They have also been linked to a number of autoimmune diseases including MS, however their precise role in the pathogenesis of MS is unclear, as B1 cells have been shown to have both protective and pathogenic roles in EAE

depending on the stage of disease (177, 178). If this lack of B1 cells contributes to autoimmune disease susceptibility in mice lacking ERAP1, or if it is just a consequence of ERAP1's ability to broadly dysregulate B cells, remains to be seen and is an interesting area of future investigation.

In a further effort to tie our B cell findings back to humans carrying the actual MS-linked ERAP1 SNP, we took advantage of publicly available scRNA-seq datasets and found well conserved transcriptional changes across multiple B cell subsets. A consistent decrease in the expression of *PTPRCAP* (CD45-associated protein [CD45-AP]) in B cells carrying the ERAP1 K528R SNP stood out. CD45-AP is an understudied protein known to interact with CD45 and modulate its behavior in a number of ways, but generally thought to augment CD45 signal transduction (179). As CD45-AP increases CD45 signaling and CD45 signaling activates Src kinases which leads to B cell proliferation (179, 180), B cells carrying the K528R SNP would be expected to have decreased CD45 signaling due to less CD45-AP and consequently may have impaired capacity to proliferate. This fits with our data showing murine B cells lacking ERAP1 have impaired proliferation when transferred into B cell deficient hosts.

We also found upregulation of eIF2 signaling and oxidative phosphorylation pathways in all B cell subsets bearing the K528R SNP, suggesting ERAP1's ability to modulate these pathways is conserved across B cells. As ERAP1 is an endoplasmic reticulum-localized peptidase, it is possible that dysfunctional ERAP1 variants may lead to issues with protein processing/production, thus requiring the cell to up-regulate translation machinery to maintain protein production. Importantly, many of the genes we see upregulated in the eIF2 signaling pathway in cells with K528R are involved in translation. Since endoplasmic reticulum function is tied to cell metabolism and immune responses (181, 182), this may explain the concerted dysregulation of these pathways in B cells in particular (183, 184), and possibly the increased

susceptibility to MS, although there is a paucity of studies regarding the effects of ER dysfunction in B cells as it relates to autoimmunity (185). It is also important to note that all of these findings are from healthy individuals at baseline and that these DEGs and pathways may be exacerbated during settings of inflammation/immune activation.

Finally, our studies here lead to the creation of the first map of the CNS resident IL-10^{+} immune compartment at the protein level in mice; an important resource for those investigating CNS regulatory mechanisms. Our map is similar to that determined using scRNA-seq, but with a couple of important differences potentially related to both the technology and animal models used. While we found microglia to be the primary source of IL-10 at steady state and CD4^{+} T cells the dominant source during EAE, Shemer, A., et al. claim microglia are unable to make IL-10 and that with LPS stimulation NK cells and neutrophils are the primary sources of IL-10 in the CNS (186). Our protein level assessment of IL-10 using a highly specific reporter mouse contradicts the idea that microglia do not make IL-10 and our results are consistent with other published work (187). One reason for the discrepancy between our datasets is likely due to Shemer, A., et al. only measuring IL-10 at the mRNA level, while we measure it at the protein level. Measurements at the protein level are critical for a cytokine such as IL-10, as its mRNA is subject to multiple post-transcriptional regulation mechanisms (188) and because IL-10 protein negatively regulates its own mRNA (189); autocrine signaling which may explain the discrepancy between our results. Lastly, while we employ the EAE model of neuroinflammation, Shemer, A., et al. use the LPS model, which may further explain why we identify different immune cell subsets are making IL-10, notably neutrophils (190). While it has been reported that this strain of IL-10^{GFP} mouse is unsuitable for IL-10 detection in myeloid cell during inflammation, through the use of spectral cytometry we are able to detect and subtract out

autofluorescence signals from microglia, thus allowing accurate IL-10 detection even on highly autofluorescent cells such as microglia.

In total, our efforts to investigate the genetic association between polymorphisms in the *ERAP1* gene and MS have begun to unravel this mystery and focus attention on B cell biology as a potential key regulator in autoimmune neuroinflammation. This correlates with the current clinical treatment of MS using non-discriminate, B cell-depleting regimens. Our work suggests that there may be an opportunity to further target these interventions to specific B cell subsets, both to enhance efficacy, as well as prevent known complications to these approaches, such as global immune-suppression.

Chapter 4: ERAP1 mediates proinflammatory responses of B cells

Authors: Maja K. Blake, Patrick O'Connell, Sarah Godbehere, Yasser A. Aldhamen, Andrea Amalfitano

Introduction

Multiple sclerosis is an incurable, severely debilitating disease which affects millions of people (3, 59). Many theories exist for what drives MS pathogenesis, including: EBV infection, Vitamin D deficiency, and genetics to name a few (5, 57). In reality, the disease is highly heterogenous and likely is due to a multitude of factors, which varies between individuals (5, 59). Furthermore, multiple types of MS disease can occur, ranging from a mild relapsing remitting disease to the devastating primary progressive disease (5, 58, 191). Many patients' diseases can be managed quite well with currently available treatments, however, for more aggressive disease types the options are limited (58, 60). Indeed, even for the well-managed diseases, MS is still incurable. In 2018, a new therapy was approved for MS which significantly improved patient outcomes as measured by stable white matter lesions and extending remission periods and survival (60). This therapy was called ocrelizumab and is a B cell targeting monoclonal antibody. The success of this therapy showed the scientific community that B cells are vital in driving MS disease and opened a new avenue to potential drug research and development. Despite the successes of ocrelizumab and clear importance of B cells in MS, the exact reasons for why B cells drive MS remain largely unclear. Therefore, more research into specific molecular mechanisms for B cells related to MS remains of utmost importance.

Although the exact cause for MS is unknown, it can be genetic in origin as hundreds of genes have been linked to the disease (165). Our lab began researching how genetics may play a role in B cells driving MS. Specifically, we studied the gene ERAP1: polymorphisms in which have been significantly linked with MS disease (8, 26). Our lab published that ERAP1 is an important mediator in pro-inflammatory B cell driven EAE, and is also a critical mediator of inflammasome and ER responses (14, 16). We determined that not only are B cells affected by

EAE to a greater extent in ERAP1-deficient mice, but also these ERAP1$^{-/-}$ B cells were responsible for causing a higher EAE phenotype. ERAP1 is an important mediator of both innate and adaptive immune responses (12, 17, 18, 97). It is an aminopeptidase localized to the ER, which trims peptides of 9-16 amino acids in length to 8-9 amino acids prior to loading onto MHC-I molecules for antigen presentation (192). In addition to its role in antigen presentation, ERAP1 also mediates NK, CD4, and CD8 T cell proinflammatory responses (13, 15, 22, 97). Furthermore, ERAP1 deficient bone marrow derived macrophages (BMDMs), have enhanced proinflammatory responses to innate stimulation (14). Specifically, they have elevated inflammasome responses. In addition to these heightened inflammasome responses, they also have elevated ER stress and downstream UPR activation (14). Together these mechanisms may begin to explain why ERAP1 deficient immune cells are highly sensitive to innate immune stimuli.

In addition to causing a worse EAE phenotype, when μMT (genetically deficient in B cells) mice were adoptively transferred with ERAP1$^{-/-}$ B cells, the B cells were actually lost after 28 days of EAE (16). We published that these B cells had impaired proliferation in comparison to WT beginning around Day 20 (16). It is known that B cells fail to proliferate to some extent after adoptive transfer (193), but ERAP1 deficient B cells had a much reduced proliferation in comparison to WT. In this chapter, we will explore mechanisms of how ERAP1 deficiency contributes to cell loss as well as intracellular mechanisms that regulate proinflammatory B cell behavior. Specifically, we will examine more closely the B cells adoptively transferred into μMT mice prior to EAE, and begin to study possible mechanisms such as inflammasome activation, ER stress and pyroptosis. These studies will help illuminate possible targetable pathways for neuroinflammatory disease and B cell driven autoimmune diseases as a whole.

Results

ERAP1 mediates the proinflammatory state of B cells

To begin investigating why mice with ERAP1 deficient B cells, specifically, have enhanced EAE phenotyping, we began by assessing proinflammatory cytokines and cell surface markers of B cells. We first isolated pan-B cells from WT and ERAP1$^{-/-}$ mice, and then further isolated CD43+ B1 cells from each genotype as well. B1 and B2 cells were examined because B1 cells are an innate-like B cell subtype which were found to be reduced in ERAP1$^{-/-}$ mice during EAE significantly more than in WT, and B2 cells are what were initially transferred into μMT mice prior to EAE induction as previously described (16). When these cells were surface stained with various activation markers, we found significant increases in CD69 and CD80 surface expression on B cells from ERAP1$^{-/-}$ mice (Fig. 17A). Furthermore, we discovered that this statistically significant elevation of CD69 and CD80 was also found on ERAP1$^{-/-}$ B2 cells, in comparison to WT B2 cells (Fig. 17B). In parallel with the increased activation marker signature on ERAP1-deficient B cells, these B cells also produced statistically more proinflammatory cytokines than WT B cells. Of the 23 cytokines assessed, IL-1β and IL-6 cytokine production was significantly enhanced in ERAP1$^{-/-}$ B cells in comparison to WT B cells with innate stimuli. Together, this data supports that the ERAP1$^{-/-}$ B cells are hyperinflammatory at baseline, which supports why mice that received ERAP1 deficient B cells had enhanced EAE phenotyping.

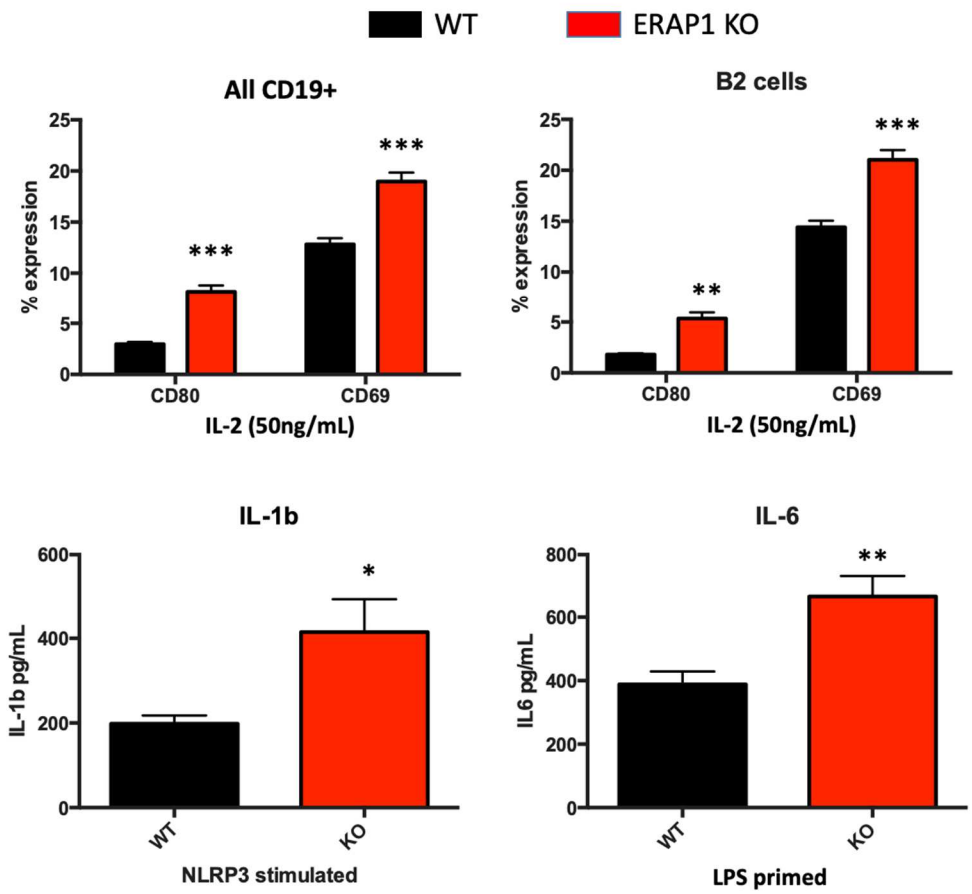

Figure 17: ERAP1$^{-/-}$ B cells have enhanced proinflammatory cytokines and activation marker expression. Splenocytes were isolated from 6 week old male WT and ERAP1$^{-/-}$ mice. CD19+ pan B cells were isolated per the manufacturer's protocol by negative selection. Pure CD19+ B cells were plated at 300,000 cells/well into a 96 well plate and stimulated with a low dose of IL-2 with or without NLRP3 inflammasome agonist Nigericin (10uM). Cells were cultured for one day, approximately 24 hours, and then collected. They were stained with surface markers CD19 (B cells), Zombie NIR (live/dead dye), B200 (B2 cells), CD80 (APC) and CD69 (PE) and flow cytometry was completed using the Cytek Aurora (A, B). Flow cytometry data was analyzed using FlowJo software v.10.7.1. When these cells were collected, the supernatant was collected, and cytokine secretion was analyzed using Bioplex 23 plex kit. The assay was

Figure 17 (cont'd)

completed per manufacturer instructions, and the top altered cytokine are shown here, IL-1β (C), and IL-6 (D). *p<0.05, **p<0.01, ***p<0.001.

ERAP1$^{-/-}$ B cells have enhanced baseline ER stress

As B cells from ERAP1$^{-/-}$ mice had proliferation defects and loss of these cells was appreciated with EAE, we next wished to begin examining some potential pathways for this reduction. We began by assessing various genes important in two mechanisms which have been related to ER stress, a state which is increased in ERAP1$^{-/-}$ bone marrow derived macrophages (BMDMs) as we previously published (14), autophagy and the UPR. At baseline, ERAP1$^{-/-}$ B cells had an increase in the autophagy genes ATG5 and ATG12, as well as the ER stress gene sXBP1 (Fig. 18A). Although not significant, when these cells were stimulated with inflammasome stimuli, there was a greater reduction in ATG5 expression in ERAP1$^{-/-}$ B cells (Fig. 18C). ATG5 expression is known to be reduced by the inflammasome, so reduction in this gene occurs with inflammasome stimuli (194).On the other hand, sXBP1 is an important downstream regulator of the p-IRE1a branch of the UPR pathway (113), and we also found it to be upregulated in ERAP1$^{-/-}$ BMDMS (14). Indeed, we also determined that the percent change of IRE1a gene expression was more greatly enhanced in ERAP1$^{-/-}$ B cells with inflammasome stimuli as well (Fig. 18C). Altogether, this data supports that similar to our previously published data in ERAP1-deficient BMDMs, ERAP1-deficient B cells also have a baseline state of enhanced ER stress.

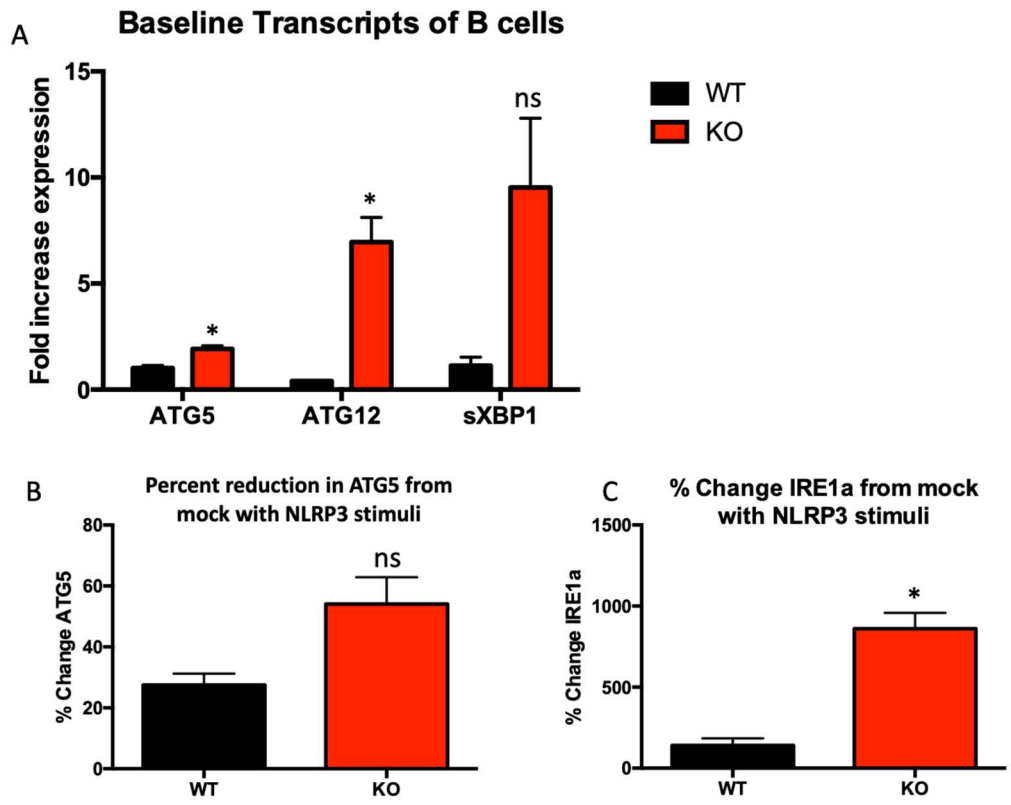

Figure 18: ER stress gene transcription is elevated in ERAP1$^{-/-}$ B cells. Pan B cells with CD19+ expression were isolated from WT and ERAP1$^{-/-}$ splenocytes. Cells were plated at a density of 1 million/well in a 48 well plate. The cells were stimulated with NLRP3 inflammasome stimuli, which includes low dose LPS for priming (40ng) and Nigericin (10uM) overnight, for approximately 16 hours. Cells were then collected and RNA was isolated using Trizol per manufacturer's protocol. cDNA was made from the RNA using the Superscript III kit and genes were assessed by fold increase in expression from WT at baseline (A). Percent reduction of ATG5 was calculated in WT and ERAP1$^{-/-}$ B cells with priming and nigericin treatment, comparing each genotype with NLRP3 stimuli to its baseline ATG5 expression value (B). Similarly, percent induction of IRE1a was calculated in WT and ERAP1$^{-/-}$ B cells,

Figure 18 (cont'd)

comparing the IRE1a expression level for each genotype with priming and nigericin to its baseline value (C). Data are expressed as mean +/- SEM. *p<0.05, **p<0.01, ***p<0.001.

The pyroptosis pathway is upregulated in ERAP1$^{-/-}$ B cells

We previously published that ERAP1$^{-/-}$ mice had reduced levels of B cells with EAE, and ERAP1$^{-/-}$ B cells failed to proliferate after 20 days of EAE (16). Furthermore, we know that ERAP1$^{-/-}$ BMDMs have enhanced ER stress and inflammasome activation as assessed by IL-1β production and caspase-1 activation (14). Pyroptosis is a unique pathway of cell death which is characterized as a proinflammatory cell death mechanism, one which involves the production of IL-1β (195, 196). Intracellularly, pyroptosis involves the cleavage of a protein called gasdermin D (GSDMD) into subunits by caspase 1, which forms pores in the membrane to allow for the release of cleaved IL-1β, also processed by caspase 1 (72, 196). As ERAP1$^{-/-}$ cells produce more IL-1β and have enhanced caspase 1 activation (14), we wished to assess this cell death pathway in B cells as a possible mechanism for why the cells are lost during EAE. We began by staining WT and ERAP1$^{-/-}$ B cells intracellularly for GSDMD with mild stimuli (IL-2). We determined that ERAP1 deficient B cells expressed significantly more GSDMD than WT B cells (Fig. 19A). This was further assessed in B cells subtypes and also found to be enhanced in ERAP1$^{-/-}$ B cells (Fig. 19B). Disulfiram was identified as a GSDMD inhibitor (197). So we next assessed whether disulfiram would reduce pyroptosis in our system. Specifically, we hypothesized that ERAP1$^{-/-}$ B cells would have a greater reduction in IL-1β (the readout of pyroptosis) production with GSDMD inhibition, if they are more reliant on this pathway. Indeed, we discovered that ERAP1$^{-/-}$ B cells had a dose dependent reduction of IL-1β release with disulfiram (Fig. 19C) with

NLRP3 inflammasome stimuli (LPS priming+Nigericin), although not significant. Importantly, WT cells also showed reduced IL-1β release with disulfiram after NLRP3 induction, which is a positive control for this experiment. However, in comparison to WT, ERAP1 deficient B cells had a much greater reduction in IL-1β release at various disulfiram concentrations (Fig. 19D), although not significant. Together, this supports that the pyroptosis mechanism may be upregulated in ERAP1 deficient B cells, and may in part explain why these cells are lost during EAE.

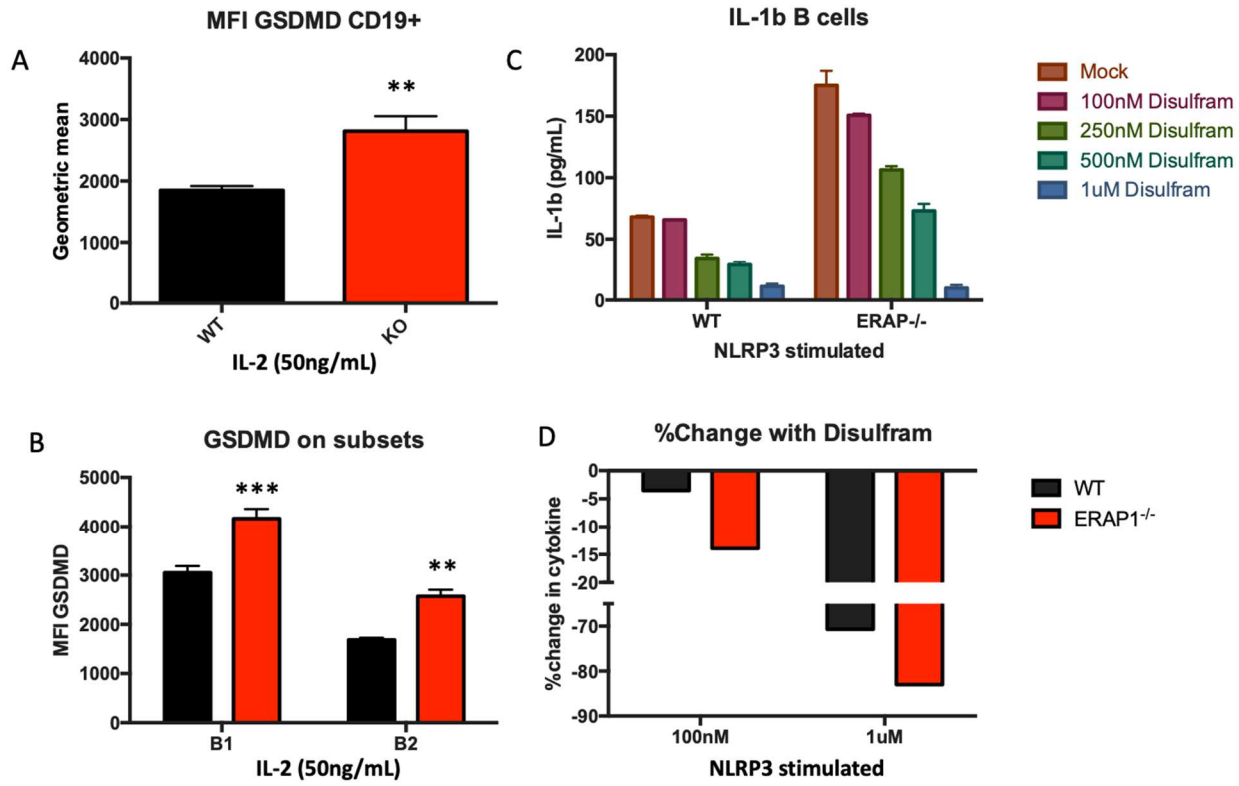

Figure 19: ERAP1 mediates pyroptotic mechanisms. Splenocytes were isolated, and CD19+ pan B cells were isolated per the manufacturer's protocol by negative selection. These CD19+ B

Figure 19 (cont'd)

cells were then plated at 300,000 cells/well into a 96 well plate. They were stained with surface markers CD19 (B cells), Zombie NIR (live/dead dye), and B200 (B2 cells), to identify different B cell subsets, and then fixed. Cells were permeabilized and stained for the intracellular marker gasdermin D and flow cytometry was completed using the Cytek Aurora (A, B). Flow cytometry data was analyzed using FlowJo software v.10.7.1. To assess the functionality of pyroptosis, isolated pan B cells were treated with the gasdermin D inhibitor disulfiram with increasing concentrations. Inhibitor was added at the same time as the LPS priming, followed by Nigericin (2.5uM) 6 hours later. Cells were cultured for an additional 12 hours, and then supernatant was collected. IL-1β ELISA was completed with the supernatants (C) and percent reduction in IL-1β production with disulfiram was calculated for multiple doses (D). Data are expressed as mean +/- SEM. **p<0.01, ***p<0.001.

Naïve ERAP1 deficient B cells have an altered gene expression profile in comparison to WT

Up to this point we have assessed various mechanisms as the cause of greater EAE phenotyping in ERAP1 deficient B cells: ER stress, autophagy, and pyroptosis. However, to discover the exact potential molecular mechanism, we decided to do RNA sequencing for gene expression analysis on ERAP1 deficient B cells. We collected spleens from naïve WT and ERAP1$^{-/-}$ mice, and then flow sorted B2 cells from the splenocytes, isolated RNA from the B2 cells, and performed RNA sequencing. We were able to isolate a pure B2 cells population with flow sorting (Fig. 20A). The RNA sequencing illuminated many differentially expressed genes (DEGs) in the various samples, including naïve WT and ERAP1$^{-/-}$ mice. Fig. 20B is a heatmap of the differentially expressed genes between naïve mice, and Fig. 20C represents a volcano plot of

the same data. Overall, we discovered a largely unique gene signature in ERAP1-deficient B cells even at baseline. To compile the many differentially expressed genes in an effective manner, the Integrative Pathway Analysis by Qiagen was used. With this, we determined the top canonical pathway altered in ERAP1 deficient naïve B cells in comparison to WT B cells was the UPR pathway (Fig. 20D). Other pathways such as aldosterone signaling and IL-17A signaling were significantly increased in ERAP1 deficient B cells as well, suggesting that ERAP1 might also regulate these pathways. This data suggests that similar to ERAP1$^{-/-}$ BMDMs, B cells also have an elevated baseline of stress, triggering an overactive UPR pathway and potential might contribute to early loss of these cells in the EAE mouse model. Furthermore, the IPA analysis software predicted the top disease related to the DEGs was neurological disease, further supporting ERAP1's role in immune tolerance and MS.

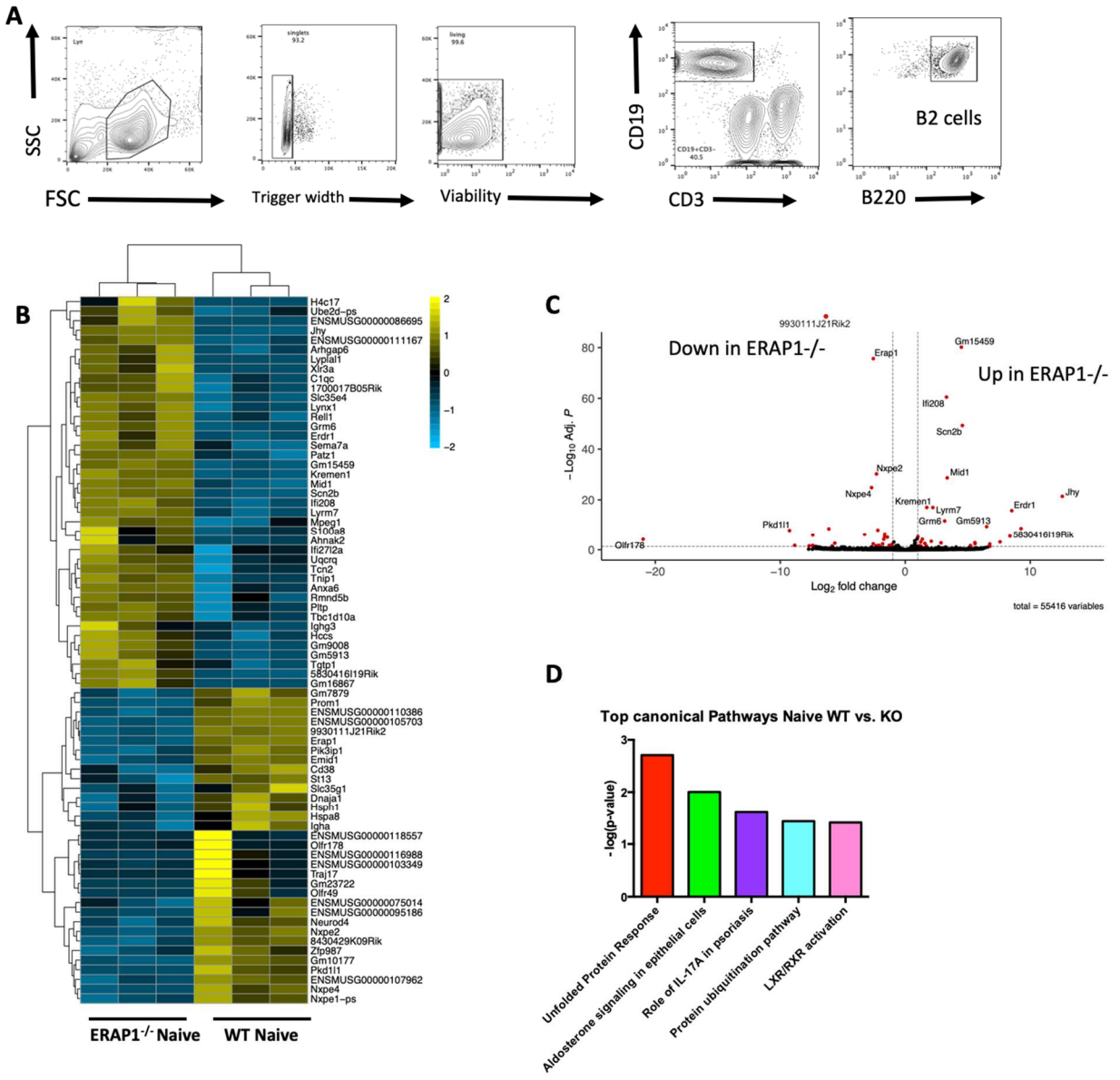

Figure 20: RNA sequencing results from Naïve WT and ERAP1$^{-/-}$ splenocytes. B2 cells were sorted out from all other splenocytes using flow sorting (A), and RNA was made from these cells. RNA was submitted to the MSU Genomics core for RNA sequencing. Results of the differentially expressed genes were collected and a heat map was generated from the data using R software (B). Volcano plot analysis for magnitude and significance of the genes was completed (C). Data was input into Qiagen's integrative analysis pathway (IPA) and the software assessed the top possibly affected pathways impacted in ERAP1$^{-/-}$ Naïve B2 cells (D).

ERAP1 alteration impacts B cell signaling

Once we assessed the baseline genomic signature related to ERAP1 deficiency, we wished to assess possible genetic alterations in response to EAE induction. We began by inducing EAE in WT and ERAP$^{-/-}$ mice. At peak EAE, around Day 21, we harvested B cells from the spleens of these EAE WT and ERAP1$^{-/-}$ mice. We then flow sorted as done in Figure 19 for B2 cells and conducted RNA sequencing. As expected, we found many more genes to be differentially expressed with EAE induction (Fig. 21A). These genes were plotted on a volcano plot to identify the top hits (Fig. 21B). Significant DEGs were similar to the ones found in naive mice, with Gm15459 (an HSP8 pseudogene) being the most significantly upregulated gene in ERAP1$^{-/-}$ B2 cells. We also compared DEGs in ERAP1$^{-/-}$ naïve and ERAP1$^{-/-}$ EAE mice. In comparison to WT, ERAP1 deficient animals had many more altered genes with EAE induction and also a completely unique signature of genes (Fig. 21C). Hundreds of DEGs were found in ERAP1$^{-/-}$ mice (Fig. 21C), with the top genes reported in a volcano plot (Fig. 21D). The gene LTF (which regulates lactoferrin protein expression) was the most upregulated gene with EAE, and Xist (which is known to regulate X chromosome inactivation) was the most downregulated, and top DEGs were validated in separate experiments (data not shown). When these DEGs were input into IPA, top canonical pathways were assessed as done in naïve mice. Overall, the top pathways were very closely correlated to known data on ERAP1 and its role in innate and adaptive immunity. Specifically, antigen presentation was the top affected pathway altered when mice with ERAP deficiency were given EAE. Surprisingly, B cell development was the next most significant pathway, which further supports the finding of B cell depletion and B cell proinflammatory signaling in ERAP deficient mice during EAE. The top predicted upstream regulator discovered through the IPA analysis was a transcription factor called TCF3 (p= 3.89 x

10^{-6}). The software predicted this gene, which is important in B cell development (198), to be reduced based on the DEGs in ERAP1$^{-/-}$ during EAE. When we validated this in the lab using qRT-PCR, we found that indeed TCF3 was reduced in ERAP1$^{-/-}$ B cells in comparison to WT B cells, at baseline and with various stimuli (Fig. S5). Altogether, this data explains why ERAP deficient mice have increase EAE scores, possibly due to ERAP1 impact on antigen presentation and possibly due to its role in B cell development. This signaling may be due to changes in the UPR, autophagy, the inflammasome, and pyroptosis, all of which are interconnected proposed pathways as shown in Figure 22.

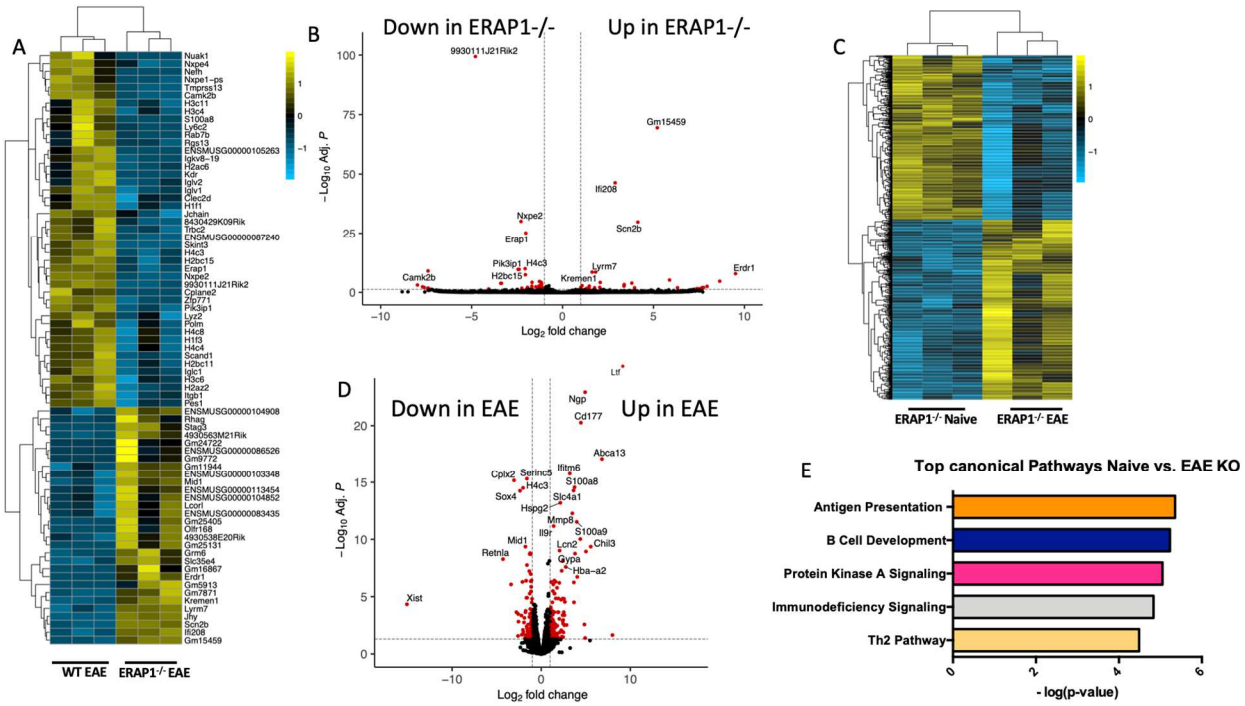

Figure 21: RNA-seq results in EAE induced WT and ERAP1$^{-/-}$ mice. EAE was induced in WT and ERAP1$^{-/-}$ mice as previously described using full length MOG protein. Upon peak EAE, at Day 21, splenocytes were collected from these mice, and flow sorted for B2 cells as described in Materials and Methods. Cells were submitted for RNA sequencing to MSU Genomics Core. Significant DEGs between WT and ERAP1$^{-/-}$ EAE B cells were identified and are shown in heat map (A). Similarly, the most significant genes with greatest changes are represented in a volcano plot (B). Cells were also compared between ERAP1$^{-/-}$ naïve mice and ERAP1$^{-/-}$ mice challenged with EAE (C). Using R software, a heatmap and volcano plot was generated as well (D). This data was input into IPA software and the top canonical pathways were identified as being affected in ERAP1$^{-/-}$ mice with EAE, in comparison to naïve ERAP1$^{-/-}$ mice (E).

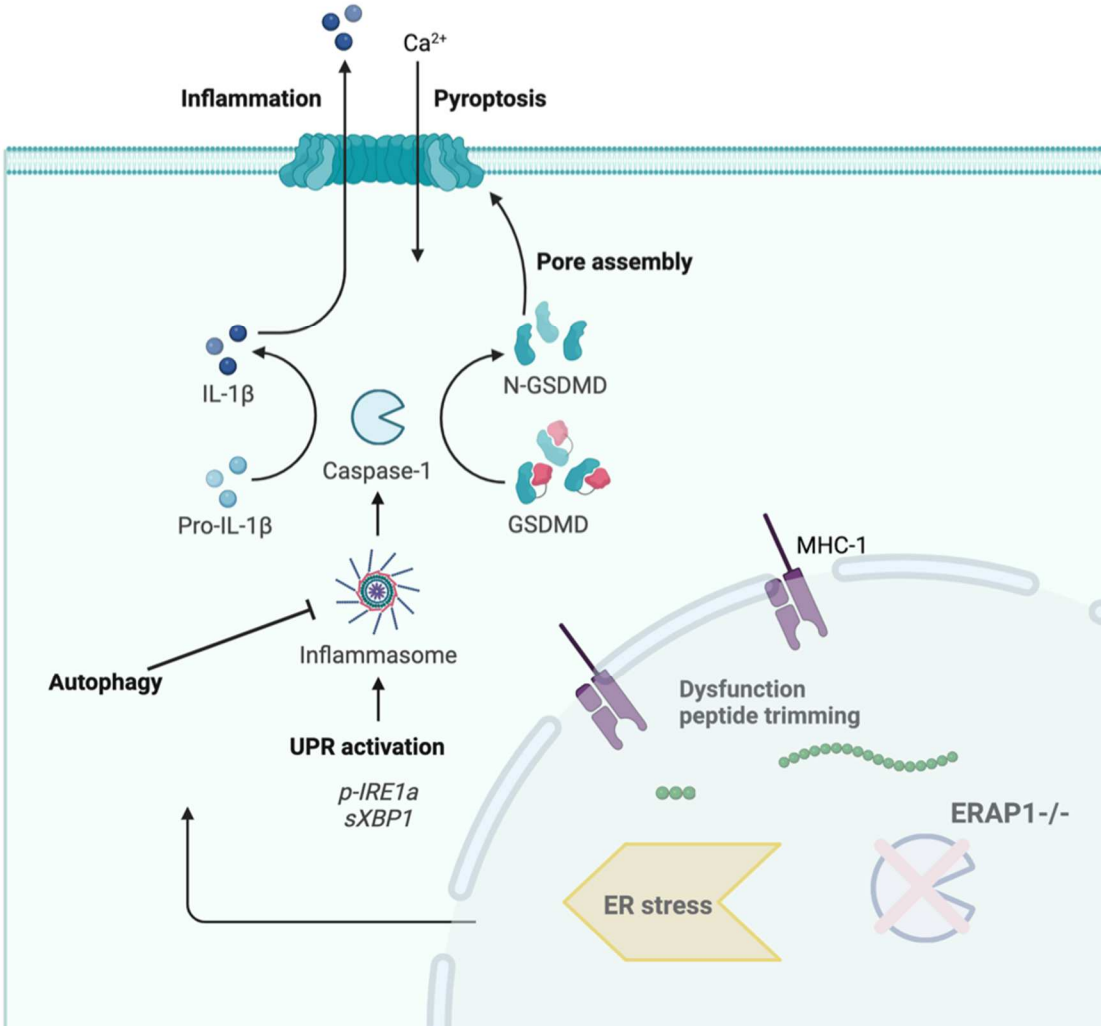

Figure 22: A proposed mechanism for B cell signaling in the setting of ERAP1 deficiency. Lack of ERAP1 activity leads to dysfunctional peptide trimming ability and unfolded protein aggregation in the ER, causing stress. This ER stress activated the UPR pathway, which triggers inflammasome activation. Autophagy may also negatively impact inflammasome activity in parallel. Inflammasome activation causes caspase 1 activation and cleavage of pro-ILβ into IL-1β, which is then secreted from the cell and induced inflammation. At the same time, caspase 1 causes cleavage of GSDMD into the N-GSDMD subunit which forms pores on the surface, further releasing IL-1β from the cell and triggering cell death.

Discussion

Polymorphisms in the ERAP1 gene have been associated with multiple sclerosis, specifically the SNP r30187 (26). Given our previous reports that ERAP1 deficient mice have enhanced EAE phenotype, a mouse model of MS, and that ERAP1 deficient B cells specifically can be attributed as the reason for such enhanced EAE phenotype, we wished to study the role of ERAP1 in B cells further. B cells are known to be pathogenic in development of MS, although the exact mechanisms as to why this is remains unknown (172). Here we wished to study the proinflammatory nature of B cells in the setting of ERAP1 modulation, with the hopes of determining differentially regulated genes and pathways to explain such proinflammatory states.

In addition to the general proinflammatory nature discovered in ERAP1$^{-/-}$ B cells, including increased activation markers and proinflammatory cytokines, we performed RNA sequencing on WT and ERAP1-deficient B cells in the naïve setting as well as with peak EAE. Overall, we determined that the gene expression in ERAP1$^{-/-}$ mice was largely unique compared to WT. Many genes were either upregulated or downregulated in ERAP1$^{-/-}$ murine B cells in both naïve and EAE in comparison to WT. Gm154859 is a heat shock protein 8 pseudogene which was significantly upregulated in mice deficient in ERAP1. Although pseudogenes are nonfunctional and do not encode for proteins (199), heat shock proteins and HSP8 are molecular chaperones which ensure proper folding and relieve ER stress (200). As intriguing at this finding is given the baseline elevation of ER stress in ERAP1 deficient cells, it is difficult to attribute meaning to this finding. Unfortunately, many of the top hit genes are either nonspecific, or pseudogenes such as this Gm154859, and are therefore difficult to attribute directly to our model.

Other better studied genes such as LTF were significantly upregulated with EAE induction in ERAP1$^{-/-}$ mice specifically. This is a gene that has been linked with proliferation

inhibition and cell death, both which were found in ERAP1$^{-/-}$ B cells after adoptive transfer (201). Overall, many more genes were altered in ERAP1$^{-/-}$ mice with EAE than WT, supporting that many more changes are occurring in B cells with ERAP1 dysfunction, which may be causing a worsened EAE disease. Importantly, the ERAP1 gene was significantly reduced in comparison to WT mice albeit not truly gone because of the nature of our mouse model. It is critical to note that the ERAP1$^{-/-}$ mouse model which is used throughout our studies is deficient in the specific enzymatic region (exons 5 and 6) of the ERAP1 protein, creating a truncated protein if expressed (30). Therefore, this truncated ERAP1 protein lacks ERAP1 enzymatic activity. The data found in these studies of ERAP1$^{-/-}$ cells or mice are therefore mainly attributed to loss of ERAP1 enzyme activity or truncation of the protein, but not loss of the total protein itself.

As so many genes were differentially expressed in ERAP1 deficient mice, we decided to use the Integrative Pathway Analysis (IPA) software program to make better sense of the data from RNA sequencing. This software was used to compare different experimental groups, namely WT Naïve vs. ERAP1$^{-/-}$ Naïve and ERAP1$^{-/-}$ Naïve vs. ERAP1$^{-/-}$ EAE, and this supported our findings about ERAP1 and MS. For example, antigen presentation was the top pathway for ERAP1$^{-/-}$ EAE mice, and ERAP1 is a well-established mediator of antigen presentation (102, 192). Also, in all settings assessed, ERAP1-deficient B cells had many more inflammatory pathways activated and most of the top diseases resulting from IPA were autoimmune. This is to be expected as polymorphisms in ERAP1 are linked with many autoimmune diseases.

In addition to antigen presentation, which has been well studied as a critical contributor to EAE/MS and impacted by ERAP1 modulation, the next top pathway for ERAP1$^{-/-}$ B cells with EAE was B cell development. With this, the top predicted mediator by IPA was a transcription

factor called TCF3. This transcription factor is known to drive B cell development, and it was predicted to be inhibited in ERAP1$^{-/-}$ B cells. We confirmed this to be the case through qRT-PCR validation experiments in the lab. In addition to TCF3 and B cell development pathway changes according to IPA, we also previously published that ERAP1$^{-/-}$ B cells fail to proliferate in comparison to WT (16). Together, this data suggests that B cell development may be impacted by ERAP1 modulation, a process which may be driving EAE. If B cells aren't properly developing, they are likely dying, and we previously published loss of B cells with ERAP1 deficiency. As we investigate here, a possible mechanism of this cell death could be pyroptosis.

Pyroptosis is an inflammatory cell death characterized by GSDMD cleavage by caspase 1 to form pores in the membrane for cytokines, namely IL-1β, to be released (72, 73). At the same time, caspase 1 also cleaves pro-IL-1β into IL-1β for release. As a main marker for pyroptotic function is IL-1β (72, 73), it is very closely interrelated to NLRP3 inflammasome activation, which also causes the release of IL-1β (71). Specifically, NLRP3 inflammasome activation is upstream of pyroptosis. Our lab published that ERAP1-deficient BMDMs have enhanced NLRP3 inflammasome activation, as measured by increases in caspase-1, IL-1β, and IL-18 production. Here, we showed that ERAP1 deficient B cells also had enhanced IL-1β production in response to inflammasome stimuli, similar to what we saw in BMDMs. Although B cells are characterized as an adaptive immune cell type, they can have innate functions as well, namely for specific B cell subtypes such as B1 (176). In addition to having elevated IL-1β production, ERAP1$^{-/-}$ B cells also were more sensitive to pyroptosis inhibitor disulfiram, which blocks GSDMD (197). This, combined with elevated IL-1β production, suggests that ERAP1 deficient B cells are both more sensitive to NLRP3 inflammasome stimuli, and are more reliant on the pyroptotic pathway. In contrast to apoptosis, pyroptosis is a proinflammatory cell death which has been linked with

EAE (196, 202). In these previous reports, mice with either GSDMD knockout or caspase 1 inhibition resulted in improved EAE scoring. Similarly, the NLRP3 inflammasome has been found to be activated in EAE and MS (77, 203), and inhibiting the inflammasome ameliorates EAE as well. Altogether, this data supports that the inflammasome and pyroptosis pathways are upregulated in ERAP1$^{-/-}$ mice, specifically within B cells, and this may be causing enhanced autoimmune phenotypes. Reasons for why pyroptosis would be occurring are unknown at this point, however mechanisms investigated here which are known to cause the pyroptosis, namely the UPR due to ER stress, may play a role.

The UPR is triggered in states of stress, such as ER stress, and has been known to promote worse neuroinflammatory phenotypes (81, 91, 113). We previously published that IRE-1α is phosphorylated in ERAP1$^{-/-}$ BMDMs in comparison to WT BMDMs, supporting that the UPR pathway is hyperactivated in ERAP1 deficient cells (14). Furthermore, we previously found that ER stress is increased at baseline and with stimuli in ERAP1$^{-/-}$ BMDMs. Here, we also show that ER stress is increased at baseline in ERAP1$^{-/-}$ B cells. The specific ER stress gene assessed was sXBP1, as this is the regulator for the IRE1a UPR pathway, and this gene was found to be consistently upregulated in other ERAP deficient immune cells (68, 131). Downstream effects of the UPR often include cell death if the stress can't be compensated for. Therefore, the increase we see in pyroptosis-related cell death may be due to increased UPR activity at baseline. This hypothesis was confirmed with RNA sequencing results showing that Naïve B cells from ERAP1$^{-/-}$ mice had significant upregulation of the UPR pathway in comparison to WT mice. Another molecular mechanism closely related to UPR and NLRP3 inflammasome which can cause cell death is autophagy. Autophagy is another way in which cells try to maintain homeostasis, and is a process reduced by NLRP3 inflammasome activity (75). We found that

autophagy was both increased at baseline, and more greatly reduced in ERAP1$^{-/-}$ B cells with NLRP3 stimuli, which supports our findings of increased inflammasome activity. Together with UPR data, this suggests a baseline level of stress is occurring in ERAP1 deficient B cells, which may be compensated for by autophagy.

Throughout this chapter we investigated why ERAP1$^{-/-}$ B cells are lost during EAE induction and determine the mechanism for their proinflammatory nature. We propose that the mechanism is dependent on a baseline level of ER stress within the cells, which causes upregulation of cellular homeostasis compensation mechanisms such as the UPR and autophagy. Despite the changes in many different pathways shown in this chapter, these pathways might be interconnected. Here we propose a possible mechanism for ERAP1 deficiency causing both B cell loss and enhanced neuroinflammation as assessed by EAE (Figure 6). We propose that ERAP1$^{-/-}$ cells have an increased level of stress at baseline as characterized by increased ER stress, UPR activity, and autophagy. Then, when these cells are stimulated by innate stimuli, like EAE-induced inflammation or during inflammasome activation, they are hypersensitive to the activation and begin producing many more proinflammatory cytokines, causing enhanced proinflammatory effects and worsened EAE. Then, as the cells were initially more stressed, they aren't able to keep up with the elevated demand and begin to die by pyroptosis, which further potentiates the inflammation as even more cytokines are released.

In conclusion, ERAP1 is an important regulator of innate and adaptive immune cell responses, including B cells. ERAP1 deficient B cells are proinflammatory and have enhanced activation and proinflammatory cytokines, inflammasome activity, autophagy and ER stress. Together, this may cause early cell death in comparison to WT B cells, possibly via pyroptosis. The combination of these traits might explain why ERAP1 deficient mice have enhanced EAE

phenotype, and why ERAP1 deficient B cells are responsible for this worsened EAE. This understanding of proinflammatory pathways, especially pyroptosis, reveals possible targetable mechanisms for autoimmune therapy related to ERAP1 polymorphisms. Furthermore, this data helps explain some potential reasons why B cell depletion therapies are effective in the clinic and should be further studied in humans. Overall, by addressing these overactive signaling cascades in ERAP1 deficient B cells, we may be able to explain B cell-related diseases better. As shown here, we believe that inflammatory cell death caused by NLRP3 activation and ER stress may play an important role in such diseases. As such, inhibiting the UPR in B cells may be a viable therapeutic strategy for neuroinflammatory disease and is something that should be further explored.

Chapter 5: Modulation of Endoplasmic Reticulum Aminopeptidase-1 in Natural Killer Cells enhances Anti-Tumor Activity

Authors: Maja K. Blake, Yasser A. Aldhamen, Andrea Amalfitano

Introduction

Cancer immunotherapy research has grown substantially over the recent decade. This growth has been characterized by new drugs and cell-based approaches to enter the clinic, many of which are based in enhancing the host's own immune response toward tumor cells and show amazing efficacy in certain patient populations (204, 205). Cancer immunotherapies have included various methods such as vaccines, checkpoint inhibitors, cellular therapy and monoclonal antibodies (204–206). However promising the results have been, these immune modulatory drugs and cell based therapies do have their drawbacks. For example, certain checkpoint inhibitors are effective for some patients and not others, and certain cellular therapies, such as CAR-T therapy, have significant risks of graft-vs. host disease (207). Additionally, patients can become resistant to such therapies and relapse, if they even respond at all (208). Also, subsets of patients on checkpoint inhibitors have even been found to have disease progression much faster than before beginning the drug, although exact reasons as to why this occurs is not known (209). Therefore, further investigation into new immune targets and development of cancer immunotherapies based in modalities other than T cells is critical to improve current clinical options for patients. A particularly promising immune cell subtype are natural killer cells, which are capable of killing pathogenic or tumor cells similarly to cytotoxic T cells. NK cells have exemplary anti-cancer potential due to low side effect profile and high targeted efficacy.

In addition to immune cell populations, new targets for cancer therapy are being discovered and explored every day. One important target that has not been studied to its full potential is ERAP1. Endoplasmic Reticulum Aminopeptidase-1 (ERAP1) is a known cellular regulator of tumor immune evasion (97, 210, 211). We and other groups have studied ERAP1

and its diverse role in autoimmune disease extensively, characterizing its importance in both innate and adaptive immune responses (12, 17, 20, 166). ERAP1 is defined as an endoplasmic reticulum (ER) enzyme which trims peptides to 8-9 residues for loading onto MHC-1 (29, 104, 145). ERAP1, in the realm of cancer biology, has been shown to induce inhibitory receptors on immune cells, in particular on NK cells, allowing tumors to evade immune recognition (22, 97). Furthermore, studies show that inhibition of ERAP1 within tumor cells is sufficient for inducing NK cell directed tumor cell death (97). ERAP1, and its role in MHC-1 presentation, is also known to regulate T cell directed tumor killing (210). Although researchers have studied ERAP1 down regulation within tumor cells as a potential anti-cancer therapy, the impact of ERAP1 inhibition within immune cell subsets has not been studied.

We previously published that ERAP1 plays an important role in NK cell activation in addition to antigen presentation function by MHC-1 (13). Using an ERAP1$^{-/-}$ mouse model, we found that mice lacking the ERAP1 gene display greater NK cell activity in comparison to WT mice (13). Thereby, in theory, a potent ERAP1 inhibitor may be able to potentiate the same anti-tumor NK cell phenotype as seen in ERAP$^{-/-}$ cells.

Such an inhibitor was recently discovered, Thimerosal, and is a potent inhibitor of ERAP1, when tested in comparison to other small molecules targeting ERAP1 (212). Thimerosal is an organomercury compound which was previously used as a preservative and immune adjuvant in vaccines (213, 214). Although the toxicity of thimerosal has been well established (213), we wished to conduct studies as a proof of principle to investigate whether ERAP1 inhibition in NK cells could elicit their enhanced activity, as we previously published in ERAP1$^{-/-}$ NK cells. Using very low, non-lethal doses of the drug, examined whether enhanced NK cell activity could target tumor cells, and explored how ERAP1 may be impacting NK cell function.

To our knowledge, this is the first report showing that ERAP1 inhibition within NK cells does indeed induce NK cell activity. In the following studies, we show that NK cells target tumor cells and enhance tumor cell death in both murine and human models to a greater extent when ERAP1 is inhibited. We also examine cellular pathways such as ER stress and the inflammasome as potential mechanisms for enhanced activity. Overall, here we a explore a potential new cancer immunotherapy principle characterized by ERAP1 inhibition within NK cells, specifically.

Results

ERAP1 regulates intrinsic NK cells activity *ex vivo*

We first verified ERAP1 inhibition by the ERAP-1 inhibitor by measuring MHC-1 levels in dendritic cells (DCs) and found reduced MHC-1 levels in a dose dependent manner (Fig. 23A). In both DCs and CD3+ lymphocytes, the ERAP1 inhibitor potently inhibited MHC-1 expression, with and without co-stimulation with interferon-gamma (IFNg) (Fig. 23B, Fig. 23C), however co-stimulation with IFNg did potentiate the reduction in CD3+ lymphocytes. Based on previous results showing enhanced NK cell activity in ERAP1$^{-/-}$ mice (13), we next wished to examine if ERAP1 inhibition would induce NK cell activity, as measured by intracellular IFNg production (215). In addition to IFNg, other stimulatory factors known to be involved in priming NK cell effector activity and proliferation such as IL-2 and IL-18 (216, 217) were also included in the splenocyte incubations, and were determined to be optimal for analyzing NK cell activity (data not shown). In addition, optimization of inhibitor dosing was done *ex vivo* in murine immune populations (data not shown). With ERAP1 inhibitor, IFNg was significantly increased in comparison to untreated cells, especially when cytokine cofactors IL-2 and IL-18 were present (Fig. 23C). Importantly, IFNg was increased in isolated murine NK1.1+ cells (Fig.23D) with ERAP1 inhibition, supporting that the increase found in IFNg production is NK cell specific. This enhanced activation altered surface markers as well, as NKP46 was upregulated on NK cells, and stimulatory molecules CD40, CD80, and CD86 were all induced on DCs with ERAP1 inhibition (Fig. S6). Additionally, proinflammatory cytokine IL-2 was induced in treated samples (Fig. S6), further indicating that NK cells, and possibly other cell types, are activated by ERAP1 inhibition. Together, this data demonstrates the heightened activation of various cell types with ERAP1 inhibition.

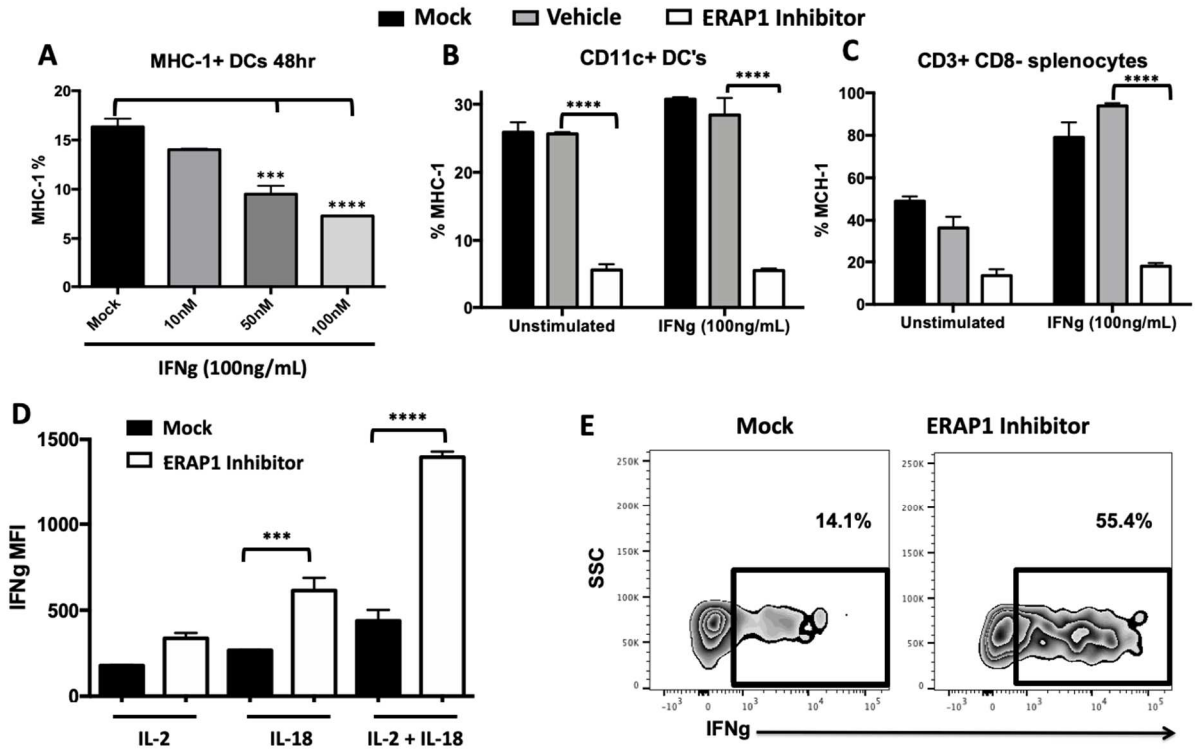

Figure 23: ERAP1 inhibition reduces MHC-1 surface expression and enhances NK cell activity. Splenocytes were collected from C57 B6 wildtype mice and incubated *in vitro* with 100ng/mL interferon-gamma (IFNg). (A) Cells were treated with thimerosal at increasing concentrations for 48 hours and flow cytometry was done for MHC-1 expression on dendritic cells. (B) Splenocytes were treated with thimerosal at 500nM for 18 hours and flow cytometry was used for analysis of specific cell types, CD11c+ DCs and CD3+ CD8- T cells. (C) Splenocytes were treated with thimerosal (350nM) in combination with co-stimulatory signals IL-2 (1ng/mL) and IL-18 (5ng/mL) for 18 hours and intracellular INFg was analyzed by flow cytometry. (D) Splenocytes were incubated with IL-2 (1ng/mL) and IL-18 (5ng/mL) +/- 350 thimerosal for 24 hours and intracellular IFNg was analyzed on NK1.1+ NK cells specifically.

Figure 23 (cont'd)

Data are expressed as means ± SEM. *** $p<0.001$, **** $p<0.0001$, significantly different from mock.

ERAP1 activity mediates tumor cell killing by NK cells

To study whether an increase in NK cell activity targeted tumor cells, we examined the NK cell-directed killing of multiple tumor cells lines with and without ERAP1 inhibition. Using increasing effector-to-target ratios (E:T), we found that multiple tumor cell lines exhibited greater cell death when incubated with splenocytes which were pre-treated with ERAP1 inhibitor. RMA-S lymphoma cells were first used to determine the inducible NK cell activity by ERAP1 inhibition, and a ratio-dependent killing response was found (Fig. 24A). Interestingly, the killing was independent of tumor cell MHC-1 expression, as RMA lymphoma cells had equal killing by NK cells when ERAP1 was inhibited within splenocytes (Fig. 24B). We next wished to determine if isolated NK cells alone were sufficient to target tumor cells. We isolated NK cells from total splenocytes and found that tumor killing was indeed induced by isolated NK cells when ERAP1 function was inhibited, although not profoundly greater than total splenocytes (Fig. 24C).

To verify whether these hyperactive NK cells would target other types of tumor cells, we analyzed their ability to kill the aggressive melanoma cell line, B16, and found a similar trend of increased killing in a ratio-dependent manner (Fig. 24D). Upon doing an antibody-dependent cell-mediated cytotoxicity (ADCC) assay, enhanced tumor killing was found in NK cells with reduced ERAP1 activity (Fig. 24E) as well. This finding further suggests that tumor targeting may be NK cell specific. Together, these findings support that ERAP1 inhibition in NK cells

potentiates their ability to kill multiple tumor cell lines. To ensure that tumor cell death was due to activated NK cells and not ERAP1 inhibition within tumor cells, we incubated tumor cells with ERAP1 inhibitor alone and found no change in cell death, suggesting the tumor cell death is indeed occurring through an immune-mediated mechanism (Fig. 24F) and that tumor cells are not susceptible to death from ERAP1 inhibition alone. These results provide rationale for pursuing ERAP1 inhibition within NK cells as a means of enhancing tumor-directed killing.

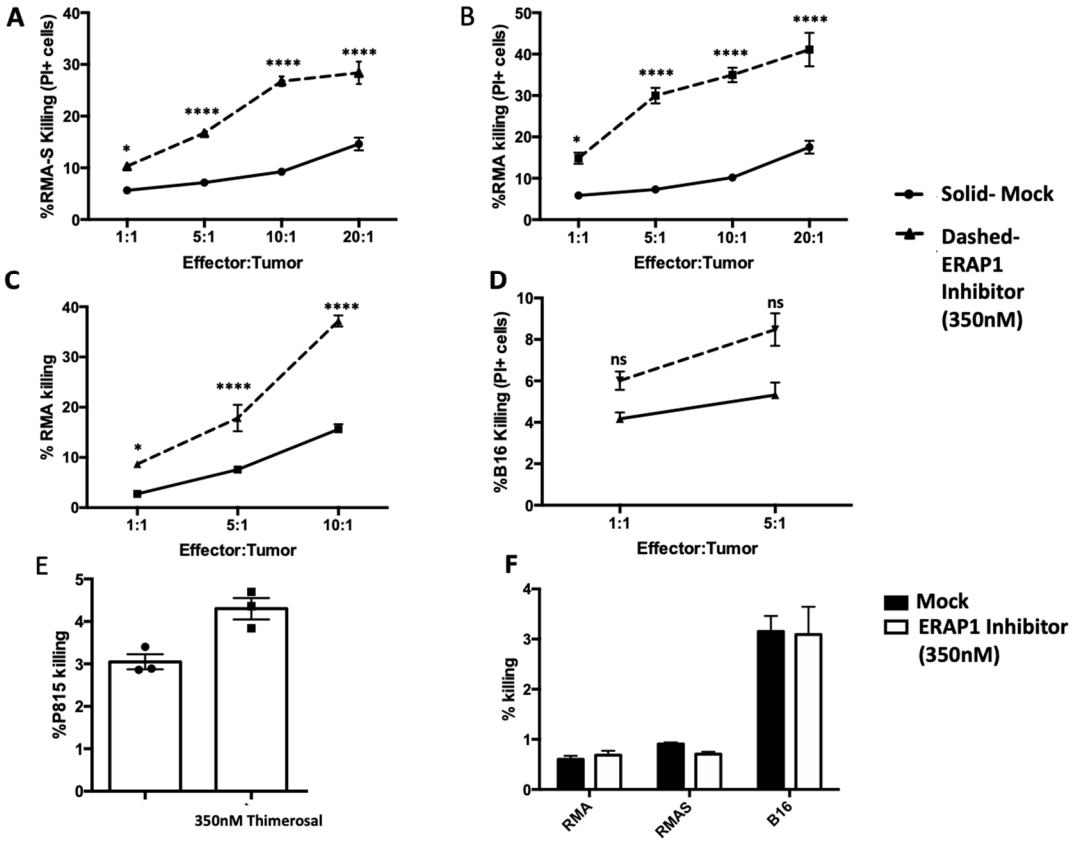

Figure 24: ERAP1 inhibition results in enhanced tumor directed killing by NK cells. (A) Murine splenocytes were stimulated for 16 hours with 1ng/mL IL-2, 5ng/mL IL-18, with or without 350nM Thimerosal. The next day, CFSE dye (5μM) labeled RMA-S (A) or RMA (B)

Figure 24 (cont'd)

cells were added to wells with splenocytes and incubated for 24 hours. Cells were collected, stained with propidium iodide (PI), and cell death was analyzed with flow cytometry. (C) NK1.1 cells were isolated from mouse splenocytes, stimulated for 16 hours with 1ng/mL IL-2, 5ng/mL IL-18, with or without 350nM Thimerosal, followed by CFSE dye (5μM) labeled RMA cell incubation for an 24 hours. Cells were collected, stained with propidium iodide (PI), and cell death was analyzed with flow cytometry as described. (D) Isolated NK1.1 cells from murine splenocytes were incubated with B16 cells with protocol described previously. (E) ADCC assay was completed by using isolated NK1.1 cells from WT splenocytes. Cells were activated for 16 hours with IL-2 and IL-18, with or without 350nM Thimerosal. P815 target cells were incubated with CFSE (5μM), then coated with CD16/CD18 anti-murine antibody for 30 minutes, followed by washing. Target cells and NK cells were cultured in a 1:1 NK-to-P815 ratio for an additional 18 hours, followed by killing assessment with PI as described. (F)Tumor cells incubated with 350nM Thimerosal alone for 24 hours followed by propidium idodide staining. Sample collection and analysis were done the same as previously described. Data are expressed as means ± SEM. * $p<0.05$, **** $p<0.001$, significantly different from mock.

Human NK cell activity is enhanced with ERAP1 inhibition

Upon determining ERAP1 inhibitor efficacy in a murine model, we next wished to pursue human NK cell modulation by ERAP1 inhibition. We found that ERAP1 inhibition was effective in inducing NK cell activity using human PBMCs, with less drug necessary to illicit INFg induction within multiple NK cell populations (Fig. 25A, B). IFNg induction was specific to certain NK cell subtypes, CD3+ CD56+ and $CD56^{bright}CD16^{dim/-}$. CPG co-stimulation, a known

inducer of NK cell activity (218), was necessary to significantly induce the effect (Fig. 25A, B), although alone did not induce any significant changes (data not shown). $CD56^{bright}CD16^{dim/-}$ is an NK cell subset of particular interest because these cells can both secrete cytokines as well as become cytotoxic, and are therefore often studied in regards to tumor biology (219). Together, this data suggests that NK cell activity is potentiated by ERAP1 inhibitor and may be specific to certain NK subtype populations.

To verify if ERAP1 inhibition in human NK cells could also induce tumor killing, ERAP1 activity was inhibited in human PBMCs and cultured with human K562 cells in various E:T ratios. Indeed, human NK cells activated by ERAP1 inhibition killed tumor cells greater than baseline, but with a higher ratio needed of 10 PBMCs: 1 tumor cell (Fig. 25A). Furthermore, although CPG was required to induce significant induction of NK cells in treated PBMCs, CPG also potentiated anti-tumor effects (Fig. 25B). A potential cause for the higher E:T ratio required to see these effects could be because a lower dose of drug was used when pre-treating human immune cells than murine cells, causing reduced overall activation in human NK cells in comparison to murine NK cells. However, a lower dose of drug was necessary due to toxicity at 350nM in human cells when dosing was optimized *in vitro* (data not shown). Together, this data represents that human NK cells are more susceptible than murine cells to Thimerosal toxicity, whereby a smaller dose is appropriate for treatment, and CPG potentiates activated cells to induce greater NK cell activity and tumor-directed killing.

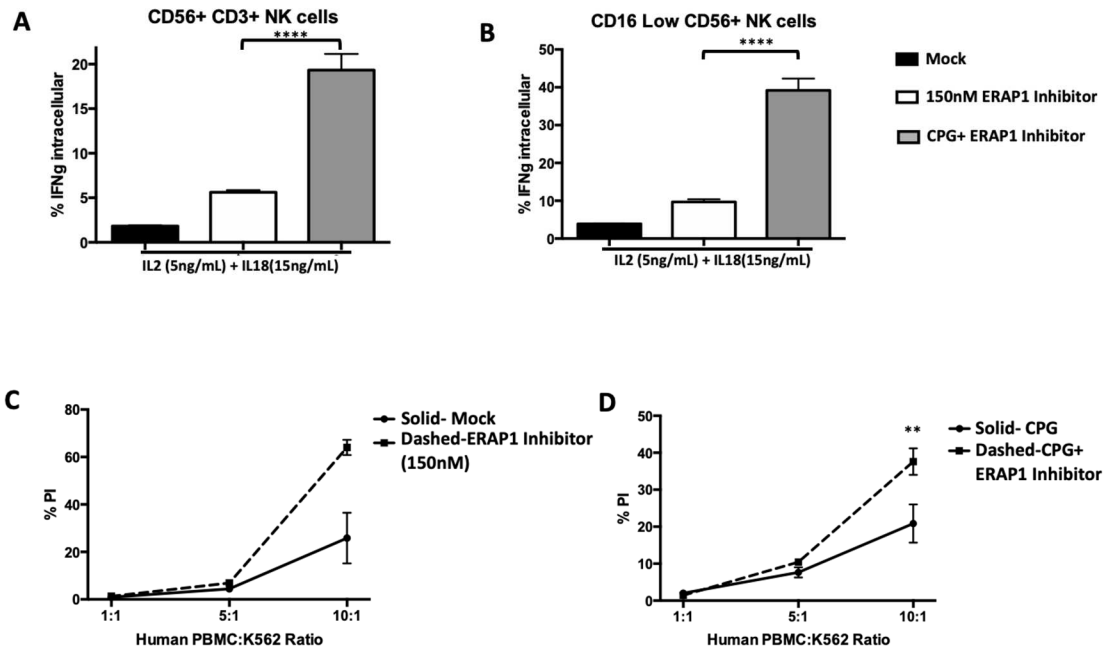

Figure 25: ERAP1 inhibition in human PBMCs results in enhanced tumor directed killing. Human PBMCs were stimulated for 16 hours with 5ng/mL IL-2 and 15ng/mL IL-18, with or without 150nM Thimerosal or DOSE CPG. CFSE dye (5μM) labeled K562 cells were added to wells in various PBMC:K562 ratios, and incubated for an additional 24 hours. Cells were collected, stained with propidium iodide (PI), and cell death was analyzed with flow cytometry. Human PBMCs were isolated and incubated with 5ng/mL IL-2 and 15ng/mL IL-18, with or without 150nM Thimerosal or DOSE CPG for 24 hours and analyzed for intracellular IFNg within various cell populations: (A) CD56+ CD3+ NK cells, (B) $CD56^{bright}CD16^{dim/-}$ cells. K562 killing was analyzed with Thimerosal alone (C) and Thimerosal with CPG (D). Data are expressed as means ± SEM. * $p<0.05$, **** $p<0.001$, significantly different from mock.

ERAP1 inhibition *in vivo* slows tumor growth and prolongs survival

To assess whether the same tumor directed NK cell killing by ERAP1 inhibition was possible *in vivo*, immunocompetent B6/C57 mice were injected with B16 aggressive melanoma cells subcutaneously. Very low doses of ERAP1 inhibitor were injected (as determined by literature review and previous in vivo studies) to account for toxicity of the drug. With just a single intertumoral injection, normalized tumor growth slowed significantly with a 10ug dose (Fig. 26A), and even a 1ug dose caused a trend towards lower tumor volume. Also, mice injected with 10ug had increased survival in comparison to naïve mice (Fig. 26B). Importantly, mice were sacrificed in the study once tumor volumes reached the humane endpoint and not due to toxicity, as this was not present. No signs of weight loss, dehydration, or illness were found in the treated mice. To assess cytokine changes from drug injection, mice were bled soon after injection. At 24 hours post intertumoral injection, various proinflammatory cytokines such as G-CSF, IL-6, and KC (CXCL-1) were elevated in treated mice in comparison to naïve (Fig. 26C). Together, this data shows that ERAP1 inhibition *in vivo* has anti-tumor effects, marked by prolonged survival and enhanced peripheral proinflammatory cytokines.

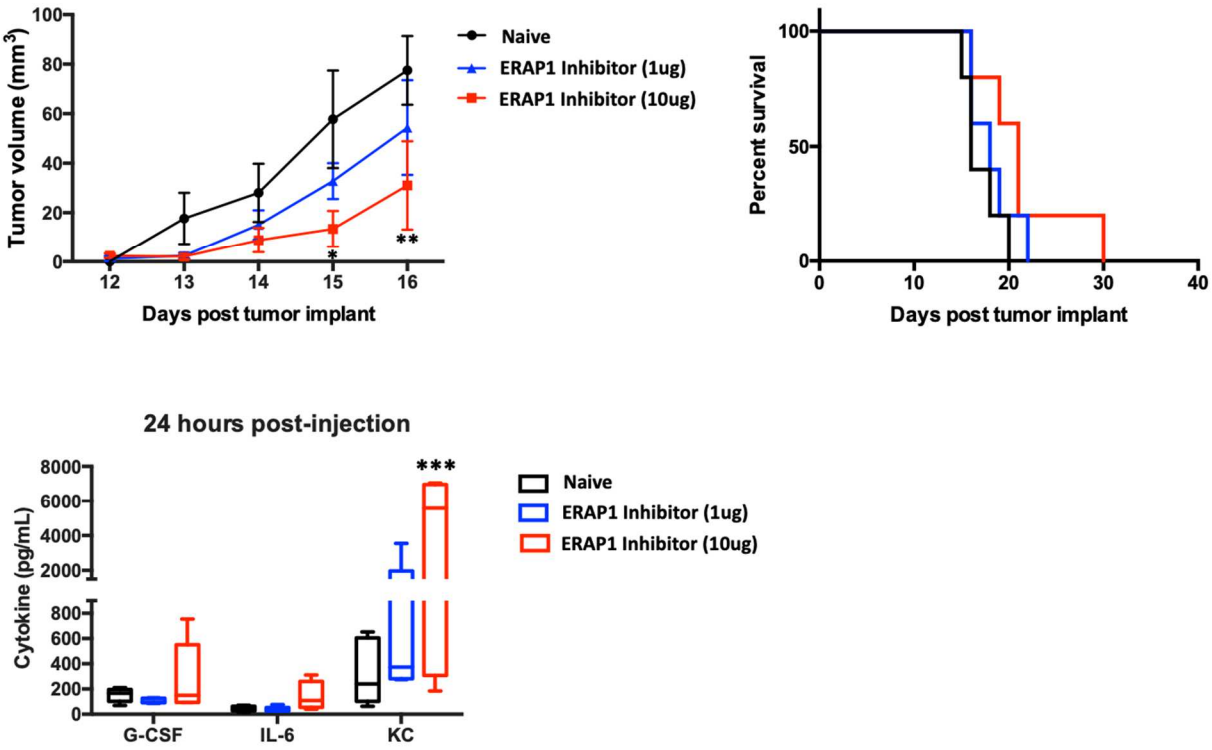

Figure 26: ERAP1 inhibition *in vivo* reduced tumor burden in mice. WT B6 mice and ERAP1$^{-/-}$ mice were injected with 150,000 B16 melanoma cells. Tumor measurements were followed for 10 days. On Day 11, mice were divided into groups of 5 and injected intratumorally with a two different doses of ERAP1 inhibitor 1ug/g and 10ug/g of thimerosal) intratumorally. Mice were closely followed for tumor measurements and signs of toxicity. Tumor measurement was done using a caliper and normalized values to baseline are reported here (A). Tumor volume is expressed as means ± SEM. * $p<0.05$, ** $p<0.01$difference between Naïve and 10ug ERAP1 inhibitor. Upon humane endpoint when tumor volume reached [add], mice were sacrificed as demonstrated by a Kaplan Meyer curve which was significant ($p<0.05$) with a logrank test for trend (B). The full study was concluded at 29 days post tumor injection. Cytokine analysis was done on murine plasma collected 24 hours after injection of ERAP1 inhibitor by retro-orbital

Figure 26 (cont'd)

bleeding technique followed by Bioplex 23-plex assay. Data are expressed as means ± SEM. *** $p<0.001$ with Two-Way ANOVA with Tukey's multiple comparison.

Tumor killing is dependent on NK MHC-1 surface expression

Since ERAP1 inhibition is known to reduce MHC-1 surface levels, and we demonstrated this phenomenon in murine immune cells, we next wished to determine whether upregulating depleted MHC-1 could reverse the anti-tumor phenotype of thimerosal treated NK cells. We used an optimized dose of ovalbumin (ova) peptide based on previous studies in these experiments, which is an effective peptide for antigen presentation on MHC-1 (120). Indeed, ERAP1 inhibitor reduced MHC-1 surface expression on NK1.1+ cells (Fig. 27A), however ova was surprisingly unable to reverse this downregulation of MHC-1. Although the surface expression of MHC-1 was not replenished by ova in presence of ERAP1 inhibitor, we wondered if MHC-1 upregulation would affect tumor killing. Ova did not affect killing in WT activated splenocytes towards RMA cells (Fig. 27B), which was expected as it was also unable to fully replenish MHC-1 levels. However, ova did significantly reduce RMA cell death in ERAP1$^{-/-}$ splenocytes with a 5:1 E:T ratio (Fig. 27C). Importantly, the initial amount of RMA directed killing was similar between treated WT and ERAP1$^{-/-}$ splenocytes (Fig. 27D), further supporting that thimerosal is a potent ERAP1 inhibitor. Together, this data suggests that ERAP1 inhibition within immune populations potentiates tumor cell killing, in a manner that may be dependent on MHC-1 surface expression. However, the reason for why MHC-1 downregulation causes increased NK cell-dependent tumor killing remains unclear.

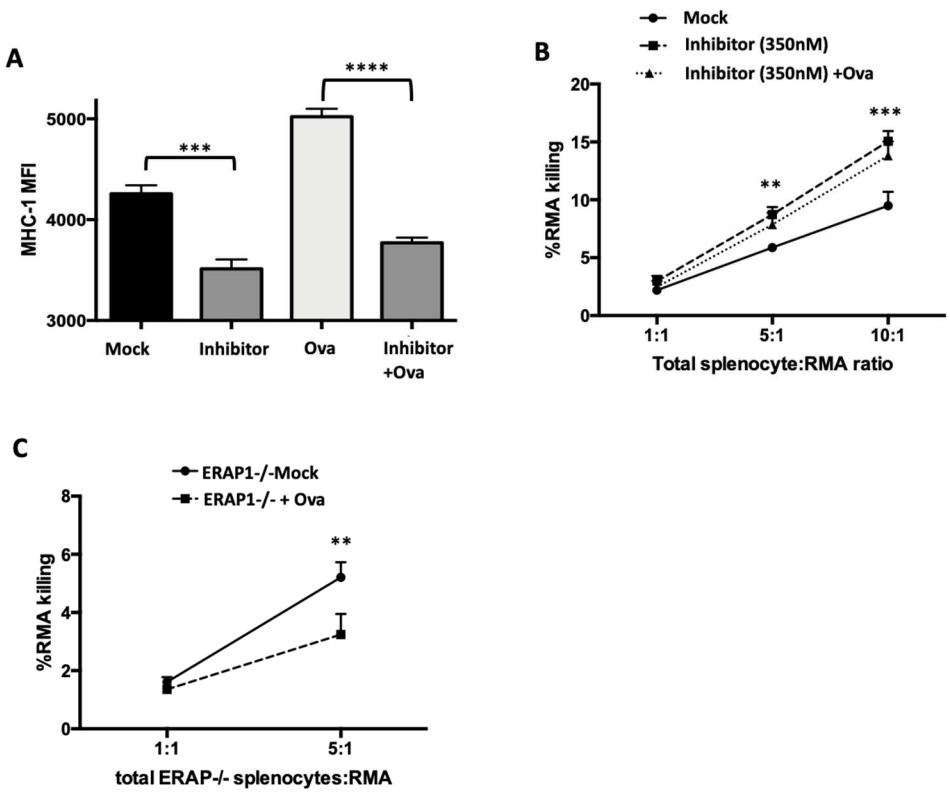

Figure 27: Tumor cell killing may be dependent on MHC-1 surface expression. Splenocytes were collected from WT and ERAP1$^{-/-}$ mice as previously described. All cells were incubated with IL-2 (1ng/mL) and IL-18 (5ng/mL). (A) WT splenocytes were treated with 25uM of Synficol peptide (Ova) alone or in combination with 350nM thimerosal. Cells were collected after 18 hours, and stained for NK1.1+ MHC-1 surface expression, followed by flow cytometry collection using the LSRII flow cytometer instrument. (B, C) Total splenocytes from WT and ERAP-/- mice were treated with 25uM Ova, with or without 350nM thimerosal, and IL-2 and IL-18 as described. Cells were cultured in varying densities in a 96 well plate for approximately 14 hours. Then, RMA tumor cells were labeled with CFSE dye (5μM) and added to splenocytes in increased Splenocyte:RMA ratios and incubated for an additional 18hrs. Cells were collected and

Figure 27 (cont'd)

stained with propidium iodine (PI) prior to flow cytometry analysis. Data are expressed as means ± SEM. * $p<0.05$, ** $p<0.005$, *** $p<0.001$, **** $p<0.0001$, significantly different from mock.

Tumor killing by ERAP1-deficient cells is enhanced during inflammasome activation.

To further study the cause of why ERAP1 inhibition enhances NK cell activity, we first analyzed various gene expression data from WT and ERAP1$^{-/-}$ NK cells (Fig. 28A). ER stress is a known potential downstream effect of the unfolded protein response (UPR) and ER stress has been found to influence MHC-1 surface expression and induce tumor killing by NK cells in cancer cells (119). This, together with our recently published data showing that ERAP1 deficient BMDMs have enhanced inflammasome and ER stress responses, led us to examine ER stress gene expression as well as other genes involved in the unfolded protein response (UPR) pathway (14). Interestingly, we found significantly enhanced ER stress gene sXBP1 (131) expression in isolated ERAP1$^{-/-}$ NK cells in comparison to WT NK cells (Fig. 28A). MyD88, an important gene in NK cells IFNg production and activity (220), was also significantly increased in ERAP1$^{-/-}$ NK cells. The MyD88/AKT pathway and XBP1 are known to work together to influence NK cell survival in humans, and could partially explain why ERAP1$^{-/-}$ NK cells exhibit greater activity in comparison to WT (221).

A potential downstream result of ER stress is inflammasome activation, and we published that ERAP1-deficient BMDMs have both elevated inflammasome activity and enhanced ER stress (14, 119, 131). We therefore decided to analyze the role of the inflammasome in ERAP1 and anti-tumor activity, and its potential for enhancing NK cell activity. When total splenocytes were primed and stimulated with inflammasome agonists MDP and Alum, the NLRP1 (Fig. 28C)

and NLRP3 (Fig. 28D) inflammasomes were activated, respectively. TLR4 stimulation by LPS potentiated both WT and ERAP1$^{-/-}$ splenocyte ability to kill RMA-S tumor cells (Fig. 28B). However, ERAP1 deficient splenocytes were significantly more sensitive to inflammasome activation. In WT cells, inflammasome activity did not have an effect on tumor killing, but interestingly, ERAP1$^{-/-}$ splenocytes showed significantly greater RMAs tumor killing when the inflammasome was stimulated, supporting that ERAP1$^{-/-}$ cells are particularly sensitive to inflammasome stimuli.

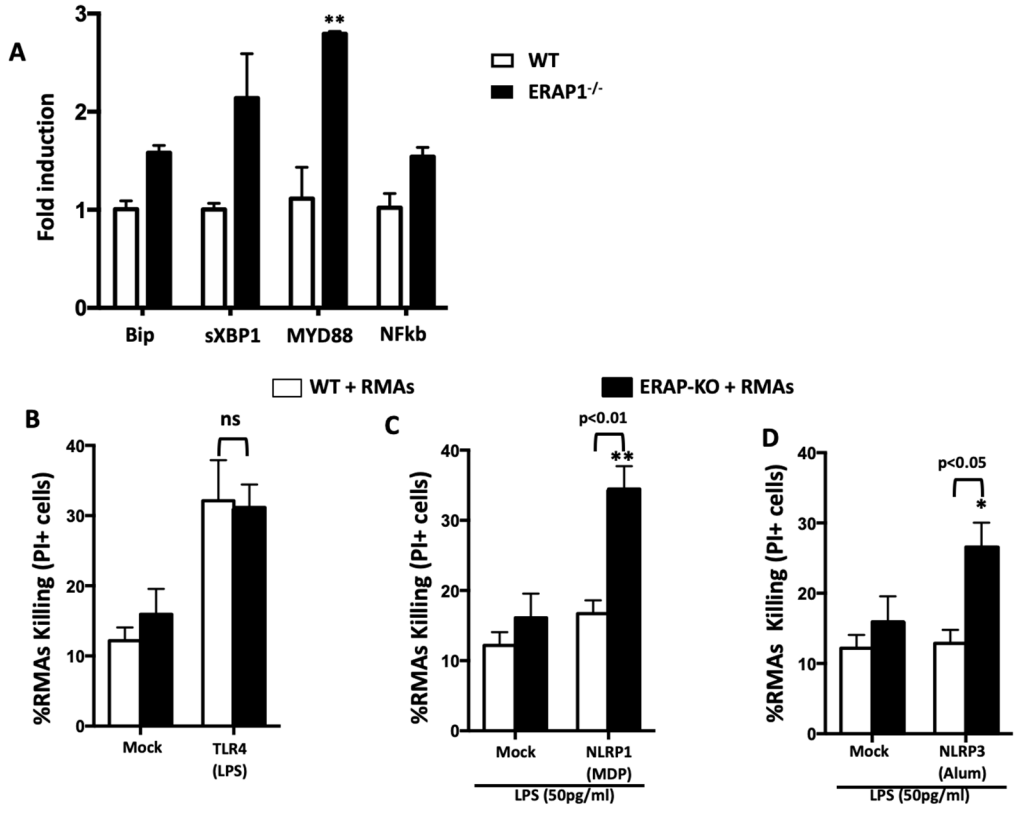

Figure 28: ERAP1 deletion induces greater tumor cell killing with inflammasome activation. Total splenocytes were isolated from WT and ERAP1$^{-/-}$ mice, followed by NK1.1

Figure 28 (cont'd)

isolation per manufacturer instructions. Cells were incubated for 6 hrs. RNA was harvested via Trizol solution and cDNA was made according to manufacturing instructions. Various genes were measured using RT-PCR including TNFa, BIP, sXBP1, MYD88, and NFkB (A). Splenocytes (3 X 10^6) were plated in triplicate in a 24-well plate with 0.5ng/ml murine IL-2. Cells were primed with LPS (50pg/ml) for 4 hours and then stimulated with (B) LPS (10μg/ml), (C) MDP (10μg/ml), and (D) Alum (1mg/ml). RMA-S were labeled with CFSE dye (5μM) and plated with a 1:1 ratio of Splenocyte:RMA-S with the splenocytes for an additional 36 hours. Propidium Iodide (PI) staining was used to evaluate killing by flow cytometry with an LSR-II cytometer. Data are expressed as means ± SEM. * $p<0.05$, ** $p<0.001$.

ERAP1 modulation is synergistic with inflammasome activation for tumor-directed killing.

To determine whether these effects were due to ERAP1 activity specifically, or if it was an off-target phenomenon in ERAP1-deficient cells, ERAP1 activity was blocked using ERAP1 inhibitor DG013. Splenocytes exhibited enhanced killing toward RMAs cells when ERAP1 was inhibited, in combination with LPS (Fig. 29A), MDP (Fig. 29B) and Alum (Fig. 29C). However, ERAP1 inhibition had no effect on killing in presence of LPS (Fig. 29A), showing that cell with and without inhibitor are equally sensitive to LPS induced killing. Furthermore, ERAP1 clearly has an important connection with the inflammasome specifically and not general TLR activation, as killing was potentiated in presence of inhibitor only when the inflammasome was stimulated as well. These results suggest that ERAP1 inhibition induces NK cell cytotoxicity through a mechanism which may rely on ER stress and inflammasome activation. Also, as RMA-S cells

lack MHC-1 surface expression, this data supports that one way to potentially overcome immune evasion by tumors is by ERAP1 inhibition within immune cells.

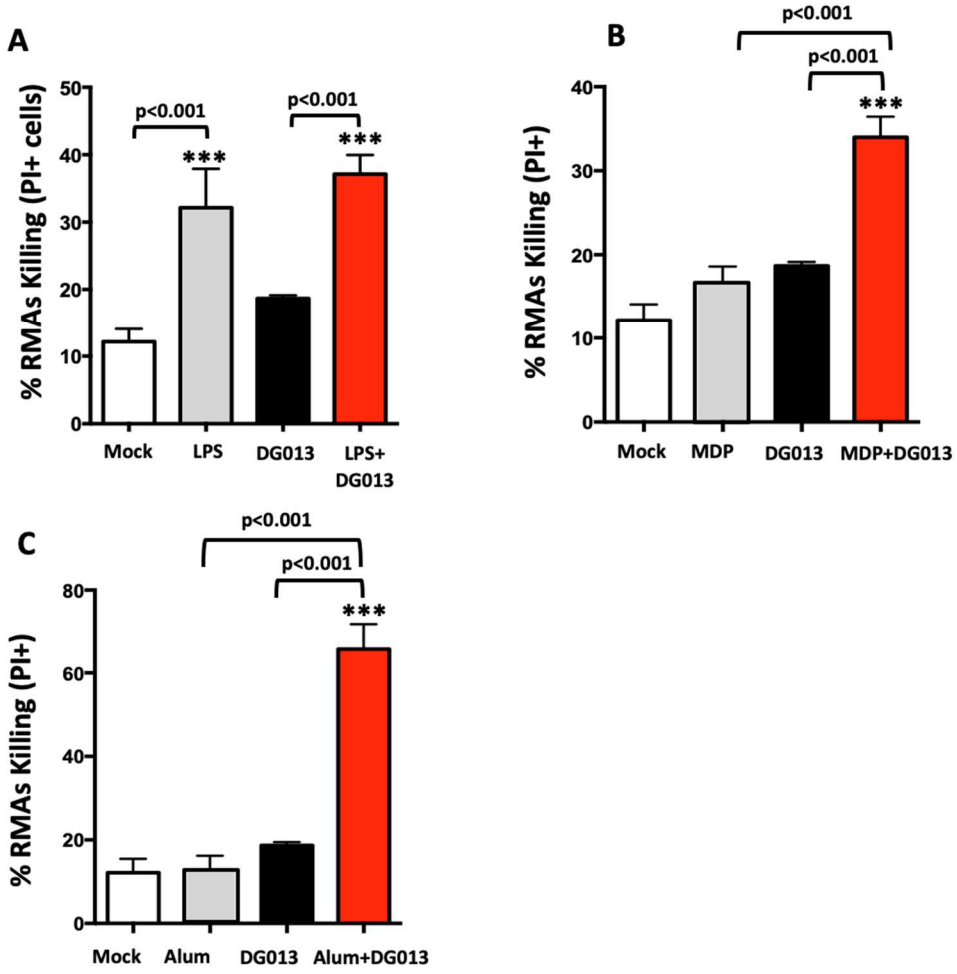

Figure 29: Killing ability of ERAP1 inhibited cells is enhanced with inflammasome stimuli, specifically. Three million splenocytes were plated in triplicate in a 24-well plate with 0.5ng/ml murine IL-2. After cells were primed with LPS (50pg/ml) for 4 hours, they were stimulated with TLR agonist (B) LPS (10µg/ml), and inflammasome agonists (C) MDP (10µg/ml) and (D) Alum (1mg/ml). Target cells, RMA-S, CFSE (5µM) labeled and plated in a 1:1 ratio with the splenocytes for 36 hours. Propidium Iodide (PI) staining was used to evaluate killing by flow

Figure 29 (cont'd)

cytometry with an LSR-II cytometer. Data are expressed as means ± SEM. * $p<0.05$, ** $p<0.001$.

Discussion

Malignancies that were once treated with cytotoxic chemotherapy are now being eradicated by less toxic, immune-based approaches. Checkpoint inhibitors such as anti-PD1 and anti-CTLA4 have shown impressive results in multiple tumor types via T cell regulation (94). Also, CAR-T cells therapies have proven highly efficacious for hematologic malignancies, but come with a toxic profile (206). Unfortunately, many tumors remain either unaffected by such therapies or grow resistant to immunotherapies over time, specifically in solid tumors (208). Moreover, recipients of CAR-T cell therapy can mount a sometimes-fatal immune response against such therapy, i.e. graft-vs. host disease. Therefore, the great success of T cell-based cancer therapies has called for the study of other immune targets, which may have greater, specific efficacy towards a wider range of tumor types. One important population being studied is NK cells, which can target tumors more specifically because they lack T cell receptors and recognize tumor signatures on cells (97). NK cells directly interact with tumor cells, destroying them in the process (22, 97). Indeed, early studies of NK cell-based therapy found remission in cancers treated with adoptively transferred NK cells (220). Given the success of adoptive transfer studies, much effort has been made to develop NK cell-based immunotherapies such as an "off-the-shelf" NK cell-based immunotherapy. However, creating immortal synthetic immune therapies proves difficult, and has yet to show safety and efficacy in humans. Methods for enhancement of NK cells function *in vivo* is of upmost importance to further the promise of NK

cell-based therapy in cancer. Certain cytokines such as IL-15 have shown promising results for activating and expanding NK cells activity towards tumor cells, but disadvantages of these therapeutic approaches such as toxicity profiles hinder excitement.

Many targets have been identified to amplify the immune response such as CAR-T and cytokines, however, an important protein involved in antigen presentation and innate and adaptive immune responses, ERAP1, remains understudied in NK cells. ERAP1 is an aminopeptidase which trims peptides to proper amino acid length for antigen presentation. Although it plays a major role in the adaptive immune response, ERAP1 also is a critical regulator of the innate response as well. ERAP1 and its role in cancer has indeed been investigated, however no treatments studied have advanced into clinical practice. Also, the approach has been to downregulate ERAP1 within tumor cells, leaving the immune system untouched to target the affected tumor cells. Here, we propose ERAP1 inhibition within NK cells specifically, as a novel approach to cancer immunotherapy.

Multiple ERAP1 inhibitors have been created, however none as specific for ERAP1 aminopeptidase activity as thimerosal, an ethyl mercury containing compound previously found in many vaccines as an immune adjuvant. Using thimerosal as an ERAP1 inhibitor, we demonstrate here as a proof of principle that ERAP1 inhibition induces NK cell activity and targeted anti-tumor responses. As we show in this manuscript, enhanced NK cell activity may be linked to inflammasome activation and ER stress, so harnessing these mechanisms may prove to be less toxic ways to enhance anti-tumor effects and should be further studied. Also, as ERAP1 inhibition is efficacious in both tumor cells (22) and NK cells, a combination therapy whereby NK cells are activated with ERAP1 inhibitor and targeted towards tumor cells by inhibiting ERAP1 within tumors, might prove highly effective in stubborn cancer subtypes. Given

thimerosal's toxic profile, conducting more *in vivo* studies to investigate this topic was beyond the scope of this paper and more research should be done into optimizing current ERAP1 inhibitors in development.

Despite using very low doses of thimerosal *in vivo*, early phase tumor growth was slowed with ERAP1 inhibitor in a dose dependent manner and overall survival was improved. Although the early phase of tumor growth was slowed, this was not stable as tumors began to grow faster after day 16, likely due to the fact that another dose of drug was not given to the mice for safety reasons. If a safe ERAP1 inhibitor was dosed more frequently, this tumor reduction may be more stable. Inflammatory changes were visibly seen after injection as well, whereby treated mice had an enhanced inflammatory response at the tumor site characterized by edema visually. Cytokines such as G-CSF, IL-6 and KC/CXCL1 were also upregulated in treated mice. CXCL-1 is a potent recruiter of neutrophils (222), so dramatic increases in this cytokine may cause more neutrophil chemotaxis to the tumor site. This, in combination with enhanced NK cell activation, could in part be the reason for enhanced inflammatory and tumor responses to treatment, although this was not fully explored in these studies.

We recently published that ERAP1 exerts its anti-inflammatory effects as an important negative regulator of the inflammasome, and here show that inflammasome activation was also required for NK cells to target tumor cells. Therefore, one possible way ERAP1 inhibition is affecting NK cell activity is by inducing the inflammasome in macrophages. Indeed, ERAP1 inhibition was found to increase activation markers such as CD80 on various cell types. Upon stimulation, macrophages release IL-18, a potent primer of NK cell activity. Previous studies have shown that mice without the NLRP3 inflammasome have uncontrolled tumor growth, due to lack of NK cell activation by IL-18 (223). In our studies, total splenocytes activated with

ERAP1 inhibitor were found to have enhanced anti-tumor activity with lower effector: tumor ratios than isolated NK cells, and therefore may be due to the priming effects of IL-18 on NK cells through inflammasome activation.

One potential cause for the enhanced inflammasome activity found in ERAP1$^{-/-}$ cells is enhanced endoplasmic reticulum (ER) stress, as we recently illustrated (14). Previous studies have shown that enhanced ER stress can drive certain disease states including type 2 diabetes and ankylosing spondylitis, and results in altered NK cell activity (112). Furthermore, cytotoxic activity of NK cells towards cancer cells can be amplified by XBP1 expression, an important regulator of unfolded protein response (UPR) genes (221). In addition, reduced MHC-1 expression itself is linked to enhanced ER stress levels and downstream enhanced NK cells activation (119). Together, these data represent ER stress as a possible mechanism for cancer cell killing, and a mechanism by which our model may be acting through as ER stress genes were induced in ERAP1$^{-/-}$ NK cells.

Interestingly, we also discovered that MyD88 is upregulated in ERAP1-deficient NK cells. MyD88 is a critical regulator of the immune response to infection in NK cells through TLR, IL-1βR, and IL-18R (224). As we previously published that ERAP1$^{-/-}$ cells have enhanced TLR signaling and inflammasome activity, this further supports that ERAP1 may be modulating the inflammasome and pro-inflammatory signaling within NK cells. Also, MyD88 and XBP1 can work together to influence NK cell survival in humans and could partially explain why ERAP1$^{-/-}$ NK cells exhibit greater activity as demonstrated here, possibly by means of prolonged survival (221).

Overall, these proof of principle studies illustrate the impact of ERAP1 inhibition on NK cell activity. Whether the cause of enhanced NK cell killing is due to enhanced inflammasome

activity, ER stress mechanisms or solely MHC-1 surface expression is not clear, but these mechanisms should be further studied as other less toxic methods for bolstering NK cell activity towards tumor cells are optimized. As the priming and enhancement of NK cells remains a limitation for NK cell-based immunotherapies, perhaps ERAP1 inhibition could be a promising answer to such dilemmas.

Chapter 6: Immune Profiling Techniques and Methods

Immune profiling techniques

In parallel with *in vivo* models, *in vitro* cell based assays are utilized throughout this dissertation to study the immune responses to ERAP1 modulation. Specifically, we studied the immune system using flow cytometry-based studies and genomic methodologies, like RNA sequencing. Recent advances in both instrumentation and computing have allowed for the quick and deep analysis of many parameters, offering a much more comprehensive view of the immune environments. These techniques helped us study and dissect molecular mechanisms and immune regulation.

Flow cytometry

Flow cytometry has revolutionized the immunology field as a whole since its development. Its ability to assess multiple different cell types and multiple parameters at once has driven its applicability to a wide variety of immune profiling projects, including studying the immune tumor microenvironment and autoimmune related diseases. Fluorescent activated cell sorting (FACS) or flow cytometry is the incredibly useful methodology in cytometry. Flow cytometry allows one to evaluate the phenotype and the frequency of a wide variety of cells in the immune microenvironment, as well as assess the expression levels of various cell surface receptors, intracellular signaling molecules, and transcription factors. However, it should be noted that most FACS data is analyzed at the level of bulk populations of immune cells and not the single-cell level.

Regarding methodology, flow cytometry first involves the processing of samples into a single-cell suspension. Cells are then stained with a viability dye and fluorescently-tagged antibodies for various cell surface or intracellular markers, and each marker is analyzed by excitation of various fluorophores with lasers. Emission of each fluorophore is then captured

with focused detectors. Over time, more and more fluorophores have been developed and become readily available. Together with new technical advancements, such as 96 well plate loaders and benchtop flow cytometers, FACS allows for highly accessible, cost effective profiling of the immune microenvironment. Similarly, flow cytometry instruments have advanced dramatically from once only being able to detect a few fluorophores, to now being able to differentiate upwards of 30 unique fluorophores at once (225).

Flow cytometry methods can now be used to detect specific cell signaling functions within a cell as well. For example, one can analyze phosphorylated proteins via Phospho-flow to examine the activation of important intracellular signaling molecules, for which antibodies are widely commercially available. Additionally, flow cytometry offers a quick and relatively straightforward way to determine cytokine expression and transcription factor levels at cell subset resolution, as compared to more conventional techniques such as ELISA's and Western blot's. Flow cytometry is also a straightforward and useful method in assessing cellular events such as autophagy and the cell cycle (226). Imaging flow cytometry has come of age as well, which can be used to visualize cell morphology and sub-cellular marker localization in single cells in real time, such as inflammasome assessment by evaluating apoptosis associated speck-like protein containing a CARD (ASC) formation and cell-cell interactions (227).

Spectral Cytometry

In comparison to conventional flow cytometry which detects fluorophores, spectral cytometry is an advanced method that analyzes the entire spectra of all fluorophores. Spectral cytometry therefore addresses some of the major concerns with conventional flow cytometry including spectral overlap and autofluorescence. Spectral cytometry uses prisms to refract photons in a wavelength-dependent manner (228). By using prisms and different detector

orientations, spectral cytometry allows for one to analyze entire fluorophore spectra. This essentially means that many more fluorophores can used in each experiment. By utilizing spectral cytometry, many more signals (i.e. cell surface receptors, intracellular cytokines, phosphorylated proteins, etc) can be detected at once; upwards of 40 markers in fact (229, 230). This allows for more markers to be assessed on each sample (as opposed to separating a sample to stain with multiple flow cytometry panels), which is highly desirable when cell number is low or sample is precious.

Analysis Approaches to High-Dimensional Cytometry

As cytometers have become more powerful and specific, and additional fluorophores have been created, high-parameter cytometry has become more widespread. High-dimensional cytometry is an explorative endeavor, often times more hypothesis driving than testing an already developed hypothesis. This is due to the large amount of parameters which can be detected. Although this is important for the scientific field as it encourages more comprehensive immunophenotyping, conventional flow cytometry analytic approaches fall short here. With increased parameters comes an increased complexity in necessary data analysis approaches. To address this, software has been created to handle high-parameter data sets. This software bridges raw data into clustering of various parameters, which will be discussed next. One such tool is an R-based workflow package called Cytometry dATa analysis Tools , or CATALYST (231). This package lets the user manipulate, cluster, and visualize data in effective manners for high-dimensional data.

Once data has been pre-processed with software such as CATALYST, clustering software like FlowSOM can be implemented, which clusters data based on cellular similarity (232). More specifically, FlowSOM creates clusters based on Self-Organizing Maps (SOMs)

within which hold events, or cells, which are most similar to one another (i.e. B cells, $CD4^+$ T cells, etc.…). This is important because subtle marker differences and similarities, which would segregate subsets, can be visualized. These subtle group differences can be easy to overlook if analyzing manually. Commonly used follow-up visualization tools to FlowSOM are t-Stochastic Neighbor Embedding (t-SNE) and Uniform Manifold Approximation and Projection (UMAP). These powerful software tools allow for visualization of two-dimensional clusters where cells that are more related to one another are grouped closer together. It is important to note that t-SNE only groups cells by local similarities, but does not retain global data structure, while UMAP does retain global data structure. These software applications can also be used through GUI-based flow cytometry software such as FlowJo.

High-dimensional flow cytometry provides researchers with many more data points and gives a broader view into the immune microenvironments. Software development for cytometry analysis not only makes data analysis much more efficient and unbiased, but also detects small differences in populations which could go unnoticed when analyzing manually, especially in small sample size populations such as the tumor microenvironment.

RNA-seq

Genomic-based approaches to immune-profiling represent both an established and rapidly evolving modality. One of the earliest genomic approaches to investigate immune cells simply involved analysis of bulk RNA-seq data with any one of a number of publicly available tools capable of predicting the frequency of different cell types present in the sample. There are a number of these computational tools available including: CIBERSORT (233), ImmuCC (a murine-specific implementation of CIBERSORT) (234), Bisque (235), MOMF (236), and MuSiC (237). These approaches predict the cellular composition of a sample subjected to bulk

RNA-seq via comparison of gene expression in the sample to a reference gene expression matrix via support vector regression or other machine learning approaches. Reference gene expression matrices can be derived from single-cell RNA-seq (scRNA-seq), FACS-sorted cell population bulk-RNA-seq, or established databases. Of these, CIBERSORT was the first developed and is currently the most widely used approach. While these methods have been shown to be fairly accurate (238), they are still limited by the fact that the provided results are predictions and do not represent ground truth measurements. However, as bulk RNA-seq data is readily available for many tissue and cell types and the cost of bulk RNA-seq is considerably lower than scRNA-seq, this makes cellular deconvolution tools widely useful for analysis of existing datasets and when resources are limited.

Methods

Animals

Mice deficient in ERAP1 (gift from Dr. Kenneth Rock (University of Massachusetts Medical School)), C57BL/6 WT and μMT mice were maintained at Michigan State University. For some experiments, ERAP1$^{-/-}$ mice were crossed to IL-10^{GFP} reporter mice (The Jackson Laboratory), identified as ERAP1$^{-/-}$/IL-10^{GFP}. Groups of mice were age- (8 to 10 weeks) and male mice were used. All animal procedures were reviewed and approved by the Michigan State University EHS, IBC, and IACUC and conformed to NIH guidelines (AUF number: 02/13-045-00). Care for mice was provided in accordance with PHS and AAALAC standards.

Ex vivo splenocyte-derived cell culture

Splenocytes were isolated from male 6-8 weeks old WT and ERAP1$^{-/-}$ mouse spleens, and red cells were removed using *ACK* lysis *buffer* (Invitrogen, Carlsbad, CA), as previously described (17). Splenocytes were cultured in RPMI medium 1640 (Invitrogen, Carlsbad, CA)

supplemented with 10% fetal bovine serum (FBS) and 1X penicillin-streptomycin-fungizone (PSF). For specific assays, mouse NK cells, human NK cells, B2 cells, or Pan-B cells were isolated using negative bead selection isolation kits (Miltenyi Biotec). For MHC-1 expression analysis, splenocytes (5×10^5 cells) were cultured with 100ng/mL INFg (Sigma Aldrich) for 48 hours followed by treatment with varying doses of Thimerosal (Sigma Aldrich). For murine NK cell activation assays, splenocytes and NK cells were incubated at 5×10^5 cells with dose IL-2 (R&D Systems) and IL-18 (R&D Systems) for 16 hours, followed by 350nM Thimerosal for an additional 24 hours. Human splenocyte and NK assays were performed by culturing 5ng/mL IL-2 (R&D Systems) and 15ng/mL IL-18 (R&D Systems) followed by 150nM Thimerosal for the same time periods described above.

Ex vivo bone marrow derived macrophage cell culture

Bone marrow cells were extracted from the femurs of male 6-8 weeks old WT and ERAP1$^{-/-}$ mice, and red cells were removed using *ACK* lysis *buffer* (Invitrogen, Carlsbad, CA), as previously described (239). Bone marrow cells were cultured in Dulbecco's Modified Eagle Medium (DMEM) supplemented with 10% fetal bovine serum (FBS), 1% penicillin-streptomycin-fungizone, and 30% supernatant derived from confluent L929 cell cultures. At day 7, immature macrophages (5×10^5 cells) were collected and plated in a 24-well plate and primed with LPS (20ng/ml) for 12 hours or primed and pre-treated with TUDCA (500µg/ml) for 12 hours. Cells were stimulated for another 16 hours with heat-killed listeria monocytogenes (HKLM) (10^8 cells/well), lipopolysaccharide (LPS) (1µg/ml), monophosphoryl lipid A (MPLA) (1µg/ml), *CpG* oligodeoxynucleotides CpG ODN (2.5ug/ml), polyriboinosinic: polyribocytidylic acid (poly(I:C)) (10µg/ ml), nigericin (10µg/ml), muramyl dipeptide (MDP) (10µg/ml), flagellin (250ng/ml), or alum (1mg/ml) (all from InvivoGen, San Diego, CA, USA). For AIM-2

inflammasome activation, cells were transfected with poly(dA:dT) (8μM) (InvivoGen, San Diego, CA, USA) using *Lipofectamine 2000* (Life Technologies Inc.) according to *manufacturer's protocol.* For MSU crystal stimulation, BMDMs were primed with LPS (15ng/mL) and stimulated with 100ug/mL MSU crystal (InvivoGen, San Diego, CA) for approximately 18 hours. Cell supernatants were collected and used for ELISA and BioPlex assays.

Cell Lines

Non-adherent tumor cell lines were cultured in RPMI medium 1640 (Invitrogen, Carlsbad, CA) supplemented with 10% fetal bovine serum (FBS) and 1X penicillin-streptomycin-fungizone (PSF). All murine cell lines used in this study were derived from C57BL/6 (B6, H-2^b) mice. RMA and RMA-S cell lines are T cell lymphomas derived from the Rauscher MuLV-induced RBL-5 cell line (240). Additionally, B16.F10 (CRL-6475), P815 (TIB-64), K562 (CCL-243) cells were obtained directly from ATCC.

Quantitative RT-PCR

To determine relative levels of ER stress related genes, 2×10^6 isolated immune cells of interest were incubated for 6 hours and RNA was harvested using TRIzol reagent (Invitrogen, Carlsbad, CA, USA) according to the manufacturer's protocol. Following RNA isolation, reverse transcription (RT) was performed on 180 ng of total RNA using SuperScript II (Invitrogen) RT and random hexamers (Applied Biosystems, Foster City, CA, USA) per manufacturer's protocol. RT reactions were diluted to a total volume of 60 μl, and 2 μl was used as the template in the subsequent PCR reactions. Primers were designed using Primer Bank web-based software (http://pga.mgh.harvard.edu/primerbank/). The primers that were used are as follows:

GAPDH: Forward: 5'AGAACATCATCCCTGCATCC3'; Reverse:

5'CACATTGGGGGTAGGAACAC3'; TNFa Forward:

5'CCCTCACACTCAGATCATCTTCT'3; Reverse: 5'GCTACGACGTGGGCTACAG3'; BiP:

Forward: 5'CGAGGAGGAGGACAAGAAGG3'; Reverse:

5'CACCTTGAACGGCAAGAACT3'; XBP1spl: Forward:

5'TGCTGAGTCCGCAGCAGGTG3' and Reverse: 5'GCTGGCAGGCTCTGGGGAAG3';

MYD88: Forward: 5'AGAGCTGCTGGCCTTGTTAG3'; Reverse:

5'TTCTCGGACTCCTGGTTCTG3';

NFkb: Forward: 5'ATGGCAGACGATGATCCCTAC3' ; Reverse:

5'CGGAATCGAAATCCCCTCTGTT3

Quantitative PCR (qPCR) was carried out on a QuantStudio 7 Fast Real-Time PCR System using SYBR Green PCR master mix (Applied Biosystems). The comparative C_t method was used to determine relative gene expression using GAPDH to standardize expression levels across all samples. Relative expression changes were calculated based on comparing experimental levels of a respective transcript of ERAP1$^{-/-}$ to WT cells.

Cytokine Measurement

Various cytokines were analyzed in total splenocytes and splenocytes cultured with RMA tumor cells following Thimerosal stimulation for 48 hours. Additionally, cytokine measurement on murine plasma samples 24 hours after ERAP1 inhibitor injection were assessed. A 23-plex multiplex cytokine assay was performed according to the manufacturer's instructions (Bio-Rad, Hercules, CA) via Luminex 100 technology (Luminex, Austin, TX), as previously described (17). The top significantly changed cytokines were reported.

Cell Staining and Flow Cytometry

Bone marrow cells were harvested and differentiated into macrophages, followed by stimulation with various NLRs and TLRs agonists. BMDMs were stained with either APC-conjugated anti-CD86, Pacific Blue CD80, APC MHC-I, PE MHC-I, PE-Cy7 CD11b, or V450 CD4. Cells were incubated with antibodies for 45 min on ice and washed with FACS buffer. For caspase-1 activity, FAM-FLICA *in vitro* caspase-1 detection kit (Immunochemistry Technologies, Bloomington, Minn., USA) was used and caspase-1 activity was measured, according to the manufacturer's protocol. For p-p65 activation, BD Phosflow Perm Buffer (BD Biosciences, San Jose, CA) was used with Alexa-Fluor 647 p-p65 (Cell Signaling, Danvers,MA) staining, and measured with flow cytometry.

Isolated NK cells were stained with MHC-I, CD56, CD3, CD16, and/or intracellular IFNg-APC (4 μg/ml; BD Biosciences, San Diego, Calif., USA). Cells were incubated on ice with the appropriate antibodies for 45 min and washed with FACS buffer. For intracellular staining, 1 million splenocytes were plated; Brefeldin A was added to a final concentration of 1 μg/mLand incubated for 3 hours at 37°C. Following incubation, splenocytes were washed with FACS buffer and surface stained, fixed and permeabilized with 2% formaldehyde for 20 minutes at room temperature and incubated on ice with IFNγ-APC (8 μg/ml) for 1 hour. A BD LSR II and Cytek Aurora instrument were used for data collection and data were analyzed using FlowJo software.

Killing Assay

NK cell killing was assessed by incubating total splenocytes, isolated NK cells from C57 or ERAP1$^{-/-}$ mice, human PBMCs or isolated human NK cells 12 hours with IL-2, IL-18 and Thimerosal in varying concentrations (100nM-500nM). Immune cells were plated in a 24-well plate based on desired Effector:Tumor ratios (1:1, 5:1, and 10:1) with varying concentrations of

Thimerosal for approximately 16 hours. Cultured tumor cell lines were labeled with 5μM CFSE dye (ThermoFisher) and added to wells. All cells were then collected and prepared for flow cytometry. Cells were stained with propidium iodide (PI) for two minutes and data was collected on an LSR II instrument for CFSE (FITC laser) and PI (PerCP-Cy5.5 laser). Data was analyzed using FlowJo software (Tree Star, San Carlos, CA).

Antibody-Dependent Cell-Mediated Cytotoxicity (ADCC) Assay

The ADCC protocol was adapted from a previously published assay (241). NK cells were isolated from C57 WT splenocytes and cultured overnight at a density of blank cells in a 96-well plate with 350nM Thimerosal, 5ng/mL IL-2 and 15ng/mL IL-18. The next day, P815 target cells were incubated separately with CFSE, and then coated with DOSE CD16/CD18 anti-murine antibody for 30 minutes at 37ºC, followed by washing the cells three times with PBS and RPMI 1640 media. Target cells and NK cells were then cultured in a 1:1 NK-to-P815 ratio for an additional 18 hours in a 24-well plate. Cells were stained with propidium iodide (PI) for two minutes and data was collected on an LSR II instrument for CFSE (FITC laser) and PI (PerCP-Cy5.5 laser). Data was analyzed using FlowJo software (Tree Star, San Carlos, CA).

Spectral Cytometry

Cells were isolated from the CNS, spleen, blood, and inguinal lymph nodes as previously described (242). Cells were stained with various antibodies as described utilizing BD Brilliant Stain Buffer (50μL per sample) whenever multiple Brilliant dyes were used in combination. Viability staining was performed with Zombie NIR (BioLegend) and Fc receptors were blocked with murine Fc block (BD Biosciences). Intranuclear staining was performed with the BD Transcription Factor Buffer Set kit (BD Biosciences) per manufacturer's instructions. Samples were acquired on a 5 laser Cytek Aurora Spectral Cytometer or a 3 laser BD LSR II and data was

analyzed using FlowJo version 10.6.1 (Tree Star) and the R computing environment. High dimensional single-cell spectral cytometry was performed in R. The CATALYST package was used to perform all analyses with a cell annotation and dimensionality reduction approach as previously described (243). After data clean up in FlowJo, files were exported as FCS files, loaded into R, and an arcsinh transformation of 6000 was applied to all spectral cytometry data. Unbiased clustering was performed with FlowSOM (244), and clusters were annotated and manually merged as necessary down to functionally distinct immune cell subsets.

For experiments using IL-10^{GFP} mice and/or *in vivo* labeling, IL-10-GFP^+ and negative (and IV^+ and negative) cells were combinatorially boolean gated in FlowJo allowing for absolute positive/negative discrimination in high dimensional analyses performed in R. In all analyses where IV labeling was performed, IV^+ cells were removed before final generation of figures and statistical analysis. Additionally, high dimensional spectral cytometry analysis was done entirely in FlowJo employing an exhaustive manual gating scheme allowing identification of nearly all immune cells, the accuracy of which was confirmed by unbiased FlowSOM clustering also performed in FlowJo.

For the *in vivo* analysis of B cell proliferation, proliferation was measured via CFSE or CTV dye dilution. Specifically, we analyzed the proportion of cells actively proliferating from the previous measurement. This was done since the baseline population will shift over time since all cells are proliferating to some degree over this extended time period. By shifting the baseline from previous timepoints we are able to assess which cells are continuing to proliferate at substantial levels.

DSS and Cytokine Measurement

To induce intestinal inflammation, mice were treated with 3% DSS (molecular mass 36-

40 kDa; MP Biologicals) dissolved in sterile distilled water. Mice were given DSS in sterile drinking water *ad libitum* for experimental days 1-7 (controls received sterile water only) followed by regular water until the end of the study. DSS solutions were made fresh on day 0 and 3 and left until day 7. Sample sizes were based on power calculations and blinded. After 7 days of DSS treatment, colons were excised and a one centimeter piece of distal colon was homogenized mechanically in PBS containing 1% NP-40 and complete protease inhibitor cocktail (Roche). Protein concentrations were determined by BCA assay. Protein (100 μg) isolated from distal colons of naïve and DSS-treated mice was used in a 23-plex multiplex cytokine assay. The assay was performed according to the manufacturer's instructions (Bio-Rad, Hercules, CA) via Luminex 100 technology (Luminex, Austin, TX), as previously described (17). *In vitro* cell supernatant cytokines were measured with the same 23-plex multiplex cytokine assay following LPS priming (20ng/mL), LPS treatment (100ng/mL), Nigericin (10ug/mL), TUDCA (500ug/mL), or GSK8612 (MedChemExpress, Monmouth Junction, NJ).

EAE Model

On day -2, mice were injected with 300μg recombinant human MOG peptide ($rhMOG_{35-55}$) (SigmaAldrich) or 33μg full-length recombinant murine MOG ($rmMOG_{1-125}$) (Anaspec) with equal parts complete Freund's adjuvant (CFA) as previously described. 400ng of pertussis toxin (MilliporeSigma) was injected intraperitoneally on days -2 and 0. Mice were scored daily on a scale of 0-5 as previously described, with a score of 0 = no symptoms, 1 = tail paresis, 2 = partial hindlimb paresis, 3 = complete hindlimb paresis, 4 = complete hindlimb paresis and front limb involvement, 5 = moribund or dead. Mice were humanely euthanized if a score of 4 or 5 was reached. Investigators were blinded to genotypes of mice during the 1st attempt at each

experiment (these are presented as representative in figures). All EAE-related mouse studies had sample sizes based on power calculations and were blinded.

Adoptive Transfer Studies

Splenocytes were collected from WT and ERAP1$^{-/-}$ mice as previously described. B cells were isolated per manufacturer's guidelines using the murine B cell isolation kit (Miltenyi Biotec) and injected I.V. retro-orbitally ($1x10^7$ cells) into μMT mice (The Jackson Laboratory). Mice were bled to confirm B cell adoptive transfer two days later via FACS. Five days after transfer, EAE was induced in mice with rmMOG$_{1-125}$ as described above. For co-transfer of both WT and ERAP1$^{-/-}$ B cells into the same mouse, WT B cells were first isolated and labeled with CFSE (5μM) and ERAP1$^{-/-}$ B cells were labeled with CellTrace Violet (10μM) per manufacturer's guidelines. Cells were mixed in a 1:1 ratio and a total of $1x10^7$ cells were injected I.V. into each μMT mouse.

CNS Immune Cell Isolation

Mice were anesthetized and trans-cardiac perfusion with 15-20mL of sterile PBS was performed. Brains (parenchyma and meninges) were then removed, placed in ice-cold 1X HBSS and minced using a scalpel. Brains were digested using a digestion cocktail for 45 minutes at 37□ as previously described (245). Samples were then homogenized with a dounce homogenizer and the digestion reaction was stopped using EDTA and 1X HBSS containing 10% FBS. The lysate was then subjected to gradient centrifugation using Percoll as previously described (246). Isolated immune cells were resuspended in FACS buffer and stained for spectral cytometry. For experiments involving *in vivo* circulating immune cell labeling, before trans-cardiac perfusion, 5μg of anti-CD45 SparkBlue 550 antibody was injected trans-cardiac through the left ventricle

and allowed to circulate for three minutes. The mouse was then trans-cardiac perfused with PBS as described above.

Integrated scRNA-seq Analysis

We first searched for scRNA-seq datasets containing publicly available raw sequencing data of PBMCs from healthy individuals. We identified seven datasets (167, 175, 247–251) meeting these criteria, six of which used the 10X Genomics platform, and one which used Seq-well (251). For 10X datasets, we downloaded the raw FASTQ files, processed them through the CellRanger pipeline and aligned reads to the GRCh38-3.0.0 human reference genome. Resulting count matrices were saved for later analysis with the Seurat package (252). We then used the output .bam file from CellRanger to call each individual sample for the presence or absence of the ERAP1 K528R SNP. This was accomplished by running mpileup from BCFtools with the following command: -Ou -A -r 5:96700273-96995983 -f ~/hg38_ref_fasta/Homo_sapiens.GRCh38.dna.primary_assembly.fa. SNPs were called from the resulting .bcf file using the call command from BCF tools with the following command: -mv -Ob -o snp_calls_XX.bcf. BCFtools was then used to index the .bcf file and a list of all SNPs in the ERAP1 region was generated using the BCFtools query command as follows: -f '%CHROM %POS %REF %END %ALT\n' -r 5:96760273-96935983 snp_calls_XX.bcf > ERAP1_snps_XX.txt. Resulting SNPs were run through a custom R script to identify the presence of the K528R SNP for each individual. Notably, for a few individuals, we tested if applying Q30 phred-score filtering affected our ERAP1 SNP calls and found that it did not (data not shown).

Seq-well data was downloaded as SRA files which were converted to FASTQ files using faster-dump from SRAtoolkit. Reads were aligned to GRCh38-3.0.0 using STAR, indexed with

SAMtools, and SNPs were called as described above. Count matrices were downloaded from publicly available pre-processed data from the original authors (251).

All count matrices were loaded into R as Seurat objects using Seurat V4.0.3 and 10X datasets were merged together. Metadata containing K528R SNP info, study info, sample_ID info, etc was appended to all cells. Seq-well data was read into R and merged together into a Seurat object using the EpicTools package (https://github.com/ajwilk/EpicTools). Metadata was appended to these files and all 10X data was merged with Seq-well data. Cells with < 200 features, > 4100 features, or > 20% of transcripts being mitochondrial were removed.

For dataset integration the harmony R package was used (253). Briefly, the Seurat object containing all cells from all datasets was processed with SCTransform, the percent of mitochondrial transcripts was regressed out, and 30 PCA dimensions were calculated. Harmony was then run on the SCT assay of this Seurat object and both study and individual donor variability were regressed out of the integration. The standard SCTransform Seurat workflow was then continued and putative B cells were identified from UMAP plots and DEGs across cell clusters. Putative B cells were subsetted out from the rest of cells. Visual inspection of data revealed that there were very few cells from the Seq-well technology, and that these cells exhibited technology-specific clustering; hence, they were removed from downstream analysis.

B cells still exhibited study-specific clustering so the B cells were subjected to further dataset integration using the SCTransform integration approach embedded in Seurat V4.0.3. Briefly, SCTranform was rerun on all cells after splitting them up by study and the SCT assay was used to find integration anchors and to integrate the data. Visual inspection of this data now revealed minimal technology-specific clustering confirming efficient integration.

Reclustering and differential marker analysis identified a few clusters of non-B cells/plasma cells which were removed. Data was re-clustered again and dimensionality reduction was also performed again. Clusters were annotated in an unbiased manner using the SingleR package. Here, we performed cluster-level annotation using three reference datasets (HPCA, Blueprint, and Monaco). SingleR effectively annotated all of our clusters with high confidence into five distinct B cell/plasma cell clusters. These clusters exhibit no study-specific biases, with the exception of the "Exhausted B cell" cluster which is composed almost entirely of cells from Kang, et al. (167).

Identification of DEG's and data visualization of the resulting high-quality single-cell dataset were performed using the normalized RNA counts (and not SCTransformed or integrated data) as recommended by the Seurat development team. DEGs were called using MAST and these DEGs were validated using a second approach (Wilcoxon rank sum test) showing very high concordance (data not shown). Pathway-level analyses were performed using IPA (Qiagen) on statistically significant DEGs from various B cell subsets. Bar plots of enriched pathways are colored according to the directionality of the changes in that pathway with more purple color indicating increased pathway activation and more tan color indicating less pathway activation in cells containing the K528R ERAP1 SNP.

RNA Sequencing

In Chapter 4 specifically, splenocytes were isolated from age-matched male WT C57bl/6 and ERAP1-KO mice at steady state (n=3 per genotype) and during peak EAE induced with rmMOG1-125 (n=3 per genotype). 2 x 10^6 B2 B cells were FACS sorted on a BD Influx cytometer into chilled 1.7 Ml Eppendorf tubes pre-coated in FBS. RNA was immediately isolated from each sample within 10 minutes post-sort with the RNeasy micro kit (Qiagen). RNA

was checked for concentration and quantity with Qubit (Thermofisher) and Bioanalyzer (Agilent technologies), respectively. Samples passing QC were ribosomal RNA depleted using the QIAseq FastSelect rRNA MHR kit (Qiagen) and libraries were prepared using the Illumina Stranded Total RNA Library Preparation Kit with IDT for Illumina Unique Dual Index adaptors. Total RNA libraries were quantified and quality control checked with Qubit and TapeStation assay's, respectively. Libraries passing QC were sequenced on a NovaSeq6000 with 2x100bp paired end sequencing using a SP flow cell. Base calling was done by Illumina Real Time Analysis (RTA) v3.4.4 and output of RTA was demultiplexed and converted to FastQ format with Illumina Bcl2fastq v2.20.0.

FastQ files were QC'd with FastQC, preprocessed with fastp, mapped to the mm10 murine genome with STAR v2.7.9, and transcripts were quantified with feature counts. Differential gene expression was performed with DESeq2. Predicted cell type composition of each samples was performed with ImmuCC. Pathway-level analyses were performed using IPA (Qiagen) on statistically significant DEGs from B cells with different genotypes.

Data and Code Availability

All raw data is available upon reasonable request. Analysis code can be found at: https://github.com/poconnel3/OConnell_et-al_ERAP1_MS_manuscript

Statistical analysis

Statistical significance for all measurements was determined by student's t-test, one-way ANOVA with *Newman*-Keuls post-test, or a two-ANOVA test with Tukey's multiple comparisons, and $p < 0.05$ was considered statistically significant. Data are represented as mean ± SEM, with * $p<0.05$, ** $p<0.01$, *** $p<0.001$, **** $p<0.0001$. All statistical analyses were performed using GraphPad Prism software version 6.0. For RNAseq and high dimensional deep

phenotyping, statistical analyses are listed in all figure legends and were performed in either GraphPad Prism V8 or the R computing environment. Cell subset frequency comparisons and differential marker expression on cell subsets from experiments employing high dimensional spectral cytometry were statistically compared with a GLMM implemented through the diffcyt R package (254). All heatmaps were locally scaled.

Chapter 7: Concluding Remarks and Future Directions

Concluding Remarks

In review, ERAP1 is an aminopeptidase localized to the ER that trims peptides for antigen presentation onto MHC-1 molecules (38, 102). These peptides are then presented to the rest of the immune system, namely CD8+ T cells, initiating a robust immune response. In addition to this specific role in adaptive immunity through antigen presentation, ERAP1 functions, (or lack thereof) impacts the innate and adaptive immune responses in various immune cell types including CD4+ T cells, NK cells, B cells, and macrophages (13, 14, 17, 18). Although ERAP1's role in adaptive immunity has been well studied, the mechanisms underlying its impacts on the innate immune response remain largely unknown. Correlative studies have found increases in proinflammatory cytokine production and activation markers in innate immune subtypes deficient in normal ERAP1 functions (13, 14, 17, 18), but the molecular mechanism for how and why this occurs has not been fully discerned. As part of this dissertation, we feel that for the first time, we have uncovered possible molecular mechanisms disrupted by lack of normal ERAP1 functionality. This work is important to study because non-synonymous polymorphisms in the ERAP1 gene are linked with multiple human diseases including MS, AS, UC, and even cancer (26, 36, 126). Our lab has utilized a unique ERAP1$^{-/-}$ mouse model with global loss of ERAP1 functions within all cell subtypes to begin to dissect how loss of normal ERAP1 functions results in disruption of immune system regulation to cause disease, as represented here throughout this dissertation.

In Chapter 2, we determined how loss of ERAP1 functions impact a subset of innate immune cells, i.e.: BMDMs. By studying ERAP1 deficient BMDMs, we are able to more fully understand ERAP1's role in innate immune responses. In Chapter 2, we found that ERAP1$^{-/-}$ BMDMs have enhanced inflammasome activity, as measured by IL-1β production. The

inflammasomes are proinflammatory enzymatic complexes that when stimulated, provoke downstream innate responses such as autophagy and pyroptosis/cell death (70, 72, 86, 196). The inflammasome has been studied in many autoimmune diseases, including MS, and is a known contributing factor to autoimmune disease pathogenesis (75, 203, 255). Our results suggest that inflammasome activation could, in theory, explain the enhanced autoimmune phenotypes we have described in studies of the ERAP1$^{-/-}$ mouse previously, and possibly correlate abnormities noted in the human populations that possess high disease risk ERAP1 SNPs. In this chapter, we also begin examining causes for the increased inflammasome activity and find that ER stress/UPR activation to likely be the culprit. Exaggerated ER stress and UPR activation has long been hypothesized as being a result of loss of normal ERAP1 aminopeptidase functions, causing improper peptide trimming and accumulations in the ER, coupled with abnormal folding of peptide chaperone molecules such as MHC-I, including HLA-B27, a variant also highly associated with human autoimmune diseases, and a gene in epistasis with ERAP1 in many of these same diseases. Indeed, ER stress and UPR activation have been linked with a multitude of autoimmune diseases (66, 81, 119), which supports the translational impact of this data. Here we began to determine why the inflammasome would be hyperactivated in ERAP1 deficient cells and verified that elevated levels of ER stress and the UPR to be enhanced, for example in ERAP1 deficient BMDMs. ER stress is a known cause of UPR activation (68, 256). Similarly, we find the same elevated baseline ER stress in CD4+ T cells, though it remains unknown whether this caused enhanced inflammasome activation in the CD4+ T cells, suggesting that lack of ERAP1 functions may cause heightened inflammasome activation throughout key segments of the mammalian immune system.

In Chapter 3, we tested the translational impact of our work by focusing on an autoimmune disease which has been linked with a specific ERAP1 variant: Multiple Sclerosis. MS is an incurable autoimmune disease affecting the neurological system. Although ERAP1 had been genetically linked to MS via GWAS studies (8, 26), the mechanisms underlying this association remained unknown until recently through our work. We began by assessing whether ERAP1 played a role in MS development by using a mouse model of MS called EAE. We induced EAE in WT and ERAP$^{-/-}$ mice and discovered that ERAP1$^{-/-}$ mice developed much more severe EAE phenotypes than WT mice. After deep phenotyping of the neuroimmune landscape by flow cytometry we identified B cell alterations in ERAP1$^{-/-}$ mice, and knowing that anti-B cell therapies have been highly effective for MS patients (174), we assessed whether ERAP1 deficient B cells were directly responsible for increased EAE severity. Within these studies we found that specific B cell subset numbers and activity was altered by ERAP1 modulation. The innate-like B cell subset B1 was greatly impacted by loss of ERAP1 function, and various activation markers such as CD69 and CD80 were induced in ERAP1 deficient B cells as well. Although loss of B cells is expected after adoptive transfer, ERAP1 deletion seemed to greatly affect the proliferation and survival of these cells. Our results show that B cells lacking ERAP1 have both exaggerated expression of T cell co-stimulatory/activation markers and fail to proliferate *in vivo*. Our findings that ERAP1$^{-/-}$ mice are more susceptible to EAE, and that this is likely a B cell mediated effect, supports GWAS studies linking human ERAP1 SNPs with susceptibility to MS, and the importance of B cells in MS disease.

In Chapter 4, we examined how loss of normal ERAP1 functions might directly affect the development, and/or functions of B cells. We first validate the exaggerated immune activation of ERAP1$^{-/-}$ B cells in comparison to WT B cells *ex vivo* with various stimulations. We show that

the enhanced proinflammatory state identified in ERAP1$^{-/-}$ B cells correlated with enhanced EAE phenotype. We also conducted global transcriptome analysis of B cell derived RNA and determined that ERAP1 deficient B cells have upregulation of many DEGs in comparison to WT both at baseline and during EAE. These findings suggest that there is increased gene transcription and overall biological processes occurring in ERAP1 deficient B cells during EAE in comparison to WT B cells undergoing an identical induction of EAE. However, certain genes such as LTF, S100A8, Gm 15439, and TCF3 may prove to be viable drivers of these differences. It is important to note that the ERAP1$^{-/-}$ mouse model used throughout this dissertation is due to a loss of function deletion (removal of exons 5 and 6) within the active site for enzymatic activity, but not the total protein, creating a truncated ERAP1 protein if expressed. This may be why ERAP1 transcriptome expression was dramatically reduced but not fully gone in ERAP1$^{-/-}$ B cells.

Using IPA software analysis, we were also able to determine that although many genes are altered in ERAP1$^{-/-}$ murine B cells, a common shared pathway that is altered is the UPR. These data support our findings of increased ER stress in other cell types throughout this dissertation and may explain, in part, why ERAP1$^{-/-}$ B cells are driving exaggerated EAE in our ERAP1 dependent models of EAE.

Given our findings that ERAP1 deficient cells have enhanced inflammasome activity due to ER stress/UPR activation, and that ERAP1$^{-/-}$ B cells also have enhanced ER stress/UPR based on the transcriptome analysis, we also evaluated the NLRP3 inflammasome in ERAP1$^{-/-}$ B cells. We found that IL-1β production was significantly upregulated in ERAP1$^{-/-}$ B cells, which is the main indicator of NLRP3 inflammasome activity. This is interesting because the role of the inflammasomes within B cells, and especially in the context of neuroimmune disease, has not

been well explored. Also, ERAP1$^{-/-}$ B cells had significantly elevated IL-6 production. IL-6 is a critical proinflammatory cytokine produced by B cells which has been linked with development of MS (257). This suggests that IL-6 neutralization may be beneficial in MS patients with ERAP1 polymorphisms.

As IL-1β was more greatly induced in ERAP1$^{-/-}$ B cells, we looked closer into pathways downstream of NLRP3 activity. As a reminder, in Chapter 3 we appreciated that ERAP1$^{-/-}$ B cells failed to proliferate as well as WT and were fully lost in μMT mice after adoptive transfer around Day 28. The idea that losing B cells would drive EAE phenotype may seem counterintuitive at first, as death of proinflammatory B cells may in theory reduce the severity of the EAE phenotype, but there are various forms of cells death. Specifically, pyroptosis is a unique mechanism for proinflammatory cell death, whereby IL-1β is released, causing even more inflammation. This type of cell death is triggered by NLRP3 activation, which we found to be upregulated in ERAP1$^{-/-}$ B cells. When we began to examine pyroptosis in ERAP1 deficient B cells, we quickly appreciated that pyroptosis was elevated as measured by GSDMD and IL-1β. Furthermore, the use of a pyroptosis inhibitor, disulfiram, caused a much greater reduction of IL-1β in ERAP1$^{-/-}$ B cells than in WT B cells, and in a dose dependent manner. Therefore, pyroptosis may likely be the mechanism for cell death during EAE, and loss of the proinflammatory ERAP1$^{-/-}$ B cells may indeed be promoting an even worse EAE phenotype due to more IL-1β release.

The global RNA sequencing results in Chapter 4 and *in vitro* data in Chapter 2 support that ER stress is indeed upregulated in ERAP1$^{-/-}$ immune cells at baseline. As the UPR is known to drive inflammation and has been linked with MS and other autoimmune diseases (66, 81, 119), this may be why ERAP1$^{-/-}$ mice have worse autoimmune phenotypes. This hypothesis

suggests that ER stress may be the starting point for all of the downstream signaling cascades seen in ERAP1 deficient immune cells, including NLRP3 inflammasome activation and cell death. Albeit that all of this research was completed in ERAP1 deficient animals and therefore is most closely related to humans with ERAP1 polymorphisms, all the pathways studied here have indeed been correlated with B cell related autoimmune diseases. As MS currently has no cure, any insight into possible new therapies for the disease is important, and these pathways may prove to be effective targets for evaluation in the clinics. Therefore, we believe that investigating the use of small molecules targeting these pathways, for which many already exist, for alleviation of autoimmune disease severity is supported.

In summary, the first three chapters of this dissertation explore the mechanisms underlying ERAP1's role in human autoimmune disease. Although many studies have been done to associate ERAP1 polymorphism with autoimmune disease, the molecular mechanism supporting why ERAP1 modulation would cause enhanced autoimmunity was truly not studied until now. Here, we propose that the reason for enhanced innate signaling and a proinflammatory signature in ERAP1 modified immune cells may be due to upregulated inflammasome activation and ER stress. Throughout this thesis, we demonstrate these pathways as being induced in multiple immune cell types. Therefore, this thesis suggests that possible avenues for treating autoimmune disease caused by either ERAP1 mutations or B cell modifications, may be through targeting the NLRP3 inflammasome or interrelated pathways.

While autoimmunity is due to enhanced immune activation, cancer progression and onset is largely due to loss of correct immune monitoring and potentially, immunosuppression. Therefore, in theory, the intense immune activity found in autoimmune disease could be used in cancer control, as a means of boosting immune activity. In this thesis, we put the theory to the

test knowing that ERAP1 modulation not only activates macrophages, T cells, and B cells, but also NK cells (13). Natural killer cell activity is indeed enhanced by ERAP1 modulation (13), and in Chapter 5 we show that this enhanced activity can target tumor cells. We also show that ERAP1$^{-/-}$ NK cells have enhanced killing with inflammasome activation, paralleling the BMDM and B cells work shown here and also further supporting the close relationship between ERAP1 modulation and inflammasome activity. Throughout Chapter 5 we use an ERAP1 inhibitor to demonstrate that inhibition of ERAP1 does impact NK cell activity and tumor directed killing. Although the data is promising, the drug used in our studies is neurotoxic and is largely not recommended for human use. Therefore, this is a "proof of principle" method for ERAP1 inhibition to examine ERAP1's possible role in cancer directed therapy.

Overall, this dissertation proves that ERAP1 is a mediator of both autoimmune responses and the tumor microenvironment. Although diverse, the reasoning for ERAP1's unique role in many diseases is likely due to its role in innate immunity. Specifically, its function in cellular stress and inflammasome mechanisms. Further development into harnessing its full immune potential will not only aid in the treatment of humans with ERAP1 polymorphisms, but also B cell driven autoimmune diseases and cancer. Therefore, ERAP1 modulation is a vessel for studying a wide variety of immune based diseases and is clearly a critical regulator of immune responses.

Future Directions

Building upon this work, it would be important to confirm our data in more *in vivo* human disease models to ensure the findings could translate to human diseases. First, to examine whether the inflammasome, in particular the NLRP3 inflammasome, can directly cause the proinflammatory phenotype of ERAP1-deficient immune cells, there are several experiments that

could be done. An NLRP3 inhibitor such as MCC950 could be administered prior to ERAP1$^{-/-}$ mice being induced to undergo inflammatory colitis with DSS or neuroinflammation with EAE, to see if the use of the inhibitor prevents or significantly lessens disease phenotypes in comparison to ERAP1$^{-/-}$ mice without treatment. Also, PBMCs from autoimmune patients with human ERAP1 polymorphisms could be assessed for overactive IL-1β release to confirm that an overactive NLRP3 is indeed correlated with ERAP1 linked autoimmune disease. Similar to the inflammasome, one could further validate the hypothesis that ER stress is causing enhanced autoimmune phenotypes in ERAP1 deficient animal models. ERAP1$^{-/-}$ mice could be treated with an ER stress inhibitor (such as TUDCA) prior to induction of ERAP1 dependent autoimmune phenotypes like EAE. Alternatively, ER stress could be inhibited in specific cell types, such as B cells prior to adoptive transfer into μMT mice and EAE disease induction. The fact that safe pharmaceuticals already exist for both inflammasome and ER stress inhibition is a great advantage. Indeed, other groups have begun developing small molecules targeting the UPR and have alluded to its possible benefit clinically. However, these drugs moving into clinical trials remains outstanding, and we believe this data supports the rationale for such work.

In Chapter 3 and 4 we find loss of B cell proliferation capabilities in the face of ERAP1 deletion, and this may be a possible mechanism for B cell loss during MOG peptide induction of EAE in ERAP1$^{-/-}$ mice, ie this is due to induction of exaggerated pyroptosis. To test this hypothesis, it would be interesting to treat ERAP1$^{-/-}$ B cells with disulfiram, a pyroptosis inhibitor, prior to adoptive transfer into uMT mice treated with MOG peptide, and assess for any improvement in the resultant EAE phenotype as compared to uMT mice treated with mock treated (with vehicle) ERAP1$^{-/-}$ B cells . We would predict improvement in B cell recovery after adoptive transfer with disulfiram therapy. Alternatively, one could generate a double knockout

mouse model, lacking both GSDMD and ERAP1, and adoptively transfer these GSDMD$^{-/-}$ /ERAP1$^{-/-}$ B cells into uMT mice induced to EAE. If pyroptosis was the reason for the enhanced EAE phenotype in mice receiving ERAP1$^{-/-}$ B cells, these mice would have EAE disease similar to WT. If significant, this result would support the use of pyroptotic inhibitors in the human clinics for ERAP1 driven MS initially, or MS in general. Indeed, use of Caspase 1 inhibitors in GSDMD$^{-/-}$ mice has been shown to attenuate EAE disease (196, 202). Disulfiram is an affordable, already FDA approved medication for alcohol use disorders, and could be an affordable and safe way for the healthcare system to treat patients with MS. On a related note, transcriptome analysis revealed that a transcription factor involved in B cell proliferation and development, TCF3, to be reduced in ERAP1$^{-/-}$ B cells. Thereby, possibly re-introducing TCF3 into ERAP1$^{-/-}$ B cells, either by plasmid transfection or lentiviral infection, could reverse the proliferation defects seen in these cells. This technology is something our lab is currently working on developing.

The common theme of this dissertation is that ERAP1 variants have been associated with a wide range of autoimmune diseases, and even cancer. In Chapter 5 we use an ERAP1 inhibitor to activate NK cells, and improve their tumor-directed killing. Higher doses (as would likely be required for cancer therapy) of this specific ERAP1 inhibitor is highly toxic (213, 214) because it is a methylmercury compound, but very low doses are safe as it was previously used as a preservative in human vaccine . Therefore, it would be necessary to modify the structure of the compound to remove the mercury group, which makes it an organomercury compound and toxic. Alternatively, other ERAP1 inhibitors which are currently in development at pharmaceutical companies (Wolf Therapeutics), could be applied to NK cells, specifically. Determining a safe and effective way to deliver ERAP1 inhibition to NK cells is of upmost importance for fully

validating whether ERAP1 inhibition within NK cells can be a viable new cancer immunotherapy. It would likely be beneficial if the ERAP1 inhibitor could be encapsulated into a nanoparticle for specific delivery to NK cells, to minimize ERAP1 inhibition in other cells. Another approach would be to make an "off-the-shelf" ERAP1$^{-/-}$ NK cell line. This would address the common concern of NK cell adoptive transfer human trials of how to activate NK cells *in vivo*, as these cells would already be in an active state because of ERAP1 inhibition.

As one can appreciate, many of the ERAP1 dependent mechanisms that perturb B cell functions examined here (inflammasome, ER stress/UPR, ERAP1, pyroptosis) are druggable targets, and many drugs are already in development. This is a major advantage for translating this work into humans and bringing new therapeutic options to patients with ERAP1 variant driven diseases. Whether targeting one of these therapies will be efficacious over another remains to be seen, but likely the inhibition of one would affect the activity of another given their close relationships. Nonetheless, we hope that the data presented here will support further development of these therapies, and future availability to patients with autoimmunity, or cancer.

REFERENCES

1. Wang, L., F.-S. Wang, and M. E. Gershwin. 2015. Human autoimmune diseases: a comprehensive update. *J. Intern. Med.* 278: 369–395.

2. Waldman, A. D., J. M. Fritz, and M. J. Lenardo. 2020. A guide to cancer immunotherapy: from T cell basic science to clinical practice. *Nat. Rev. Immunol.* 20: 651–668.

3. Ascherio, A., and K. L. Munger. 2016. Epidemiology of Multiple Sclerosis: From Risk Factors to Prevention-An Update. *Semin. Neurol.* 36: 103–114.

4. Sollid, L. M., W. Pos, and K. W. Wucherpfennig. 2014. Molecular mechanisms for contribution of MHC molecules to autoimmune diseases. *Curr. Opin. Immunol.* 31: 24–30.

5. Leray, E., T. Moreau, A. Fromont, and G. Edan. 2016. Epidemiology of multiple sclerosis. *Rev. Neurol. (Paris).* 172: 3–13.

6. Reveille, J. D. 2012. Genetics of spondyloarthritis - Beyond the MHC. *Nat. Rev. Rheumatol.*

7. Brown, M. A., T. Kenna, and B. P. Wordsworth. 2016. Genetics of ankylosing spondylitis - Insights into pathogenesis. *Nat. Rev. Rheumatol.*

8. Romania, P., L. Cifaldi, B. Pignoloni, N. Starc, V. D'Alicandro, O. Melaiu, G. Li Pira, E. Giorda, R. Carrozzo, M. Bergvall, T. Bergström, L. Alfredsson, T. Olsson, I. Kockum, I. Seppälä, T. Lehtimäki, M. A. Hurme, H. Hengel, A. Santoni, C. Cerboni, F. Locatelli, M. D'Amato, and D. Fruci. 2017. Identification of a Genetic Variation in ERAP1 Aminopeptidase that Prevents Human Cytomegalovirus miR-UL112-5p-Mediated Immunoevasion. *Cell Rep.* 20: 846–853.

9. Hanson, A. L., T. Cuddihy, K. Haynes, D. Loo, C. J. Morton, U. Oppermann, P. Leo, G. P. Thomas, K.-A. Lê Cao, T. J. Kenna, and M. A. Brown. 2018. Genetic Variants in ERAP1 and ERAP2 Associated With Immune-Mediated Diseases Influence Protein Expression and the Isoform Profile. *Arthritis Rheumatol. (Hoboken, N.J.)* 70: 255–265.

10. Momburg, F., J. Roelse, J. C. Howard, G. W. Butcher, G. J. Hämmerling, and J. J. Neefjes. 1994. Selectivity of MHC-encoded peptide transporters from human, mouse and rat. *Nature* 367: 648–651.

11. Chang, S.-C., F. Momburg, N. Bhutani, and A. L. Goldberg. 2005. The ER aminopeptidase, ERAP1, trims precursors to lengths of MHC class I peptides by a molecular ruler mechanism. *Proc. Natl. Acad. Sci.* 102: 17107–17112.

12. Rastall, D. P. W., Y. A. Aldhamen, S. S. Seregin, S. Godbehere, and A. Amalfitano. 2014. ERAP1 functions override the intrinsic selection of specific antigens as immunodominant peptides, thereby altering the potency of antigen-specific cytolytic and effector memory T-cell responses. *Int. Immunol.* 26: 685–695.

13. Rastall, D. P. W., F. S. Alyaquob, P. O'Connell, Y. Pepelyayeva, D. Peters, S. Godbehere-Roosa, C. Pereira-Hicks, Y. A. Aldhamen, and A. Amalfitano. 2017. Mice expressing human ERAP1 variants associated with ankylosing spondylitis have altered T-cell repertoires and NK cell functions, as well as increased in utero and perinatal mortality. *Int. Immunol.*

14. Blake, M. K., P. O'Connell, Y. Pepelyayeva, S. Godbehere, Y. A. Aldhamen, and A. Amalfitano. 2022. ERAP1 is a critical regulator of inflammasome-mediated proinflammatory and ER stress responses. *BMC Immunol.* 23: 9.

15. Pepelyayeva, Y., D. P. W. Rastall, Y. A. Aldhamen, P. O'Connell, S. Raehtz, F. S. Alyaqoub, M. K. Blake, A. M. Raedy, A. M. Angarita, A. M. Abbas, C. N. Pereira-Hicks, S. G. Roosa, L. McCabe, and A. Amalfitano. 2018. ERAP1 deficient mice have reduced Type 1 regulatory T cells and develop skeletal and intestinal features of Ankylosing Spondylitis. *Sci. Rep.* 8.

16. O'Connell, P., M. K. Blake, S. Godbehere, Y. A. Aldhamen, and A. Amalfitano. 2021. Absence of ERAP1 in B Cells Increases Susceptibility to Central Nervous System Autoimmunity, Alters B Cell Biology, and Mechanistically Explains Genetic Associations between ERAP1 and Multiple Sclerosis. *J. Immunol.*

17. Aldhamen, Y. A., S. S. Seregin, D. P. W. Rastall, C. F. Aylsworth, Y. Pepelyayeva, C. J. Busuito, S. Godbehere-Roosa, S. Kim, and A. Amalfitano. 2013. Endoplasmic Reticulum Aminopeptidase-1 Functions Regulate Key Aspects of the Innate Immune Response. *PLoS One*.

18. Aldhamen, Y. A., Y. Pepelyayeva, D. P. W. Rastall, S. S. Seregin, E. Zervoudi, D. Koumantou, C. F. Aylsworth, D. Quiroga, S. Godbehere, D. Georgiadis, E. Stratikos, and A. Amalfitano. 2015. Autoimmune disease-associated variants of extracellular endoplasmic reticulum aminopeptidase 1 induce altered innate immune responses by human immune cells. *J. Innate Immun.*

19. Cui, X., F. Hawari, S. Alsaaty, M. Lawrence, C. A. Combs, W. Geng, F. N. Rouhani, D. Miskinis, and S. J. Levine. 2002. Identification of ARTS-1 as a novel TNFR1-binding protein that promotes TNFR1 ectodomain shedding. *J. Clin. Invest.*

20. Goto, Y., K. Ogawa, A. Hattori, and M. Tsujimoto. 2011. Secretion of endoplasmic reticulum aminopeptidase 1 is involved in the activation of macrophages induced by lipopolysaccharide and interferon-gamma. *J. Biol. Chem.* 286: 21906–21914.

21. Goto, Y., K. Ogawa, T. J. Nakamura, A. Hattori, and M. Tsujimoto. 2015. Substrate-dependent nitric oxide synthesis by secreted endoplasmic reticulum aminopeptidase 1 in macrophages. *J. Biochem.*

22. Cifaldi, L., P. Romania, M. Falco, S. Lorenzi, R. Meazza, S. Petrini, M. Andreani, D. Pende, F. Locatelli, and D. Fruci. 2015. ERAP1 Regulates Natural Killer Cell Function by Controlling the Engagement of Inhibitory Receptors. *Cancer Res.* 75: 824 LP – 834.

23. Wang, X., J. Ma, J. Ma, Y. Wen, L. Meng, H. Yang, R. Zhang, and D. Hao. 2017. Bioinformatics analysis of genetic variants of endoplasmic reticulum aminopeptidase 1 in ankylosing spondylitis. *Mol Med Rep* 16: 6532–6543.

24. Lee, Y. H., and G. G. Song. 2016. Associations between ERAP1 polymorphisms and susceptibility to ankylosing spondylitis: a meta-analysis. *Clin. Rheumatol.* 35: 2009–2015.

25. Kirino, Y., G. Bertsias, Y. Ishigatsubo, N. Mizuki, I. Tugal-Tutkun, E. Seyahi, Y. Ozyazgan, F. S. Sacli, B. Erer, H. Inoko, Z. Emrence, A. Cakar, N. Abaci, D. Ustek, C. Satorius, A. Ueda, M. Takeno, Y. Kim, G. M. Wood, M. J. Ombrello, A. Meguro, A. Gül, E. F. Remmers, and D. L. Kastner. 2013. Genome-wide association analysis identifies new susceptibility loci for Behçet's disease and epistasis between HLA-B*51 and ERAP1. *Nat. Genet.*

26. Guerini, F. R., R. Cagliani, D. Forni, C. Agliardi, D. Caputo, A. Cassinotti, D. Galimberti, C. Fenoglio, M. Biasin, R. Asselta, E. Scarpini, G. P. Comi, N. Bresolin, M. Clerici, and M. Sironi. 2012. A functional variant in ERAP1 predisposes to multiple sclerosis. *PLoS One* 7: e29931–e29931.

27. Zvyagin, I. V, V. Y. Dorodnykh, I. Z. Mamedov, D. B. Staroverov, A. G. Bochkova, D. V Rebrikov, and Y. B. Lebedev. 2010. Association of ERAP1 Allelic Variants with Risk of Ankylosing Spondylitis. *Acta Naturae* 2: 72–77.

28. Pepelyayeva, Y., and A. Amalfitano. 2019. The role of ERAP1 in autoinflammation and autoimmunity. *Hum. Immunol.* 80: 302–309.

29. York, I. A., S. C. Chang, T. Saric, J. A. Keys, J. M. Favreau, A. L. Goldberg, and K. L. Rock. 2002. The Er aminopeptidase ERAP I enhances or limits antigen presentation by trimming epitopes to 8-9 residues. *Nat. Immunol.*

30. York, I. A., M. A. Brehm, S. Zendzian, C. F. Towne, and K. L. Rock. 2006. Endoplasmic reticulum aminopeptidase 1 (ERAP1) trims MHC class I-presented peptides in vivo and plays an important role in immunodominance. *Proc. Natl. Acad. Sci.* 103: 9202 LP – 9207.

31. Babaie, F., R. Hosseinzadeh, M. Ebrazeh, N. Seyfizadeh, S. Aslani, S. Salimi, M. Hemmatzadeh, G. Azizi, F. Jadidi-Niaragh, and H. Mohammadi. 2020. The roles of ERAP1 and ERAP2 in autoimmunity and cancer immunity: New insights and perspective. *Mol. Immunol.* 121: 7–19.

32. Mehta, A. M., E. S. Jordanova, T. van Wezel, H.-W. Uh, W. E. Corver, K. M. C. Kwappenberg, W. Verduijn, G. G. Kenter, S. H. van der Burg, and G. J. Fleuren. 2007. Genetic variation of antigen processing machinery components and association with cervical carcinoma. *Genes, Chromosom. Cancer* 46: 577–586.

33. Harvey, D., J. J. Pointon, D. M. Evans, T. Karaderi, C. Farrar, L. H. Appleton, R. D. Sturrock, M. A. Stone, U. Oppermann, M. A. Brown, and B. P. Wordsworth. 2009. Investigating the genetic association between ERAP1 and ankylosing spondylitis . *Hum. Mol. Genet.* 18: 4204–4212.

34. R., R. A., A. L. H., C. Adrian, V. Matteo, L. Jonathan, W. Laura, B. M. A., and W. Paul. 2017. ERAP1 association with ankylosing spondylitis is attributable to common genotypes rather than rare haplotype combinations. *Proc. Natl. Acad. Sci.* 114: 558–561.

35. Burton, P. R., D. G. Clayton, L. R. Cardon, N. Craddock, P. Deloukas, A. Duncanson, D. P. Kwiatkowski, M. I. McCarthy, W. H. Ouwehand, N. J. Samani, J. A. Todd, P. Donnelly, J. C. Barrett, D. Davison, D. Easton, D. M. Evans, H. T. Leung, J. L. Marchini, A. P. Morris, C. C. A. Spencer, M. D. Tobin, A. P. Attwood, J. P. Boorman, B. Cant, U. Everson, J. M. Hussey, J. D. Jolley, A. S. Knight, K. Koch, E. Meech, S. Nutland, C. V. Prowse, H. E. Stevens, N. C. Taylor, G. R. Walters, N. M. Walker, N. A. Watkins, T. Winzer, R. W. Jones, W. L. McArdle, S. M. Ring, D. P. Strachan, M. Pembrey, G. Breen, D. S. Clair, S. Caesar, K. Gordon-Smith, L. Jones, C. Fraser, E. K. Green, D. Grozeva, M. L. Hamshere, P. A. Holmans, I. R. Jones, G. Kirov, V. Moskivina, I. Nikolov, M. C. O'Donovan, M. J. Owen, D. A. Collier, A. Elkin, A. Farmer, R. Williamson, P. McGuffin, A. H. Young, I. N. Ferrier, S. G. Ball, A. J. Balmforth, J. H. Barrett, T. D. Bishop, M. M. Iles, A. Maqbool, N. Yuldasheva, A. S. Hall, P. S. Braund, R. J. Dixon, M. Mangino, S. Stevens, J. R. Thompson, F. Bredin, M. Tremelling, M. Parkes, H. Drummond, C. W. Lees, E. R. Nimmo, J. Satsangi, S. A. Fisher, A. Forbes, C. M. Lewis, C. M. Onnie, N. J. Prescott, J. Sanderson, C. G. Matthew, J. Barbour, M. K. Mohiuddin, C. E. Todhunter, J. C. Mansfield, T. Ahmad, F. R. Cummings, D. P. Jewell, J. Webster, M. J. Brown, M. G. Lathrop, J. Connell, A. Dominiczak, C. A. B. Marcano, B. Burke, R. Dobson, J. Gungadoo, K. L. Lee, P. B. Munroe, S. J. Newhouse, A. Onipinla, C. Wallace, M. Xue, M. Caulfield, M. Farrall, A. Barton, I. N. Bruce, H. Donovan, S. Eyre, P. D. Gilbert, S. L. Hilder, A. M. Hinks, S. L. John, C. Potter, A. J. Silman, D. P. M. Symmons, W. Thomson, J. Worthington, D. B. Dunger, B. Widmer, T. M. Frayling, R. M. Freathy, H. Lango, J. R. B. Perry, B. M. Shields, M. N. Weedon, A. T. Hattersley, G. A. Hitman, M. Walker, K. S. Elliott, C. J. Groves, C. M. Lindgren, N. W. Rayner, N. J. Timpson, E. Zeggini, M. Newport, G. Sirugo, E. Lyons, F. Vannberg, A. V. S. Hill, L. A. Bradbury, C. Farrar, J. J. Pointon, P. Wordsworth, M. A. Brown, J. A. Franklyn, J. M. Heward, M. J. Simmonds, S. C. L. Gough, S. Seal, M. R. Stratton, N. Rahman, M. Ban, A. Goris, S. J. Sawcer, A. Compston, D. Conway, M. Jallow, K. A. Rockett, S. J. Bumpstead, A. Chaney, K. Downes, M. J. R. Ghori, R. Gwilliam, S. E. Hunt, M. Inouye, A. Keniry, E. King, R. McGinnis, S. Potter, R. Ravindrarajah, P. Whittaker, C. Widden, D. Withers, N. J. Cardin, T. Ferreira, J. Pereira-Gale, I. B. Hallgrimsdóttir, B. N. Howie, Z. Su, Y. Y. Teo, D. Vukcevic, D. Bentley, S. L. Mitchell, P. R. Newby, O. J. Brand, J. Carr-Smith, S. H. S. Pearce, S. C. L. Gough, R. McGinnis, A. Keniry, P. Deloukas, J. D. Reveille, X. Zhou, A. M. Sims, A. Dowling, J. Taylor, T. Doan, J. C. Davis, L. Savage, M. M. Ward, T. L. Learch, and M. H. Weisman. 2007. Association scan of 14,500 nonsynonymous SNPs in four diseases identifies autoimmunity variants. *Nat. Genet.*

36. Reeves, E., C. J. Edwards, T. Elliott, and E. James. 2013. Naturally Occurring ERAP1 Haplotypes Encode Functionally Distinct Alleles with Fine Substrate Specificity. *J. Immunol.* 191: 35 LP – 43.

37. Zhang, L., H. Yu, M. Zheng, H. Li, Y. Liu, A. Kijlstra, and P. Yang. 2015. Association of ERAP1 Gene Polymorphisms With Behçet's Disease in Han Chinese. *Invest. Ophthalmol. Vis. Sci.* 56: 6029–6035.

38. D'amico, S., P. Tempora, V. Lucarini, O. Melaiu, S. Gaspari, M. Algeri, and D. Fruci. 2021. ERAP1 and ERAP2 enzymes: A protective shield for ras against COVID-19? *Int. J. Mol. Sci.* 22: 1–10.

39. Yamamoto, N., J. Nakayama, K. Yamakawa-Kobayashi, H. Hamaguchi, R. Miyazaki, and T. Arinami. 2002. Identification of 33 polymorphisms in the adipocyte-derived leucine aminopeptidase (ALAP) gene and possible association with hypertension. *Hum. Mutat.* 19: 251–257.

40. Rysz, S., J. Al-Saadi, A. Sjöström, M. Farm, F. Campoccia Jalde, M. Plattén, H. Eriksson, M. Klein, R. Vargas-Paris, S. Nyrén, G. Abdula, R. Ouellette, T. Granberg, M. Jonsson Fagerlund, and J. Lundberg. 2021. COVID-19 pathophysiology may be driven by an imbalance in the renin-angiotensin-aldosterone system. *Nat. Commun.* 12: 2417.

41. Ranjit, S., J. Y. Wong, J. W. Tan, C. Sin Tay, J. M. Lee, K. Yin Han Wong, L. H. Pojoga, D. L. Brooks, A. E. Garza, S. A. Maris, I. A. Katayama, J. S. Williams, A. Rivera, G. K. Adler, G. H. Williams, and J. R. Romero. 2019. Sex-specific differences in endoplasmic reticulum aminopeptidase 1 modulation influence blood pressure and renin-angiotensin system responses. *JCI insight* 4: e129615.

42. Xu, Y., J. Wu, and J. Wu. 2020. Expression and role of ERAP1 in placental tissues of preeclampsia. *Hypertens. pregnancy* 39: 165–171.

43. Ferreira, L. C., C. E. M. Gomes, P. Duggal, I. De Paula Holanda, A. S. de Lima, P. R. P. do Nascimento, and S. M. B. Jeronimo. 2021. Genetic association of ERAP1 and ERAP2 with eclampsia and preeclampsia in northeastern Brazilian women. *Sci. Rep.* 11: 6764.

44. Taurog, J. D., A. Chhabra, and R. A. Colbert. 2016. Ankylosing Spondylitis and Axial Spondyloarthritis. *N. Engl. J. Med.* 374: 2563–2574.

45. Zhu, W., X. He, K. Cheng, L. Zhang, D. Chen, X. Wang, G. Qiu, X. Cao, and X. Weng. 2019. Ankylosing spondylitis: etiology, pathogenesis, and treatments. *Bone Res.* 7: 22.

46. Cortes, A., S. L. Pulit, P. J. Leo, J. J. Pointon, P. C. Robinson, M. H. Weisman, M. Ward, L. S. Gensler, X. Zhou, H.-J. Garchon, G. Chiocchia, J. Nossent, B. A. Lie, Ø. Førre, J. Tuomilehto, K. Laiho, L. A. Bradbury, D. Elewaut, R. Burgos-Vargas, S. Stebbings, L. Appleton, C. Farrah, J. Lau, N. Haroon, J. Mulero, F. J. Blanco, M. A. Gonzalez-Gay, C. Lopez-Larrea, P. Bowness, K. Gaffney, H. Gaston, D. D. Gladman, P. Rahman, W. P. Maksymowych, J. B. A. Crusius, I. E. van der Horst-Bruinsma, R. Valle-Oñate, C. Romero-Sánchez, I. M. Hansen, F. M. Pimentel-Santos, R. D. Inman, J. Martin, M. Breban, B. P. Wordsworth, J. D. Reveille, D. M. Evans, P. I. W. de Bakker, M. A. Brown. 2015. Major histocompatibility complex associations of ankylosing spondylitis are complex and involve further epistasis with ERAP1. *Nat. Commun.* 6: 7146.

47. Ma, Y., D. Fan, S. Xu, J. Deng, X. Gao, S. Guan, X. Zhang, and F. Pan. 2021. Ankylosing Spondylitis Patients Display Aberrant ERAP1 Gene DNA Methylation and Expression. *Immunol. Invest.* 1–13.

48. Takeuchi, M., D. L. Kastner, and E. F. Remmers. 2015. The immunogenetics of Behçet's disease: A comprehensive review. *J. Autoimmun.* 64: 137–148.

49. Zhou, Z. Y., S. L. Chen, N. Shen, and Y. Lu. 2012. Cytokines and Behcet's Disease. *Autoimmun. Rev.* 11: 699–704.

50. Alpsoy, E. 2016. Behçet's disease: A comprehensive review with a focus on epidemiology, etiology and clinical features, and management of mucocutaneous lesions. *J. Dermatol.* 43: 620–632.

51. Alpsoy, E., P. Leccese, G. Emmi, and S. Ohno. 2021. Treatment of Behçet's Disease: An Algorithmic Multidisciplinary Approach. *Front. Med.* 8.

52. Guasp, P., E. Barnea, M. F. González-Escribano, A. Jiménez-Reinoso, J. R. Regueiro, A. Admon, and J. A. López de Castro. 2017. The Behcet's disease-associated variant of the aminopeptidase ERAP1 shapes a low-affinity HLA-B*51 peptidome by differential subpeptidome processing. *J. Biol. Chem.* 292: 9680–9689.

53. Constantinescu, C. S., N. Farooqi, K. O'Brien, and B. Gran. 2011. Experimental autoimmune encephalomyelitis (EAE) as a model for multiple sclerosis (MS). *Br. J. Pharmacol.* 164: 1079–1106.

54. Klineova, S., and F. D. Lublin. 2018. Clinical Course of Multiple Sclerosis. *Cold Spring Harb. Perspect. Med.* 8.

55. Attfield, K. E., L. T. Jensen, M. Kaufmann, M. A. Friese, and L. Fugger. 2022. The immunology of multiple sclerosis. *Nat. Rev. Immunol.*

56. Parnell, G. P., and D. R. Booth. 2017. The Multiple Sclerosis (MS) Genetic Risk Factors Indicate both Acquired and Innate Immune Cell Subsets Contribute to MS Pathogenesis and Identify Novel Therapeutic Opportunities. *Front. Immunol.* 8: 425.

57. Bjornevik, K., M. Cortese, B. C. Healy, J. Kuhle, M. J. Mina, Y. Leng, S. J. Elledge, D. W. Niebuhr, A. I. Scher, K. L. Munger, and A. Ascherio. 2022. Longitudinal analysis reveals high prevalence of Epstein-Barr virus associated with multiple sclerosis. *Science* 375: 296–301.

58. Filipi, M., and S. Jack. 2020. Interferons in the Treatment of Multiple Sclerosis: A Clinical Efficacy, Safety, and Tolerability Update. *Int. J. MS Care* 22: 165–172.

59. Olsson, T., L. F. Barcellos, and L. Alfredsson. 2017. Interactions between genetic, lifestyle and environmental risk factors for multiple sclerosis. *Nat. Rev. Neurol.* 13: 25–36.

60. Syed, Y. Y. 2018. Ocrelizumab: A Review in Multiple Sclerosis. *CNS Drugs* 32: 883–890.
61. Chassaing, B., J. D. Aitken, M. Malleshappa, and M. Vijay-Kumar. 2014. Dextran sulfate sodium (DSS)-induced colitis in mice. *Curr. Protoc. Immunol.* 104: 15.25.1-15.25.14.

62. Bauer, C., P. Duewell, C. Mayer, H. A. Lehr, K. A. Fitzgerald, M. Dauer, J. Tschopp, S. Endres, E. Latz, and M. Schnurr. 2010. Colitis induced in mice with dextran sulfate sodium (DSS) is mediated by the NLRP3 inflammasome. *Gut*.

63. McCarthy, D. P., M. H. Richards, and S. D. Miller. 2012. Mouse models of multiple sclerosis: experimental autoimmune encephalomyelitis and Theiler's virus-induced demyelinating disease. *Methods Mol. Biol.* 900: 381–401.

64. Liu, G., K. A. Muili, V. V Agashe, and J.-A. Lyons. 2012. Unique B cell responses in B cell-dependent and B cell-independent EAE. *Autoimmunity* 45: 199–209.

65. Ransohoff, R. M. 2012. Animal models of multiple sclerosis: the good, the bad and the bottom line. *Nat. Neurosci.* 15: 1074–1077.

66. Junjappa, R. P., P. Patil, K. R. Bhattarai, H.-R. Kim, and H.-J. Chae. 2018. IRE1α Implications in Endoplasmic Reticulum Stress-Mediated Development and Pathogenesis of Autoimmune Diseases. *Front. Immunol.* 9: 1289.

67. Yan, M.-M., J.-D. Ni, D. Song, M. Ding, and J. Huang. 2015. Interplay between unfolded protein response and autophagy promotes tumor drug resistance. *Oncol. Lett.* 10: 1959–1969.

68. Hetz, C., E. Chevet, and H. P. Harding. 2013. Targeting the unfolded protein response in disease. *Nat. Rev. Drug Discov.* 12: 703–719.

69. Marré, M. L., and J. D. Piganelli. 2017. Environmental Factors Contribute to β Cell Endoplasmic Reticulum Stress and Neo-Antigen Formation in Type 1 Diabetes. *Front. Endocrinol. (Lausanne).* 8: 262.

70. Sun, Q., J. Fan, T. R. Billiar, and M. J. Scott. 2017. Inflammasome and autophagy regulation - a two-way street. *Mol. Med.* 23: 188–195.

71. Swanson, K. V, M. Deng, and J. P.-Y. Ting. 2019. The NLRP3 inflammasome: molecular activation and regulation to therapeutics. *Nat. Rev. Immunol.* 19: 477–489.

72. Shi, J., Y. Zhao, K. Wang, X. Shi, Y. Wang, H. Huang, Y. Zhuang, T. Cai, F. Wang, and F. Shao. 2015. Cleavage of GSDMD by inflammatory caspases determines pyroptotic cell death. *Nature* 526: 660–665.

73. He, W., H. Wan, L. Hu, P. Chen, X. Wang, Z. Huang, Z.-H. Yang, C.-Q. Zhong, and J. Han. 2015. Gasdermin D is an executor of pyroptosis and required for interleukin-1β secretion. *Cell Res.* 25: 1285–1298.

74. Paik, S., J. K. Kim, P. Silwal, C. Sasakawa, and E.-K. Jo. 2021. An update on the regulatory mechanisms of NLRP3 inflammasome activation. *Cell. Mol. Immunol.* 18: 1141–1160.

75. Zhong, Z., E. Sanchez-Lopez, and M. Karin. 2016. Autophagy, NLRP3 inflammasome and auto-inflammatory/immune diseases. *Clin. Exp. Rheumatol.* 34: 12–16.

76. Guggino, G., D. Mauro, A. Rizzo, R. Alessandro, S. Raimondo, A.-S. Bergot, M. A. Rahman, J. J. Ellis, S. Milling, R. Lories, D. Elewaut, M. A. Brown, R. Thomas, and F. Ciccia. 2021. Inflammasome Activation in Ankylosing Spondylitis Is Associated With Gut Dysbiosis. *Arthritis Rheumatol. (Hoboken, N.J.)* 73: 1189–1199.

77. Hou, B., Y. Zhang, P. Liang, Y. He, B. Peng, W. Liu, S. Han, J. Yin, and X. He. 2020. Inhibition of the NLRP3-inflammasome prevents cognitive deficits in experimental autoimmune encephalomyelitis mice via the alteration of astrocyte phenotype. *Cell Death Dis.* 11: 377.

78. Kim, S.-K., Y. J. Cho, and J.-Y. Choe. 2018. NLRP3 inflammasomes and NLRP3 inflammasome-derived proinflammatory cytokines in peripheral blood mononuclear cells of patients with ankylosing spondylitis. *Clin. Chim. Acta.* 486: 269–274.

79. Perazzio, S. F., L. E. C. Andrade, and A. W. S. de Souza. 2020. Understanding Behçet's Disease in the Context of Innate Immunity Activation. *Front. Immunol.* 11.

80. Heshmatpanah, M., N. Zarrabi Ahrabi, F. Shahram, M. Akhlaghi, M. Akhtari, E. Shamsian, S. Mostafaee, and M. Mahmoudi. 2020. Altered Expression of Unfolded Protein Response Genes in Macrophages from Behcet's Disease. *Rheumatol. Res.* 5: 65–72.

81. Lin, W., and S. Stone. 2015. The unfolded protein response in multiple sclerosis. *Front. Neurosci.* 9.

82. Huang, W.-X., P. Huang, and J. Hillert. 2004. Increased expression of caspase-1 and interleukin-18 in peripheral blood mononuclear cells in patients with multiple sclerosis. *Mult. Scler. J.* 10: 482–487.

83. Malhotra, S., C. Costa, H. Eixarch, C. W. Keller, L. Amman, H. Martínez-Banaclocha, L. Midaglia, E. Sarró, I. Machín-Díaz, L. M. Villar, J. C. Triviño, B. Oliver-Martos, L. N. Parladé, L. Calvo-Barreiro, F. Matesanz, K. Vandenbroeck, E. Urcelay, M.-L. Martínez-Ginés, A. Tejeda-Velarde, N. Fissolo, J. Castilló, A. Sanchez, A. A. B. Robertson, D. Clemente, M. Prinz, P. Pelegrin, J. D. Lünemann, C. Espejo, X. Montalban, and M. Comabella. 2020. NLRP3 inflammasome as prognostic factor and therapeutic target in primary progressive multiple sclerosis patients. *Brain* 143: 1414–1430.

84. Yin, H., H. Wu, Y. Chen, J. Zhang, M. Zheng, G. Chen, L. Li, and Q. Lu. 2018. The Therapeutic and Pathogenic Role of Autophagy in Autoimmune Diseases. *Front. Immunol.* 9: 1512.

85. Ye, X., X.-J. Zhou, and H. Zhang. 2018. Exploring the Role of Autophagy-Related Gene 5 (ATG5) Yields Important Insights Into Autophagy in Autoimmune/Autoinflammatory Diseases. *Front. Immunol.* 9.

86. Harris, J., M. Hartman, C. Roche, S. G. Zeng, A. O'Shea, F. A. Sharp, E. M. Lambe, E. M. Creagh, D. T. Golenbock, J. Tschopp, H. Kornfeld, K. A. Fitzgerald, and E. C. Lavelle. 2011. Autophagy controls IL-1beta secretion by targeting pro-IL-1beta for degradation. *J. Biol. Chem.* 286: 9587–9597.

87. Wang, X., J. Wang, H. Zheng, M. Xie, E. L. Hopewell, R. A. Albrecht, S. Nogusa, A. Garc\'\ia-Sastre, S. Balachandran, and A. A. Beg. 2014. Differential Requirement for the IKKβ/NF-κB Signaling Module in Regulating TLR- versus RLR-Induced Type 1 IFN Expression in Dendritic Cells. *J. Immunol.* 193: 2538–2545.

88. Pattingre, S., A. Tassa, X. Qu, R. Garuti, X. H. Liang, N. Mizushima, M. Packer, M. D. Schneider, and B. Levine. 2005. Bcl-2 antiapoptotic proteins inhibit Beclin 1-dependent autophagy. *Cell* 122: 927–939.

89. Margariti, A., H. Li, T. Chen, D. Martin, G. Vizcay-Barrena, S. Alam, E. Karamariti, Q. Xiao, A. Zampetaki, Z. Zhang, W. Wang, Z. Jiang, C. Gao, B. Ma, Y.-G. Chen, G. Cockerill, Y. Hu, Q. Xu, and L. Zeng. 2013. XBP1 mRNA splicing triggers an autophagic response in endothelial cells through BECLIN-1 transcriptional activation. *J. Biol. Chem.* 288: 859–872.

90. Suzuki, H., K. Kanekura, T. P. Levine, K. Kohno, V. M. Olkkonen, S. Aiso, and M. Matsuoka. 2009. ALS-linked P56S-VAPB, an aggregated loss-of-function mutant of VAPB, predisposes motor neurons to ER stress-related death by inducing aggregation of co-expressed wild-type VAPB. *J. Neurochem.* 108: 973–985.

91. Colbert, R. A., M. L. DeLay, G. Layh-Schmitt, and D. P. Sowders. 2009. HLA-B27 misfolding and spondyloarthropathies. *Adv. Exp. Med. Biol.*

92. Rezaiemanesh, A., M. Mahmoudi, A. A. Amirzargar, M. Vojdanian, A. R. Jamshidi, and M. H. Nicknam. 2017. Ankylosing spondylitis M-CSF-derived macrophages are undergoing unfolded protein response (UPR) and express higher levels of interleukin-23. *Mod. Rheumatol.* 27: 862–867.

93. Rezaiemanesh, A., M. Mahmoudi, A. A. Amirzargar, M. Vojdanian, F. Babaie, J. Mahdavi, M. Rajabinejad, A. R. Jamshidi, and M. H. Nicknam. 2022. Upregulation of Unfolded Protein Response and ER Stress-Related IL-23 Production in M1 Macrophages from Ankylosing Spondylitis Patients. *Inflammation* 45: 665–676.

94. Seidel, J. A., A. Otsuka, and K. Kabashima. 2018. Anti-PD-1 and Anti-CTLA-4 Therapies in Cancer: Mechanisms of Action, Efficacy, and Limitations. *Front. Oncol.* 8: 86.

95. Hodi, F. S., S. J. O'Day, D. F. McDermott, R. W. Weber, J. A. Sosman, J. B. Haanen, R. Gonzalez, C. Robert, D. Schadendorf, J. C. Hassel, W. Akerley, A. J. M. van den Eertwegh, J. Lutzky, P. Lorigan, J. M. Vaubel, G. P. Linette, D. Hogg, C. H. Ottensmeier, C. Lebbé, C. Peschel, I. Quirt, J. I. Clark, J. D. Wolchok, J. S. Weber, J. Tian, M. J. Yellin, G. M. Nichol, A. Hoos, and W. J. Urba. 2010. Improved Survival with Ipilimumab in Patients with Metastatic Melanoma. *N. Engl. J. Med.* 363: 711–723.

96. Joyce, S. 2015. Immunoproteasomes edit tumors, which then escapes immune recognition. *Eur. J. Immunol.* 45: 3241–3245.

97. Cifaldi, L., E. Lo Monaco, M. Forloni, E. Giorda, S. Lorenzi, S. Petrini, E. Tremante, D. Pende, F. Locatelli, P. Giacomini, and D. Fruci. 2011. Natural killer cells efficiently reject lymphoma silenced for the endoplasmic reticulum aminopeptidase associated with antigen processing. *Cancer Res.*

98. Steinbach, A., J. Winter, M. Reuschenbach, R. Blatnik, A. Klevenz, M. Bertrand, S. Hoppe, M. von Knebel Doeberitz, A. K. Grabowska, and A. B. Riemer. 2017. ERAP1 overexpression in HPV-induced malignancies: A possible novel immune evasion mechanism. *Oncoimmunology* 6: e1336594.

99. Reeves, E., O. Wood, C. H. Ottensmeier, E. V King, G. J. Thomas, T. Elliott, and E. James. 2019. HPV Epitope Processing Differences Correlate with ERAP1 Allotype and Extent of CD8+ T-cell Tumor Infiltration in OPSCC. *Cancer Immunol. Res.* 7: 1202–1213.

100. Koumantou, D., E. Barnea, A. Martin-Esteban, Z. Maben, A. Papakyriakou, A. Mpakali, P. Kokkala, H. Pratsinis, D. Georgiadis, L. J. Stern, A. Admon, and E. Stratikos. 2019. Editing the immunopeptidome of melanoma cells using a potent inhibitor of endoplasmic reticulum aminopeptidase 1 (ERAP1). *Cancer Immunol. Immunother.* 68: 1245–1261.

101. Joyce, P., L. Young, M. Quibell, J. Shiers, C. Tong, K. Clark, E. James, E. Reeves, A. Remtulla, H. Leonard, C. de Almeida, E. Lori, N. Ternette, F. Poynton, and A. Leishman. 2020. 446 Immunopeptidome changes mediated by a novel ERAP1 inhibitor leads to tumor growth inhibition. *J. Immunother. Cancer* 8: A271 LP-A271.

102. Fierabracci, A., A. Milillo, F. Locatelli, and D. Fruci. 2012. The putative role of endoplasmic reticulum aminopeptidases in autoimmunity: Insights from genomic-wide association studies. *Autoimmun. Rev.*

103. Tsujimoto, M., and A. Hattori. 2005. The oxytocinase subfamily of M1 aminopeptidases. In *Biochimica et Biophysica Acta - Proteins and Proteomics*.

104. Saric, T., S. C. Chang, A. Hattori, I. A. York, S. Markant, K. L. Rock, M. Tsujimoto, and A. L. Goldberg. 2002. An IFN-γ-induced aminopeptidase in the ER, ERAP I, trims precursors to MHC class I-presented peptides. *Nat. Immunol.*

105. Goto, Y., K. Ogawa, A. Hattori, and M. Tsujimoto. 2011. Secretion of endoplasmic reticulum aminopeptidase 1 is involved in the activation of macrophages induced by lipopolysaccharide and interferon-γ. *J. Biol. Chem.*

106. Goto, Y., K. Ogawa, T. J. Nakamura, A. Hattori, and M. Tsujimoto. 2014. TLR-Mediated Secretion of Endoplasmic Reticulum Aminopeptidase 1 from Macrophages. *J. Immunol.*

107. Muñoz-Planillo, R., P. Kuffa, G. Martínez-Colón, B. L. Smith, T. M. Rajendiran, and G. Núñez. 2013. K^+ efflux is the common trigger of NLRP3 inflammasome activation by bacterial toxins and particulate matter. *Immunity* 38: 1142–1153.

108. Iwasaki, A., and R. Medzhitov. 2015. Control of adaptive immunity by the innate immune system. *Nat. Immunol.*

109. Weber, A., P. Wasiliew, and M. Kracht. 2010. Interleukin-1β (IL-1β) processing pathway. *Sci. Signal.*

110. Dinarello, C. A. 2000. Interleukin-18, a proinflammatory cytokine. *Eur. Cytokine Netw.* .
111. Rudwaleit, M., and D. Baeten. 2006. Ankylosing spondylitis and bowel disease. *Best Pract. Res. Clin. Rheumatol.*

112. Marciniak, S. J., and D. Ron. 2006. Endoplasmic Reticulum Stress Signaling in Disease. *Physiol. Rev.* 86: 1133–1149.

113. Wang, S., and R. J. Kaufman. 2012. The impact of the unfolded protein response on human disease. *J. Cell Biol.* 197: 857 LP – 867.

114. Hornung, V., A. Ablasser, M. Charrel-Dennis, F. Bauernfeind, G. Horvath, D. R. Caffrey, E. Latz, and K. A. Fitzgerald. 2009. AIM2 recognizes cytosolic dsDNA and forms a caspase-1-activating inflammasome with ASC. *Nature*.

115. Sakai, J., E. Cammarota, J. A. Wright, P. Cicuta, R. A. Gottschalk, N. Li, I. D. C. Fraser, and C. E. Bryant. 2017. Lipopolysaccharide-induced NF-κB nuclear translocation is primarily dependent on MyD88, but TNFα expression requires TRIF and MyD88. *Sci. Rep.* 7: 1428.
116. Liu, T., L. Zhang, D. Joo, and S.-C. Sun. 2017. NF-κB signaling in inflammation. *Signal Transduct. Target. Ther.* 2: 17023.

117. Perkins, N. D. 2007. Integrating cell-signalling pathways with NF-κB and IKK function. *Nat. Rev. Mol. Cell Biol.* 8: 49–62.

118. Shenderov, K., N. Riteau, R. Yip, K. D. Mayer-Barber, S. Oland, S. Hieny, P. Fitzgerald, A. Oberst, C. P. Dillon, D. R. Green, V. Cerundolo, and A. Sher. 2014. Cutting Edge: Endoplasmic Reticulum Stress Licenses Macrophages To Produce Mature IL-1β in Response to TLR4 Stimulation through a Caspase-8– and TRIF-Dependent Pathway. *J. Immunol.*

119. Ulianich, L., G. Terrazzano, M. Annunziatella, G. Ruggiero, F. Beguinot, and B. Di Jeso. 2011. ER stress impairs MHC Class I surface expression and increases susceptibility of thyroid cells to NK-mediated cytotoxicity. *Biochim. Biophys. Acta - Mol. Basis Dis.* 1812: 431–438.

120. Wick, M. J., and J. D. Pfeifer. 1996. Major histocompatibility complex class I presentation of ovalbumin peptide 257–264 from exogenous sources: protein context influences the degree of TAP-independent presentation. *Eur. J. Immunol.* 26: 2790–2799.

121. Popa, O. M., M. Cherciu, L. I. Cherciu, M. I. Dutescu, M. Bojinca, V. Bojinca, C. Bara, and L. O. Popa. 2016. ERAP1 and ERAP2 Gene Variations Influence the Risk of Psoriatic Arthritis in Romanian Population. *Arch. Immunol. Ther. Exp. (Warsz).* 64: 123–129.

122. Martinon, F., V. Pétrilli, A. Mayor, A. Tardivel, and J. Tschopp. 2006. Gout-associated uric acid crystals activate the NALP3 inflammasome. *Nature* 440: 237–241.

123. Zhu, J., A. Li, E. Jia, Y. Zhou, J. Xu, S. Chen, Y. Huang, X. Xiao, and J. Li. 2017. Monosodium urate crystal deposition associated with the progress of radiographic grade at the sacroiliac joint in axial SpA: a dual-energy CT study. *Arthritis Res. Ther.* 19: 83.

124. Evans, D. M., C. C. A. Spencer, J. J. Pointon, Z. Su, D. Harvey, G. Kochan, U. Opperman, A. Dilthey, M. Pirinen, M. A. Stone, L. Appleton, L. Moutsianis, S. Leslie, T. Wordsworth, T. J. Kenna, T. Karaderi, G. P. Thomas, M. M. Ward, M. H. Weisman, C. Farrar, L. A. Bradbury, P. Danoy, R. D. Inman, W. Maksymowych, D. Gladman, P. Rahman, A. Morgan, H. Marzo-Ortega, P. Bowness, K. Gaffney, J. S. H. Gaston, M. Smith, J. Bruges-Armas, A. R. Couto, R. Sorrentino, F. Paladini, M. A. Ferreira, H. Xu, Y. Liu, L. Jiang, C. Lopez-Larrea, R. Díaz-Peña, A. Lóepez-Vázquez, T. Zayats, G. Band, C. Bellenguez, H. Blackburn, J. M. Blackwell, E. Bramon, S. J. Bumpstead, J. P. Casas, A. Corvin, N. Craddock, P. Deloukas, S. Dronov, A. Duncanson, S. Edkins, C. Freeman, M. Gillman, E. Gray, R. Gwilliam, N. Hammond, S. E. Hunt, J. Jankowski, A. Jayakumar, C. Langford, J. Liddle, H. S. Markus, C. G. Mathew, O. T. McCann, M. I. McCarthy, C. N. A. Palmer, L. Peltonen, R. Plomin, S. C. Potter, A. Rautanen, R. Ravindrarajah, M. Ricketts, N. Samani, S. J. Sawcer, A. Strange, R. C. Trembath, A. C. Viswanathan, M. Waller, P. Weston, P. Whittaker, S. Widaa, N. W. Wood, G. McVean, J. D. Reveille, B. P. Wordsworth, M. A. Brown, and P. Donnelly. 2011. Interaction between ERAP1 and HLA-B27 in ankylosing spondylitis implicates peptide handling in the mechanism for HLA-B27 in disease susceptibility. *Nat. Genet.*

125. Reeves, E., T. Elliott, E. James, and C. J. Edwards. 2014. ERAP1 in the pathogenesis of ankylosing spondylitis. *Immunol. Res.*

126. Fung, E. Y. M. G., D. J. Smyth, J. M. M. Howson, J. D. Cooper, N. M. Walker, H. Stevens, L. S. Wicker, and J. A. Todd. 2009. Analysis of 17 autoimmune disease-associated variants in type 1 diabetes identifies 6q23/TNFAIP3 as a susceptibility locus. *Genes Immun.* 10: 188–191.

127. Grigoriadis, G., Y. Zhan, R. J. Grumont, D. Metcalf, E. Handman, C. Cheers, and S. Gerondakis. 1996. The Rel subunit of NF-kappaB-like transcription factors is a positive and negative regulator of macrophage gene expression: distinct roles for Rel in different macrophage populations. *EMBO J.* 15: 7099–7107.

128. Kagan, J. C., T. Su, T. Horng, A. Chow, S. Akira, and R. Medzhitov. 2008. TRAM couples endocytosis of Toll-like receptor 4 to the induction of interferon-β. *Nat. Immunol.* 9: 361–368.

129. Toshchakov, V., B. W. Jones, P.-Y. Perera, K. Thomas, M. J. Cody, S. Zhang, B. R. G. Williams, J. Major, T. A. Hamilton, M. J. Fenton, and S. N. Vogel. 2002. TLR4, but not TLR2, mediates IFN-β–induced STAT1α/β-dependent gene expression in macrophages. *Nat. Immunol.* 3: 392–398.

130. Zhou, R., A. S. Yazdi, P. Menu, and J. Tschopp. 2011. A role for mitochondria in NLRP3 inflammasome activation. *Nature*.

131. Kaser, A., A. H. Lee, A. Franke, J. N. Glickman, S. Zeissig, H. Tilg, E. E. S. Nieuwenhuis, D. E. Higgins, S. Schreiber, L. H. Glimcher, and R. S. Blumberg. 2008. XBP1 Links ER Stress to Intestinal Inflammation and Confers Genetic Risk for Human Inflammatory Bowel Disease. *Cell*.

132. Shkoda, A., P. A. Ruiz, H. Daniel, S. C. Kim, G. Rogler, R. B. Sartor, and D. Haller. 2007. Interleukin-10 Blocked Endoplasmic Reticulum Stress in Intestinal Epithelial Cells: Impact on Chronic Inflammation. *Gastroenterology*.

133. Sivakumar, P. V., G. M. Westrich, S. Kanaly, K. Garka, T. L. Born, J. M. J. Derry, and J. L. Viney. 2002. Interleukin 18 is a primary mediator of the inflammation associated with dextran sulphate sodium induced colitis: Blocking interleukin 18 attenuates intestinal damage. *Gut*.

134. Villani, A. C., M. Lemire, G. Fortin, E. Louis, M. S. Silverberg, C. Collette, N. Baba, C. Libioulle, J. Belaiche, A. Bitton, D. Gaudet, A. Cohen, D. Langelier, P. R. Fortin, J. E. Wither, M. Sarfati, P. Rutgeerts, J. D. Rioux, S. Vermeire, T. J. Hudson, and D. Franchimont. 2009. Common variants in the NLRP3 region contribute to Crohn's disease susceptibility. *Nat. Genet.*

135. Dowds, T. A., J. Masumoto, L. Zhu, N. Inohara, and G. Núñez. 2004. Cryopyrin-induced interleukin 1β secretion in monocytic cells: Enhanced activity of disease-associated mutants and requirement for ASC. *J. Biol. Chem.*

136. Hosokawa, T., K. Kusugami, K. Ina, T. Ando, M. Shinoda, A. Imada, M. Ohsuga, T. Sakai, T. Matsuura, K. Ito, and K. Kaneshiro. 1999. Interleukin-6 and soluble interleukin-6 receptor in the colonic mucosa of inflammatory bowel disease. *J. Gastroenterol. Hepatol.*

137. Cui, X., F. N. Rouhani, F. Hawari, and S. J. Levine. 2003. An aminopeptidase, ARTS-1, is required for interleukin-6 receptor shedding. *J. Biol. Chem.*

138. Compston, A., and A. Coles. 2008. Multiple sclerosis. *Lancet (London, England)* 372: 1502–1517.

139. Yadav, S. K., J. E. Mindur, K. Ito, and S. Dhib-Jalbut. 2015. Advances in the immunopathogenesis of multiple sclerosis. *Curr. Opin. Neurol.* 28: 206–219.

140. McGinley, A. M., S. C. Edwards, M. Raverdeau, and K. H. G. Mills. 2018. Th17 cells, γδ T cells and their interplay in EAE and multiple sclerosis. *J. Autoimmun.*

141. Voge, N. V, and E. Alvarez. 2019. Monoclonal antibodies in multiple sclerosis: present and future. *Biomedicines* 7: 20.

142. Didonna, A., and J. R. Oksenberg. 2017. The genetics of multiple sclerosis. *Exon Publ.* 3–16.

143. Consortium*†, I. M. S. G., ANZgene, IIBDGC, and WTCCC2. 2019. Multiple sclerosis genomic map implicates peripheral immune cells and microglia in susceptibility. *Science (80-.).* 365: eaav7188.

144. (IIBDGC), I. I. B. D. G. C., C. Agliardi, L. Alfredsson, M. Alizadeh, C. Anderson, R. Andrews, H. B. Søndergaard, A. Baker, and G. Band. 2013. Analysis of immune-related loci identifies 48 new susceptibility variants for multiple sclerosis. *Nat. Genet.* 45: 1353–1360.

145. Serwold, T., F. Gonzalez, J. Kim, R. Jacob, and N. Shastri. 2002. ERAAP customizes peptides for MHC class I molecules in the endoplasmic reticulum. *Nature* 419: 480–483.

146. Mrdjen, D., A. Pavlovic, F. J. Hartmann, B. Schreiner, S. G. Utz, B. P. Leung, I. Lelios, F. L. Heppner, J. Kipnis, and D. Merkler. 2018. High-dimensional single-cell mapping of central nervous system immune cells reveals distinct myeloid subsets in health, aging, and disease. *Immunity* 48: 380–395.

147. Dixon, K. O., M. Tabaka, M. A. Schramm, S. Xiao, R. Tang, D. Dionne, A. Anderson, O. Rozenblatt-Rosen, A. Regev, and V. K. Kuchroo. 2021. TIM-3 restrains anti-tumour immunity by regulating inflammasome activation. *Nature* 595: 101–106.

148. Ocaña-Guzman, R., L. Torre-Bouscoulet, and I. Sada-Ovalle. 2016. TIM-3 regulates distinct functions in macrophages. *Front. Immunol.* 7: 229.

149. Wolf, Y., A. C. Anderson, and V. K. Kuchroo. 2020. TIM3 comes of age as an inhibitory receptor. *Nat. Rev. Immunol.* 20: 173–185.

150. Battaglia, M., S. Gregori, R. Bacchetta, and M.-G. Roncarolo. 2006. Tr1 cells: from discovery to their clinical application. In *Seminars in immunology* vol. 18. Elsevier. 120–127.

151. Gagliani, N., C. F. Magnani, S. Huber, M. E. Gianolini, M. Pala, P. Licona-Limon, B. Guo, D. R. Herbert, A. Bulfone, and F. Trentini. 2013. Coexpression of CD49b and LAG-3 identifies human and mouse T regulatory type 1 cells. *Nat. Med.* 19: 739–746.

152. Petereit, H. F., R. Pukrop, F. Fazekas, S. U. Bamborschke, S. Röpele, H. W. Kölmel, S. Merkelbach, G. Japp, P. J. H. Jongen, and H. P. Hartung. 2003. Low interleukin-10 production is associated with higher disability and MRI lesion load in secondary progressive multiple sclerosis. *J. Neurol. Sci.* 206: 209–214.

153. Ersoy, E., C. N. S. Kuş, U. Şener, I. Coker, and Y. Zorlu. 2005. The effects of interferon□β on interleukin 10 in multiple sclerosis patients. *Eur. J. Neurol.* 12: 208–211.

154. Zhang, X., D. N. Koldzic, L. Izikson, J. Reddy, R. F. Nazareno, S. Sakaguchi, V. K. Kuchroo, and H. L. Weiner. 2004. IL10 is involved in the suppression of experimental autoimmune encephalomyelitis by CD25+ CD4+ regulatory T cells. *Int. Immunol.* 16: 249–256.

155. Wei, Y., H. Chang, H. Feng, X. Li, X. Zhang, and L. Yin. 2019. Low serum interleukin 10 is an independent predictive factor for the risk of second event in clinically isolated syndromes. *Front. Neurol.* 10: 604.

156. Boyden, A. W., A. A. Brate, and N. J. Karandikar. 2020. Novel B cell-dependent multiple sclerosis model using extracellular domains of myelin proteolipid protein. *Sci. Rep.* 10: 5011.

157. Harp, C. R. P., A. S. Archambault, J. Sim, S. T. Ferris, R. J. Mikesell, P. A. Koni, M. Shimoda, C. Linington, J. H. Russell, and G. F. Wu. 2015. B cell antigen presentation is sufficient to drive neuroinflammation in an animal model of multiple sclerosis. *J. Immunol.* 194: 5077–5084.

158. Wu, G. F., K. S. Shindler, E. J. Allenspach, T. L. Stephen, H. L. Thomas, R. J. Mikesell, A. H. Cross, and T. M. Laufer. 2011. Limited sufficiency of antigen presentation by dendritic cells in models of central nervous system autoimmunity. *J. Autoimmun.* 36: 56–64.

159. Fillatreau, S., C. H. Sweenie, M. J. McGeachy, D. Gray, and S. M. Anderton. 2002. B cells regulate autoimmunity by provision of IL-10. *Nat. Immunol.* 3: 944–950.

160. Kitamura, D., J. Roes, R. Kühn, and K. Rajewsky. 1991. AB cell-deficient mouse by targeted disruption of the membrane exon of the immunoglobulin μ chain gene. *Nature* 350: 423–426.

161. Yang, Y., J. Weiner, Y. Liu, A. J. Smith, D. J. Huss, R. Winger, H. Peng, P. D. Cravens, M. K. Racke, and A. E. Lovett-Racke. 2009. T-bet is essential for encephalitogenicity of both Th1 and Th17 cells. *J. Exp. Med.* 206: 1549–1564.

162. Damsker, J. M., A. M. Hansen, and R. R. Caspi. 2010. Th1 and Th17 cells: adversaries and collaborators. *Ann. N. Y. Acad. Sci.* 1183: 211–221.

163. Matsushita, T., K. Yanaba, J.-D. Bouaziz, M. Fujimoto, and T. F. Tedder. 2008. Regulatory B cells inhibit EAE initiation in mice while other B cells promote disease progression. *J. Clin. Invest.* 118: 3420–3430.

164. Pierson, E. R., I. M. Stromnes, and J. M. Goverman. 2014. B cells promote induction of experimental autoimmune encephalomyelitis by facilitating reactivation of T cells in the central nervous system. *J. Immunol.* 192: 929–939.

165. Wellcome Trust Case Control Consortium, Australo-Anglo-American Spondylitis Consortium (TASC), P. R. Burton, D. G. Clayton, L. R. Cardon, N. Craddock, P. Deloukas, A. Duncanson, D. P. Kwiatkowski, M. I. McCarthy, W. H. Ouwehand, N. J. Samani, J. A. Todd, P. Donnelly, J. C. Barrett, D. Davison, D. Easton, D. M. Evans, D. M. Evans, H.-T. Leung, J. L. Marchini, A. P. Morris, C. C. A. Spencer, M. D. Tobin, A. P. Attwood, J. P. Boorman, B. Cant, U. Everson, J. M. Hussey, J. D. Jolley, A. S. Knight, K. Koch, E. Meech, S. Nutland, C. V Prowse, H. E. Stevens, N. C. Taylor, G. R. Walters, N. M. Walker, N. A. Watkins, T. Winzer, R. W. Jones, W. L. McArdle, S. M. Ring, D. P. Strachan, M. Pembrey, G. Breen, D. St Clair, S. Caesar, K. Gordon-Smith, L. Jones, C. Fraser, E. K. Green, D. Grozeva, M. L. Hamshere, P. A. Holmans, I. R. Jones, G. Kirov, V. Moskivina, I. Nikolov, M. C. O'Donovan, M. J. Owen, D. A. Collier, A. Elkin, A. Farmer, R. Williamson, P. McGuffin, A. H. Young, I. N. Ferrier, S. G. Ball, A. J. Balmforth, J. H. Barrett, T. D. Bishop, M. M. Iles, A. Maqbool, N. Yuldasheva, A. S. Hall, P. S. Braund, R. J. Dixon, M. Mangino, S. Stevens, J. R. Thompson, F. Bredin, M. Tremelling, M. Parkes, H. Drummond, C. W. Lees, E. R. Nimmo, J. Satsangi, S. A. Fisher, A. Forbes, C. M. Lewis, C. M. Onnie, N. J. Prescott, J. Sanderson, C. G. Matthew, J. Barbour, M. K. Mohiuddin, C. E. Todhunter, J. C. Mansfield, T. Ahmad, F. R. Cummings, D. P. Jewell, J. Webster, M. J. Brown, M. G. Lathrop, J. Connell, A. Dominiczak, C. A. B. Marcano, B. Burke, R. Dobson, J. Gungadoo, K. L. Lee, P. B. Munroe, S. J. Newhouse, A. Onipinla, C. Wallace, M. Xue, M. Caulfield, M. Farrall, A. Barton, Biologics in RA Genetics and Genomics Study Syndicate (BRAGGS) Steering Committee, I. N. Bruce, H. Donovan, S. Eyre, P. D. Gilbert, S. L. Hilder, A. M. Hinks, S. L. John, C. Potter, A. J. Silman, D. P. M. Symmons, W. Thomson, J. Worthington, D. B. Dunger, B. Widmer, T. M. Frayling, R. M. Freathy, H. Lango, J. R. B. Perry, B. M. Shields, M. N. Weedon, A. T. Hattersley, G. A. Hitman, M. Walker, K. S. Elliott, C. J. Groves, C. M. Lindgren, N. W. Rayner, N. J. Timpson, E. Zeggini, M. Newport, G. Sirugo, E. Lyons, F. Vannberg, A. V. S. Hill, L. A. Bradbury, C. Farrar, J. J. Pointon, P. Wordsworth, M. A. Brown, J. A. Franklyn, J. M. Heward, M. J. Simmonds, S. C. L. Gough, S. Seal, Breast Cancer Susceptibility Collaboration (UK), M. R. Stratton, N. Rahman, M. Ban, A. Goris, S. J. Sawcer, A. Compston, D. Conway, M. Jallow, M. Newport, G. Sirugo, K. A. Rockett, S. J. Bumpstead, A. Chaney, K. Downes, M. J. R. Ghori, R. Gwilliam, S. E. Hunt, M. Inouye, A. Keniry, E. King, R. McGinnis, S. Potter, R. Ravindrarajah, P. Whittaker, C. Widden, D. Withers, N. J. Cardin, D. Davison, T. Ferreira, J. Pereira-Gale, I. B. Hallgrimsdo'ttir, B. N. Howie, Z. Su, Y. Y. Teo, D. Vukcevic, D. Bentley, M. A. Brown, A. Compston, M. Farrall, A. S. Hall, A. T. Hattersley, A. V. S. Hill, M. Parkes, M. Pembrey, M. R. Stratton, S. L. Mitchell, P. R. Newby, O. J. Brand, J. Carr-Smith, S. H. S. Pearce, R. McGinnis, A. Keniry, P. Deloukas, J. D. Reveille, X. Zhou, A.-M. Sims, A. Dowling, J. Taylor, T. Doan, J. C. Davis, L. Savage, M. M. Ward, T. L. Learch, M. H. Weisman, and M. Brown. 2007. Association scan of 14,500 nonsynonymous SNPs in four diseases identifies autoimmunity variants. *Nat. Genet.* 39: 1329—1337.

166. Reeves, E., and E. James. 2018. The role of polymorphic ERAP1 in autoinflammatory disease. *Biosci. Rep.* 38: BSR20171503.

167. Kang, H. M., M. Subramaniam, S. Targ, M. Nguyen, L. Maliskova, E. McCarthy, E. Wan, S. Wong, L. Byrnes, and C. M. Lanata. 2018. Multiplexed droplet single-cell RNA-sequencing using natural genetic variation. *Nat. Biotechnol.* 36: 89–94.

168. Piccirillo, C. A., E. Bjur, I. Topisirovic, N. Sonenberg, and O. Larsson. 2014. Translational control of immune responses: from transcripts to translatomes. *Nat. Immunol.* 15: 503–511.

169. Ganeshan, K., and A. Chawla. 2014. Metabolic regulation of immune responses. *Annu. Rev. Immunol.* 32: 609.

170. La Rocca, C., F. Carbone, V. De Rosa, A. Colamatteo, M. Galgani, F. Perna, R. Lanzillo, V. B. Morra, G. Orefice, and I. Cerillo. 2017. Immunometabolic profiling of T cells from patients with relapsing-remitting multiple sclerosis reveals an impairment in glycolysis and mitochondrial respiration. *Metabolism* 77: 39–46.

171. Häusser-Kinzel, S., and M. S. Weber. 2019. The role of B cells and antibodies in multiple sclerosis, neuromyelitis optica, and related disorders. *Front. Immunol.* 10: 201.

172. Michel, L., H. Touil, N. B. Pikor, J. L. Gommerman, A. Prat, and A. Bar-Or. 2015. B cells in the multiple sclerosis central nervous system: trafficking and contribution to CNS-compartmentalized inflammation. *Front. Immunol.* 6: 636.

173. Levin, L. I., K. L. Munger, E. J. O'Reilly, K. I. Falk, and A. Ascherio. 2010. Primary infection with the Epstein Barr virus and risk of multiple sclerosis. *Ann. Neurol.* 67: 824–830.

174. Montalban, X., S. L. Hauser, L. Kappos, D. L. Arnold, A. Bar-Or, G. Comi, J. De Seze, G. Giovannoni, H.-P. Hartung, and B. Hemmer. 2017. Ocrelizumab versus placebo in primary progressive multiple sclerosis. *N. Engl. J. Med.* 376: 209–220.

175. Schafflick, D., C. A. Xu, M. Hartlehnert, M. Cole, A. Schulte-Mecklenbeck, T. Lautwein, J. Wolbert, M. Heming, S. G. Meuth, and T. Kuhlmann. 2020. Integrated single cell analysis of blood and cerebrospinal fluid leukocytes in multiple sclerosis. *Nat. Commun.* 11: 1–14.

176. Morris, G., B. K. Puri, L. Olive, A. F. Carvalho, M. Berk, and M. Maes. 2019. Emerging role of innate B1 cells in the pathophysiology of autoimmune and neuroimmune diseases: Association with inflammation, oxidative and nitrosative stress and autoimmune responses. *Pharmacol. Res.* 148: 104408.

177. Peterson, L. K., I. Tsunoda, and R. S. Fujinami. 2008. Role of CD5+ B-1 cells in EAE pathogenesis. *Autoimmunity* 41: 353–362.

178. Rovituso, D., S. Heller, M. Schroeter, C. Kleinschnitz, and S. Kuerten. 2014. B1 cells are unaffected by immune modulatory treatment in remitting-relapsing multiple sclerosis patients. *J. Neuroimmunol.* 272: 86–90.

179. Takeda, A., A. Matsuda, R. M. J. Paul, and N. R. Yaseen. 2004. CD45-associated protein inhibits CD45 dimerization and up-regulates its protein tyrosine phosphatase activity. *Blood* 103: 3440–3447.

180. Saunders, A. E., P. Johnson, A. Samarakoon, and K. W. Harder. 2012. CD45 (PTPRC). In *Encyclopedia of Signaling Molecules* Springer Nature. 328–334.

181. Wang, X., C. O. Eno, B. J. Altman, Y. Zhu, G. Zhao, K. E. Olberding, J. C. Rathmell, and C. Li. 2011. ER stress modulates cellular metabolism. *Biochem. J.* 435: 285–296.

182. Oakes, S. A., and F. R. Papa. 2015. The role of endoplasmic reticulum stress in human pathology. *Annu. Rev. Pathol.* 10: 173.

183. Gaudette, B. T., D. D. Jones, A. Bortnick, Y. Argon, and D. Allman. 2020. mTORC1 coordinates an immediate unfolded protein response-related transcriptome in activated B cells preceding antibody secretion. *Nat. Commun.* 11: 1–16.

184. So, J.-S. 2018. Roles of endoplasmic reticulum stress in immune responses. *Mol. Cells* 41: 705.

185. Li, A., N.-J. Song, B. P. Riesenberg, and Z. Li. 2020. The emerging roles of endoplasmic reticulum stress in balancing immunity and tolerance in health and diseases: mechanisms and opportunities. *Front. Immunol.* 10: 3154.

186. Shemer, A., I. Scheyltjens, G. R. Frumer, J.-S. Kim, J. Grozovski, S. Ayanaw, B. Dassa, H. Van Hove, L. Chappell-Maor, and S. Boura-Halfon. 2020. Interleukin-10 prevents pathological microglia hyperactivation following peripheral endotoxin challenge. *Immunity* 53: 1033–1049.

187. Lobo-Silva, D., G. M. Carriche, A. G. Castro, S. Roque, and M. Saraiva. 2016. Balancing the immune response in the brain: IL-10 and its regulation. *J. Neuroinflammation* 13: 1–10.

188. Iyer, S. S., and G. Cheng. 2012. Role of interleukin 10 transcriptional regulation in inflammation and autoimmune disease. *Crit. Rev. Immunol.* 32.

189. Brown, C. Y., C. A. Lagnado, M. A. Vadas, and G. J. Goodall. 1996. Differential regulation of the stability of cytokine mRNAs in lipopolysaccharide-activated blood monocytes in response to interleukin-10. *J. Biol. Chem.* 271: 20108–20112.

190. Zhang, X., L. Majlessi, E. Deriaud, C. Leclerc, and R. Lo-Man. 2009. Coactivation of Syk kinase and MyD88 adaptor protein pathways by bacteria promotes regulatory properties of neutrophils. *Immunity* 31: 761–771.

191. Frischer, J. M., S. Bramow, A. Dal-Bianco, C. F. Lucchinetti, H. Rauschka, M. Schmidbauer, H. Laursen, P. S. Sorensen, and H. Lassmann. 2009. The relation between inflammation and neurodegeneration in multiple sclerosis brains. *Brain* 132: 1175–1189.

192. York, I. A., S.-C. Chang, T. Saric, J. A. Keys, J. M. Favreau, A. L. Goldberg, and K. L. Rock. 2002. The ER aminopeptidase ERAP1 enhances or limits antigen presentation by trimming epitopes to 8–9 residues. *Nat. Immunol.* 3: 1177–1184.

193. Cabatingan, M. S., M. R. Schmidt, R. Sen, and R. T. Woodland. 2002. Naive B lymphocytes undergo homeostatic proliferation in response to B cell deficit. *J. Immunol.* 169: 6795–6805.

194. Biasizzo, M., and N. Kopitar-Jerala. 2020. Interplay Between NLRP3 Inflammasome and Autophagy. *Front. Immunol.* 11.

195. Chen, S., and B. Sun. 2013. Negative regulation of NLRP3 inflammasome signaling. *Protein Cell*.

196. Li, S., Y. Wu, D. Yang, C. Wu, C. Ma, X. Liu, P. N. Moynagh, B. Wang, G. Hu, and S. Yang. 2019. Gasdermin D in peripheral myeloid cells drives neuroinflammation in experimental autoimmune encephalomyelitis. *J. Exp. Med.* 216: 2562–2581.

197. Hu, J. J., X. Liu, S. Xia, Z. Zhang, Y. Zhang, J. Zhao, J. Ruan, X. Luo, X. Lou, Y. Bai, J. Wang, L. R. Hollingsworth, V. G. Magupalli, L. Zhao, H. R. Luo, J. Kim, J. Lieberman, and H. Wu. 2020. FDA-approved disulfiram inhibits pyroptosis by blocking gasdermin D pore formation. *Nat. Immunol.* 21: 736–745.

198. Wöhner, M., H. Tagoh, I. Bilic, M. Jaritz, D. K. Poliakova, M. Fischer, and M. Busslinger. 2016. Molecular functions of the transcription factors E2A and E2-2 in controlling germinal center B cell and plasma cell development. *J. Exp. Med.* 213: 1201–1221.

199. Tutar, Y. 2012. Pseudogenes. *Comp. Funct. Genomics* 2012: 424526.

200. Liu, Y., and A. Chang. 2008. Heat shock response relieves ER stress. *EMBO J.* 27: 1049–1059.

201. Ni, L., C. Yuan, C. Zhang, Y. Xiang, J. Wu, X. Wang, and X. Wu. 2020. Co-Expression Network Analysis Identified LTF in Association with Metastasis Risk and Prognosis in Clear Cell Renal Cell Carcinoma. *Onco. Targets. Ther.* 13: 6975–6986.

202. A., M. B., M. M. K., S. L. B., B. Roobina, M. M. Chiara, M. E. O., L. Jian-Qiang, B. W. G., and P. Christopher. 2018. Caspase-1 inhibition prevents glial inflammasome activation and pyroptosis in models of multiple sclerosis. *Proc. Natl. Acad. Sci.* 115: E6065–E6074.

203. Inoue, M., and M. L. Shinohara. 2013. NLRP3 Inflammasome and MS/EAE. *Autoimmune Dis.* 2013: 859145.

204. Borghaei, H., M. R. Smith, and K. S. Campbell. 2009. Immunotherapy of cancer. *Eur. J. Pharmacol.* 625: 41–54.

205. Mellman, I., G. Coukos, and G. Dranoff. 2011. Cancer immunotherapy comes of age. *Nature* 480: 480–489.

206. Voena, C., and R. Chiarle. 2016. Advances in cancer immunology and cancer immunotherapy. *Discov. Med.*

207. Topalian, S. L., F. S. Hodi, J. R. Brahmer, S. N. Gettinger, D. C. Smith, D. F. McDermott, J. D. Powderly, R. D. Carvajal, J. A. Sosman, M. B. Atkins, P. D. Leming, D. R. Spigel, S. J. Antonia, L. Horn, C. G. Drake, D. M. Pardoll, L. Chen, W. H. Sharfman, R. A. Anders, J. M. Taube, T. L. McMiller, H. Xu, A. J. Korman, M. Jure-Kunkel, S. Agrawal, D. McDonald, G. D. Kollia, A. Gupta, J. M. Wigginton, and M. Sznol. 2012. Safety, activity, and immune correlates of anti-PD-1 antibody in cancer. *N. Engl. J. Med.* 366: 2443–2454.

208. Klemen, N. D., M. Wang, P. L. Feingold, K. Cooper, S. N. Pavri, D. Han, F. C. Detterbeck, D. J. Boffa, S. A. Khan, K. Olino, J. Clune, S. Ariyan, R. R. Salem, S. A. Weiss, H. M. Kluger, M. Sznol, and C. Cha. 2019. Patterns of failure after immunotherapy with checkpoint inhibitors predict durable progression-free survival after local therapy for metastatic melanoma. *J. Immunother. Cancer* 7: 196.

209. Ferrara, R., L. Mezquita, M. Texier, J. Lahmar, C. Audigier-Valette, L. Tessonnier, J. Mazieres, G. Zalcman, S. Brosseau, S. Le Moulec, L. Leroy, B. Duchemann, C. Lefebvre, R. Veillon, V. Westeel, S. Koscielny, S. Champiat, C. Ferté, D. Planchard, J. Remon, M.-E. Boucher, A. Gazzah, J. Adam, E. Bria, G. Tortora, J.-C. Soria, B. Besse, and C. Caramella. 2018. Hyperprogressive Disease in Patients With Advanced Non–Small Cell Lung Cancer Treated With PD-1/PD-L1 Inhibitors or With Single-Agent Chemotherapy. *JAMA Oncol.* 4: 1543–1552.

210. Schmidt, K., C. Keller, A. A. Kühl, A. Textor, U. Seifert, T. Blankenstein, G. Willimsky, and P.-M. Kloetzel. 2018. ERAP1-Dependent Antigen Cross-Presentation Determines Efficacy of Adoptive T-cell Therapy in Mice. *Cancer Res.* 78: 3243 LP – 3254.

211. Compagnone, M., L. Cifaldi, and D. Fruci. 2019. Regulation of ERAP1 and ERAP2 genes and their disfunction in human cancer. *Hum. Immunol.*

212. Stamogiannos, A., A. Papakyriakou, F.-X. Mauvais, P. van Endert, and E. Stratikos. 2016. Screening Identifies Thimerosal as a Selective Inhibitor of Endoplasmic Reticulum Aminopeptidase 1. *ACS Med. Chem. Lett.* 7: 681–685.

213. Dórea, J. G., M. Farina, and J. B. T. Rocha. 2013. Toxicity of ethylmercury (and Thimerosal): a comparison with methylmercury. *J. Appl. Toxicol.* 33: 700–711.

214. Kern, J. K., D. A. Geier, K. G. Homme, and M. R. Geier. 2020. Examining the evidence that ethylmercury crosses the blood-brain barrier. *Environ. Toxicol. Pharmacol.* 74: 103312.

215. Lünemann, A., B. Tackenberg, T. DeAngelis, R. Barreira da Silva, B. Messmer, L. D. Vanoaica, A. Miller, B. Apatoff, F. D. Lublin, J. D. Lünemann, and C. Münz. 2011. Impaired IFN-γ production and proliferation of NK cells in Multiple Sclerosis. *Int. Immunol.* 23: 139–148.

216. Chaix, J., M. S. Tessmer, K. Hoebe, N. Fuséri, B. Ryffel, M. Dalod, L. Alexopoulou, B. Beutler, L. Brossay, E. Vivier, and T. Walzer. 2008. Cutting edge: Priming of NK cells by IL-18. *J. Immunol.* 181: 1627–1631.

217. Sharma, R., and A. Das. 2018. IL-2 mediates NK cell proliferation but not hyperactivity. *Immunol. Res.* 66: 151–157.

218. Sivori, S., M. Falco, M. Della Chiesa, S. Carlomagno, M. Vitale, L. Moretta, and A. Moretta. 2004. CpG and double-stranded RNA trigger human NK cells by Toll-like receptors: induction of cytokine release and cytotoxicity against tumors and dendritic cells. *Proc. Natl. Acad. Sci. U. S. A.* 101: 10116–10121.

219. Michel, T., A. Poli, A. Cuapio, B. Briquemont, G. Iserentant, M. Ollert, and J. Zimmer. 2016. Human CD56^{bright} NK Cells: An Update. *J. Immunol.* 196: 2923 LP – 2931.

220. Ge, Y., J. Chen, X. Qiu, J. Zhang, L. Cui, Y. Qi, X. Liu, J. Qiu, Z. Shi, Z. Lun, J. Shen, and Y. Wang. 2014. Natural killer cell intrinsic toll-like receptor MyD88 signaling contributes to IL-12-dependent IFN-γ production by mice during infection with Toxoplasma gondii. *Int. J. Parasitol.* 44: 475–484.

221. Wang, Y., Y. Zhang, P. Yi, W. Dong, A. P. Nalin, J. Zhang, Z. Zhu, L. Chen, D. M. Benson, B. L. Mundy-Bosse, A. G. Freud, M. A. Caligiuri, and J. Yu. 2019. The IL-15–AKT–XBP1s signaling pathway contributes to effector functions and survival in human NK cells. *Nat. Immunol.* 20: 10–17.

222. Ritzman, A. M., J. M. Hughes-Hanks, V. A. Blaho, L. E. Wax, W. J. Mitchell, and C. R. Brown. 2010. The chemokine receptor CXCR2 ligand KC (CXCL1) mediates neutrophil recruitment and is critical for development of experimental lyme arthritis and carditis. *Infect. Immun.*

223. Dupaul-Chicoine, J., A. Arabzadeh, M. Dagenais, T. Douglas, C. Champagne, A. Morizot, I. G. Rodrigue-Gervais, V. Breton, S. L. Colpitts, N. Beauchemin, and M. Saleh. 2015. The Nlrp3 Inflammasome Suppresses Colorectal Cancer Metastatic Growth in the Liver by Promoting Natural Killer Cell Tumoricidal Activity. *Immunity* 43: 751–763.

224. Dixon, K. J., J. R. Siebert, D. Wang, A. M. Abel, K. E. Johnson, M. J. Riese, S. S. Terhune, V. L. Tarakanova, M. S. Thakar, and S. Malarkannan. 2021. MyD88 is an essential regulator of NK cell-mediated clearance of MCMV infection. *Mol. Immunol.* 137: 94–104.

225. Bonilla, D. L., G. Reinin, and E. Chua. 2021. Full Spectrum Flow Cytometry as a Powerful Technology for Cancer Immunotherapy Research. *Front. Mol. Biosci.* 7: 612801.

226. Pozarowski, P., and Z. Darzynkiewicz. 2004. Analysis of cell cycle by flow cytometry. *Methods Mol. Biol.* 281: 301–311.

227. Barteneva, N. S., E. Fasler-Kan, and I. A. Vorobjev. 2012. Imaging flow cytometry: coping with heterogeneity in biological systems. *J. Histochem. Cytochem.* 60: 723–733.

228. Nolan, J. P., and D. Condello. 2013. Spectral flow cytometry. *Curr. Protoc. Cytom.* Chapter 1: Unit1.27-Unit1.27.

229. Park, L. M., J. Lannigan, and M. C. Jaimes. 2020. OMIP-069: Forty-Color Full Spectrum Flow Cytometry Panel for Deep Immunophenotyping of Major Cell Subsets in Human Peripheral Blood. *Cytom. Part A* 97: 1044–1051.

230. O'Connell, P., M. K. Blake, Y. Pepelyayeva, S. Hyslop, S. Godbehere, A. M. Angarita, C. Pereira-Hicks, A. Amalfitano, and Y. A. Aldhamen. 2021. “Adenoviral delivery of an immunomodulatory protein to the tumor microenvironment controls tumor growth” *Mol. Ther. - Oncolytics*.

231. Crowell, H. L., C. Soneson, P.-L. Germain, D. Calini, L. Collin, C. Raposo, D. Malhotra, and M. D. Robinson. 2020. muscat detects subpopulation-specific state transitions from multi-sample multi-condition single-cell transcriptomics data. *Nat. Commun.* 11: 6077.

232. Quintelier, K., A. Couckuyt, A. Emmaneel, J. Aerts, Y. Saeys, and S. Van Gassen. 2021. Analyzing high-dimensional cytometry data using FlowSOM. *Nat. Protoc.* 16: 3775–3801.

233. Chen, B., M. S. Khodadoust, C. L. Liu, A. M. Newman, and A. A. Alizadeh. 2018. Profiling Tumor Infiltrating Immune Cells with CIBERSORT. *Methods Mol. Biol.* 1711: 243–259.

234. Chen, Z., A. Huang, J. Sun, T. Jiang, F. X.-F. Qin, and A. Wu. 2017. Inference of immune cell composition on the expression profiles of mouse tissue. *Sci. Rep.* 7: 40508.

235. Jew, B., M. Alvarez, E. Rahmani, Z. Miao, A. Ko, K. M. Garske, J. H. Sul, K. H. Pietiläinen, P. Pajukanta, and E. Halperin. 2020. Accurate estimation of cell composition in bulk expression through robust integration of single-cell information. *Nat. Commun.* 11: 1971.

236. Sun, X., S. Sun, and S. Yang. 2019. An Efficient and Flexible Method for Deconvoluting Bulk RNA-Seq Data with Single-Cell RNA-Seq Data. *Cells* 8.

237. Wang, X., J. Park, K. Susztak, N. R. Zhang, and M. Li. 2019. Bulk tissue cell type deconvolution with multi-subject single-cell expression reference. *Nat. Commun.* 10: 380.

238. Newman, A. M., C. L. Liu, M. R. Green, A. J. Gentles, W. Feng, Y. Xu, C. D. Hoang, M. Diehn, and A. A. Alizadeh. 2015. Robust enumeration of cell subsets from tissue expression profiles. *Nat. Methods* 12: 453–457.

239. Aldhamen, Y. A., D. M. Appledorn, S. S. Seregin, C. J. Liu, N. J. Schuldt, S. Godbehere, and A. Amalfitano. 2011. Expression of the SLAM Family of Receptors Adapter EAT-2 as a Novel Strategy for Enhancing Beneficial Immune Responses to Vaccine Antigens. *J. Immunol.*

240. Kärre, K., H. G. Ljunggren, G. Piontek, and R. Kiessling. 1986. Selective rejection of H-2-deficient lymphoma variants suggests alternative immune defence strategy. *Nature* 319: 675–678.

241. Gómez-Román, V. R., R. H. Florese, L. J. Patterson, B. Peng, D. Venzon, K. Aldrich, and M. Robert-Guroff. 2006. A simplified method for the rapid fluorometric assessment of antibody-dependent cell-mediated cytotoxicity. *J. Immunol. Methods* 308: 53–67.

242. Aldhamen, Y. A., S. S. Seregin, N. J. Schuldt, D. P. W. Rastall, J. L. Chyong-jy, S. Godbehere, and A. Amalfitano. 2012. Vaccines expressing the innate immune modulator EAT-2 elicit potent effector memory T lymphocyte responses despite pre-existing vaccine immunity. *J. Immunol.* 189: 1349–1359.

243. Chevrier, S., H. L. Crowell, V. R. T. Zanotelli, S. Engler, M. D. Robinson, and B. Bodenmiller. 2018. Compensation of signal spillover in suspension and imaging mass cytometry. *Cell Syst.* 6: 612–620.

244. Van Gassen, S., B. Callebaut, M. J. Van Helden, B. N. Lambrecht, P. Demeester, T. Dhaene, and Y. Saeys. 2015. FlowSOM: Using self□organizing maps for visualization and interpretation of cytometry data. *Cytom. Part A* 87: 636–645.

245. Grabert, K., and B. W. McColl. 2018. Isolation and phenotyping of adult mouse microglial cells. In *Macrophages* Springer. 77–86.

246. Lee, J.-K., and M. G. Tansey. 2013. Microglia isolation from adult mouse brain. In *Microglia* Springer. 17–23.

247. Cillo, A. R., C. H. L. Kürten, T. Tabib, Z. Qi, S. Onkar, T. Wang, A. Liu, U. Duvvuri, S. Kim, and R. J. Soose. 2020. Immune landscape of viral-and carcinogen-driven head and neck cancer. *Immunity* 52: 183–199.

248. Wen, W., W. Su, H. Tang, W. Le, X. Zhang, Y. Zheng, X. Liu, L. Xie, J. Li, and J. Ye. 2020. Immune cell profiling of COVID-19 patients in the recovery stage by single-cell sequencing. *Cell Discov.* 6: 1–18.

249. Zhang, J.-Y., X.-M. Wang, X. Xing, Z. Xu, C. Zhang, J.-W. Song, X. Fan, P. Xia, J.-L. Fu, and S.-Y. Wang. 2020. Single-cell landscape of immunological responses in patients with COVID-19. *Nat. Immunol.* 21: 1107–1118.

250. Zheng, G. X. Y., J. M. Terry, P. Belgrader, P. Ryvkin, Z. W. Bent, R. Wilson, S. B. Ziraldo, T. D. Wheeler, G. P. McDermott, and J. Zhu. 2017. Massively parallel digital transcriptional profiling of single cells. *Nat. Commun.* 8: 1–12.

251. Wilk, A. J., A. Rustagi, N. Q. Zhao, J. Roque, G. J. Martínez-Colón, J. L. McKechnie, G. T. Ivison, T. Ranganath, R. Vergara, and T. Hollis. 2020. A single-cell atlas of the peripheral immune response in patients with severe COVID-19. *Nat. Med.* 26: 1070–1076.

252. Hao, Y., S. Hao, E. Andersen-Nissen, W. M. Mauck III, S. Zheng, A. Butler, M. J. Lee, A. J. Wilk, C. Darby, and M. Zager. 2021. Integrated analysis of multimodal single-cell data. *Cell* 184: 3573–3587.

253. Korsunsky, I., N. Millard, J. Fan, K. Slowikowski, F. Zhang, K. Wei, Y. Baglaenko, M. Brenner, P. Loh, and S. Raychaudhuri. 2019. Fast, sensitive and accurate integration of single-cell data with Harmony. *Nat. Methods* 16: 1289–1296.

254. Weber, L. M., M. Nowicka, C. Soneson, and M. D. Robinson. 2019. diffcyt: Differential discovery in high-dimensional cytometry via high-resolution clustering. *Commun. Biol.* 2: 1–11.

255. Soares, J. L. S., E. M. L. Oliveira, and A. Pontillo. 2019. Variants in NLRP3 and NLRC4 inflammasome associate with susceptibility and severity of multiple sclerosis. *Mult. Scler. Relat. Disord.* 29: 26–34.

256. Tam, A. B., E. L. Mercado, A. Hoffmann, and M. Niwa. 2012. ER stress activates NF-κB by integrating functions of basal IKK activity, IRE1 and PERK. *PLoS One* 7: e45078–e45078.

257. Serada, S., M. Fujimoto, M. Mihara, N. Koike, Y. Ohsugi, S. Nomura, H. Yoshida, T. Nishikawa, F. Terabe, T. Ohkawara, T. Takahashi, B. Ripley, A. Kimura, T. Kishimoto, and T. Naka. 2008. IL-6 blockade inhibits the induction of myelin antigen-specific Th17 cells and Th1 cells in experimental autoimmune encephalomyelitis. *Proc. Natl. Acad. Sci.* 105: 9041 LP – 9046.

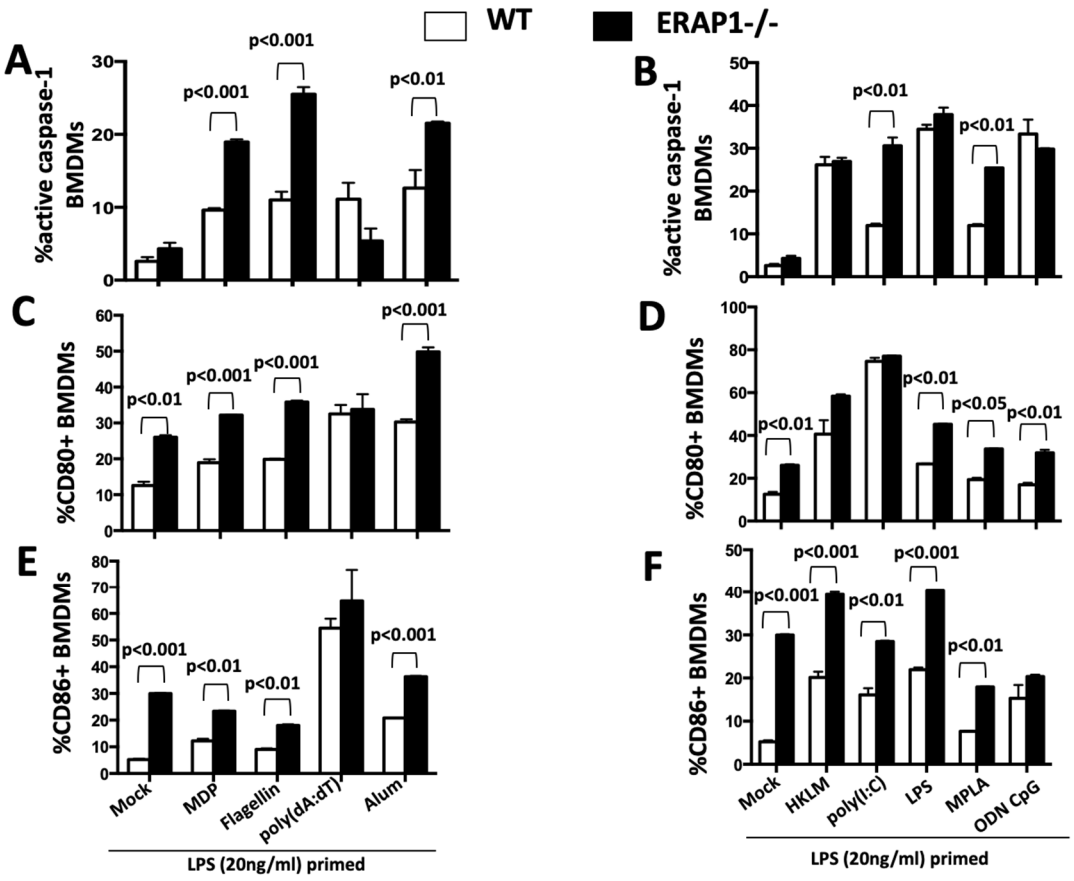

Figure S1: Characterization of macrophages with multiple inflammasome agonists.

Bone marrow-derived macrophages (5× 105 cells) were plated into 24-well plates, and then cells were primed with LPS (20ng/ml) for 16 hours. Cells were then stimulated for another 24 hours with various NLR inflammasome agonists, as indicated. Cells were stained with Pacific Blue conjugated-CD80 (C, D) and APC conjugated anti-CD86 (E,F) and flow cytometry was completed. Data are expressed as means ± SEM. $p<0.01$, $p<0.001$, significantly different from mock.

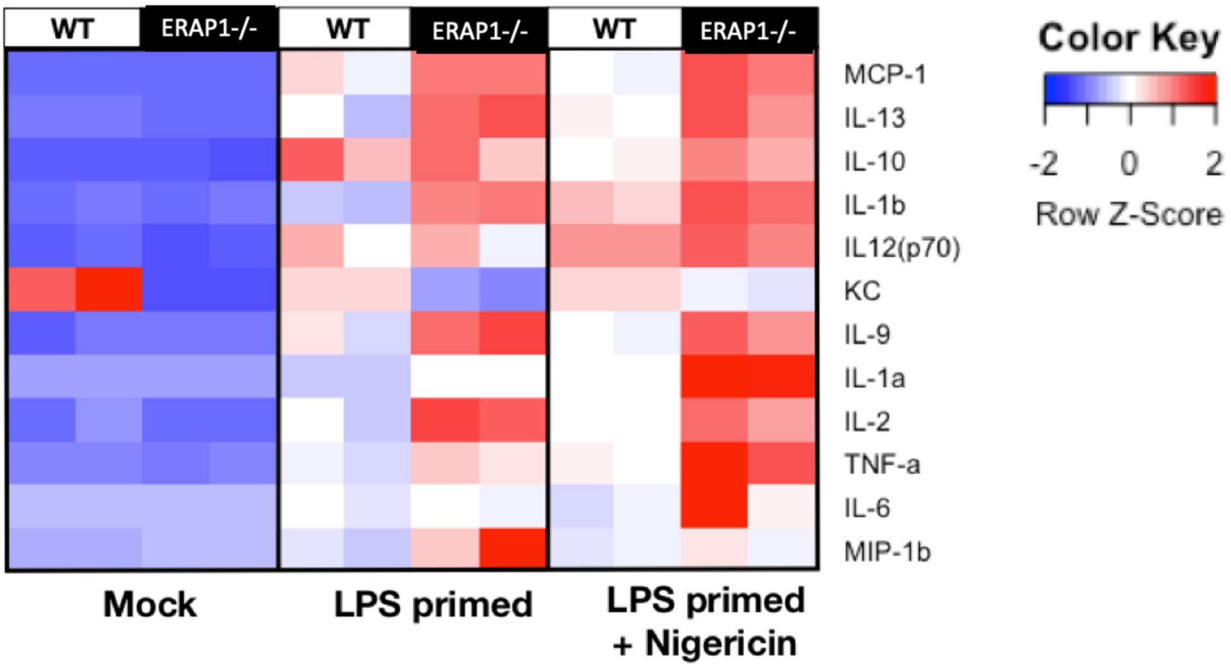

Figure S2: Increased cytokine and chemokine production from ERAP1$^{-/-}$ macrophages following NLRP3 inflammasome activation.

Heat map depicting the top 12 upregulated and downregulated cytokines by ERAP1. Bone marrow-derived macrophages (BMDMs) from C57 WT and ERAP1$^{-/-}$ mice were primed with LPS (20ng/mL) for 12 hours. Cells were then stimulated with nigericin (10ug/mL) for an additional 20 hours. Supernatants were collected and analyzed used in a 23-plex multiplex assay using Bioplex.

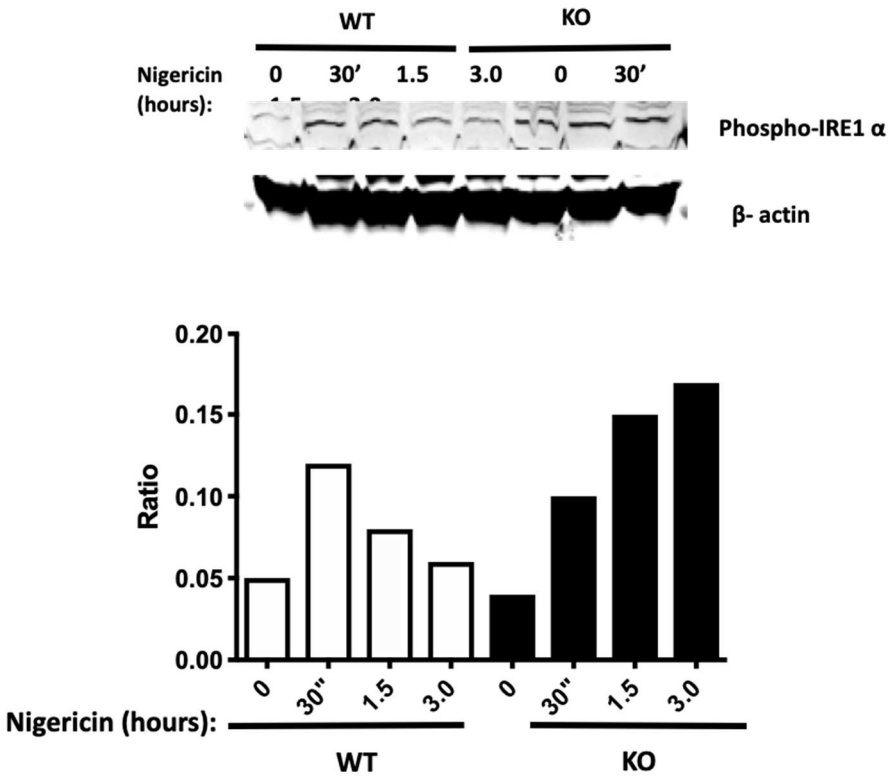

Figure S3: p-IRE1a expression with NLRP3 inflammasome stimulation. Bone marrow-derived macrophages (2×10^6 cells) were plated into 6-well plates, and then cells were primed with LPS (15ng/ml) for 12 hours. Cells were then stimulated for various timepoints with Nigericin (10uM). BMDMs were collected, protein was isolated and western blot was run for p-IRE1a and loading control.

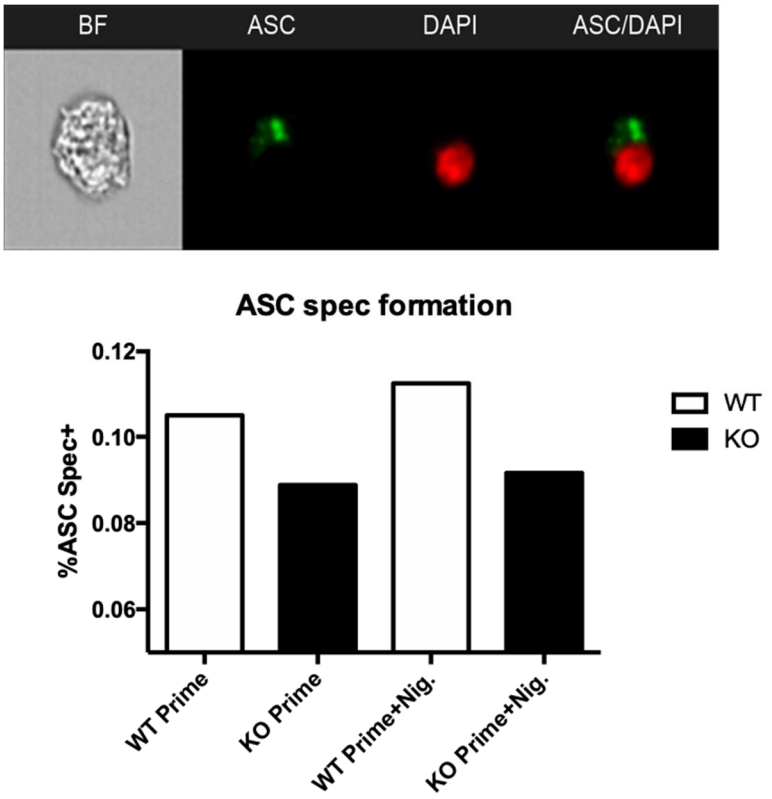

Figure S4: ASC speck formation analysis with NLRP3 inflammasome stimulation. Bone marrow-derived macrophages (1×10^6 cells) were plated into 6-well plates, and then cells were primed with LPS (15ng/ml) for 12 hours. Cells were then stimulated for 30 minutes with Nigericin (Nig.). Cells were stained with Alexa 488-conjugated ASC and DAPI nuclear stain, followed by sample collection and analysis via ImageStream X.

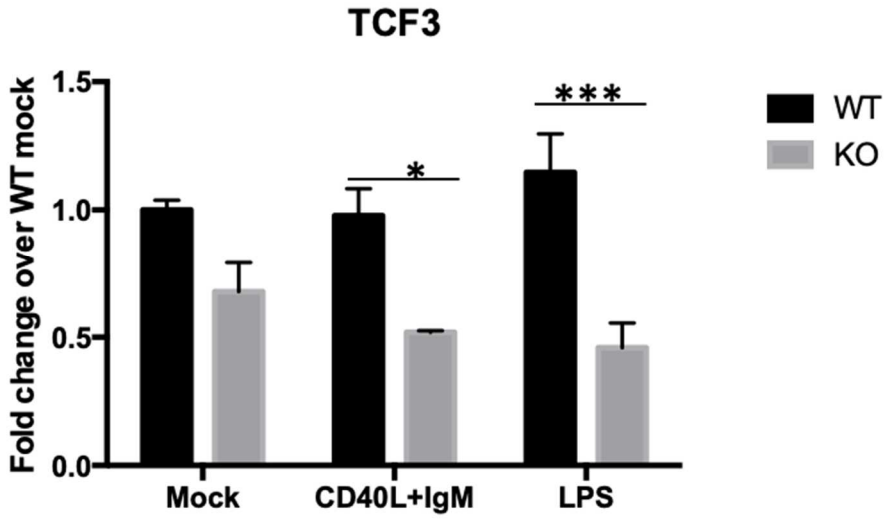

Figure S5: Confirmation of reduced TCF3 expression in ERAP1-deficient B cells. Isolated B cells (1×10^6 cells) were plated into 6-well plates, and then cells were treated with LPS (100ng/ml), or CD40L and Fragmented IgM for 12 hours. RNA was harvested via Trizol solution and cDNA was made according to manufacturing instructions. The TCF3 gene was measured using RT-PCR. Data are expressed as means ± SEM. * $p<0.05$, *** $p<0.0001$.

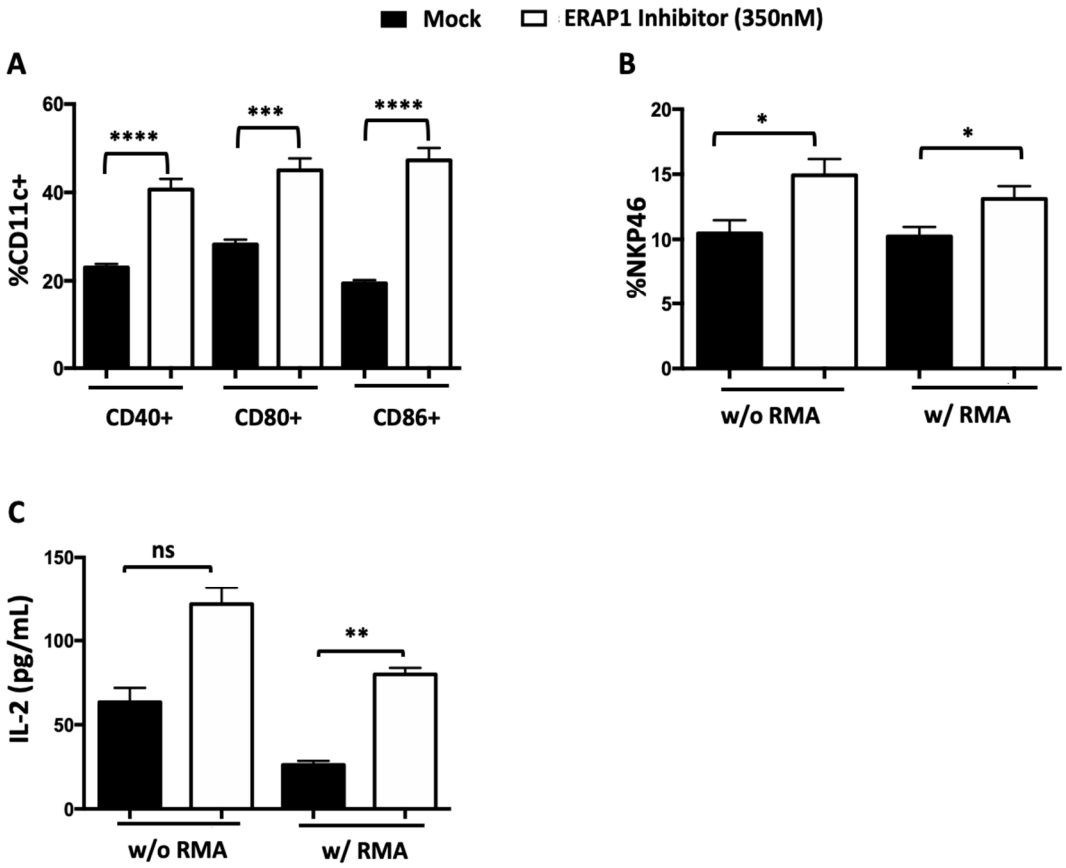

Figure S6: ERAP1 deficient NK cells have increased activation marker surface expression.

(A) Splenocytes were isolated from WT mice, and cultured for 48 hours with 350nM Thimerosal. Cells were collected and stained for CD40, CD80 and CD86 on CD11c+ Dendritic Cells (DCs). Isolated splenocytes from WT mice were cultured for 48 hours with 350nM Thimerosal, with (w/) or without (w/o) RMA cells in a 5:1 Splenocyte:RMA ratio for 48 hours. (B) Cells were collected and stained for NKP46 on NK1.1 cells. Flow cytometry was conducted using LSRII instrument. (C) Supernatant was collected after 48 hours and IL-2 cytokine analysis was completed for total splenocytes alone and splenocytes with RMA co-culture, with or without 350nM Thimerosal. Data are expressed as means ± SEM. *$p<0.005$, **$p<0.002$, **** $p<0.0001$